VOLUME 30 APRIL 1952 NUMBER 4

Canadian Journal of Chemistry

Editor: J. W. T. SPINKS

Published by THE NATIONAL RESEARCH COUNCIL
OTTAWA CANADA

CANADIAN JOURNAL OF CHEMISTRY

(Formerly Section B, Canadian Journal of Research)

The CANADIAN JOURNAL OF CHEMISTRY is published monthly by the National Research Council of Canada under the authority of the Chairman of the Committee of the Privy Council on Scientific and Industrial Research. Matters of general policy are the responsibility of a joint Editorial Board consisting of members of the National Research Council of Canada and the Royal Society of Canada.

The National Research Council of Canada publishes also: *Canadian Journal of Botany, Canadian Journal of Medical Sciences, Canadian Journal of Physics, Canadian Journal of Technology, Canadian Journal of Zoology.*

The CANADIAN JOURNAL OF CHEMISTRY and the CANADIAN JOURNAL OF TECHNOLOGY have been chosen by the Chemical Institute of Canada as its medium of publication for scientific papers.

EDITORIAL BOARD

Representing
NATIONAL RESEARCH COUNCIL

DR. J. H. L. JOHNSTONE (*Chairman*),
Professor of Physics,
Dalhousie University,
Halifax, N.S.

DR. OTTO MAASS,
Macdonald Professor of
Physical Chemistry,
McGill University,
Montreal, P.Q.

DR. CHARLES W. ARGUE,
Dean of Science,
University of New Brunswick,
Fredericton, N.B.

DR. A. G. MCCALLA,
Department of Plant Science,
University of Alberta,
Edmonton, Alta.

Representing
ROYAL SOCIETY OF CANADA

DR. G. M. VOLKOFF,
Professor of Physics,
University of British Columbia,
Vancouver, B.C.

DR. J. W. T. SPINKS,
Dean, College of Graduate
Studies,
University of Saskatchewan,
Saskatoon, Sask.

} Section III

DR. H. S. JACKSON,*
Head, Department of Botany,
University of Toronto,
Toronto, Ont.

DR. E. HORNE CRAIGIE,
Department of Zoology,
University of Toronto,
Toronto, Ont.

} Section V

Ex officio

DR. LÉO MARION (*Editor-in-Chief*),
Division of Chemistry,
National Research Laboratories,
Ottawa.

DR. H. H. SAUNDERSON,
Director, Division of Information Services,
National Research Council,
Ottawa.

Representing
THE CHEMICAL INSTITUTE OF CANADA

DR. H. G. THODE,
Department of Chemistry
McMaster University,
Hamilton, Ont.

Manuscripts should be addressed to:

DR. LÉO MARION,
Editor-in-Chief,
Canadian Journal of Chemistry,
National Research Council,
Ottawa, Canada.

Each manuscript should be typewritten, double-spaced, and the original and one extra copy submitted (see **Notice to Contributors** inside of back cover).

Subscriptions, renewals, and orders for back numbers should be addressed to:

Administrative Services,
National Research Council,
Ottawa, Canada.

Subscription rate: **$4.00** a year; single numbers: 50 cents. Special rates can be obtained for subscriptions to more than one of the Journals published by the National Research Council.

**Deceased.*

Canadian Journal of Chemistry

Issued by THE NATIONAL RESEARCH COUNCIL OF CANADA

VOL. 30 APRIL, 1952 NUMBER 4

THE ACTION OF LIQUID AMMONIA ON WHEAT STRAW HOLOCELLULOSE[1]

BY C. T. BISHOP

ABSTRACT

Exhaustive extraction with anhydrous liquid ammonia removed 8.0% of wheat straw holocellulose. Acetamide was isolated from the extract and identified as the dihydrogen bromide salt. A polyuronide fraction, making up 1.3% of the holocellulose, was isolated and shown to consist of D-xylose, L-arabinose, D-glucose, D-galactose, and D-glucuronic acid in approximate molar ratios of 11 : 3 : 3 : 1 : 2.5. Analysis and hydrogenation of the noncarbohydrate portion of the liquid ammonia extract showed it to consist of low molecular weight degradation products among which methylamine was identified. A separate experiment showed that anhydrous liquid ammonia degraded an isolated polyuronide by 8.4%; all components of the polyuronide were equally affected.

INTRODUCTION

Anhydrous liquid ammonia has been used as a solvent for carbohydrate reactions since 1931 (12, 13, 14, 18). However, its use in investigating crude plant materials is more recent. Yan (24) studied the use of liquid ammonia as a solvent for lignin in rye straw and found that it removed 0.8% of polysaccharide material as well as 50% of the lignin. He also showed that anhydrous liquid ammonia completely deacetylated the straw. In 1937 Hess and Gunderman (9) showed that liquid ammonia would swell cellulose and form a derivative similar to hydrocellulose. More recently Wolff, Olds, and Hilbert (22) found that starch was more readily esterified after treatment with anhydrous liquid ammonia. Neubauer (15) made use of this swelling action of liquid ammonia to increase the accessibility of polyuronides in maple wood.

In a previous publication (4) it was reported that anhydrous liquid ammonia increased the accessibility of polyuronides to solvents and in this way aided in the fractionation of wheat straw holocellulose. In that fractionation, material soluble in liquid ammonia was left in the holocellulose and removed in the aqueous extract. The purpose of the present work was to determine what action liquid ammonia had on wheat straw holocellulose apart from the physical swelling of the cellulose fiber structure.

MATERIALS AND METHODS

Wheat straw holocellulose was prepared from extractive free wheat straw by a delignification procedure using sodium chlorite (1). Pentoses were determined as furfural, by an excess bromine oxidation method (10) after distillation from 12% hydrochloric acid. Lignin was determined by the 72% sulphuric

[1] *Manuscript received December 4, 1951.*
Contribution from the Division of Applied Biology, National Research Laboratories, Ottawa. Issued as paper No. 135 on Uses of Plant Products and as N.R.C. No. 2677.

acid method of Ritter *et al.* (17); uronic acid anhydride by the method of Tracy (21); methoxyl by the procedure described by Clarke (5). Acetyl content was determined by alkali saponification followed by steam distillation and titration of the acetic acid (5). Reducing power was determined by the method of Somogyi (20) and individual sugars, liberated by acid hydrolysis, were determined both qualitatively and quantitatively by a combination of chromatographic techniques previously described (4). Nitrogen was determined by the Kjeldahl procedure and carbon–hydrogen by dry combustion. All results were on an ash-free, moisture-free basis unless otherwise stated.

EXPERIMENTAL PROCEDURES AND RESULTS

Liquid Ammonia Extraction

The extractions with liquid ammonia were carried out in the apparatus previously described (4) and under the same anhydrous conditions. A solid–solvent ratio of 1 : 30 (w/v) was used and the extractions were done at atmospheric pressure. At the end of each extraction period the liquid ammonia extract was removed by suction through a glass dispersion sinter, the system being protected from moisture by anhydrous calcium chloride drying tubes. As a result of the evaporation of the liquid ammonia under diminished pressure and of the drying of the residue to constant weight at 0.1 mm. over phosphoric anhydride, the extracted material was obtained as a dark brown syrup. Four successive 24 hr. extractions of 366.4 gm. of wheat straw holocellulose with anhydrous liquid ammonia removed 13.2 gm., 10.6 gm., 5.5 gm., and 0.0 gm. or a total of 8.0%. Original values of 5.8%, 1.9%, and 1.8% for uronic acid anhydride, acetyl, and lignin respectively in wheat straw holocellulose were reduced to 5.3%, 0.3%, and 1.4% by liquid ammonia extraction.

Identification of Acetamide

After removal of liquid ammonia, the extract was dissolved in 700 ml. of water and the solution (pH 7) exhaustively extracted with chloroform in a liquid–liquid extractor. The chloroform solution was dried over anhydrous sodium sulphate and evaporated, under diminished pressure, to a dark brown glass from which 0.10 gm. of white crystals were isolated by vacuum sublimation. The crystals were dissolved in 5 ml. of water to which 15 ml. of 48% hydrobromic acid was added, and the solution evaporated to dryness at 60°C. The resulting hydrobromide was recrystallized from 75% methanol to a constant m.p. of 138°-140°C. which was not depressed on admixture with an authentic sample of dihydrobromide salt of acetamide.

Polyuronide Fraction

The aqueous solution from the chloroform extraction was concentrated, under diminished pressure, to 250 ml. The addition of four volumes of 95% ethanol precipitated 4.8 gm. (1.3%) of polyuronide material. After dialysis against water and drying through solvent exchange to a white powder, the following analysis of the polyuronide was obtained: $[\alpha]_D^{20} = -89.0$, pentose = 53.6%, uronic acid anhydride ($CO_2 \times 4$) = 10.8%, and methoxyl/uronic acid anhydride = 0.84. An aliquot (0.55 gm.) of the polyuronide was

hydrolyzed to constant reducing power by heating on a boiling water bath with 50 ml. of 1% sulphuric acid. The acid was neutralized with barium carbonate, the barium salts removed by filtration, washed with warm water, and the combined washings and filtrate concentrated to 10 ml. Barium uronates (0.1 gm.) were precipitated from this solution by adding four volumes of 95% ethanol and the filtrate was again concentrated to 10 ml. D-xylose, L-arabinose, D-glucose, and D-galactose were identified in this filtrate by comparison with known sugars run on the same paper chromatogram using a solvent system of ethyl acetate – water – pyridine (11). The reliability of this method was previously demonstrated by isolation of crystalline derivatives (4). Molar ratios of 11 : 3 : 3 : 1 respectively of the above sugars were found by quantitative chromatography (8, 16) in which the sugars, separated on the paper, were extracted by water and their amounts in the extracts determined by the Somogyi method (20).

Analysis of the polyuronide indicated the presence of 2.5 moles of uronic acid anhydride. Methoxylated uronic acids are difficult to oxidize to mucic or saccharic acid (3). The presence of a methoxyl group in the uronic acid from wheat straw holocellulose (4) probably accounts for repeated unsuccessful attempts to isolate a crystalline oxidation product.

In a separate investigation, subsequent to this work, the uronic acid has been identified as D-glucuronic acid. A polyuronide, similar to the one described here, was isolated from wheat straw holocellulose by extraction with alkali. Prolonged hydrolysis of this polyuronide with sulphuric acid yielded an aldobiuronic acid which was isolated as the barium salt. Further hydrolysis of this compound and paper chromatography of the hydrolyzate showed it to consist of D-xylose and a uronic acid. Methoxyl determinations showed that only one-third of the uronic acid contained a methyl ether group. The methyl ester of this aldobiuronic acid was reduced with sodium borohydride (23) and the product was hydrolyzed with dilute acid. Paper chromatography of the hydrolyzate showed the presence of D-glucose and this was confirmed by isolation of D-glucose phenylosotriozole (7) which had a m.p. and mixed m.p. of 195-196°C. Because D-glucose was absent in the aldobiuronic acid before reduction it could only have been formed from the uronic acid. The uronic acid in the polyuronide of wheat straw holocellulose is therefore D-glucuronic acid.

Noncarbohydrate Fraction

The ethanol-soluble material from the polyuronide precipitation had a reducing power of 0.20 ml. of 0.005 *N* thiosulphate per 10 mgm. This value remained constant after heating with 2% sulphuric acid at 96°C. for six hours, showing the absence of polysaccharide material. Examination by paper chromatography showed that no monosaccharides were present. This material was dried to constant weight over phosphoric anhydride at 0.1 mm. Analysis showed: C = 41.7%, H = 5.14%, N = 6.75%, methoxyl = 5.9%, and molecular weight = 124 (determined by depression of the freezing point of water).

The noncarbohydrate material (11.5 gm.) in absolute ethanol (200 ml.) was hydrogenated in a stainless steel bomb of 500 ml. capacity which was fitted to a mechanical rocker. Copper–chrome oxide was freshly prepared according to Connor *et al.* (6) and was used immediately. Two hydrogenations were done with 5 gm. charges of the catalyst and an initial hydrogen pressure of 2000 p.s.i. The temperature of the bomb was raised to 240°C. in two hours and maintained at that point for six hours. Hydrogen consumption of 0.7 moles was calculated from pressure readings at room temperature before and after the hydrogenations. Raney nickel was prepared by the method of Adkins (2) and stored under absolute ethanol until used. Three more hydrogenations using 4 gm. of Raney nickel under the same conditions increased the total hydrogen consumption to a constant amount of 2.8 moles. Evaporation of the solvent left 1.34 gm. of a brown syrup, a yield of 11.7%. The ethanolic distillate had a fishy odor and gave off white fumes with hydrochloric acid, indicating the presence of low molecular weight, aliphatic amines. The ethanol solution was saturated with dry hydrogen chloride at 5°C. and redistilled leaving a light brown oil. After decolorizing with charcoal and cooling at 0°C., 0.77 gm. of an amine hydrochloride were obtained. Its melting point, 186°-208°, was unchanged on recrystallization. The crystals were benzoylated by the standard method (19) using sodium hydroxide and benzoyl chloride. The resulting benzamide was recrystallized from ethanol–water to a constant m.p. of 79°-80°C. which was not depressed on admixture with an authentic sample of the benzamide of methyl amine.

The brown syrup (1.34 gm.), left after removal of ethanol from the hydrogenate, was distilled at 0.07 mm. A heavy straw-colored syrup (0.18 gm.) came over at a bath temperature of 250°C. Analysis of this syrup showed: C = 72.0%, H = 11.0%, N = 0.0%, methoxyl = 0.0%, and molecular weight = 215 (determined by the vapor pressure lowering of methanol). Analysis of the nondistillable residue gave: C = 54.2%, H = 8.03%, N = 2.9%, methoxyl = 1.2%, and molecular weight = 980 (determined by elevation of the boiling point of ethanol).

Action of Anhydrous Liquid Ammonia on a Polyuronide Material

A polyuronide fraction, extracted from wheat straw holocelluose by 12% potassium hydroxide, had $[\alpha]_D^{27} = -88.5°$, pentose = 82.8%, uronic acid anhydride = 7.16%, and methoxyl = 0.8%. A sample (0.50 gm.) of this polyuronide was soaked in anhydrous liquid ammonia (150 ml.) for 36 hr. under the previously described conditions (4). The liquid ammonia only partially dissolved the polyuronide which became slightly darkened in color. After removal of the liquid ammonia, by vaporization under diminished pressure, the polyuronide was hydrolyzed to constant reducing power by 2% sulphuric acid at 96°C. A recovery of 70.6% of the weight of sample was obtained as reducing material. Duplicate hydrolysis of a sample of the same polyuronide that had not been treated with anhydrous liquid ammonia gave a recovery of 79.0%. The loss of 8.4% in reducing power can therefore be attributed to treatment with anhydrous liquid ammonia. Individual sugars

in both hydrolyzates were estimated quantitatively by chromatography. The proportions of the sugars to each other were the same showing that the degradation was general.

DISCUSSION

The anhydrous liquid ammonia extract of wheat straw holocellulose contained 1.3% of polyuronide material and 6.7% of noncarbohydrate material. The acetyl content of the holocellulose was reduced from 1.9% to 0.3% and this deacetylating action was confirmed by the identification of acetamide. The extraction also reduced the content of residual lignin in the wheat straw holocellulose from 1.8% to 1.4%. These results are in good agreement with those of Yan (24) who used anhydrous liquid ammonia to extract lignin from rye straw and found that 0.8% of a polysaccharide was removed and that the material was completely deacetylated.

The bulk (6.7% of the wheat straw holocellulose) of the liquid ammonia extract was noncarbohydrate. After complete hydrogenation only 11.7% of material was recoverable with the rest being lost as volatile products among which methyl amine was identified. Distillation of the recovered material and analyses of both distillate and residue indicated a mixture of products from which no identifiable compound could be isolated. These results showed that the noncarbohydrate material was a complex mixture of low molecular weight compounds together with a small amount of higher molecular weight material, possibly lignin extracted by the liquid ammonia.

Except for 1.8% residual lignin, wheat straw holocellulose consists entirely of carbohydrates. Therefore, the 6.7% of noncarbohydrate material must have been formed by a degradative chemical action of anhydrous liquid ammonia on wheat straw holocellulose. This degradation was confirmed by soaking a polyuronide fraction in anhydrous liquid ammonia and determining the amount recoverable as reducing material after hydrolysis. A loss of 8.4% was caused by the liquid ammonia. Anhydrous conditions precluded the possibility of degradation by alkali. Isolation of such nitrogenous compounds as acetamide and methyl amine showed that this complex, degradative reaction was directly associated with the ammonia. It appears that although anhydrous liquid ammonia can be used with success to swell or activate cellulose (9) or starch (22), the smaller polyuronide molecule is less resistant to its chemical action. It must be concluded that anhydrous liquid ammonia is not a good solvent for extracting polyuronide material. However, its use as a swelling agent to increase the accessibility of polyuronides to other solvents (4, 15) is justified if the time of treatment is kept short.

ACKNOWLEDGMENTS

The author wishes to thank Dr. G. A. Adams for supplying the wheat straw holocellulose used in this work, and for many helpful discussions.

REFERENCES

1. Adams, G. A. and Castagne, A. E. Can. J. Research, B, 26: 325. 1948.
2. Adkins, H. Reactions of hydrogen. University of Wisconsin Press, Madison. 1937. p. 20.

3. ANDERSON, E. and OTIS, L. J. Am. Chem. Soc. 52: 4461. 1930.
4. BISHOP, C. T. and ADAMS, G. A. Can. J. Research, B, 28: 753. 1950.
5. CLARKE, E. P. Semimicro quantitative organic analysis. Academic Press, Inc., New York. 1943.
6. CONNOR, R., FOLKERS, K., and ADKINS, H. J. Am. Chem. Soc. 54: 1138. 1932.
7. HANN, R. M. and HUDSON, C. S. J. Am. Chem. Soc. 66: 735. 1944.
8. HAWTHORNE, J. R. Nature, 160: 714. 1947.
9. HESS, K. and GUNDERMANN, J. Ber. 70(B): 1788. 1937.
10. HUGHES, E. E. and ACREE, S. F. Ind. Eng. Chem., Anal. Ed. 6: 123. 1934.
11. JERMYN, M. A. and ISHERWOOD, F. A. Biochem. J. 44: 402. 1949.
12. MILLER, C. O. and SIEHRS, A. E. Proc. Soc. Exptl. Biol. Med. 29: 535. 1931.
13. MUSKAT, I. E. J. Am. Chem. Soc. 56: 693. 1934.
14. MUSKAT, I. E. J. Am. Chem. Soc. 56: 2449. 1934.
15. NEUBAUER, L. G. Ph.D. Thesis, McGill University, Montreal, Que. 1949.
16. PARTRIDGE, S. M. Nature, 158: 270. 1946.
17. RITTER, G. J., SEBORG, R. M., and MITCHELL, R. L. Ind. Eng. Chem., Anal. Ed. 4: 202. 1932.
18. ROBBINS, G. B. and UPSON, F. W. J. Am. Chem. Soc. 62: 1074. 1940.
19. SHRINER, R. L. and FUSON, R. C. Identification of organic compounds. John Wiley and Sons, Inc., New York. 1940. p. 147.
20. SOMOGYI, M. J. Biol. Chem. 160: 61. 1945.
21. TRACY, M. V. Biochem. J. 43: 185. 1948.
22. WOLFF, I. A., OLDS, D. W., and HILBERT, G. E. J. Am. Chem. Soc. 73: 346. 1951.
23. WOLFROM, M. L., WOOD, H. B., and ANNO, K. Abstracts Papers Am. Chem. Soc. 119: 8Q. 1951.
24. YAN., M. M. Ph.D. Thesis, McGill University, Montreal, Que. 1947.

THE REACTION BETWEEN SILVER AND TRIPHENYLMETHYL CHLORIDE[1]

By E. J. Perry[2] and C. A. Winkler

ABSTRACT

Kinetic evidence has been obtained to indicate that, in toluene, the reaction between silver and triphenylmethyl chloride is a tarnishing reaction involving the growth of a silver chloride film on silver. Logarithmic, linear, and parabolic rates were observed, as well as a characteristic, very sudden decrease in reaction rate under certain conditions. The film thicknesses at which most of these phenomena occurred were those predicted by the Cabrera–Mott theory for the oxidation of metals.

INTRODUCTION

The reaction between silver and triphenylmethyl chloride,

$$Ag + (C_6H_5)_3CCl \rightarrow AgCl + (C_6H_5)_3C^{\cdot},$$

has long been known (7), but has been the subject of kinetic study only to the extent that reaction times for satisfactory yields of triphenylmethyl free radicals have been determined (14), and the reactivity of silver relative to that of a number of other metals towards triphenylmethyl chloride has been assessed (16). The present study was made since it seemed likely that the reaction should represent a liquid phase tarnishing reaction in which silver chloride, which is practically insoluble in most organic solvents, would grow as a film on the metallic silver because of the strong attractive forces which are known (3) to exist between the positive and negative ions of a metal salt and a metal substrate. The presently accepted view on the growth of such a film, a process termed "Anlaufvorgang" by Wagner (17), is that, as tarnishing occurs, metal passes outwards through the metal salt film, either by the outward diffusion of interstitial metal cations and electrons if the metal salt is an excess semiconductor, or by the inward diffusion of vacant cation sites and of positive holes if the metal salt is a deficit semiconductor. For the oxidation of metals, Cabrera and Mott (3) have differentiated various growth laws and mechanisms, according as the growing film is "very thin" (up to $\sim 10^{-6} - 10^{-5}$ cm.), "thin" (up to $\sim 10^{-4}$ cm.) or "thick". They also postulated that below a "critical temperature" the initially very rapid growth should suddenly come to a virtual standstill, a phenomenon they termed the attainment of a "limiting film thickness", the value of which would depend on the temperature and other parameters.

The growth of "very thin" and "thin" metal oxide films has already been the subject of experimental investigations (13, 4). However, only the growth of "thick" silver chloride films has so far been studied because of the elevated temperatures at which the film forming reaction used in the past,

[1] *Manuscript received November 20, 1951.*
Contribution from the Physical Chemistry Laboratory, McGill University, Montreal, Que., with financial assistance from the National Research Council of Canada. Presented at the June, 1951 Meeting of the Chemical Institute of Canada at Winnipeg, Man.
[2] *Holder of a Fellowship under the National Research Council of Canada. Present address: Department of National Health and Welfare, Ottawa, Ont.*

i.e., the action of gaseous chlorine on silver, was made to take place. Both Tammann (15) and Wagner (18) found this reaction to follow a parabolic rate law. Tammann's mechanism, which postulates an inward diffusion of gaseous chlorine through the silver chloride film, is obsolete and Wagner's mechanism is accepted at the present time (12). Wagner (17) was able to show quantitatively that the entire amount of product formed during a tarnishing reaction could be ascribed to the outward motion of metal cations and electrons through the film. He described (18) the process at the silver chloride – chlorine interface in the following manner:

$$\text{Cl (gaseous)} + \text{Ag}^+ (i) + e^- (l) \rightleftharpoons \text{Cl}^-(l) + \text{Ag}^+(l) + \square\ (e^-)$$

where $e^-(l)$, $\text{Cl}^-(l)$, and $\text{Ag}^+(l)$ are an electron, a chloride anion, and a silver cation respectively, all in regular lattice sites. $\text{Ag}^+(i)$ represents an interstitial silver cation present as a Frenkel lattice defect and $\square\ (e^-)$ is the symbol for a positive hole. The final steps in the tarnishing mechanism are then the inward diffusion of the positive hole to the silver – silver chloride interface where it is filled by an electron from a silver atom which, after thus becoming a cation, dissolves interstitially in the silver chloride film.

EXPERIMENTAL

Materials

Precipitated silver obtained from Johnson, Matthey, and Mallory Ltd., Montreal, was used without further purification. According to measurements by the B.E.T. method (1) at − 195.8°C., this silver had a surface area of 0.90 m.^{2} per gm. Loeser and Harkins (11) recently obtained a similar surface area (1.05 − 1.22 m.^{2} per gm.) for silver "powder" as the result of surface area determinations by the B.E.T. and H.J. methods (10).

Triphenylmethyl chloride was prepared from triphenylmethylcarbinol (Brickman and Co., Montreal) by Gomberg's method (8).

Mallinckrodt's reagent grade toluene was distilled, in a dry nitrogen stream, from sodium directly into the reaction system.

Technical grade acetonitrile (Brickman and Co., Montreal) was dried over anhydrous sodium sulphate and distilled, in a dry nitrogen stream, from phosphorus pentoxide directly into the reaction system.

Apparatus and General Procedure

The apparatus (Fig. 1) consisted essentially of a round-bottomed flask *F*, a long mercury seal stirrer *U*, a manometer *M*, and an iron nail sealed into a glass tube *T* which, by means of a magnet, could be drawn up into a small side-arm *E*. To a large S.T. joint at the top of the mercury seal stirrer could be fitted an attachment that consisted of a bulb *A* to contain mercury, together with appropriate stopcocks. It was used for the introduction of gases (nitrogen or oxygen) and of mercury into the apparatus.

At the beginning of each experiment weighed quantities of precipitated silver and of pyrogallol were put into the flask *F* and a known quantity of solvent then introduced. A small and very thin glass vial containing a weighed amount of triphenylmethyl chloride was placed into the side-arm

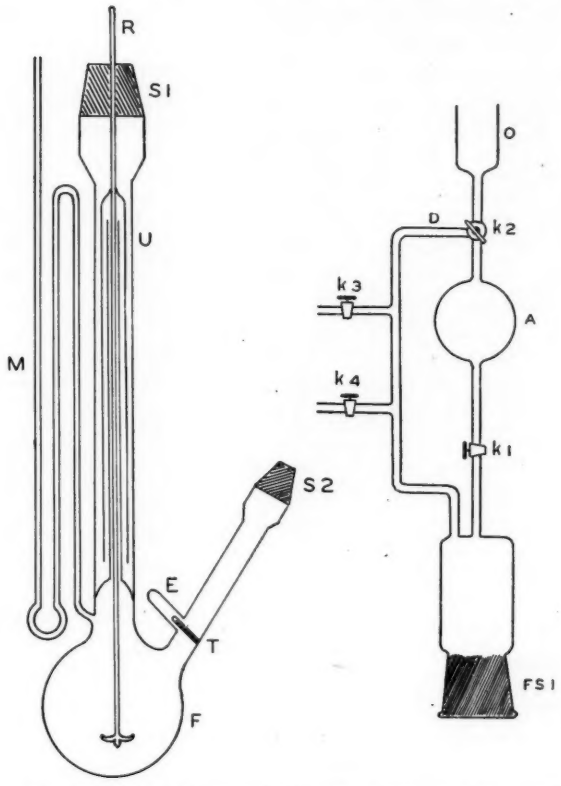

FIG. 1. View of top (right) and bottom (left) parts of apparatus before the side-arm has been sealed off.

and allowed to come to rest on *T* (Fig. 1). The contents of the flask were frozen and the side-arm sealed off just below S.T. joint *S*-2. The nitrogen atmosphere inside the apparatus was then replaced by oxygen which was trapped at a suitable initial pressure by filling *M* and *U* with mercury. An electromagnet was placed around *E* and the entire apparatus immersed in a glass-walled thermostat so that pressure readings could be taken with a cathetometer focused on *M*. After half an hour of preliminary stirring, during which the apparatus attained the temperature of the thermostat, the tube *T* was drawn up into side-arm *E*. When the thin vial fell to the bottom of the apparatus it was broken by the stirrer and the triphenylmethyl chloride went into solution to initiate reaction. In the presence of oxygen and of pyrogallol, the triphenylmethyl free radicals formed by the interaction of silver and of triphenylmethyl chloride immediately formed triphenylmethyl hydroperoxide,

$$(C_6H_5)_3C^{\cdot} + O_2 + H^{\cdot} \text{ (from pyrogallol)} \rightarrow (C_6H_5)_3COOH.$$

According to Ziegler and his coworkers (19), this reaction takes place very

rapidly and in stoichiometric proportions and can therefore be made the basis of an analytical method for the determination of triphenylmethyl and many other triarylmethyl free radicals.

Frequent pressure readings were then taken, and from the fall in oxygen pressure and the dimensions of the system (determined by calibration with due regard for volume changes caused by movement of the mercury in M and U) it was possible to calculate the amount of triphenylmethyl or of silver chloride formed. To make the data directly comparable, all pressure changes were corrected to an arbitrary standard volume, V, of 263.7 ml. and an arbitrary standard temperature, T, of 338°K. All of the Δp values in Figs. 2 to 6 may thus be changed to gram-molecules of triphenylmethyl free radical or of silver chloride formed by making use of the relation $\Delta p = \Delta nRT/V$. The quantity Δn is the number of moles of oxygen consumed, corresponding to the number of moles of triphenylmethyl free radical or of silver chloride formed during the pressure change Δp. The weights of silver chloride formed may then be converted to film thicknesses by reference to the initial weight and surface area (0.90 m.^{2} per gm.) of the silver used and the specific gravity (5.56 gm. per cc.) of silver chloride.

EXPERIMENTAL RESULTS AND DISCUSSION

The practicability of using metal powder rather than metal cylinders or plates during a kinetic study of this type of reaction is evident from the good reproducibility (within 5%) observed throughout this work. While the usual stirring speed was about 460 r.p.m., controlled experiments at 300, 460, and 600 r.p.m. were also made and they showed that variations in the rate of stirring within these limits had no effect on the reaction rate. No "blank" due to oxygen absorption by silver powder suspended in the solvent, or by dissolved pyrogallol or triphenylmethyl chloride was observed.

The reaction plots contained in this paper are characterized by the applicability of logarithmic, parabolic, and linear rate laws, by the occurrence of characteristic changes from one law to another, and by a very sudden decrease in rate below a certain reaction temperature. These phenomena form such a unique and distinctive pattern, known to occur only in tarnishing reactions, that it seems well justified to postulate a rate-controlling tarnishing mechanism. Because the growing film is one of silver chloride on silver, with triphenylmethyl chloride clearly in the role of the electronegative tarnishing agent, Wagner's mechanism for the basic step of the growth process can here be written in the following manner:

$$(C_6H_5)_3CCl\,(\text{dissolved}) + e^-(l) + Ag^+(i) \rightarrow Cl^-(l) + Ag^+(l) + \square(e^-) + (C_6H_5)_3C^{\cdot}.$$

Among the various theories on tarnishing processes, that of Cabrera and Mott (3) is the only one that provides an explanation for the striking effect (Fig. 2) observed with a temperature change of as little as 20°C. Initially the reaction was very fast and in accordance with a logarithmic growth law, both at 65.4°C. and at 44.9°C. At the former temperature, the logarithmic growth law was valid (Fig. 3) up to a well-defined and reproducible film

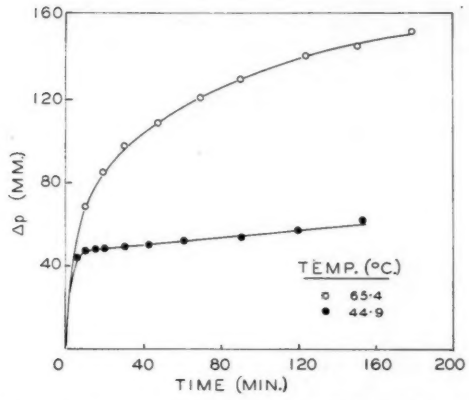

FIG. 2. The effect of temperature (with 1 gm. Ph_3CCl, 2 gm. silver; in toluene).

thickness of 1.6×10^{-6} cm. Such a "critical film thickness" X_1 should occur, according to the Cabrera–Mott theory (3) for gas phase oxidations, and be usually observable at $10^{-6} - 10^{-5}$ cm. The value of X_1 is given by qaV/kT, where q is the charge on the cation of the metal salt film, a is the distance from the metal – metal salt interface to the top of the first potential barrier in the path of a diffusing interstitial cation, V is the contact potential difference

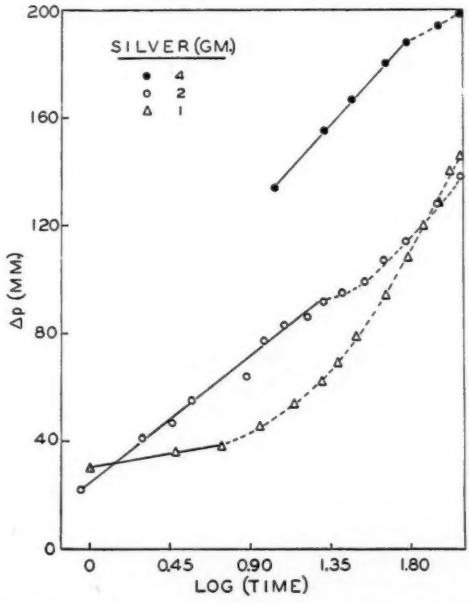

FIG. 3. Applicability of a logarithmic growth law with three different amounts of silver (at 65.4°C.; in toluene).

between metal and tarnishing agent, k is Boltzmann's constant, and T is the absolute temperature. X_1 also delimits "very thin" films from "thin" ones. "Very thin" oxide films, according to Cabrera and Mott (3), obey the following growth law which involves (13) a logarithmic dependence of film thickness on time:

$$\frac{dX}{dt} = N\Omega\nu \exp(-W/kT) \exp\left(\frac{qaF}{kT}\right)$$

where, in addition to the symbols already defined above, N is the number of metal ions per unit metal surface area at the metal–metal salt interface, Ω is the volume of metal salt formed per metal salt cation, ν is the frequency of atomic vibration, and W, for excess semiconductors, is the sum of the heat of solution of a metal cation in the metal salt plus the activation energy for its interstitial diffusion in the metal salt. With deficit semiconductors, where a physical model for the growth of "very thin" films has not yet been worked out, W is probably related to the energy required to create a vacant positive hole and a vacant cation site plus an activation energy term for the diffusion of these lattice defects. The quantity F represents the strength of an electric field which is postulated to exist in a growing "very thin" or "thin" oxide film because of a layer of adsorbed O^- ions at the oxide–oxygen interface. The formation of these ions, according to Cabrera and Mott, is due to adsorbed oxygen atoms at this interface which possess energy levels below the surface of the Fermi distribution in the metal. As long as the film thickness is small, electrons, passing from metal to oxygen, will penetrate the oxide film by a process of quantum mechanical tunneling or of thermionic emission. An electrostatic potential V will be set up at the oxide–oxygen interface because of the attainment of an electronic quasi equilibrium such that, in a time short compared with that in which the metal ions diffuse, as many electrons pass from metal to oxygen as in the opposite direction. The strength of the electric field F is then equal to V/X, where X is the film thickness.

At 44.9°C., a logarithmic growth law would be expected to be valid beyond a film thickness of 1.6×10^{-6} cm. because of the inverse relation between the critical film thickness and reaction temperature. At this temperature of 44.9°C., however, there occurred, long before this film thickness was reached, a very sudden decrease in rate of reaction at a well-defined and quite reproducible film thickness of 80 Å (Fig. 4). Provided the temperature is low enough, the Cabrera–Mott theory predicts the occurrence of such a sudden decrease in rate at a film thickness of 20 – 100 Å corresponding to the attainment of a limiting film thickness $X_L = Vaq/(W - 39kT)$. In accordance with this definition, X_L increases with reaction temperature and the highest temperature at which, for a given tarnishing reaction, the phenomenon of the limiting film thickness still occurs is the critical temperature $T_c = W/39k$. From Fig. 2 it would appear that a temperature of 65.4°C. lies well above this critical temperature T_c, while 44.9°C. lies slightly above T_c so that a very sudden decrease in rate of reaction still occurs. The film thickness of 80 Å at which the sudden decrease in rate occurs (Fig. 4) therefore appears to be

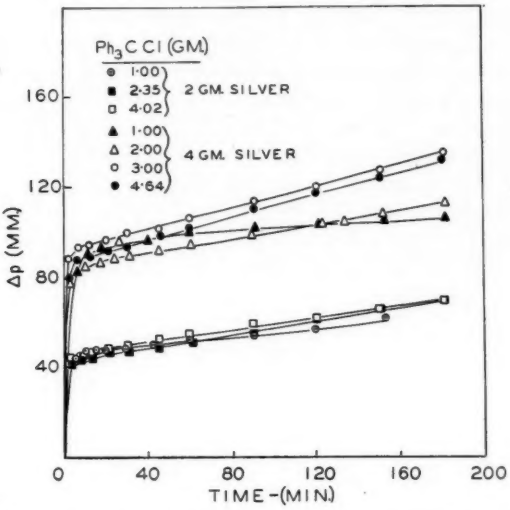

FIG. 4. The effect of initial Ph_3CCl concentration (with two different amounts of silver; in toluene at 44.9°C.).

slightly greater than the value corresponding to the limiting film thickness X_L at a temperature just below the critical temperature T_c.

At 44.9°C., the reaction continues at a constant rate (Fig. 4). For a given amount of silver, this rate is directly proportional to the triphenylmethyl chloride concentration existing at the beginning of the linear rate, for low values, but becomes independent of the concentration at high values. Here the rate is directly proportional to the amount of silver present.

A linear rate observed (9) for the oxidation of aluminum has been explained by Cabrera and Mott (3) as due to the fact that in the transition region between "thin" and "thick" films, a transition from a parabolic rate with a smaller rate constant to a different parabolic rate with a larger constant may occur. The film thickness considered in this interpretation ($\sim 10^{-4}$ cm.) is, however, quite different from that at which the observed linear rate in the silver – triphenylmethyl chloride reaction takes place (i.e., beginning at 80 Å). For very small concentrations of oxygen, Cabrera (2) predicted the nonattainment of the Mott electronic quasi equilibrium because of an insufficient amount of adsorbed tarnishing agent at the metal salt – tarnishing agent interface. The rate controlling factor would then be the adsorption of tarnishing agent at this interface and the observed rate would be expected to be linear and first order with respect to concentration of tarnishing agent. If such a mechanism were valid for the present reaction the rate presumably would become nonlinear at concentrations of tarnishing agent sufficient to set up the Mott electronic quasi equilibrium. Actually the rate remained linear and did not increase beyond a maximum value even with large excess of triphenyl-

methyl chloride. Older theories (5) on tarnishing processes predict the occurrence of a linear rate by the mere generalization that such a rate would be due to processes at the film interfaces rather than inside the film itself. The sudden appearance of rifts through which tarnishing agent could pass without hindrance is, according to Evans (6), another reason for the validity of a linear law but it is doubtful that this occurs here because of the complete reproducibility with which the linear rate begins at 44.9°C. once a film thickness of 80 Å has been reached. The occurrence of a linear rate under these reaction conditions appears, therefore, to be a newly observed experimental fact for which existing theoretical treatments make no provision.

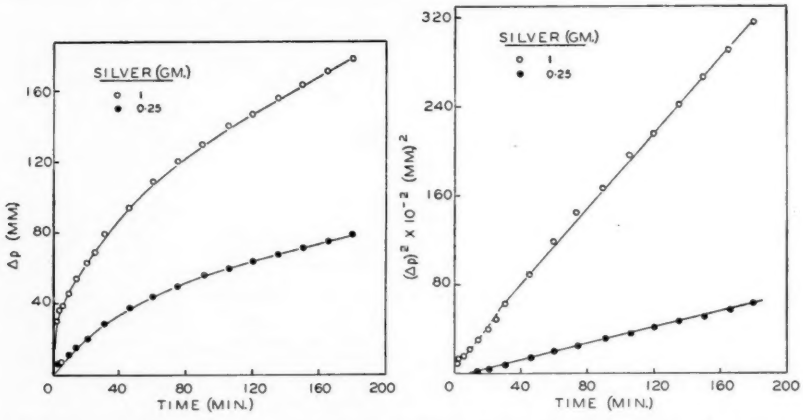

FIG. 5. The effect of excess Ph_3CCl at 65.4°C. (with 4.60 gm. Ph_3CCl; in toluene). Plot on right shows applicability of a parabolic growth law.

If, at a reaction temperature of 65.4°C., the ratio of triphenylmethyl chloride to silver in the reaction mixture lies above a certain minimum value, then a parabolic growth law is valid (Fig. 5). As the maximum film thickness attained in the two reaction curves shown was 1.13×10^{-5} cm., the depicted growth is that of "thin" films in the sense of the Cabrera–Mott theory (3) according to which only films which become thicker than about 10^{-4} cm. within a few hours are designated "thick" films. Because silver chloride is a deficit semiconductor, the observed parabolic growth is in contrast to the conclusion by the Cabrera–Mott theory (3) that a "thin" film which is a deficit semiconductor should grow according to a cubic growth law of the type

$$X^3 = 3At$$

where X is the film thickness at time t, and the constant A is proportional to $\exp\{-(W_i + U)/kT\}$, where W_i is the energy required to form a vacant cation site and U is the activation energy for its diffusion in the metal salt.

It is evident from Fig. 6 that the over-all rate in acetonitrile is considerably faster than in toluene and that the sudden slowing down of the reaction, a

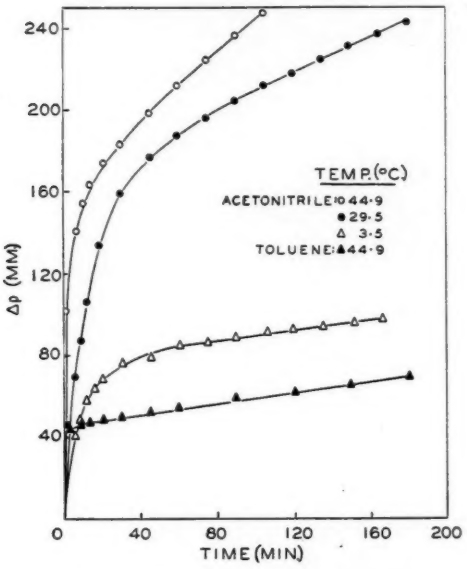

FIG. 6. The effect of solvent and of temperature.

phenomenon apparently resulting from the attainment of Cabrera and Mott's limiting film thickness X_L, occurs at a temperature about 40°C. below the corresponding temperature in toluene. Because of this difference in the value of the critical temperature $W/39k$, it would appear that a molecule of the tarnishing agent, triphenylmethyl chloride, polarized or ionized by dissolution in a dissociating solvent such as acetonitrile, requires less energy for the abstraction of an electron out of a silver chloride lattice than a triphenylmethyl chloride molecule dissolved in a nondissociating or nonpolarizing solvent such as toluene.

The over-all conclusion from the work described in this paper appears to be that, although the silver – triphenylmethyl chloride reaction occurs in a liquid phase and with a chemical compound instead of an element in the role of tarnishing agent, its general characteristics are quite similar to those observed for gas phase oxidations. Some extension of accepted theoretical treatments would appear to be necessary, however, to account for such observations as a parabolic rather than a cubic growth law for a "thin" deficit semiconductor, and a linear law with definite characteristics at a temperature just above Cabrera and Mott's critical temperature.

ACKNOWLEDGMENT

The authors wish to express their appreciation to Dr. Arnell and Dr. McDermott of the Defence Research Board of Canada for measurement of the surface area of the silver used in this work.

REFERENCES

1. BRUNAUER, S., EMMETT, P. H., and TELLER, E. J. Am. Chem. Soc. 60: 309. 1938.
2. CABRERA, N. Phil. Mag. 40: 175. 1949.
3. CABRERA, N. and MOTT, N. F. Repts. Progress Phys. Phys. Soc. (London), 12: 163. 1949.
4. CAMPBELL, W. E. and THOMAS, U. B. Trans. Electrochem. Soc. 91: 345. 1947.
5. EVANS, U. R. Trans. Electrochem. Soc. 46: 247. 1924.
6. EVANS, U. R. Trans. Electrochem. Soc. 91: 547. 1947.
7. GOMBERG, M. J. Am. Chem. Soc. 22: 757. 1900.
8. GOMBERG, M. Ber. 36: 384. 1903.
9. GULBRANSEN, E. A. and WYSONG, W. S. J. Phys. & Colloid Chem. 51: 1087. 1947.
10. HARKINS, W. D. and JURA, G. J. Am. Chem. Soc. 66: 1362. 1944.
11. LOESER, E. H. and HARKINS, W. D. J. Am. Chem. Soc. 72: 3427. 1950.
12. MOTT, N. F. and GURNEY, R. W. Electronic processes in ionic crystals. Clarendon Press, Oxford. 1948. p. 259.
13. RHODIN, T. N. J. Am. Chem. Soc. 72: 5102. 1950.
14. SCHMIDLIN, J. and GARCIA-BANUS, A. Ber. 45: 1344. 1912.
15. TAMMANN, G. and KOSTER, W. Z. anorg. u. allgem. Chem. 123: 196. 1922.
16. THOMAS, J. C., BOWDEN, S. T., and JONES, W. J. J. Chem. Soc. 473. 1930.
17. WAGNER, C. Z. physik. Chem., B, 21: 25. 1933.
18. WAGNER, C. Z. physik. Chem., B, 32: 447. 1936.
19. ZIEGLER, K., SEIB, A., KNOEVENAGEL, K., HERTE, P., and ANDREAS, F. Ann. 551: 150. 1942.

DICUMAROL-2-C^{14}: SYNTHESIS AND METABOLISM STUDIES[1]

By H. R. Eisenhauer,[2] J. M. Pepper, L. B. Jaques, and J. W. T. Spinks

ABSTRACT

Dicumarol (3,3′-methylene *bis*(4-hydroxycoumarin)) has been synthesized labeled with C^{14} in the 2-position. Starting with active barium carbonate of specific activity 1.6 μc. per mgm., the intermediate compounds diethyl carbonate-1-C^{14} and 4-hydroxycoumarin-2-C^{14} were prepared. Subsequent reaction of the latter compound with aqueous formaldehyde yielded dicumarol-2-C^{14}. The specific activity of the final product, once recrystallized from cyclohexanone, was 4.3×10^5 counts per min. per mgm. corrected for geometry and absorption. The expired carbon dioxide from a mouse injected with this C^{14}-labeled product was collected and found to contain no radioactivity. This indicated that, in this animal, the 2-carbon of dicumarol does not enter into a metabolic process whereby it is expired as carbon dioxide.

Recent investigations (4, 6) into the mechanism whereby dicumarol lowers the prothrombin level in the blood have emphasized the valuable results to be obtained in using dicumarol labeled with C^{14}. In these experiments inactive 4-hydroxycoumarin was condensed with formaldehyde-C^{14} (5), thereby placing the labeled carbon atom in the methylene bridge position. On administration to animals, the labeled dicumarol was shown to reach the liver in an unchanged form but the radioactive material which was excreted either in the urine or in the feces was no longer dicumarol. A program of research was therefore begun to examine the chemical nature of these metabolic products.

One approach to this problem would be to synthesize dicumarol labeled in various other positions in the molecule and, by a comparison of the active* metabolic products isolated from the excretions of animals fed with these differently labeled samples, to obtain some insight into their chemical constitution. It appeared quite feasible to effect such labeling in any of the 2-, 3-, or 4-carbon atoms of the 4-hydroxycoumarin molecule and subsequent reaction with inactive formaldehyde would yield the required dicumarol.

Using the reactions outlined by Anschutz (1), 4-hydroxycoumarin could be labeled with C^{14} in the *3-position* if methylene-labeled malonic ester were used or in the *2- or 4-positions*** if carboxyl-labeled malonic acid were used. Labeling in the *2-position* would be achieved using the method reported by Link (9) starting from carboxyl-labeled acetic anhydride. The application of a recently reported synthesis of 4-hydroxycoumarin (3) from *o*-hydroxyacetophenone and carbonyl-labeled diethyl carbonate would yield a product labeled in the *2-position*.

The initial choice for an attempted synthesis was the last method mentioned above, partly because it appeared to offer the simplest method of preparing

[1] *Manuscript received December 3, 1951.*

Contribution from the Departments of Chemistry and Physiology, University of Saskatchewan, Saskatoon, Sask. This paper constitutes part of a thesis submitted by H. R. Eisenhauer in partial fulfillment of the requirements for the degree of Master of Arts in Chemistry and was presented at the Seventh Annual Conference of the Chemical Institute of Canada, Winnipeg, June 1951.

[2] *Present address: Department of Biochemistry, College of Agriculture, University of Wisconsin, Madison, Wis.*

**"Active" is used here in the sense of "radioactive".*

***In any one molecule either the 2- or 4-positions would be labeled but not both.*

a product of high specific activity and partly because of the reasons outlined below.

Pulver and von Kaulla (8) in studying the physiological action of the compound "Tromexan" (I) isolated a metabolite (II) which they assumed was formed by hydrolysis in the animal body.

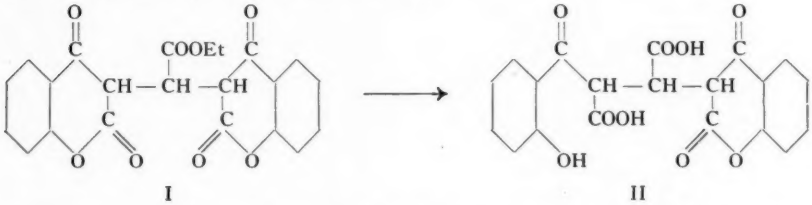

I II

Furthermore Link has shown (9) that the treatment of dicumarol (III) with 10% potassium hydroxide at 100°C. gives rise to the degradation product disalicylpropane (IV) which involves the loss of two carbon atoms per mole-

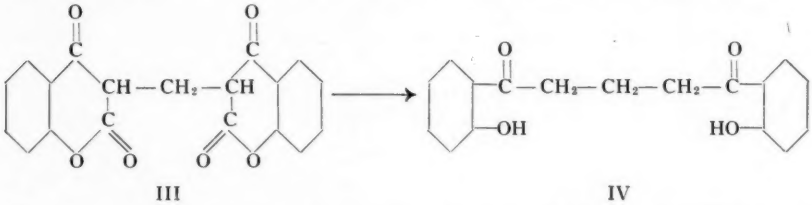

III IV

cule. It was thought, therefore, that if dicumarol labeled with C^{14} in the 2-position (V) were used in an animal experiment, then, if the metabolism of dicumarol involved a similar reaction, some carbon atoms which contained the activity would be removed. If this carbon were expired as $C^{14}O_2$ it should be possible to detect this activity and thereby provide some insight into the metabolism of this chemical.

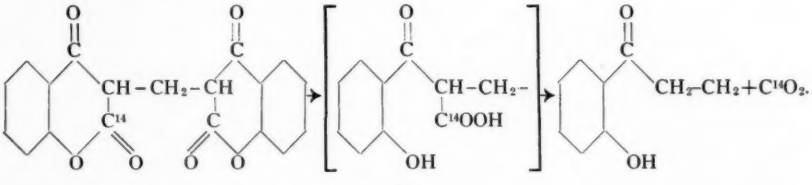

V

The purpose of the present investigation was to synthesize the dicumarol with C^{14} in the 2-position. The series of reactions finally used to effect this synthesis, starting from C^{14}-labeled barium carbonate, is shown as follows:

$$BaC^{14}O_3 \xrightarrow[\text{acid}]{\text{perchloric}} C^{14}O_2 \xrightarrow{NaOH} Na_2C^{14}O_3 \xrightarrow{AgNO_3} Ag_2C^{14}O_3$$

$$Ag_2C^{14}O_3 + 2CH_3CH_2I \xrightarrow{(C_2H_5)_3N} (CH_3CH_2)_2C^{14}O_3 + 2AgI.$$

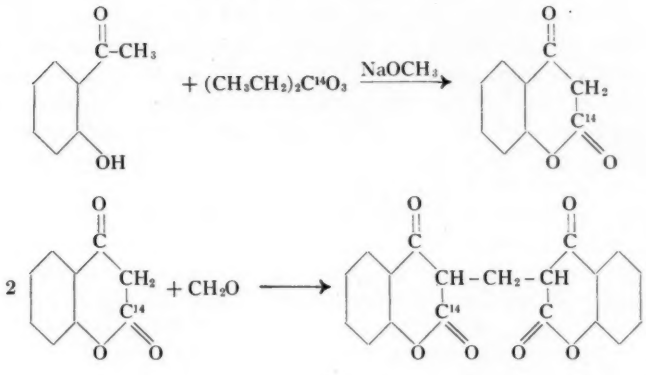

V

The synthesis was at first carried out on a macro scale to determine the approximate conditions and yields which could be expected for each individual step. Subsequently, based on this information, each step was worked out on a semimicro (approximately millimolar) scale and these individual reactions then combined to effect a complete synthesis of dicumarol starting from 100 mgm. of barium carbonate. Finally the semimicro-scale synthesis was repeated using C^{14}-labeled barium carbonate.

To determine whether the 2-carbon atom of dicumarol was expired in the manner suggested above, a mouse was injected with a small amount of this labeled product. The collection of the expired carbon dioxide for 18 hr. followed by its precipitation as barium carbonate and by counting, showed that no activity was lost in this manner.

EXPERIMENTAL

For the macro-scale experiments carbon dioxide was released quantitatively from barium carbonate by the addition of perchloric acid and was absorbed in a stoichiometric amount of sodium hydroxide solution. The sodium carbonate solution thus formed was added to a solution of silver nitrate to give a quantitative yield of silver carbonate. The conversion of silver carbonate to diethyl carbonate presented the first difficulty. In 1854, de Clermont had reported that this synthesis occurred by heating equivalent amounts of ethyl iodide and silver carbonate in a sealed tube, but attempts to repeat this gave very low (9%) yields of diethyl carbonate. However, it was found that yields up to 30% were obtained if catalytic amounts of triethylamine or pyridine were used under refluxing conditions. It was thought that the mechanism may involve the formation of the quaternary ammonium salt which thereby labilizes the carbon to iodine bond. For the larger quantities required in the many inactive trial experiments, diethyl carbonate was prepared by the interaction of phosgene and absolute ethanol (7).

Following closely a procedure outlined in a United States patent by Dickenson in 1947 (3), diethyl carbonate and *o*-hydroxy acetophenone were

reacted to give 4-hydroxycoumarin in 68% yield with respect to the *o*-hydroxyacetophenone. In this process the ethanol formed is continuously removed as an ethanol-benzene azeotrope at its boiling point, thereby displacing the equilibrium of the reaction in the required direction. As a result of numerous runs it was found that the best yields of 4-hydroxycoumarin were obtained if the catalyst, sodium ethylate, were present in twice the equivalent amount in relation to the *o*-hydroxyacetophenone; it was also found that under none of the conditions tried was any of the desired product formed if *o*-hydroxyacetophenone were present in an amount representing an excess over that theoretically required. This was, of course, unfortunate since in the series of radioactive syntheses the diethyl carbonate would be the labeled reagent. The preferred ratio of reactants was as follows: *o*-hydroxyacetophenone: sodium ethylate: diethyl carbonate as 0.62 : 1.25 : 1.

On reducing the scale of the synthesis to that using one millimole of diethyl carbonate, difficulties in obtaining useful yields were encountered. However, the modified procedures herein reported were found to be satisfactory. The dilution of the diethyl carbonate-1-C^{14} with inactive diethyl carbonate was made in order to ensure that this reagent was present in an amount representing an excess over that theoretically required. It had been shown previously that unless this condition was fulfilled no yield of 4-hydroxycoumarin was obtained.

Throughout the active synthesis, absorption towers containing 5% sodium hydroxide were attached to the outlets of all reaction vessels containing active material in order to trap any escaping carbon dioxide.

Diethyl Carbonate-1-C^{14}

Barium carbonate-C^{14} (104 mgm.) (specific activity 1.6 μc. per mgm.*) was placed in one bulb of a small glass apparatus attached to a second bulb containing an easily removable small test tube holding 0.5127 *N* sodium hydroxide (2 ml.). Water (2 ml.) was added to cover the barium carbonate, both aqueous components frozen, and the system evacuated and closed. By means of a dropping funnel, 30% perchloric acid (5 ml.) was added onto the carbonate and the closed system allowed to warm to room temperature and to stand for 24 hr. The contents of the small tube were then added with stirring to a solution of silver nitrate (185 mgm.) in water (20 ml.). The resulting precipitate was filtered (2), washed with water, acetone, ether, and finally dried for two hours, *in vacuo*, at 20°C. (1 mm.). This silver carbonate -C^{14} was powdered, placed in a small (4 ml.) flask, and ethyl iodide (3.0 ml.) and triethyl amine (0.1 ml.) were added. The reaction mixture was refluxed at 100°C. for two hours, during which time dry nitrogen gas was bubbled through and into a sodium hydroxide trap.

After cooling, inactive diethyl carbonate (0.10 ml.) was added, the mixture filtered through a small sintered glass filter, and the residue washed with five 1 ml. portions of dry benzene. The combined filtrate and washings were

**Barium carbonate (5 mgm.) with an activity of 0.5 mc. per 15 mgm., obtained from the Atomic Energy Project at Chalk River, Ont., was diluted with 99 mgm. of inactive carbonate.*

slowly fractionated through a small Vigreaux column attached to a small flask fitted with a dropping funnel and thermometer. Distillation was continued until the vapor temperature reached that of boiling benzene and then for an additional 10 min., the volume of liquid being maintained at 2 ml. by the addition of dry benzene.

4-Hydroxycoumarin-2-C^{14}

To the resulting benzene solution of diethyl carbonate-1-C^{14} were added a solution of sodium (23 mgm.) in absolute ethanol (0.5 ml.) and 0.060 ml. of *o*-hydroxyacetophenone. The benzene–ethanol azeotrope was slowly distilled, while dry benzene was added continuously at such a rate that the level of liquid remained constant. Heating was continued for an additional 2.5 hr. after the temperature of the distillate reached the boiling point of benzene at which time water (7 ml.) was added to dissolve the resulting 4-hydroxycoumarin-2-C^{14}. The aqueous and benzene layers were readily separated.

Dicumarol-2-C^{14}

The above water solution was placed in a test tube (15 ml.), fitted with a reflux condenser, and the solution acidified with 6 *N* hydrochloric acid (1.0 ml.) under an atmosphere of carbon dioxide-free nitrogen. The resulting suspension of 4-hydroxycoumarin-2-C^{14} was heated at 100°C. until it clarified, at which point a 38% solution of formaldehyde (2 ml.) was added. The resulting dicumarol-2-C^{14} was allowed to coagulate overnight, filtered (2), and air-dried. The product was crystallized from cyclohexanone; m.p. 287° to 288°C., yield 12.2 mgm.; mixed melting point with an authentic sample of dicumarol showed no depression. Radioactive measurements using an end-window type of Geiger–Müller counter with a scale of 128 indicated a specific activity of 4.3×10^5 counts per min. per mgm., corrected for geometry and absorption.

Animal Experiments

Dicumarol-2-C^{14} (0.25 mgm.) was injected intravenously into a mouse (15.2 gm.) which was immediately placed in a metabolism cage (6). For the next 18 hr. the expired carbon dioxide was collected in sodium hydroxide. The resulting solution was diluted to 300 ml., the carbonate precipitated as barium carbonate from a 20 ml. aliquot, dried on two platinum dishes, weighed, and counted. No count was observed using either the Geiger–Müller end-window counting tube or a gas-flow type counter.

With the counting equipment and techniques used a 5% conversion could have been detected and a 15% conversion fairly accurately measured.

This indicated that, in the body, there is no significant liberation of carbon in the 2-position from dicumarol. Parallel experiments with dicumarol labeled in the methylene bridge (6) also showed no appreciable fraction of the activity in the expired carbon dioxide. This suggested that the 2-carbon and the methylene bridge carbon remain attached to the 3-carbon, and in view of the known rapid metabolism of 2- to 5-carbon carboxylic acids, it may be inferred that these carbons remained attached to the benzenoid nucleus. Chromatographic analysis of the urine (10), after administration of methylene labeled dicumarol, has indicated the production of at least four metabolic products

of low water solubility. This also is in agreement with the view that the radioactivity remains attached to the benzenoid nucleus.

The mouse was sacrificed and counts taken on many of the isolated tissues and excreta. The results obtained, with the activity expressed as a percentage of the injected dose, were as follows: liver, 6.04; gall bladder, 0.6; intestine, 2.8; intestinal content, 40.5; urine, 9.8; and feces, 4.85. No activity was detected in the spleen, kidney, lung, muscle, sternum, or blood. It is perhaps of some interest that the per cent activities reported here are about the same as those reported for similar experiments using dicumarol labeled in the methylene bridge position (6).

ACKNOWLEDGMENTS

We should like to thank Dr. L. W. Trevoy of the Department of Chemistry for his kind interest in this work. We are indebted to Mrs. R. L. Eager of the Department of Chemistry and Miss E. Lepp of the Department of Physiology for assistance in the radioactive measurements and in the animal experiments. Grateful acknowledgment is given to the National Research Council of Canada for financial assistance including a Bursary and two Summer Scholarships to one of us (H.R.E.).

REFERENCES

1. ANSCHUTZ, R. Ann. 367: 174, 194, 196. 1909.
2. CALVIN, M., HEIDELBERGER, C., REID, J. C., TOLBERT, B. M., and YANKWICH, P.E. Isotopic carbon. John Wiley and Sons, Inc., New York. 1949. p. 116.
3. DICKENSON, H. G. U.S. Patent 2,449,162. September 14, 1948.
4. JAQUES, L. B. and SPINKS, J. W. T. Blood clotting and allied problems. Trans. Third Conference, Josiah Macy, Jr. Foundation, New York. 1950. p. 68.
5. LEE, C. C., TREVOY, L. W., JAQUES, L. B., and SPINKS, J. W. T. Can. J. Research, B, 28: 170. 1950.
6. LEE, C. C., TREVOY, L. W., SPINKS, J. W. T., and JAQUES, L. B. Proc. Soc. Exptl. Biol. Med. 74: 151. 1950.
7. LUX, H. Ber. 62: 1824. 1929.
8. PULVER, R. and VON KAULLA, K. N. Schweiz. med. Wochschr. 78: 956. 1948.
9. STAHMANN, M. A., HUEBNER, C. F., and LINK, K. P. J. Biol. Chem. 138: 513, 529. 1941.
10. WALDMAN, M. H. Master's Thesis, University of Saskatchewan, Saskatoon, Sask. 1951.

SOME METHYL ETHERS AND ACETATES OF PURPUROGALLIN[1]

By G. Denis Thorn[2] and L. R. C. Barclay

ABSTRACT

The preparation and ultraviolet absorption spectra of a number of methyl ethers and acetates of purpurogallin are given. The following derivatives of purpurogallin are, to our knowledge, not mentioned in the literature: a monoacetate, m.p. 182-183°C.; a diacetate I, m.p. 159-160°C.; a diacetate II, m.p. 208-209°C.; a triacetate, m.p. 161.5-162.5°C.; a monomethyl ether diacetate, m.p. 156-157°C.; a dimethyl ether diacetate, m.p. 194-196°C. Comparison of the ultraviolet absorption spectra with those determined for derivatives of known structure suggested the positions of the acetyl groups in the new substances now prepared.

A research, as yet unpublished, on the oxidation of pyrogallol with alkaline hypoiodite, made it probable that at pH 12 the initial product was 3-hydroxy-1, 2-benzoquinone (11). Attempts at isolation of the quinone by addition to the reaction solution of dimethyl sulphate or acetic anhydride yielded a methyl ether of purpurogallin on one hand and a mixture of acetates of purpurogallin on the other. In order to characterize these compounds, the various methyl ethers and acetates of purpurogallin were prepared. This work is reported herein.

The methyl ether in question, m.p. 194.5-195°C., proved to be (I, $R_1 = R_2 = H$, $R_3 = Me$), identical with that prepared by Willstätter and Heiss (12) and by Critchlow, Haworth, and Pauson (5). The structure assigned is based on the evidence of the latter workers.

A dimethyl ether, m.p. 156°C., and a trimethyl ether, m.p. 179.5-180°C., were obtained by treating a solution of purpurogallin with, respectively, two equivalents (7) and an excess of diazomethane (8).

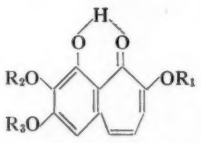

I

The dimethyl ether has been proved recently by synthesis to possess the structure (I, $R_1 = H$, $R_2 = R_3 = Me$) (2, 3, 4). The trimethyl ether has the structure (I, $R_1 = R_2 = R_3 = Me$) (7). Purpurogallin tetramethyl ether, m.p. 91-92°C., was prepared as described by Willstätter and Heiss (12).

A monoacetate, m.p. 182-183°C., two diacetates, m.p. 159-160°C. and m.p. 208-209°C., and a triacetate, m.p. 161.5-162.5°C., were prepared by treating solutions of purpurogallin in pyridine with the appropriate amounts

[1] *Manuscript received December 18, 1951.*
Contribution from the Department of Chemistry, Mount Allison University, Sackville, N.B.

[2] *Present address: Science Service Laboratory, Department of Agriculture, London, Ont.*

of acetic anhydride. Purpurogallin tetracetate was prepared according to Perkin and Steven (10). The positions of the acetyl groups on the purpurogallin moiety can be shown with a fair degree of certainty by a simple analysis of the ultraviolet absorption spectra of these derivatives and of the methyl ethers and their acetates.

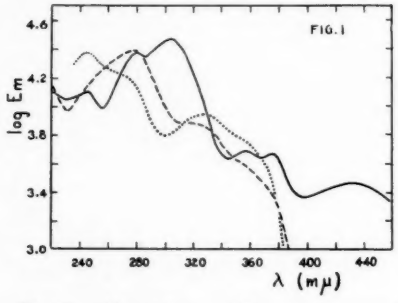

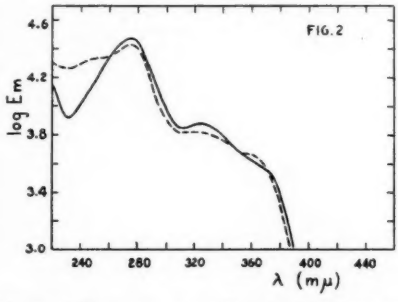

FIG. 1. Absorption spectra. ——— Purpurogallin. - - - - Purpurogallin tetramethyl ether. ..... Purpurogallin tetracetate.
FIG. 2. Absorption spectra. ——— Purpurogallin trimethyl ether monoacetate. - - - - Purpurogallin dimethyl ether diacetate.

The absorption spectra of purpurogallin tetramethyl ether (Fig. 1), purpurogallin tetracetate (Fig. 1), purpurogallin trimethyl ether monoacetate (Fig. 2), and purpurogallin dimethyl ether diacetate (Fig. 2) are similar. They differ from the spectrum of purpurogallin especially in lacking the absorption maxima at 430 and 304 mμ, and in having absorption peaks in the neighborhood of 325 and 275 mμ. These differences are attributable to the etherification and/or acetylation of all four hydroxyl groups of purpurogallin, preventing the formation of the chelate ring (I).

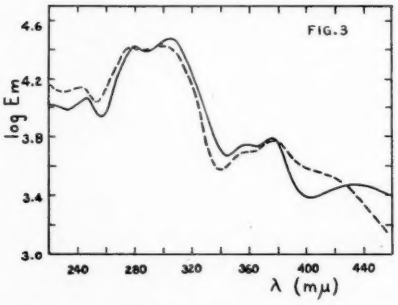

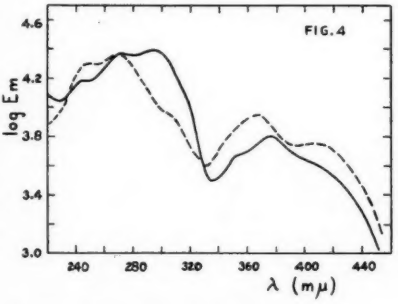

FIG. 3. Absorption spectra. ——— Purpurogallin monomethyl ether. - - - - Purpurogallin dimethyl ether.
FIG. 4. Absorption spectra. ——— Purpurogallin monoacetate. - - - - Purpurogallin diacetate I (m.p. 159-160°C.).

For purpurogallin monomethyl ether (I, $R_1 = R_2 = H$, $R_3 = Me$) and purpurogallin dimethyl ether (I, $R_1 = H$, $R_2 = R_3 = Me$), the spectra (Fig. 3) are almost superimposable on the spectrum of purpurogallin itself (Fig. 1).

Differences (lack of an absorption maximum at 430 mμ, shifting of the two peaks at 357 and 377 mμ to shorter wave length to form a broad band with slightly greater extinction, and structural changes below 320 mμ) appear in the spectra of the derivatives in which the hydroxyl group of the tropolone ring is not free (i.e., I, R_1 = Me or Ac), as in purpurogallin trimethyl ether (Fig. 5) (and purpurogallin triacetate (Fig. 5), purpurogallin monomethyl ether diacetate (Fig. 6); see Postulates 4 and 5, below).

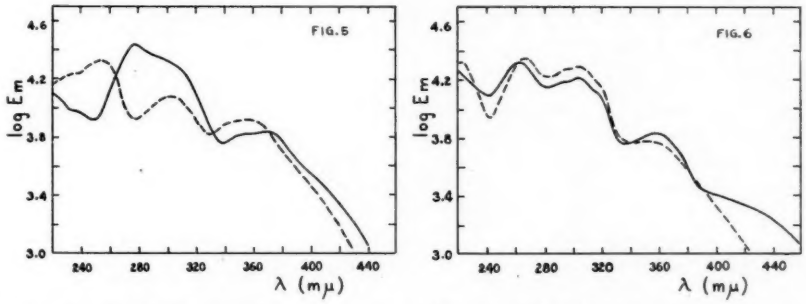

FIG. 5. Absorption spectra. ———— Purpurogallin trimethyl ether. - - - - Purpurogallin triacetate.
FIG. 6. Absorption spectra. ———— Purpurogallin diacetate II (m.p. 208-209°C.). - - - - Purpurogallin monomethyl ether diacetate.

From these observations, it may be postulated that:

(1) Purpurogallin monoacetate, m.p. 182-183°C., (Fig. 4) has the structure I, R_1 = H, and either R_2 = Ac, R_3 = H or R_2 = H, R_3 = Ac.

(2) Purpurogallin diacetate I, m.p. 159-160°C., (Fig. 4) is I, R_1 = H, R_2 = R_3 = Ac.

(3) Purpurogallin diacetate II, m.p. 208-209°C. (Fig. 6) has the structure R_1 = Ac and either R_2 = Ac, R_3 = H or R_2 = H, R_3 = Ac.

It may be suggested further, that, because the spectra of the diacetate II and the monomethyl ether diacetate (Fig. 6) are so similar and because diacetate II can be made from the monoacetate of purpurogallin, (*a*) diacetate II has the structure I, R_1 = R_2 = Ac, R_3 = H, and (*b*) purpurogallin monoacetate has the structure I, R_1 = R_3 = H, R_2 = Ac.

(4) Purpurogallin triacetate is I, R_1 = R_2 = R_3 = Ac.

(5) Purpurogallin monomethyl ether diacetate has the structure I, R_1 = R_2 = Ac, R_3 = Me.

Nierenstein and Spiers (9) mention a monoacetate of purpurogallin, m.p. 169-170°C. In our hands, no trace of a monoacetate of this melting point was obtainable by acetylation of purpurogallin, and treatment of the tetracetate with acetic acid according to Nierenstein and Spiers yielded only mixtures of purpurogallin monoacetate, m.p. 182-183°C., and purpurogallin diacetate I, m.p. 159-160°C. Deacetylation of the acetates of purpurogallin was observed to occur also in ethanol solution.

EXPERIMENTAL*

Purpurogallin

Purpurogallin was obtained by oxidation of pyrogallol with potassium iodate (6) and purified by crystallization from a solution of phenol in acetic acid (7), glistening copper-colored needles, m.p. 276°C. Calc. for $C_{11}H_8O_5$: C, 60.0; H, 3.6%. Found: C, 60.0, 59.9; H, 3.7, 3.8%.

Purpurogallin Monomethyl Ether

This derivative was prepared by Thorn and Purves (11), m.p. 194.5-195°C. (corr.). It has been prepared by Willstätter and Heiss (12), m.p. 182-183°C., and by Critchlow, Haworth, and Pauson (5), m.p. 193°C.

Purpurogallin Dimethyl Ether (7)

To 1 gm. of purpurogallin in ether–dioxane solution at 0°C. was added a cold ether solution of two equivalents of diazomethane prepared from nitrosomethylurea. Evaporation of the solution to dryness and crystallization of the residue from ethanol gave shiny orange needles, m.p. 156°C. Calc. for $C_{13}H_{12}O_5$: CH_3O, 25.0%. Found: CH_3O, 24.9, 24.6%.

Purpurogallin Trimethyl Ether

This was prepared according to the method of Herzig (8) by treating a solution of purpurogallin in ether–ethanol with excess diazomethane. Fine yellow needles formed on standing overnight, m.p. 179.5-180°C.; literature (12), m.p. 175-177°C., (7), m.p. 176°C. Calc. for $C_{14}H_{14}O_5$: CH_3O, 35.5%. Found: CH_3O, 35.4, 35.5%.

Purpurogallin Tetramethyl Ether

This ether was prepared according to the method of Willstätter and Heiss (12) by methylation of the trimethyl ether with potassium hydroxide and dimethyl sulphate, m.p. 91-92°C., from aqueous methanol; literature, m.p. 92°C. (1), m.p. 93°C. (12).

Purpurogallin Monoacetate

Acetic anhydride, 0.86 cc. (0.0091 mole), was added slowly with shaking over a period of one-half hour to a solution of 2.00 gm. (0.0091 mole) of purpurogallin in 25 cc. of pyridine on the steam bath. After a further 20 min. on the steam bath, most of the solvent was removed by distillation in vacuum, and 30 cc. of ether was added to the residue to precipitate 2.23 gm. of light brown material, m.p. 165-170°C. Three crystallizations from ether – ethyl acetate (Norite) raised the melting point to 182-183°C. Calc. for $C_{13}H_{10}O_6$: C, 59.6; H, 3.84; CH_3CO, 16.4%. Found: C, 59.6, 59.7; H, 3.82, 3.86; CH_3CO, 16.5%.

Purpurogallin Diacetate I

Acetic anhydride, 1.72 cc., was added slowly with shaking to 2.00 gm. of purpurogallin in 25 cc. of pyridine. The flask was stoppered, shaken vigorously for five minutes, and after 30 min. the reaction mixture was poured into 300 cc. of ice-water to give a yellow precipitate, 1.06 gm. The diacetate melted after several crystallizations from ether – ethyl acetate (Norite) at 159-160°C. Calc. for $C_{15}H_{12}O_7$: CH_3CO, 28.3%. Found: CH_3CO, 28.1%.

**All melting points were uncorrected, unless otherwise noted.*

Purpurogallin Diacetate II

(*a*) Acetic anhydride, 1.92 cc., was added drop by drop to 2.24 gm. of purpurogallin in 30 cc. of pyridine and heated on the steam bath for 40 min. Removal of most of the solvent by distillation in vacuum, followed by addition of ether, gave an orange precipitate, 2.90 gm., m.p. 165-172°C. Three crystallizations from ether – ethyl acetate (Norite) gave shining orange-red prisms, m.p. 208°C.

(*b*) Acetic anhydride, 0.19 cc., was added dropwise with shaking to 0.516 gm. of purpurogallin monoacetate in 7 cc. of pyridine on a boiling water bath. The reaction mixture was left on the water bath a further 10 min., then most of the pyridine was evaporated in vacuum and a few cubic centimeters of ether added to the residue gave an orange precipitate, 0.548 gm., m.p. 168-173°C. Two crystallizations from ethyl acetate raised the melting point to 208-209°C. Calc. for $C_{18}H_{12}O_7$: CH_3CO, 28.3%. Found: CH_3CO, 27.0%.

A mixture of diacetate I and diacetate II melted at 145–150°C.

Purpurogallin Triacetate

Acetic anhydride, 3.86 cc., was added in small portions with shaking to 3.00 gm. of purpurogallin in 30 cc. of pyridine. The flask was stoppered, shaken vigorously, let stand for 30 min., and the contents poured into 300 cc. of ice-water with stirring. A bright yellow precipitate was obtained, 3.47 gm., m.p. 154-156°C. The triacetate melted after two crystallizations from ether – ethyl acetate at 161.5-162.5°C. Calc. for $C_{17}H_{14}O_8$: C, 59.0; H, 4.08; CH_3CO, 37.3%. Found: C, 58.5, 58.5; H, 4.18, 4.16; CH_3CO, 35.4, 36.1%.

Purpurogallin Tetracetate

This was obtained in 50% yield by acetylation of purpurogallin according to Perkin and Steven (10), m.p. 192-193.5°C. from ethanol; literature (10), m.p. 186°C.

Diacetate of Purpurogallin Monomethyl Ethyl Ether

A solution of 0.2 gm. of purpurogallin monomethyl ether in 10 cc. of acetic anhydride containing 1 cc. of pyridine was heated under reflux for 30 min., then diluted with water. Yellow material separated, 0.17 gm., m.p. 148-150°C. Repeated crystallization from ethanol raised the melting point to 156-157°C. Calc. for $C_{16}H_{14}O_7$: C, 60.4; H, 4.43; CH_3CO, 27.0; CH_3O, 9.8%. Found: C, 59.3, 60.0; H, 4.68, 4.60; CH_3CO, 27.4; CH_3O, 9.8, 9.7%.

Diacetate of Purpurogallin Dimethyl Ether

A solution of 0.25 gm. of purpurogallin dimethyl ether in 5 cc. of acetic anhydride was heated under reflux for two hours, then diluted with water. Pale yellow material separated, 0.25 gm. Two crystallizations from ether – ethyl acetate yielded the pale greenish-yellow diacetate, m.p. 194-196°C. Calc. for $C_{17}H_{16}O_7$: CH_3O, 18.37%. Found: CH_3O, 18.32, 18.38%.

Monoacetate of Purpurogallin Trimethyl Ether

A solution of 0.10 gm. of purpurogallin trimethyl ether in 5 cc. of acetic anhydride and 1 cc. of pyridine was heated under reflux for 45 min. Most of the solvent was removed in vacuum and a few cubic centimeters of ether was

added. Transparent plates, 0.10 gm., separated out, m.p. 145-146°C. Crystallization from ether – ethyl acetate gave colorless crystals of m.p. 145.5-146°C.; literature (10) gives m.p. 140-143°C. Calc. for $C_{16}H_{16}O_6$: CH_3O, 30.6%. Found: CH_3O, 30.5%.

Absorption Spectra

Absorption spectra were measured on a Beckman Model DU spectrophotometer. The solvent employed in all cases was purified dioxane.

ACKNOWLEDGMENTS

Financial assistance given by the National Research Council of Canada during the progress of this research is gratefully acknowledged.

REFERENCES

1. BARLTROP, J. A. and NICHOLSON, J. S. J. Chem. Soc. 116. 1948.
2. CAUNT, D., CROW, W. D., HAWORTH, R. D., and VODOZ, C. A. Chemistry & Industry, 149. 1950.
3. CAUNT, D., CROW, W. D., HAWORTH, R. D., and VODOZ, C. A. J. Chem. Soc. 1631. 1950.
4. CAUNT, D., CROW, W. D., and HAWORTH, R. D. J. Chem. Soc. 1313. 1951.
5. CRITCHLOW, A., HAWORTH, R. D., and PAUSON, P. L. J. Chem. Soc. 1318. 1951.
6. EVANS, T. W. and DEHN, W. M. J. Am. Chem. Soc. 52: 3647. 1930.
7. HAWORTH, R. D., MOORE, B. P., and PAUSON, P. L. J. Chem. Soc. 1045. 1948.
8. HERZIG, J. Monatsh. 31: 799. 1910.
9. NIERENSTEIN, M. and SPIERS, C. W. Ber. 46: 3151. 1913.
10. PERKIN, A. G. and STEVEN, A. B. J. Chem. Soc. 83: 192. 1903.
11. THORN, G. D. and PURVES, C. B. Manuscript in preparation.
12. WILLSTÄTTER, R. and HEISS, H. Ann. 433: 17. 1923.

THE QUANTITATIVE DETERMINATION OF THE FREE MONOXIDES OF CALCIUM, STRONTIUM, AND BARIUM AND OF CALCIUM ETHYLATE BY THE ALCOHOL–GLYCEROL METHOD[1]

By E. G. Swenson and T. Thorvaldson

ABSTRACT

The alcohol–glycerol method for the determination of free calcium oxide in solid systems can be used to determine the monoxides of strontium and barium with a similar degree of precision. The determination of calcium ethylate by this method shows promise. The soluble magnesium salts, magnesium chloride and magnesium acetate, interfere with the determination of the oxides through a replacement reaction liberating magnesium oxide. The chlorides of calcium, strontium, and barium increase the initial titer obtained in the determination of the monoxides of calcium and strontium, but have no such effect in the determination of barium oxide. For calcium oxide this increase in titer for equimolecular concentrations of the chlorides is in the ascending order: barium, strontium, calcium; for strontium oxide the effectiveness is in the reverse order. The method involves reactions between the monoxides and glycerol to form titratable metal triglycerol hydroxides and possibly two nontitratable products, the mono- and di-glyceroxides of the metals. The relative amounts of these compounds appear to be determined by the physical state of the oxide, the period of heating, the ratio of alcohol to glycerol, and the amount of water present.

The original object of this work was to determine whether the alcohol–glycerol method for free lime (6) is also applicable to the quantitative determination of the free monoxides of barium and strontium. It was later extended to the study of the effect of accelerators and of the inhibiting action of magnesium chloride on the process.

The experimental procedure used has already been described (7). The glycerol was redistilled at reduced pressure. As samples of barium oxide and strontium oxide of unquestioned purity were not available, the ammonium acetate solution was standardized against pure calcium oxide. Later work with barium hydroxide indicated that calcium oxide may be used for this purpose without introducing error.

THE DETERMINATION OF FREE BARIUM OXIDE

A sample of barium oxide was obtained by the decomposition of a "reagent" grade of hydrated barium nitrate, with final heating at 1000° to 1050°C. for one hour. The sample was ground rapidly and stored in a weighing bottle in a desiccator over magnesium perchlorate and calcium oxide. Preparation of the oxide from the nitrate in this manner produced some barium peroxide which was determined separately (8). It was found, however, that barium peroxide, after refluxing with the alcohol–glycerol solution, does not give any titer with ammonium acetate. Table I gives the results of the application of the alcohol–glycerol method to this sample of barium oxide with and without the addition of some anhydrous salts, which give accelerating action in

[1] *Manuscript received November 9, 1951.*
Contribution from the Division of Building Research, National Research Council, Ottawa, Canada, and the Department of Chemistry, University of Saskatchewan, Saskatoon, Sask. Issued as N.R.C. No. 2676.

the determination of free lime (1, 7). The period of refluxing between titrations was 20 min.

TABLE I
DETERMINATION OF BaO BY THE ALCOHOL–GLYCEROL METHOD

Weight of sample, gm.	Accelerator, gm.	Titer NH_4OAc solution		Total Time, hr. : min.	% BaO obtained
		Initial, ml.	Total, ml.		
0.2973	none	15.6	17.12	4 : 20	94.3
0.3018	none	16.0	17.52	4 : 20	95.1
0.3063	$CaCl_2$ – 0.200	16.2	17.69	4 : 20	94.6
0.3099	$SrCl_2$ – 0.285	16.5	18.00	4 : 20	95.1
0.3044	$BaCl_2$ – 0.375	16.1	17.48	4 : 20	94.0
					Mean 94.6

Analysis of the sample used in Table I gave the following results: barium dioxide, 1.52% (8); silica, 1.34%; loss on ignition at 980°C., 0.8%; total barium, determined as sulphate and calculated to barium oxide, 97.2%. Correcting for barium dioxide, the value for barium oxide becomes 95.7% as compared with 94.6% free barium oxide by the alcohol–glycerol method. It is probable that there was some combination of barium oxide with silica during the preparation of the sample, thus lowering the value for the free oxide. Only traces of other elements were found.

Another grade of commercial barium nitrate of somewhat inferior quality was converted to barium oxide in the same manner. The results were similar except that the value obtained for free barium oxide was 92.0%.

It was found that different samples of barium oxide, prepared from the same sample of hydrated barium nitrate by heating, gave widely different rates of extraction in the alcohol–glycerol solution, indicating that the reactivity of barium oxide is affected by slight variations in the method of preparation.

The presence of the chlorides of calcium, strontium, and barium which produce acceleration in the determination of calcium oxide have no effect either on the rate or on the value obtained in the determination of barium oxide. In Table I the salts are present in equimolecular concentrations. In other series, quantities varying from 0.2 to 1.0 gm. were used with similar results. Furthermore, for a variation in the weight of the sample of barium oxide from 0.1 to 0.3 gm., a proportional change occurred in the first 20 min. titer. The oxide in the quantities used dissolved rapidly in the alcohol–glycerol mixture to give in the main a titratable product so that over 90% of the BaO present is determined by the first titer.

A sample of barium hydroxide octahydrate of very high purity (A.C.S. Specifications) was also used. This was dehydrated at room temperature *in vacuo* to the monohydrate ($Ba(OH)_2.H_2O$) and by heating at 260°C. to the hydroxide. The octahydrate dissolved rapidly in the alcohol–glycerol solution at room temperature and was titrated by a single titration. The end point must, however, be determined in the hot solution, as in the determination

of calcium oxide, to avoid overtitration. The monohydrate dissolved somewhat more slowly, but after refluxing 0.2 gm. samples for 10 min. about 99% of the total was titratable, the end point being reached after boiling for an additional 10 min. The end point with the hydroxide was reached after three 10 min. refluxing periods. This compares with more than four hours required for the corresponding determination of anydrous barium oxide (Table I). The values obtained for the barium oxide in the three products were consistent on the basis of the original weight of the octahydrate, the latter containing about 1% of barium carbonate which remains unchanged during the dehydration of the octahydrate to barium hydroxide.

Standardization of the ammonium acetate solution with pure calcium oxide thus appears satisfactory. This avoids the difficulties involved in the preparation of pure barium oxide which attacks platinum at the temperature necessary for complete dehydration and removal of carbon dioxide.

As in the case of the determination of free lime (7), the presence of magnesium chloride was found to interfere with the determination of free barium oxide. Presence of magnesium sulphate had no effect. The last named is only very slightly soluble in the 5 to 1 alcohol–glycerol mixture.

THE DETERMINATION OF FREE STRONTIUM OXIDE

A sample of strontium oxide was obtained by ignition of "reagent" strontium nitrate at about 1000°C. with subsequent grinding. Table II gives the results of the application of the alcohol–glycerol method to this sample without accelerator and with chlorides of calcium, strontium, and barium in equimolecular proportions.

TABLE II

DETERMINATION OF SrO BY THE ALCOHOL–GLYCEROL METHOD

Weight of sample, gm.	Accelerator, gm.	Titer NH_4OAc solution		Total time, hr. : min.	% SrO obtained
		Initial, ml.	Total, ml.		
0.2002	None	2.4	17.26	5 : 00	95.4
0.2052	None	4.8	17.64	5 : 00	95.2
0.1979	$CaCl_2$ – 0.200	9.0	16.99	6 : 00	95.0
0.1949	$SrCl_2$ – 0.285	13.1	16.83	3 : 20	95.6
0.1914	$BaCl_2$ – 0.375	14.6	16.57	3 : 20	95.8
					Mean 95.4

Analysis of the samples of strontium oxide, of Table II, gave 0.49% strontium dioxide (8), 0.92% silica, and a loss on ignition at 980°C. of 0.8%. Only traces of other elements were found. Determination of total strontium as the oxalate gave 96.7% SrO which, after correction for strontium dioxide, gives 96.3%, as compared to 95.4% for free SrO. The difference is probably due to combination of silica with strontium oxide and a small amount of carbonate present.

Several samples of strontium oxide were prepared and a series of analyses were made varying the weights of the oxide used as well as the amounts of

the salt accelerators added. The initial titer was not proportional to the amount of oxide used (for quantities of 0.1 to 0.2 gm. SrO) thus behaving more like CaO than BaO. The chlorides of calcium, strontium, and barium all act as accelerators on the first titer, the effect of equimolecular concentration increasing in the above order. This is in the reverse order to that found in the determination of calcium oxide (7). The total time was reduced with $SrCl_2$ and $BaCl_2$ but not so with calcium chloride, perhaps partly because the white precipitate formed made decision of end points difficult. There appears to be no significant change in the total value for free SrO obtained with or without accelerators. The method of preparation of the strontium oxide appeared to have less effect on the progress of the determination than was the case with barium oxide. The presence of magnesium chloride was found to interfere with the determination.

Magnesium oxide, when refluxed with 5:1 alcohol–glycerol mixture containing phenolphthalein, gives no color in the solution and is therefore not titratable. The solid, however, takes on a pink tint.

From the experimental work recorded, it would appear that the alcohol–glycerol method, as used for the quantitative determination of free lime, is also suitable for the determination of free barium oxide and strontium oxide probably with a similar order of precision as for free lime. The chlorides of calcium, strontium, and barium have no effect on the determination of free barium oxide, but give an accelerating effect with strontium oxide and calcium oxide (7). Magnesium oxide can not be determined by the method and the presence of magnesium chloride interferes with the determination of the other oxides.

THE DETERMINATION OF CALCIUM ETHYLATE

The possibility that calcium ethylate may play a part as a titratable intermediate product in the alcohol–glycerol determination of free lime was considered. If so, one might expect that this compound could be determined by a single titration with ammonium acetate. The ethylate was prepared by refluxing anhydrous ethyl alcohol (99.9%) with freshly cut shavings of metallic calcium in an atmosphere of dry oxygen-free nitrogen. The system was protected against access of air or moisture. The product was recrystallized from absolute alcohol and the adhering alcohol removed *in vacuo* at room temperature. Several crystalline samples were thus obtained. The samples appeared to behave like calcium oxide on alcohol–glycerol extraction and titration except that the time required without accelerator was somewhat shorter than with pure calcium oxide. Strontium chloride gave good acceleration, cutting the time required to about one-half or less. The similarity of the titration of calcium ethylate and calcium oxide and the fact that when the ratio of alcohol to glycerol is increased above 5 to 1 there is a rapid falling off in the rate of titration of free lime indicate that the ethylate does not play a part in the titration of calcium oxide. Furthermore the solid products formed on prolonged refluxing of calcium oxide with 5 : 1 alcohol–glycerol solution contained no alcohol.

The method may be of use in determining calcium ethylate. The precision was very good and the values obtained with and without the use of an accelerator were in good agreement. Further experimental work would be necessary to determine the accuracy of the method.

The presence of magnesium chloride interfered with the determination as in the case of the alkaline earth oxides.

THE INHIBITING ACTION OF MAGNESIUM CHLORIDE

A further study was made of the interference of magnesium chloride in the determination of the free oxides of the alkaline earths by the alcohol–glycerol method. Incidentally, it was found that the presence of magnesium acetate interferes in a similar manner.

Anhydrous magnesium chloride was prepared by passing pure dry hydrogen chloride over the heated hexahydrate of magnesium ammonium chloride until all the water and ammonium chloride had been volatilized. The sample was then cooled in a current of purified dry air and transferred quickly to weighing bottles. A gravimetric determination of magnesium gave 98.9% magnesium chloride while a volumetric determination of chloride gave 98.5% magnesium chloride. A solution containing 1 gm. magnesium chloride in 100 ml. of anhydrous 5:1 alcohol–glycerol mixture remained permanently clear and gave an equivalent conductivity of 4.3 reciprocal ohms at 25°C.

The quantitative determinations were made in the usual manner. A weighed quantity of the alkaline earth oxide was introduced into a dry 125 ml. florence flask; 60 ml. of the alcohol–glycerol solution containing the requisite quantity of magnesium chloride was added, and the digestion carried out with titration with standard ammonium acetate solution at 20 min. intervals until no pink color appeared in the solution after an hour's boiling.

TABLE III

EFFECT OF $MgCl_2$ ON THE DETERMINATION OF BaO, SrO, AND CaO

	BaO		SrO		CaO	
	Molar ratio, $\frac{MgCl_2}{BaO}$	% BaO recovered by titration	Molar ratio, $\frac{MgCl_2}{SrO}$	% SrO recovered by titration	Molar ratio, $\frac{MgCl_2}{CaO}$	% CaO recovered by titration
*A**	0.55	55.5	0.53	53.7	0.45	64.5
	0.76	42.0				
	0.85	28.7	0.92	23.0	0.90	30.5
	1.08	22.5	1.04	18.3		
	1.10	22.0	1.06	16.6	1.35	13.4
	1.64	5.2	1.59	7.0		
	2.19	0.0	2.12	0.0	1.80	0.0
*B***	0.43	62.1			0.43	64.0
	0.45	60.9			0.50	53.8
	0.86	26.4			0.75	35.6
	0.95	22.3			0.86	26.8
	1.00	17.2			0.95	21.8
					1.00	17.3
	1.48	trace			1.50	4.1

**Using $MgCl_2.6H_2O$ in Series A.*
***Using $MgCl_2$ (anhydrous) in Series B.*

Table III gives the effect of varying the magnesium chloride present, while Table IV gives the effect of the presence of water in the reaction mixture.

TABLE IV

EFFECT OF WATER IN THE PRESENCE OF $MgCl_2$ ON THE DETERMINATION OF BaO AND CaO

BaO			CaO		
Molar ratio, $\frac{MgCl_2}{BaO}$	Moles H_2O per mole $MgCl_2$	% BaO recovered by titration	Molar ratio, $\frac{MgCl_2}{CaO}$	Moles H_2O per mole $MgCl_2$	% CaO recovered by titration
0.85	6	28.7	0.50	0	53.8
	6.5	26.0		6	53.4
	8	24.2		18	49.8
	16	16.2	1.00	0	17.3
				6	0.9
				18	0.0

Fig. 1 is a plot of the values obtained for the free oxide against the initial molar ratio of magnesium chloride to free oxide. The points for BaO and CaO with anhydrous magnesium chloride and for SrO with the hexahydrate of magnesium chloride fall upon a straight line (Curve 1) up to a ratio approaching unity, at which point the recovery of the free oxides by titration has fallen to less than 20%, while at a ratio of about 1.5 the recovery approaches

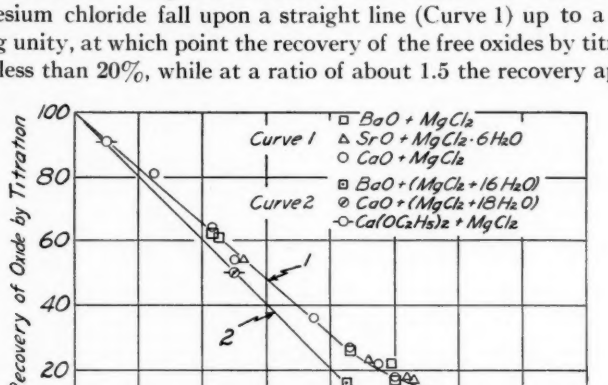

FIG. 1. The effect of magnesium chloride on the titration of the free monoxides of barium, strontium, and calcium by the alcohol–glycerol method.

zero. The values obtained for barium oxide and calcium oxide with $MgCl_2.6H_2O$ present are not essentially different. Lengthening the initial refluxing time from 20 to 120 min. did not reduce further the total titratable barium oxide, but the initial titer was slightly reduced.

Addition of small amounts of water to the reaction mixture decreased progressively the titratable amount of oxide. Occasionally the results were erratic. Values obtained with 16 to 18 moles of water per mole of magnesium

chloride (Curve 2 of Fig. 1) fall upon a straight line with no recovery of the oxide by titration when the ratio of magnesium chloride to free oxide reaches unity.

With a freshly prepared sample of crystalline calcium ethylate and magnesium chloride in anhydrous alcohol–glycerol solution the total titer was reduced to 91% for a magnesium chloride to ethylate molar ratio of 0.100; to 49.3% for a ratio of 0.503; and to 1.0% for a ratio of 1.04. These points fall close to Curve 2.

It would therefore appear that one mole of magnesium chloride is capable of neutralizing one mole of the free oxide or ethylate under the conditions of these experiments. In all cases, a solid, rendered slightly pink by the phenolphthalein present, remained at the end of the run. As a solution of 1 gm. of magnesium chloride in 100 ml. of the alcohol–glycerol solution remains clear on standing for more than a year, the reaction producing the precipitate appears to be between the magnesium salt and the free oxides.

Two alternative explanations of the effect of magnesium chloride might be suggested:

1. The formation of compounds of the type, $MgCl_2.CaO$,

2. Reactions of the type, $CaO + MgCl_2 \rightarrow CaCl_2 + MgO$, with an alkaline earth hydroxide or a glycerol metal hydroxide as an intermediate product.

To determine the nature of the reaction the following experiments were undertaken. Anhydrous magnesium chloride and calcium oxide in a molar ratio slightly above unity were refluxed with 60 ml. of alcohol–glycerol for approximately four hours. The solid was filtered off and washed with absolute alcohol. It was composed of magnesium oxide with minute traces of calcium and chloride.

Barium hydroxide (containing a small amount of barium carbonate) was refluxed with alcohol–glycerol for about two and one-half hours in a similar manner with a 15% *M* excess of magnesium chloride. The solid, which was mainly in suspension, was separated by centrifuging and washed first with alcohol containing a little glycerol and then with absolute alcohol. The solid was composed of magnesium oxide with a small amount of barium (as carbonate) and a trace of chloride.

It appears that the interference of magnesium chloride in the alcohol–glycerol determination of the free oxides is due to a reaction of Type 2 above. The high values for the free oxides (Table III and Curve 1, Fig. 1), at first thought to be due to the slowness of the double decomposition, are probably caused by a second parallel reaction occurring in the nearly anhydrous medium with the formation of a glyceroxide (see below) which on further refluxing becomes titratable. This explanation is supported by the fact that the length of the initial refluxing period had no material effect on the final result, the lower initial titer being balanced by higher successive titers on further refluxing. Experiments described below also support this view.

THE MECHANISM OF THE ALCOHOL–GLYCEROL METHOD FOR DETERMINING THE FREE ALKALINE EARTH OXIDES

Destrem (2) reported the preparation of anhydrous glyceroxides of the composition $C_3H_5(OH)O_2Ca$ and $C_3H_5(OH)O_2Ba$. Grün and Bockisch (3) reported the preparation of triglycerol calcium hydroxide, $Ca(OH)_2.3C_3H_5(OH)_3$, and Grün and Husman (4), of the analogous compounds of strontium and barium. The latter also reported the formation of a hydrated diglycerol calcium hydroxide, which they state liberates one molecule of glycerol on heating to 130°C. Wheeler (9) prepared a calcium diglyceroxide, $Ca(C_3H_5(OH)_2O)_2$ as well as the calcium monoglyceroxide of Destrem and proposed the following chart to illustrate the relationship between the various compounds of calcium oxide and glycerol.

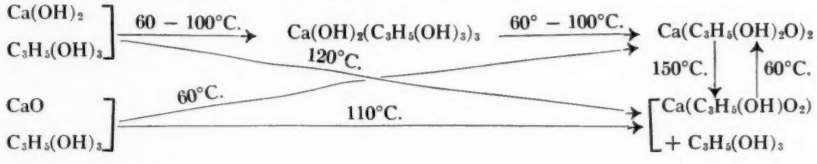

On the basis of the above and of experiments reported in this and in a previous paper (7) it is possible to propose a mechanism for the alcohol–glycerol determination of the free oxides of the alkaline earth metals.

When a 5:1 alcohol–glycerol solution containing a small amount of water is refluxed with calcium oxide the first product formed is the triglycerol calcium hydroxide of Grün and Bockisch, or the diglycerol calcium hydroxide of Grün and Husman, or possibly a mixture of these. The product is only moderately soluble in the 5:1 alcohol–glycerol mixture, but when suspended in the hot liquid redissolves during the titration with the ammonium acetate solution.

In a completely anhydrous alcohol–glycerol mixture the easily titratable product, which is intensely colored by phenolphthalein, does not form. A product not colored by phenolphthalein, the diglyceroxide of Wheeler, or the monoglyceroxide of Destrem, or a mixture of these, separates out. This is not directly titratable with ammonium acetate. For nearly anhydrous solutions the initial titer is very small, but owing to the formation of water in the titration, successive titers show an increase to a maximum and then decrease with the exhaustion of the free lime. The accelerating effect of the presence of small amounts of water is thus explained as well as the inhibiting effect of the presence of large amounts of tricalcium aluminate, pentacalcium trialuminate, and other dehydrating agents (7).

On continued refluxing of the alcohol–glycerol mixture (containing a small amount of water) with calcium oxide, without titration, the easily titratable product first formed is changed to the almost insoluble diglyceroxide or monoglyceroxide of calcium or a mixture of the two. Both the formation of the titratable product and the subsequent production of the nontitratable glyceroxides are fairly slow processes at the boiling temperature of the mixture.

The first reaction is accelerated, and the second reaction is retarded by increasing the amount of water present but overtitration with ammonium acetate in the early part of the determination does not materially reduce the total time required for the determination (7). However, prolonging the initial refluxing period beyond a critical value reduces the initial titer, a point being reached when the rate of formation of the glyceroxides exceeds the rate of formation of titratable glycerol calcium hydroxide. The experimental evidence indicates that in a normal alcohol–glycerol determination of free lime a portion of the free lime is transformed into the very slightly soluble glyceroxides and thus escapes titration in the early part of the process. As the free lime in the sample approaches exhaustion, the reverse process, i.e., the formation of the glycerol calcium hydroxide from the glyceroxides, proceeds slowly giving rise to a prolonged series of very small titers.

The authors' experience with the alcohol–glycerol determination of free lime over a period of many years appears to be wholly in accord with the above views as to the mechanism involved. A number of special experiments were also made to test these assumptions. Samples of calcium oxide were refluxed for 20 min. with 5:1 alcohol–glycerol solution and a portion of the hot supernatant liquid was removed by filtration. The titer of the filtered liquid was very small compared with the titer of the liquid containing the suspended solid, showing that some of the solid redissolves during the titration. In a similar experiment refluxing for six hours gave extremely small titers for both the filtered liquid and the liquid containing the solid, showing that the solid had been transformed to a nontitratable form. In another experiment with two hours of refluxing, the color of the clear filtered solution was discharged by the addition of a few drops of 0.1 *M* solution of ammonium acetate, but the color returned on further refluxing of the clear solution and it required three further refluxing periods of 10 min. each for a permanent end point to be reached. This supports the view that a small amount of the solid formed on prolonged refluxing is in solution but is not directly titratable, and that an equilibrium between the titratable and nontitratable glycerol–lime compounds exists in the solution, giving rise at least in part to the gradually diminishing titers towards the end of the determination of free lime.

It was found that calcium oxide heated with glycerol in a bath at 120°C. for short periods of time (about 10 min.) and then diluted with absolute alcohol gave mainly a titratable product; after the first titration there remained a light suspension of a solid, which was not colored by phenolphthalein. This suspended solid reverted slowly to the titratable form on repeated refluxing and titrating in the usual manner. On the other hand similar treatment of calcium oxide and glycerol for five hours at 150°C. gave only a small amount of titratable product with a large amount of precipitate remaining after the first titration. Reversal to the titratable product on further refluxing was very slow.

Analysis of the solid products present after short periods of refluxing, under conditions comparable to those used in the determination of free lime, cannot

be expected to give any conclusive information as to the mechanism on account of the mixtures involved. Some of the solid products obtained after lengthy refluxing were analyzed. Several samples of calcium oxide weighing less than 0.05 gm. were refluxed with 60 ml. of 5:1 alcohol–glycerol mixture for from three to six hours; the solids were filtered off by suction, washed with hot absolute alcohol, and brought to constant weight *in vacuo*. The molar ratio of glycerol* to calcium oxide varied from 1.02 to 1.07. Average values on the basis of the product as 100 were glycerol, 70; calcium oxide, 41. This indicates that the nontitratable solid produced may be a mixture of Destrem's calcium monoglyceroxide (corresponding calculated values, glycerol, 70.8; calcium oxide 43.0) and Wheeler's calcium diglyceroxide (glycerol, 82.9; calcium oxide, 25.2), mainly the former. Another series with larger amounts of calcium oxide and another preparation of alcohol–glycerol, refluxed for two to five hours, gave an average glycerol – calcium oxide ratio of 1.55 and average values of 76.8% glycerol and 30.5% calcium oxide, indicating a mixture of the same compounds in different proportions. No clear-cut relation of the values obtained to the time of refluxing was observed.

The mechanism involved in the determination of the free oxides of barium and strontium appears to be essentially the same as for calcium oxide. According to Grün and Husman (4) triglycerol barium hydroxide forms when the octahydrate of barium hydroxide is added to glycerol. As stated above the titratable product is completely soluble in anhydrous 5:1 alcohol–glycerol solution, and appears to be much more stable in the solution than the corresponding slightly soluble calcium compound. The barium glyceroxide of Destrem (2) probably does not form under these conditions even on prolonged refluxing on account of the water present. According to Destrem the monoglyceroxide forms when barium oxide is heated with anhydrous glycerol at 70°C. so it would appear that when barium oxide is refluxed with the alcohol–glycerol solution this compound will form if there is not enough water present to form the triglycerol barium hydroxide. The large initial titer of the determinations of Table I with the subsequent long series of small titers before a permanent end point is reached supports the view that a nontitratable glyceroxide is formed to a small extent in this case and that on further refluxing a slow reconversion to the titratable form takes place. On this basis the difference in the behavior of the octahydrate and the monohydrate of barium hydroxide, and barium oxide described above may be explained.

The solubility of triglycerol strontium hydroxide is intermediate between that of the corresponding compounds of barium and calcium. The determination of strontium oxide resembles that of calcium oxide more than barium oxide.

The accelerating effect of the chlorides of the alkaline earth metals on the determination of the monoxides of calcium and strontium is probably related to the capacity of these salts to form soluble complexes with large amounts of glycerol as shown by Grün and collaborators. Similar soluble complexes are

*See Strebinger and Streit method (5).

possibly formed with the glycerol compounds of the metallic oxides. The net result appears to be the stabilization of the titratable glycerol compounds of the oxides. In the case of the more stable titratable compound of barium oxide there is some evidence of slight inhibiting effect. It was found that when the three oxides are added to the alcohol–glycerol solution containing phenolphthalein, the color appears immediately in the solution with barium oxide while some time elapses before it appears with the other oxides. When the accelerating salts are present the reverse is the case.

Further study and standardization of the alcohol–glycerol method for determining free lime in Portland cement on the basis of the optimum amount of water in the reagents appears to be desirable.

REFERENCES

1. BRANDENBURG, H. R. Rock Products, 34: 8, 68. 1931.
2. DESTREM, M. A. Ann. chim. et phys. Ser. 5, 27: 7. 1882.
3. GRÜN, AD. and BOCKISCH, F. Ber. 41: 3456. 1908.
4. GRÜN, AD. and HUSMAN, J. Ber. 43: 1291. 1910.
5. LAWRIE, J. W. Glycerol and glycols. Chemical Catalogue Company, Inc., New York. 1928. p. 245.
6. LERCH, W. and BOGUE, R. H. Ind. Eng. Chem. Anal. Ed. 2: 296. 1930.
7. SWENSON, E. G. and THORVALDSON, T. Can. J. Chem. 29: 140. 1951.
8. TREADWELL, F. P. and HALL, W. T. Analytical chemistry. Vol. 2. 7th ed. John Wiley and Sons, Inc., New York. 1930. p. 534.
9. WHEELER, T. S. Chem. News. 142: 241. 1931.

REACTION OF OXYMERCURIALS WITH HYDRAZINE[1]

By George F Wright

ABSTRACT

The reduction of 2-methoxyalkylmercuric halides by hydrazine hydrate is thought to proceed through mercuri-*bis*-2-methoxyalkane, which decomposes to give 2-methoxyalkane radicals. These radicals may lose or gain a hydrogen atom to form 2-methoxyalkene or alkane. The reaction seems to be definitive for structure proof. The *bis*-mercurial from the (α) 2-methoxycyclohexylmercuric chloride which is formed directly from cyclohexene is less stable than the diastereomeric (β) *bis*-mercurial, which can be purified by distillation. Conversion of this (β) *bis*-mercurial to pure β-2-methoxycyclohexylmercuric chloride shows that this reaction occurs by direct replacement. The hydrazine reduction may be used to convert β-1-chloromercuri-2-methoxy-1,2-diphenylethane (from *trans*-stilbene) to the α-diastereomer. Since the β-isomer in this case is more readily hydrolyzable than the α-isomer, and each isomer may be converted cleanly back to its parent alkene, the series of reactions provides a method of converting *trans*- into *cis*-stilbene.

There are two chemical methods for structure proof of organoöxymercurials but neither is of general or reliable applicability. Firstly, the mercuri group may be replaced by bromine or iodine, but configuration is lost by this halogenation and the α-oxyalkyl halide decomposes easily. The second method, used originally by Sand and Singer (7), involves conversion of an alkoxyalkylmercurial to the alkoxyalkane with sodium amalgam. Oftentimes this alloy simply regenerates the original alkene from which the alkoxyalkylmercurial was prepared. This result is predictable since it is known that other α-alkoxyorganometallic compounds behave similarly, and the α-methoxyalkylsodium presumably is an intermediate in the reduction of the mercurial. In view of the limitations of these two methods it seemed worthwhile to seek a novel technique for structure proof.

Some years ago Gilman and Wright (4) found that organomercuric salts could be "reduced" to the corresponding mercuri-*bis*-organic compound by hydrazine hydrate. Later, it was found by Romeyn and Wright (5) that a partial conversion of this type could be utilized to establish an equilibrium between the two 1-methoxy-2-chloromercuricyclohexanes. The low yields in this equilibration indicated the possibility that further reduction was occurring. A reinvestigation has now shown that the precipitation of metallic mercury is greater than can be accounted for by formation of 2-mercuri-*bis*-1-methoxycyclohexane. A second product has been sought and found largely to be methoxycyclohexane.

The reduction is carried out by solution of α-1-methoxy-2-cyclohexylmercuric chloride (I) in boiling alkali to which the hydrazine hydrate is then added. Precipitation of metallic mercury and a heavy oil of low volatility occurs. Analysis of this heavy oil shows that it is largely 2-mercuri-*bis*-1-methoxycyclohexane (II). More slowly a volatile liquid, largely methoxycyclohexane (IV), collects in the reflux condensate, from which it may be

[1] *Manuscript received November 2, 1951.*
Contribution from the Department of Chemistry, University of Toronto, Toronto, Ont.

separated. It thus appears that II is formed initially and it then decomposes to IV. However, the formation of volatile liquid ceases before all of the heavy oil has decomposed.

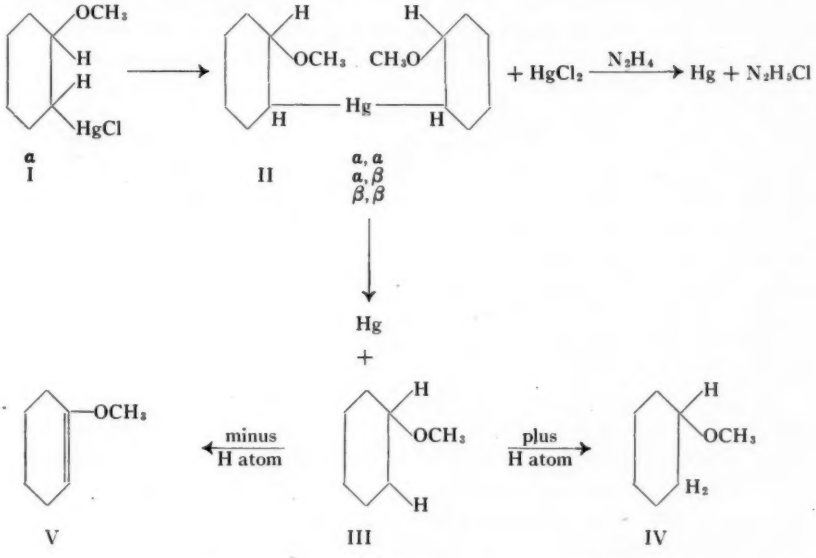

The methoxycyclohexane is contaminated with methoxycyclohexene (V, identified as the dinitrophenylhydrazone of its hydrolysis product, cyclohexanone) in inverse ratio to the excess of hydrazine hydrate used in the reaction. This behavior would not be unexpected if the initially formed mercuri-*bis*-methoxycyclohexane (II) were to decompose into metallic mercury and methoxycyclohexyl radicals (III). The latter would then disproportionate to give IV and V by hydrogen atom exchange, or else would be reduced by hydrazine to give methoxycyclohexane (IV) alone.

Support for this mechanism is afforded by a close examination of the heavy oil which is designated as the *bis*-mercurial (II). When this oil was isolated (in low yield) after a long period of reaction and then was converted by methanolic mercuric acetate and aqueous sodium chloride to 2-methoxycyclohexylmercuric chloride (I) the latter derivative was found to comprise entirely the β-diastereomer. On the other hand, comparable treatment of the heavy oil isolated (in larger yield) after a short reaction period gave a diastereomeric mixture of I. Presumably the α,α-mercuri-*bis*-methoxycyclohexane is less stable over a period of time than the β, β-diastereomer, the α, β-isomer probably being intermediate in stability.

This instability probably is due to thermal decomposition. The heavy oil isolated from a reduction of short duration could be distilled at 0.01 mm. but metallic mercury separated during the process, while both methoxycyclo-

hexane (IV) and methoxycyclohexene (V) were found in the dry-ice trap connected in series with the receiver. The distillate which condensed in the water-cooled receiver gave a diastereomeric mixture of 2-methoxycyclohexylmercuric chlorides when it was treated with mercuric acetate and sodium chloride. The composition of this high-boiling distillate was found by elemental analysis to conform with that of the *bis*-mercurial (II). However, when this distillate was redistilled repeatedly the separation of metallic mercury finally became negligible, although the elemental analysis of the distillate did not change. When this repeatedly-distilled mercuri-*bis*-2-methoxycyclohexane was treated with methanolic mercuric acetate and then with aqueous sodium chloride, the resulting 1-methoxy-2-cyclohexylmercuric chloride was found to be the pure β-diastereomer.

When the thermal decomposition at the same temperature (135°C.) was carried out at atmospheric pressure the same products (IV and V) were obtained together with methanol and cyclohexene. The latter substances must have been formed from the methoxycyclohexyl radicals since methoxycyclohexane and methoxycyclohexene are stable at this temperature.

Further evidence that the decomposition is homopolar (i.e., radical) is provided by the observation that the mercuri-*bis* mixture is stabilized by isolation under nitrogen or by addition of an antioxidant such as hydroquinone.

It must be considered significant that the stable *bis*-mercurial II (which is undoubtedly the β, β'-diastereomer) should be converted by mercuric salt into diastereomerically pure β-2-methoxycyclohexylmercuric salt. The replacement of R–Hg–C by Cl–Hg–C evidently must take place in a direct manner, perhaps according to the following mechanism:

$$\mathrm{R{-}Hg{-}R + HgX_2} \longrightarrow \underset{\substack{\uparrow \\ \mathrm{X} \\ | \\ \mathrm{Hg{-}X}}}{\mathrm{R{-}Hg{-}R}} \xrightarrow[\text{rearr.}]{1,3} \mathrm{XHgR + RHgX}\,.$$

Since the opposite reaction (conversion of 2RHgX into R_2Hg and HgX_2) does not produce diastereomerically-pure *bis*-mercurial, it evidently does not follow this mechanism. Alternatively it is suggested that cyclohexylmercuric hydroxide loses hydroxyl radical to the hydrazine, while dimercuri-*bis*-methoxycyclohexane,

$$\begin{array}{l} \mathrm{2RHgOH} \\ \uparrow \mathrm{NaOH} \\ \mathrm{2RHgCl} \end{array} \longrightarrow \underset{\mathrm{2-OH}}{\mathrm{R{-}Hg{-}Hg{-}R}} \longrightarrow \underbrace{\mathrm{(RHg{-}) + Hg + (R{-})}}_{\mathrm{RHgR + Hg}}$$

initially formed, may decompose into methoxycyclohexylmercuri radical and methoxycyclohexyl radical. These two radicals may then combine to give mercuri-*bis*-methoxycyclohexane II. Subsequently this diastereomeric mixture (α, α and α, β) of II may decompose, preferentially at the α-linkage,

$$RHgR \rightleftharpoons (RHg-) + (R-)$$

and subsequently recombine directly or (if the (R–) radical disproportionates to RH/R minus H) via recombination to R–Hg–Hg–R. The dimercuri-*bis*-compound (R–Hg–Hg–R) which is the essential feature of this mechanism was originally postulated by Sand (6).

In addition to its usefulness as a reaction for structure proof of organoöxymercurials the reduction with hydrazine hydrate may be useful as a synthetic method. Thus one of the interesting diastereomeric pairs of methoxymercurials is the pair of 1-chloromercuri-2-methoxy-1,2-diphenylethanes. However, stereochemical study of these has been limited by the troublesome preparation of pure *cis*-stilbene.

On the other hand *trans*-stilbene is readily available. This geoisomer may be converted to the low melting β-1-chloromercuri-2-methoxy-1,2-diphenylethane (VI) (1) in 60% direct yield or 85% on the basis of the stilbene actually consumed. If now this mercurial is treated with hydrazine hydrate in alkaline methanol a sponge of mercury is formed. The mercuri-*bis*-diastereomers (VII) thus formed are converted by mercuric acetate to the acetoxymercuri diastereomers and thence, by sodium chloride to the mixture of chloromercurials VIII (none of these compounds having been isolated). Now when a methanolic solution of VIII is treated briefly with hydrochloric acid the isolable mercurial is α-1-chloromercuri-2-methoxy-1,2-diphenylethane, together with *trans*-stilbene from which it can readily be separated. A further description of this latter reaction will be outlined because of its theoretical significance.

If a solution comprising one equivalent of each of the diastereomers (VIII) in methanol is treated for one minute with three equivalents of concentrated hydrochloric acid and then quickly diluted with water and neutralized, a solid separates. When stilbene is washed out of this solid by ether, the remainder is almost pure α-1-methoxy-2-chloromercuri-1,2-diphenylethane (VIII, α). The β-diastereomer has been decomposed by the mineral acid.

The mode of addition (with single Walden inversion) during methoxymercuration has only been demonstrated in the case of cyclohexene (2), and it must be assumed to be the same for the two geometric isomers of stilbene. Supporting evidence for this assumption is provided by an observation in this laboratory that each diastereomer may be decomposed into its parent geoisomer (3). This observation has now been extended and substantiated. If β-1-methoxy-2-chloromercuri-1,2-diphenylethane (VIII, β) is decomposed by treatment with strong hydrochloric only *trans*-stilbene is formed. Similar, though much slower, decomposition of the α-diastereomer (VIII, α) gives only *cis*-stilbene from which it is formed by methoxymercuration.

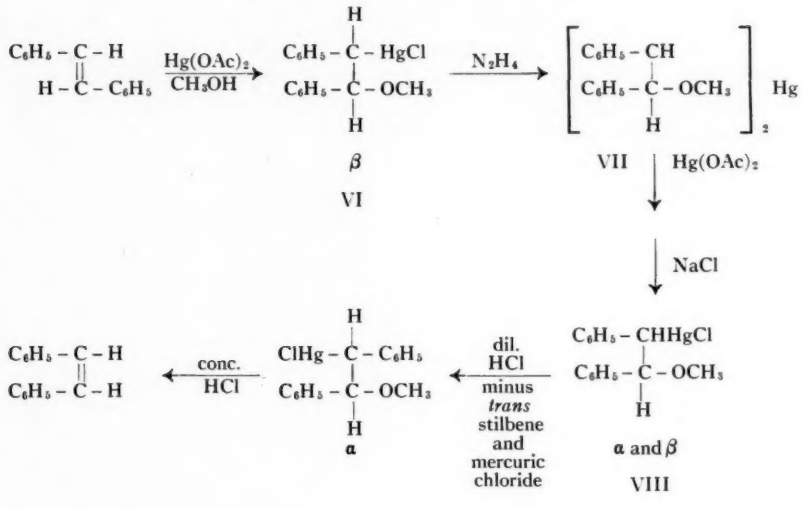

Parenthetically it may be observed that the entire series of reactions from *trans*-stilbene through VI, VII, and VIII to *cis*-stilbene provides a method for conversion of one geoisomer to the other.

The formation of the methoxymercurial from, and reversion to, the same geometric isomer is a reasonable indication that the configurational relationships are the same among the several diastereomeric pairs. The difference in rate of decomposition of the two β-diastereomers relative to their α-isomers would seem therefore to be due to differences in conformation.

It has been suggested (2) that the reversion of 2-methoxy-1-cyclohexylmercuric chloride to cyclohexene, methanol, and mercuric salt proceeds most easily through a quasi-bicyclic intermediate. This hypothesis was advanced because the quasi rings formed from α-2-methoxy-1-cyclohexylmercuric chloride (which reverts more easily than the β-diastereomer) would exist in the stable *trans*-decalin form. No such cyclic restriction exists in the case of the diastereomeric 1-chloromercuri-2-methoxy-1,2-diphenylethanes. Any extension of the hypothesis must therefore depend on the relative symmetries of the quasi-monocyclic intermediates.

Structures (X) and (XI) are stereochemical representatives of α- and β-1-chloromercuri-2-methoxy-1,2-diphenylethane. According to the hypothesis outlined above, the addition of hydrogen chloride to each would lead to the quasi-cyclic intermediates XII and XIII. Inspection of these reveals the distinction that in XII both phenyl groups are polar (or else equatorial) if the 'crown' form of the six-membered ring is to be maintained. On the other hand the polar-equatorial relationship of phenyl groups exists in the quasi ring (XIII) representative of the β-isomer.

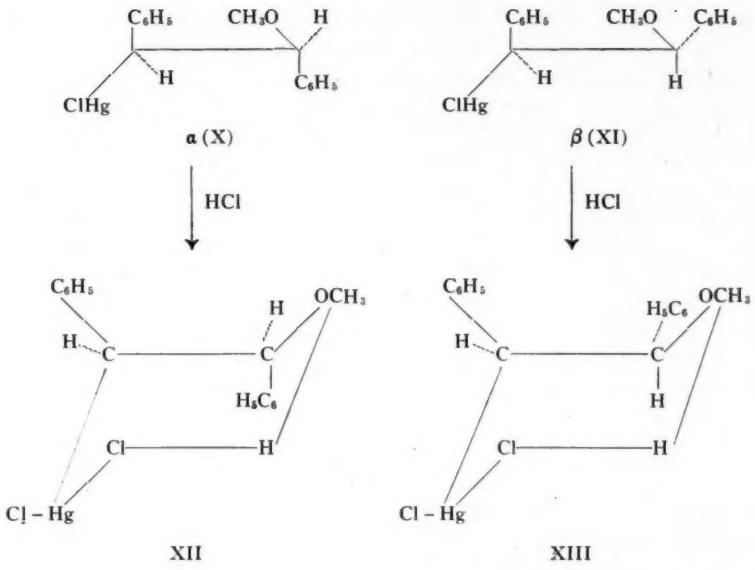

Since no restriction is apparent respecting the ease with which such quasi rings might be formed, the conformation of such intermediates may well decide the relative tendencies to decompose either to alkene, mercuric chloride, and methanol, or else to methoxyalkylmercuric chloride and hydrogen chloride. Structure XII and, especially, its bipolar hydrogen equivalent is more symmetrical than XIII. It seems reasonable to presume tentatively that less tendency toward π bond formation would exist from XII than from XIII. On this basis XIII ought to revert to the alkene more readily than XII, in accordance with the fact.

EXPERIMENTAL*

Reduction of α-2-Methoxycyclohexylmercuric Chloride

A solution of 34.9 gm. (0.1 mole) of 2-methoxycyclohexylmercuric chloride in 80 ml. (0.2 mole) of 10% aqueous sodium hydroxide was added equivalently with 50 ml. (0.87 mole) of 85% hydrazine hydrate to 80 ml. of boiling 10% aqueous sodium hydroxide during one hour under reflux. The volatile product was steam distilled off and, after collection in ether and drying with sodium sulphate, was distilled, b.p. 130-133° (750 mm.), wt. 1.60 gm., $n_D^{2.05}$ 1.4358. This distillate was found by treatment with acid and dinitrophenylhydrazine to contain about 10% of methoxycyclohexene, converted thus to cyclohexanone dinitrophenylhydrazone. The remainder was distilled off, b.p. 133°, n_D^{20} 1.4340, D_4^{20} 0.875 and thus is methoxycyclohexane. The percentage of methoxycyclohexene increased with longer time of reflux. The

**Melting points have been corrected against reliable standards.*

combined yield of 15% was increased to 20% when the hydrazine hydrate was added to the boiling alkaline solution of mercurial.

The residual solution after steam distillation was cooled, extracted with ether, and the metallic mercury phase separated, wt. 15.4 gm. The etherous solution was dried with magnesium sulphate and distilled, finally at 0.02 mm. with a few mgm. of hydroquinone. The distillate weighed 11 gm. and contained some metallic mercury, b.p. 130-147°$_{.02}$, D_4^{20} 1.622, $n_D^{20.5}$ 1.534. Yield is 49% of theoretical. Anal. calcd. for $C_{14}H_{26}O_2Hg$: C, 39.6; H, 6.14. Found: C, 39.6; H, 5.95. After repeated redistillation at 0.02 mm. the precipitation of mercury during distillation ceased. The stable β-mercuri-*bis*-2-methoxycyclohexane boiled 135-40°$_{.02}$, n_D^{20} 1.5365, D_4^{20} 1.664. The elemental analysis was identical with that of the initial distillate. When a portion of this purified *bis*-mercurial was treated with mercuric acetate in methanol, and subsequently with aqueous sodium chloride it yielded pure β-2-methoxycyclohexylmercuric chloride, authenticated by mixed melting point. On the other hand, similar treatment of the initial distillate gave a diastereomeric mixture of the chloromercurials, m.p. 88-90°.

Decomposition of Mercuri-bis-2-methoxycyclohexane

The decomposition of 11 gm. (0.026 mole) of the initial distillate (diastereomeric mixture) of mercuri-*bis*-2-methoxycyclohexane was carried out in a 25 ml. flask heated (175°) by an *o*-dichlorobenzene vapor bath. Mercury precipitated and a distillate appeared (85°C.) during two hours. Further distillation at 25° and 0.15 mm. gave a total distillate of 3.04 gm. This was redistilled to give 0.2 gm. of methanol (oxidized to formaldehyde for identification), then 1.60 gm. of cyclohexene (identified by conversion to the α-methoxychloromercurial), and finally at 90-130° a mixture of methoxycyclohexene and methoxycyclohexane (1 gm.) which contained about 50% of the former. This content of methoxycyclohexene was demonstrated by hydrolysis with hot 10% sulphuric acid to cyclohexanone, identified as its dinitrophenylhydrazone.

The residue after distillation at 25° (0.15 mm.) was completely distilled at 140°, wt. 2.81 gm. This crude yield indicates that at least 30% of the original mixture was β,β-mercuri-*bis*-2-methoxycyclohexane. It was redistilled at 0.4 mm. to yield 0.2 gm., n_D^{20} 1.50 (probably 2,2′-dimethoxybicyclohexyl), b.p. 105-110° and then 1.83 gm., b.p. 125-30°, n_D^{20} 1.5366 which could be converted to almost pure β-2-methoxycyclohexylmercuric chloride by treatment with mercuric acetate and then aqueous sodium chloride. The distillate did not precipitate mercury after a period of several weeks.

β-1-Chloromercuri-2-methoxy-1,2-diphenylethane

A suspension of 180 gm. (1 mole) of *trans*-stilbene, 636 gm. (2 moles) of mercuric acetate, and 24.2 gm. (0.1 mole) of benzoyl peroxide in 4 liters of methanol was stirred for two days. Filtration removed mercurous acetate which weighed 9.7 gm. after washing with diethyl ether. The filtrate was added during two hours to a stirred solution of 174 gm. (3 moles) of sodium chloride in 7.5 liters of water. After three more hours the stirring was inter-

rupted. Ten hours later the crude precipitate was filtered off. The filtrate was discarded (after metallic mercury was recovered from it by treatment with aluminum foil). The crude precipitate was washed with ether to remove stilbene, 1,2-dimethoxy-1,2-diphenylethane, and methyl benzoate. The remaining β-1-chloromercuri-2-methoxy-1,2-diphenylethane weighed 270 gm. (60% of theoretical), m.p. 123-125°. This was purified by solution in 350 ml. of warm chloroform (plus 2 gm. of Darco), filtration, and crystallization induced by addition of 400 ml. of petroleum ether (b.p. 60-70°). After chilling to 4° for 12 hr., 249 gm. (92% recovery) was filtered off, m.p. 130-130.5°. Partial evaporation of the filtrate yielded 15 gm. more, m.p. 128-129°.

The combined etherous washing liquors were combined and evaporated. The residue was crystallized from 850 ml. of boiling 95% ethanol containing 20 ml. concentrated hydrochloric acid. In this way 40 gm. of *trans*-stilbene, m.p. 122-123°, was recovered. The filtrate contained an appreciable amount of mercuric chloride.

α-1-Chloromercuri-2-methoxy-1,2-diphenylethane

A. With Aqueous Hydrazine

A suspension of 31 gm. (0.069 mole) of β-1-chloromercuri-2-methoxy-1,2-diphenylethane in 160 ml. (0.2 mole) of 5% aqueous sodium hydroxide at 55° was treated with 23 ml. (0.4 mole) of hydrazine hydrate and the whole was boiled for 20 min. The original solid almost dissolved, then metallic mercury and a heavy oil appeared. Diethyl ether extraction of the cooled mixture enabled separation of 8.99 gm. (67% of total) metallic mercury.

The ether solution was treated with 18.6 gm. (0.069 mole) of mercuric chloride and 50 ml. of methanol. The ether was distilled off during two hours. The hot solution was filtered to remove 1.1 gm. of mercurous chloride. The cold filtrate yielded 10 gm. of impure α-diastereomer, m.p. 135°. This product was purified by three crystallizations from hot ethanol, m.p. 143°, 50% recovery.

B. With Hydrazine Hydrate in Methanol

A solution of 22.3 gm. (0.05 mole) of β-1-chloromercuri-2-methoxy-1,2-diphenylethane in 200 ml. of boiling methanol was obtained by addition of 10 ml. (0.1 mole) of 40% aqueous sodium hydroxide. After the solution was cooled to 35°, 2.9 ml. (0.05 mole) of 85% hydrazine hydrate was added at once. Gas was evolved as a greenish-yellow precipitate appeared. After 12 hr. the gray metallic sponge was filtered off and washed with methanol and diethyl ether. The filtrate was poured into 500 ml. of water and this solution was extracted with diethyl ether.

The extract was evaporated. A suspension of 15.9 gm. (0.05 mole) of mercuric acetate in 100 ml. of methanol was added and the whole shaken for 15 min. After 150 min., this mixture was filtered into dilute aqueous sodium chloride. The semisolid precipitate could be crystallized from 95% ethanol to yield impure α-diastereomer (m.p. 137°) but it was more convenient to purify by destruction of the β-isomer.

To this end the semisolid precipitate was dissolved partially in 200 ml. of hot methanol. This solution was cooled and then shaken with 5 ml. of concentrated hydrochloric acid for exactly one minute. The solution was then diluted to a volume of 400 ml. with water plus 22 ml. of 10% aqueous sodium hydroxide. After several hours the dirty yellow precipitate was filtered, washed with 4 ml. of ethanol and three 10 ml. portions of diethyl ether to remove *trans*-stilbene. The remainder (4.34 gm., m.p. 137-139°) was crystallized from 130 ml. of hot 95% ethanol. The pure α-diastereomer thus obtained weighed 3.3 gm., m.p. 143.9-144.2°. This low yield (15%) may be doubled by increase in amount of mercuric acetate used. Mercuric chloride may be used, but some oxidation occurs in this instance. The yield is critical in respect of the amount of hydrochloric acid used, as the following experiment shows.

A mixture of 0.1 gm. each of the two diastereomeric chloromercurimethoxydiphenylethanes in 5 ml. methanol was treated exactly one minute with 0.05 ml. of concentrated hydrochloric acid, then diluted into 5 ml. of water and neutralized to pH 5 with alkali. The precipitate was washed with ether, wt. 0.06 gm., m.p. 137°. The etherous filtrate yielded 0.1 gm. of impure stilbene, m.p. 104-105°.

Decomposition of β-1-Chloromercuri-2-methoxy-1,2-diphenylethane

A slurry of 4.47 gm. (0.01 mole) of β-1-chloromercuri-2-methoxy-1,2-diphenylethane (m.p. 131°) in 5 ml. ethanol was stirred with 10 ml. concentrated hydrochloric acid. The temperature rose to 45° and cooling was necessary. After one hour the mixture was filtered to yield 1.80 gm. (100%) of *trans*-stilbene, m.p. 124-124.6°. A mixed melting point was not lowered. The filtrate, made alkaline, yielded impure mercuric oxide, 2.29 gm. These results were duplicated exactly when 5 ml. of 70% perchloric acid in 10 ml. of water replaced the hydrochloric acid.

Decomposition of α-1-Chloromercuri-2-methoxy-1,2-diphenylethane

There was no observable heat evolution when the decomposition with hydrochloric acid described above was repeated with the α-diastereomer, m.p. 144°. After eight hours of stirring the oily phase finally became lighter than the aqueous phase. The whole was diluted with water to a volume of 75 ml. and then extracted thrice with a total of 15 ml. of ether. Evaporation left 1.58 gm. which was distilled at 8 mm. The *cis*-stilbene, b.p. 134-135°, weighed 1.34 gm., n_D^{20} 1.6270, D_4^{20} 1.011. Although the yield was only 75% of theoretical no *trans*-stilbene could be detected either in the residue after distillation or in the distillate. The *cis*-stilbene was identified by conversion to the α-methoxymercurial, m.p. 143-144°. The *trans*-isomer would have been recovered unchanged from the uncatalyzed methoxymercuration, but none was found.

When the decomposition of the α-diastereomer was carried out with perchloric rather than hydrochloric acid all of the available mercury was converted to mercurous salt. The yield of impure *cis*-stilbene was 30% of

theoretical n_D^{20} 1.615 but no *trans*-stilbene could be detected. The remainder comprised distillable oxidation products (b.p. 140-170°, 8 mm.) which have not been identified.

REFERENCES

1. BIRKS, A. M. and WRIGHT, G. F. J. Am. Chem. Soc. 62: 2412. 1940.
2. BROOK, A. G. and WRIGHT, G. F. Acta Cryst. 4: 50. 1951.
3. DOWNING, D. C. M.A. Thesis, University of Toronto, Toronto, Ont. 1940.
4. GILMAN, H. and WRIGHT, G. F. J. Am. Chem. Soc. 55: 3302. 1933.
5. ROMEYN, J. and WRIGHT, G. F. J. Am. Chem. Soc. 69: 697. 1947.
6. SAND, J. Ber. 34: 2910. 1901.
7. SAND, J. and SINGER, F. Ber. 35: 3170. 1902. Ann. 329: 166. 1903.

THERMAL DECARBOXYLATION OF URONIC ACIDS[1]

By A. S. Perlin

ABSTRACT

A novel decarboxylation of uronic acids by merely heating the material without the use of a solvent or added catalyst is described. At approximately 255°C. decarboxylation for uronic and polyuronic acids and salts within 15 min. reaction time is nearly quantitative. Vigorous dehydration occurs simultaneously, the residue corresponding basically to a 5-carbon skeleton that contains 1.5 atoms of oxygen. Other products of the reaction are minor and include carbon monoxide, and traces of acid and oils. Sugar acids, such as gluconic and ascorbic, are not as extensively decarboxylated. The reaction is employed for analysis of several nitrogen dioxide oxidized celluloses and starches and the results are in good agreement with those given by titration and the 12% hydrochloric acid method.

INTRODUCTION

A striking property of uronic acids is the ease with which they are decarboxylated by boiling with strong mineral acids (7). Preliminary tests by the author indicated that decarboxylation may be achieved also by heat in the absence of added catalyst. Since this property of uronic acids had not been previously reported it invited further investigation. The present paper describes some aspects of the reaction; attention is also given to its possible use for estimating uronic acids, as an alternative to the methods commonly employed—modifications of the Lefevre-Tollens reaction, reviewed by Nevell (11), and titration procedures, reviewed by Davidson and Nevell (2).

EXPERIMENTAL

Apparatus and Procedure

The reaction was first carried out at diminished pressure (5×10^{-3} mm.) as suggested by the work of Puddington on the thermal decomposition of reducing sugars and starch (14). Carbon dioxide produced was trapped with liquid air and absorbed in standard barium hydroxide solution. Subsequent experiments were performed at atmospheric pressure in the following manner. The sample tube, containing 0.1 to 0.2 gm. of material, was held in a horizontal position to prevent water formed in the reaction from condensing and falling back onto the sample. Heating was effected with an air bath consisting of a glass retort in which a stable liquid was refluxed at the desired reaction temperature (e.g., diphenyl ether, 255°C.; methyl phthalate, 280°C.). A steady stream of carbon dioxide free nitrogen was passed successively over the sample, through a U-tube surrounded by brine, and through two gas-scrubbers of concentrated sulphuric acid. The entrained, dry carbon dioxide was absorbed with ascarite and weighed. In some experiments traces of oxygen were removed from the nitrogen stream with Fieser's solution (3), but this procedure did not alter the results. After a given heating time the tube was quickly cooled and the system flushed with nitrogen for a further 15 min. For estimation of water the U-trap was surrounded with dry

[1] *Manuscript received November 9, 1951.*
Contribution from the Division of Applied Biology, National Research Laboratories, Ottawa, Canada. Issued as N.R.C. No. 2690.

ice – toluene and was evacuated together with the sample tube, so that the water distilled into the trap at room temperature; volatile acid dissolved in the water was titrated. Sometimes the nitrogen stream issuing from the ascarite tube was collected under water and analyzed gasometrically for carbon monoxide.

A continuous rate curve could not be obtained from an individual sample, since several minutes flushing was required after a given heating period to sweep carbon dioxide completely into the ascarite tube. Each carbon dioxide value therefore represents a separate experimental run which, in many instances, was repeated. Temperature equilibration time as compared with total reaction time was slow. For example, at a retort temperature of 255°C. the interior of the sample tube reached 245°C. in 5 min., whereas most total reaction periods were less than 20 min. The actual reaction temperature was therefore only a function of the reflux temperature of the liquid in the retort. However, at a given retort temperature, results were generally reproducible with less than 5% error and appeared to reflect the true *relative* reaction temperature. All temperatures are in degrees Centigrade (°C.).

Materials and Methods

Alginic acid was prepared from commercial sodium alginate by precipitation as the calcium salt (15); the free acid was liberated with cold 0.1 *N* hydrochloric acid, washed successively with water and alcohol, and dried *in vacuo* over phosphorus pentoxide. Mucic acid, m.p. 204-206°C., was prepared by the oxidation of D-galactose with nitric acid. Barium-D-glucuronate and -D-galacturonate of theoretical barium content (26%) were prepared by Dr. C. T. Bishop. Nitrogen dioxide oxidized celluloses were obtained from Tennessee Kodak Corporation, except for oxycell *A*, a commercial preparation ("Oxycell", Parke-Davis). Nitrogen dioxide oxidized starches were supplied by Dr. R. W. Kerr, Corn Products Refining Co. Wheat straw hemicelluloses (1) and wheat flour pentosans (13) were prepared in these laboratories. The other materials referred to later in the text were commercial preparations of the best quality obtainable. All samples were dried *in vacuo* over phosphorus pentoxide.

Uronic acid was estimated by the 12% hydrochloric acid modification of Tracy (17) and by calcium acetate titration according to Meesook and Purves (10). In analysis of the nitrogen dioxide oxidized starches with calcium acetate the reaction temperature was 18°C. so as to minimize yellowing of the solutions. Furfural was estimated by the bromine oxidation method of Hughes and Acree (4).

RESULTS

Decarboxylation at Reduced and Atmospheric Pressures

Puddington (14) found that starch and several sugars at a pressure of 10^{-4} mm. and temperatures ranging about 200° did not evolve appreciable quantities of carbon dioxide in reaction periods of three to four hours. In contrast (Fig. 1), the carbon dioxide yield from alginic acid under similar conditions was substantial, within two hours being about two-thirds of that

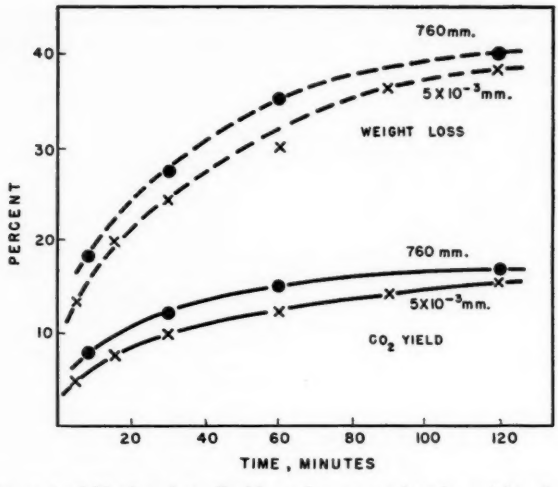

FIG. 1. Per cent yield of carbon dioxide and per cent loss in weight of alginic acid at 200°C. at atmospheric and diminished pressures.

theoretically possible (25%) by complete decarboxylation of the uronic carboxyl groups. Weight loss in this period reached 40%, and the difference between this and the carbon dioxide yield was due chiefly to water formed in the reaction (shown below) equivalent to about three moles per mole of carbon dioxide. The reaction was not a function of diminished pressure but of the elevated temperature since the results were not materially altered at atmospheric pressure (Fig. 1). For easier manipulation subsequent runs were therefore carried out at atmospheric pressure.

Although uronic carboxyl groups were the most likely source of the carbon dioxide, some may have come from new carboxyl groups created in the residues of already decarboxylated units through internal oxidation–reduction, while other uronic units remained intact. The former source would be favored if one mole of carbon dioxide were found for each uronic acid unit decomposed. Decomposition could not be measured directly. However, to derive some indication of its extent the partially-decomposed samples, at the end of the

TABLE I

RELATION OF CARBON DIOXIDE YIELD TO AMOUNT OF ALGINIC ACID DECOMPOSED

200°/0.005 mm.		200°/760 mm.	
% Theoretical* CO_2	% Loss potential furfural	% Theoretical* CO_2	% Loss potential furfural
17.6	14.0	30.0	35.0
29.6	26.4	39.2	46.2
37.0	43.0	48.0	52.7
56.8	63.0	61.0	71.3

Based on 25% carbon dioxide as the theoretical yield.

reaction period, were analyzed in the usual way (4) for furfural production. It was assumed that few, if any, pentose residues were present in these samples as reaction products because of the extensive dehydration; also, that furfural or derivatives, if formed, would have distilled or condensed to tar at the temperature employed. Accordingly, the only sources of furfural for analysis were the uronic acid units which had escaped decomposition. Since the quantity obtainable from intact alginic acid was known (22.0%), the decrease in this original amount as the reaction proceeded (i.e., the loss of potential furfural) gave an index of the number of units decomposed. Table I shows that the amounts of decomposition measured in this way corresponded reasonably well to the accompanying yields of carbon dioxide. The results therefore indicated that perhaps 90%, if not the entire yield, of the carbon dioxide was produced by decarboxylation of the uronic carboxyl groups.

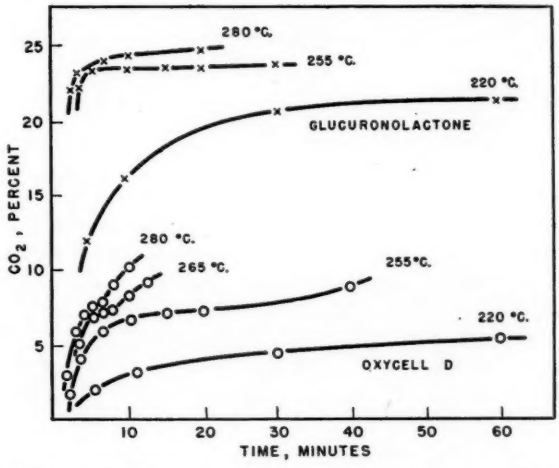

FIG. 2. Variation with temperature in the rate of evolution of carbon dioxide from glucuronolactone and oxycell *D*.

Influence of Temperature

The influence on decarboxylation of temperatures higher than 200° is illustrated in Fig. 2 which gives rates of evolution of carbon dioxide for a pure uronic acid (glucuronolactone) and for a polyuronide of low uronic acid content (oxycell *D*, described in a succeeding section). The respective carboxyl values (COO^-) were 24.5% by alkali titration, and 7.3% by calcium acetate titration. At 220° the rates were logarithmic, falling off at 70 to 80% of these values. The initial rates at 255° were considerably more rapid and evolution of carbon dioxide virtually ceased during the period 10-20 min. reaction time when the total amounts evolved approximated the expected values. The actual values found at 15 min. (as representative of the near-level portions of the curves) were 23.5 and 7.0% carbon dioxide, respectively. Pronounced breaks at approximately the same values were attained at 280°

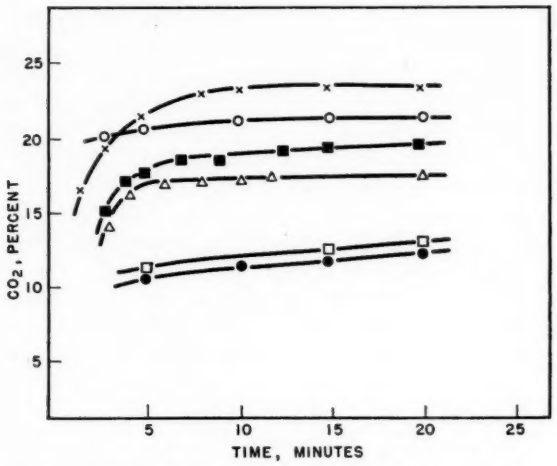

FIG. 3. Evolution of carbon dioxide by uronic acids and salts at 255°C.
– × – alginic acid; – ○ – sodium alginate; – ■ – galacturonic acid monohydrate;
– Δ – citrus pectin; – □ – barium glucuronate; – ● – barium galacturonate.

in about five minutes reaction time, with oxycell *D* then showing a secondary evolution of carbon dioxide. The latter was again evident at 265° after a slightly larger time interval, and was attributed to degradation of the anhydroglucose units comprising the non-uronide portion of the polymer. These and similar results for other uronic acids and polyuronides indicated that a temperature of about 255° was satisfactory for complete decarboxylation. The reaction period required for this was about 15 min. in marked contrast to reflux periods of at least 5 hr. usually reported for theoretical decarboxylation with mineral acids.

Rates of thermal decarboxylation for other uronic and polyuronic acids and salts at 255° (Fig. 3) were also characterized by an initial rapid rate of reaction followed by a pronounced falling off to a slow steady state in 10-15 min. reaction time. The yields of carbon dioxide for each at 15 min. corresponded closely to theoretical (Table II).

TABLE II

YIELDS OF CARBON DIOXIDE FROM URONIC ACIDS AND SALTS IN 15 MIN. AT 255°

Material	Expected CO_2, %	Found CO_2, %
Alginic acid	25.0*	23.4
Galacturonic acid .H_2O	20.5**	19.4
Citrus pectin	16.5***	17.3
Sodium alginate	22.2*	21.5
Barium glucuronate	16.8*	16.7
Barium galacturonate	16.8*	17.0

**Calculated.*
***By calcium acetate titration.*
****By 12% hydrochloric acid (17).*

Decarboxylation of the salts was especially vigorous, and for sodium alginate was accompanied by formation, with almost explosive violence, of a dense smoke. This behavior was not observed with any of the other materials examined and was presumed to be due to the reaction of the sodium ion with water in the reaction tube. The rate for sodium alginate fell off somewhat at 220° but still was more rapid than that for glucuronolactone (Fig. 2) at the same temperature, the yields of carbon dioxide being 16.8, 19.0, 20.4, and 20.6% at 5, 10, 20, and 30 min., respectively. All this suggested the possibility of basic catalysis, but alginic acid (60 mesh) admixed with an excess of sodium carbonate showed no enhanced rate of decarboxylation. In this connection, powdered glass, copper–chrome oxide catalyst, and potassium acid sulphate also failed to alter the rate of decarboxylation of alginic acid at 255°.

Products of the Reaction

Loss in weight of the reactant compounds at 255° was almost entirely recoverable as carbon dioxide and water (Table III). Other products were carbon monoxide in amount ranging about 1%, traces of volatile acid and admixed lactone, distillable oil, and a product which formed a char in the first sulphuric acid bubbler. The latter was not trapped with brine nor with dry ice – toluene; tests for formaldehyde with chromatropic acid reagent were negative. Measured as the increase in weight of the bubbler, the char comprised 1-2% of the products. Distillable oil accounted for much of the discrepancy (5-10%) observed in total recovery.

Extent of dehydration is indicated in another manner by comparing the last two columns in Table III. The number of oxygen atoms per monomer unit, which were removed as water at approximately theoretical decarboxylation, accounted for all but 1.5 atoms of the noncarboxyl oxygen of the acids and 2.0 to 2.5 of the salts. Since the metal cations of the latter should form alkali or alcoholates instead of water, theoretical becomes 4.0 for the barium uronates and 3.0 for sodium alginate. Thus combined dehydration and decarboxylation uniformly reduced the oxygen contents to about 1.5 atoms per monomer unit.

From the decreasing water/carbon dioxide ratios found with increasing degree of decarboxylation over the temperature range of 200-280° (Fig. 4), it appeared that dehydration was particularly intensive during early stages of the reaction. The very high ratios for galacturonic $.H_2O$ (*A*) at the outset were probably due to the loss of water of hydration, which was expected to require a much lower energy of activation than the loss of water of constitution. Recalculation of the results to the basis of the anhydrous acid gave the broken-line plot (*B*), which more closely parallels that for glucuronolactone (*C*). Extrapolation of *B* and *C* shows that dehydration during the early stages accounted for all of the oxygen theoretically available for water formation (Table III)—five atoms for galacturonic and four atoms for glucuronic. One interpretation is that decarboxylation at first was accompanied by complete deoxygenation (and dehydrogenation) with carbon dioxide and water

TABLE III

PRODUCTS OF THE THERMAL DECARBOXYLATION OF URONIC ACIDS AND SALTS

Material	Reaction time, min.	% CO_2	% H_2O	% Wt. loss	% Recovery	Moles H_2O/CO_2	Theoretical O atoms available/mole
Glucuronolactone	5	23.6	24.4	50.6	94.8	2.5	4.0
	15	23.6	24.4	51.6	93.0	2.4	
Alginic acid	5	21.1	23.1	46.8	94.4	2.7	4.0
	15	23.5	24.5	49.7	96.6	2.6	
Galacturonic.H_2O	5	17.7	34.9	53.4	98.5	4.8	6.0
	15	19.2	35.5	56.4	97.0	4.5	
Sodium alginate	5	20.7	17.1	41.9	90.2	2.0	4.0
	20	21.0	19.0	44.8	89.3	2.2	
Barium glucuronate	5	15.9	15.0	33.3	92.8	2.3	5.0
	15	16.7	15.7	34.3	94.5	2.3	
Barium galacturonate	5	16.1	16.2	34.0	95.0	2.4	5.0
	15	17.0	16.7	35.4	95.2	2.4	

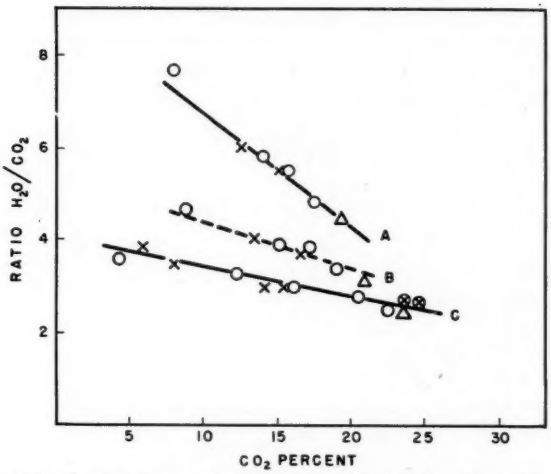

FIG. 4. Variation in the water/carbon dioxide ratio with decarboxylation. (*A*) galacturonic acid monohydrate, (*B*) galacturonic acid (calculated as anhydrous acid), (*C*) glucuronolactone. Reaction temperatures, °C. : 200° (×) 220° (○), 255° (Δ), 280° (⊗).

being, presumably, the only products. Later, other types of degradation occurred to small extent to form carbon monoxide, volatile acids, etc., and the relative amount of water was less. Polymerization possibly became the important side-reaction since at theoretical decarboxylation the residues contained 1.5 atoms of oxygen per monomer unit, corresponding basically to a 5-carbon skeleton having one atom of oxygen and sharing another with an adjacent 5-carbon skeleton (except for sodium alginate in which only 1.0 atom of oxygen remained). Polymerization was further indicated by the charred appearance of the residues, and since thermal decomposition of reducing sugars and starch involves preliminary dehydration and polymerization (5, 14).

Thermal Decomposition of Related Carbohydrates

Thermal decomposition of sugar acids, reducing sugars, and polysaccharides was also examined under the conditions described above. Sugar acids— gluconic, mucic, and ascorbic— were readily decarboxylated at 255°. They differed from uronic acids, however, by yielding somewhat less than the theoretical amounts of carbon dioxide in 15 min. reaction time; the respective amounts were 70, 65, and 85% (Fig. 5). Other differences between their behavior and that of uronic acids were evident at 220° if the rates of decarboxylation of ascorbic and gluconic acids were compared with that for glucuronolactone (Table IV). In contrast to the logarithmic evolution rate of carbon dioxide for glucuronolactone, that for ascorbic acid showed a decided break reaching a constant value within 10 min. when, instead of 22.0% as at 255°, the total carbon dioxide yield was only 17.5%. The rate for gluconic acid was much slower and the induction period evident at 255° was now more prolonged.

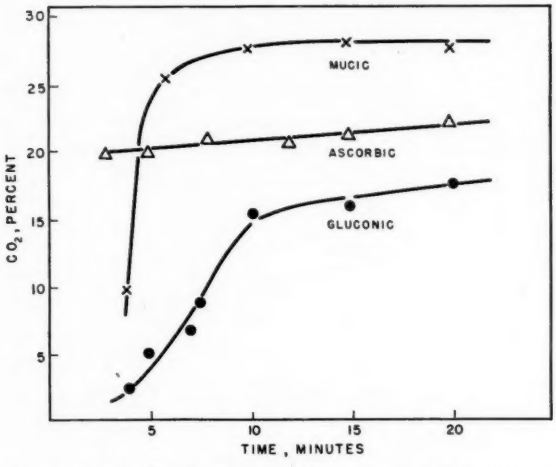

FIG. 5. Evolution of carbon dioxide by sugar acids at 255°C.

To some extent these results paralleled the relative response of these acids to decarboxylation with 12% hydrochloric acid. Kenyon *et al.* (16) showed ascorbic acid to yield carbon dioxide at a rate somewhat faster than did uronic acids, while gluconic acid was decarboxylated only to a small extent. They attributed these differences to steric effects exerted by the carbonyl groups which lessened the stability of the carboxyl groups. According to this interpretation the enediol group of ascorbic acid was most effective, the potential aldehyde of the uronic acid somewhat less effective, while the absence of a carbonyl group in gluconic acid accounted for its relatively greater stability. It is possible that similar influences operated in the compounds decarboxylated thermally, the carboxyl groups accordingly being more resistant or less resistant to thermal decarboxylation.

Reducing sugars examined were L-arabinose, D-xylose, D-glucose, and D-galactose, each of which gave only about 3% of carbon dioxide in 15 min. at 255°, although from the charred appearance of the residues, extensive decomposition had occurred. Under the same conditions good quality wheat and corn starch and cotton linters all yielded negligible amounts of carbon

TABLE IV

DECARBOXYLATION OF GLUCURONOLACTONE, ASCORBIC ACID, AND GLUCONIC ACID AT 220°

Time, min.	% CO_2			
	5	10	30	60
Glucuronolactone	12.0	16.0	20.5	21.2
Ascorbic acid	15.5	17.4	17.6	—
Gluconic acid	0	1.5	7.1	12.7

dioxide. However, wheat straw hemicelluloses evolved carbon dioxide equivalent to two and three times the small uronic acid values (3-4%) indicated by the 12% hydrochloric acid method. A wheat flour pentosan, of negligible uronide content by the same method, yielded 3-4% of carbon dioxide by thermal decomposition. However, when the arabofuranose units present were removed from the pentosan by graded hydrolysis (13) the carbon dioxide yield became negligible. This behavior perhaps accounts for the anomalous results given by the straw hemicelluloses since they also contained arabofuranose units (1).

Thermal Decarboxylation of Nitrogen Dioxide Oxidized Celluloses and Starches

Kenyon *et al.* (8, 9, 16, 18, 19) have shown that the action of nitrogen dioxide on cellulose predominantly effects oxidation of primary hydroxyl groups, the products being polyuronides to an extent depending on the degree of oxidation. Ketone groups were thought to be present in small quantities (8), an interpretation supported by Nevell (12) who also suggested formation of non-uronide carboxyl groups. Starch oxidized with nitrogen dioxide is known to be structurally akin to the oxidized celluloses (6). It was therefore of special interest to examine the thermal decarboxylation of these synthetic polyuronides since they provided well-characterized substrates having widely different amounts of uronide residues in combination with non-uronide sugar units.

The rates of carbon dioxide evolution for several oxidized celluloses and starches (Figs. 6 and 7), as found previously for the natural uronic acids and polyuronides, were initially rapid and then fell off markedly at 10-20 min. reaction time. Values for carbon dioxide represented by the near-level portions of the curves generally agreed reasonably well with the corresponding

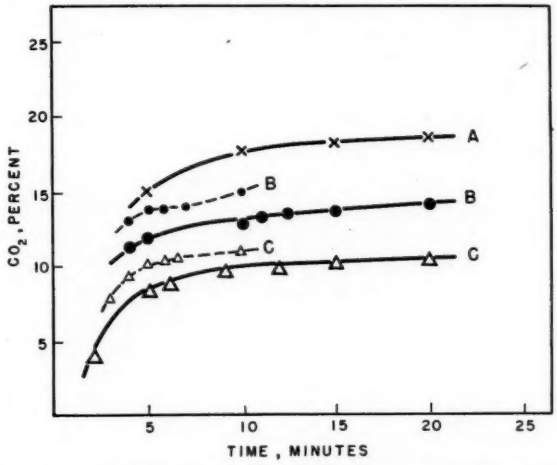

FIG. 6. Evolution of carbon dioxide by nitrogen dioxide oxidized cellulose (Oxycells *A*, *B*, and *C*); temperatures: —— 255°C.; - - 280°C.

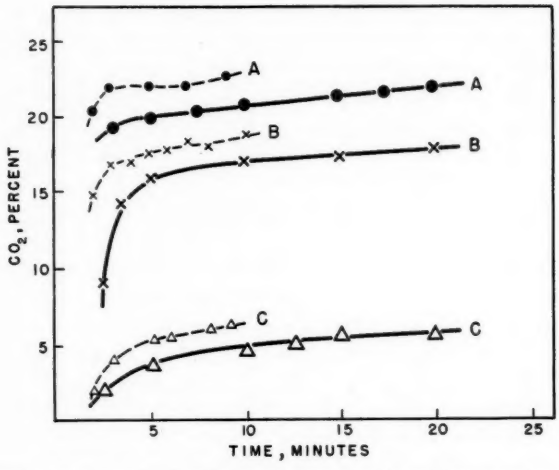

FIG. 7. Evolution of carbon dioxide by nitrogen dioxide oxidized starches (Oxystarch *A*, *B*, and *C*); temperatures: —— 255°C.; – – 280°C.

values for uronic acid obtained by conventional methods of analysis (Table V). Significance of the thermal values is emphasized by reference to the rates of evolution at 280° represented by the broken-line plots of Figs. 6 and 7. It is seen that a line drawn parallel to the abscissa from the 15 min. point at 255° and through the broken-line curve coincides with the region of maximum inflection of the curve in each instance. Results of the titration and 12% hydrochloric acid techniques were, themselves, not always in good agreement. Perhaps this disagreement was to be expected since Kenyon *et al.* (9) generally found higher results for the oxidized celluloses by titration than with hydrochloric acid, whereas Nevell (11) found the opposite to be the case. In view of these contradictions, the thermal decarboxylation procedure appears to be no less trustworthy for measuring the uronic acid content of these materials than the methods currently in use.

TABLE V

CARBOXYL VALUES OF NITROGEN DIOXIDE, OXIDIZED CELLULOSES, AND STARCHES

Material	Calcium acetate COO^-, %	Thermal* CO_2, %	12% HCl** CO_2, %
Oxycell *A*	—	18.0	18.2
Oxycell *B*	14.9	13.7	14.3
Oxycell *C*	10.8	10.5	8.4
Oxycell *D****	7.3	7.0	6.2
Oxystarch *A*	23.7	21.5	23.5
Oxystarch *B*	14.5	17.3	22.5
Oxystarch *C*	5.6	5.5	7.0

**15 min. reaction time.*
***11 hr. reflux.*
****See Fig. 1.*

The water/carbon dioxide ratios for oxidized celluloses *A*, *B*, and *C* were each about 3.6 at 5 min. and changed to 3.4, 4.2, and 4.7, respectively, at 15 min. reaction time. These results indicated only a moderate degree of dehydration of the non-uronide portions, particularly in the early stages of the reaction.

DISCUSSION

The foregoing results indicate that all uronic acids may be decarboxylated thermally in the absence of added catalyst, the respective rates differing little. The reaction applies equally well whether the material exists as the free acid, lactone, or salt, and whether alone or combined with other uronic acid or carbohydrate units. At temperatures close to 255° and above, decarboxylation is very rapid and yields almost theoretical quantities of carbon dioxide within a period of 15 min. reaction time.

The carbon dioxide appears to come from the uronic carboxyl groups exclusively. Support for this contention is found in the fact that no pure uronic acid yielded more than that expected by complete decarboxylation, and that expected in the relation between the carbon dioxide and furfural yields of progressively decomposed alginic acid. An explanation for these results may be found in the intensive dehydration which accompanies thermal decarboxylation, especially in the early stages of the reaction. The oxygen content of the molecule is thus depleted to a point where there is little chance of new carboxyl groups arising by internal rearrangements, and oxygen of the air appears to have little influence on the carbonaceous residue. Since non-uronide sugar units, when present, are dehydrated more slowly than uronide groups, intermolecular oxidation–reduction has more opportunity to occur and may result in formation of new carboxyl groups. Thus, in oxidized celluloses and starches with varying amounts of anhydroglucose residues, substantial secondary evolution of carbon dioxide follows initial decarboxylation of the uronic component. The two phases are satisfactorily differentiated under proper conditions with these materials, but some of the hemicelluloses examined do not respond in like manner. The ease with which sugar acids are decarboxylated suggests that similar structures, if present, would also interfere with the carbon dioxide value. A satisfactory means for separating this kind of decarboxylation from that of uronic acids is not suggested by the present results, although a partial separation may be achieved by lowering the reaction temperature.

The thermal reaction is thus intermediate in scope between titration methods and the 12% hydrochloric acid procedure since (in addition to uronic carboxyl) all non-uronide carboxyl groups are titrated, whereas they are perhaps 70% decarboxylated thermally and 15% by acid. Titration methods, however, have the disadvantage of interference from ash and acidic impurities and may not measure stable lactone forms of the uronic acids (9). These shortcomings do not apply in either decarboxylation method. On the other hand, evolution of carbon dioxide from oxidized celluloses and alginic acid by acid decarboxylation does not reach a constant value, and the method is

therefore regarded by Nevell (11) as only a rough measure of the proportion of uronic acid groups present. In contrast, the evolution of carbon dioxide by thermal decarboxylation at a proper temperature reaches a constant value within the theoretical range for many uronide materials. However, not all of the materials tested behaved satisfactorily. Hence wider application of this reaction must await further examination.

ACKNOWLEDGMENTS

The technical assistance of Mr. J. Giroux and the helpful interest of Dr. I. E. Puddington are gratefully acknowledged. Tennessee Kodak Corporation kindly donated samples of nitrogen dioxide oxidized cellulose, and nitrogen dioxide oxidized starches were the gift of Dr. R. W. Kerr, Corn Products Refining Company. Analyses for carbon monoxide were kindly made by Mr. A. K. Light.

REFERENCES

1. ADAMS, G. A. and CASTAGNE, A. E. Can. J. Chem. 29: 109. 1951.
2. DAVIDSON, G. F. and NEVELL, T. P. J. Textile Inst. 39: T102. 1948.
3. FIESER, L. J. Am. Chem. Soc. 46: 2639. 1924.
4. HUGHES, E. E. and ACREE, S. F. J. Research Natl. Bur. Standards, 21: 327. 1938.
5. HURD, C. D. and EDWARDS, O. E. J. Org. Chem. 14: 680. 1949.
6. KERR, R. W. J. Am. Chem. Soc. 72: 816. 1950.
7. LEFEVRE, K. V. and TOLLENS, B. Ber. 40: 4513. 1907.
8. MCGEE, P. A., FOWLER, W. F. Jr., UNRUH, C. C., and KENYON, W. O. J. Am. Chem. Soc. 70: 2700. 1948.
9. MCGEE, P. A., FOWLER, W. F. Jr., and KENYON, W. O. J. Am. Chem. Soc. 69: 347. 1947.
10. MEESOOK, B. and PURVES, C. B. Paper Trade J. 123 (No. 18): 35. 1946.
11. NEVELL, T. P. J. Text. Inst. 39: T118. 1948.
12. NEVELL, T. P. J. Textile Inst. 42: T91. 1951.
13. PERLIN, A. S. Cereal Chem. 28: 370. 1951.
14. PUDDINGTON, I. E. Can. J. Research, B, 26: 415. 1948.
15. ROSE, R. C. Can. J. Technol. 29: 19. 1951.
16. TAYLOR, E. W., FOWLER, W. F. Jr., MCGEE, P. A., and KENYON, W. O. J. Am. Chem. Soc. 69: 342. 1947.
17. TRACY, M. V. Biochem. J. 43: 185. 1948.
18. UNRUH, C. C. and KENYON, W. O. J. Am. Chem. Soc. 64: 127. 1942.
19. YACKEL, E. C. and KENYON, W. O. J. Am. Chem. Soc. 64: 121. 1942.

SYNTHESIS OF PARA-BRIDGED BENZENE COMPOUNDS. III[1]

By M. F. Bartlett, S. K. Figdor, and K. Wiesner

ABSTRACT

2-5-Octamethylene tetrahydrophthalic anhydride does not form even a trace of the corresponding phthalic anhydride on dehydrogenation, but partly dissociates back into cyclododecadiene and maleic anhydride. 2-5-Nonamethylene tetrahydrophthalic anhydride dehydrogenates with considerable difficulty.

In a previous communication (2) we have shown that 2-5-decamethylene and 2-5-tetradecamethylene tetrahydrophthalic acids can be converted smoothly to the corresponding phthalic acids by dehydrogenation with Pd-charcoal in boiling naphthalene. We have now synthesized in exactly the same manner the 2-5-nonamethylene (II) and 2-5-octamethylene (I) tetrahydrophthalic acids and investigated their dehydrogenation. Under the conditions where the 10-membered bridge compound was formed smoothly neither of the two new compounds (I and II) gave a trace of dehydrogenated product. In both cases only starting material was recovered, with complete absence of the typical ultraviolet absorption spectrum of phthalic acid. If the dehydrogenation of Compound I was carried out without solvent with Pd-charcoal at 340° a small amount of a neutral volatile compound was obtained which gave an infrared spectrum identical with cyclododecadiene, showing that dissociation of the Diels-Alder adduct has taken place. The acidic fraction was starting material as checked by the complete absence of the typical ultraviolet absorption.

In the solvent free dehydrogenation of Compound II, no diene was found but the recovered acidic substance which was essentially starting material showed an absorption spectrum which corresponded to approximately 10% of the phthalic acid.

It was therefore concluded that although the dehydrogenation is hindered very strongly in this case, it nevertheless could be achieved under conditions that are sufficiently drastic. We have therefore subjected a larger amount of Compound II to a selenium dehydrogenation and analyzed carefully the products. The acidic material obtained by saponification of the dehydrogenation mixture was converted into an oily anhydride by sublimation.

The ultraviolet absorption spectrum of this product was perfectly in agreement with those of our previous 2-5-polymethylene phthalic anhydrides and is shown in Fig. 1, Curve I. (Curve II is the ultraviolet spectrum of 2-5-diethyl phthalic anhydride.)

The oily anhydride failed to crystallize and therefore it was not possible to make it analytically pure.

It was necessary to resort to oxidation studies to prove the structure. Oxidation with permanganate gave a good yield of 1,2,3,4-benzene tetra-

[1] *Manuscript received October 18, 1951.*
Contribution from the Chemistry Laboratories of the University of New Brunswick, Fredericton, N.B.

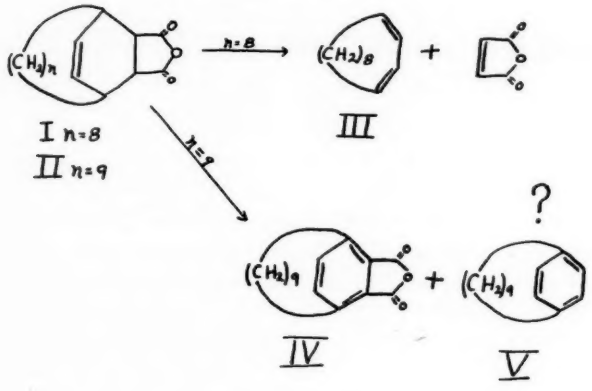

carboxylic acid, identified as methylester by mixed melting point and infrared spectrum. If we therefore combine this result with the agreement of the ultraviolet absorption there is hardly any doubt that we really had 2-5-nonamethylene phthalic anhydride IV.

The only other explanation, which is not considered likely, is that the nonamethylene bridge was ruptured in the middle during the dehydrogenation. The neutral fraction of the dehydrogenation mixture was chromatographed and a hydrocarbon was isolated which analyzed perfectly for 1-4-nonamethylene benzene. The quantity was not sufficient to allow structure proof by oxidation. The infrared spectrum showed bands at 1510 and 1600 cm.$^{-1}$, which are quite characteristic of an aromatic ring. Para substitution also causes characteristic bands at 800 and 875 cm.$^{-1}$ Bands at 796, 808, 858 cm.$^{-1}$, and 876 cm.$^{-1}$ are really present in the spectrum but they are weak. In view of the extremely small amount of the compound a definite decision as to whether or not the compound is 1-4-nonamethylene benzene was not possible.

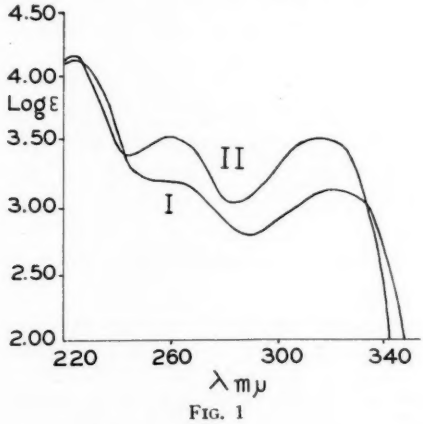

FIG. 1

EXPERIMENTAL

Synthesis of the tetrahydrophthalic acids I and II was performed exactly as previously (1). Therefore we give here only the analyses constants and yields of all new compounds.

Cyclododecene-one-3.—Yield 34%; b.p. 142°-153°C. at 16-18 mm.

Cyclododecene-ol-3.—Yield 90%; b.p. 105°-110°C. at 2-4 mm. Calculated for $C_{12}H_{22}O$: C, 79.06; H, 12.17; act. H, 0.54%. Found C, 79.09; H, 12.11; act. H, 0.54%.

Phenylurethane m.p. 95-96°C. Calculated for $C_{19}H_{27}O_2N$: C, 75.71; H, 9.03; N, 4.65%. Found: C, 75.54; H, 9.08; N, 4.78%.

Cyclododecadiene.—Yield 68%; b.p. 84°C. at 4 mm. Ultraviolet max. 230 mμ. Calculated for $C_{12}H_{20}$: C, 87.73; H, 12.27%. Found: C, 87.54; H, 12.27%.

2-5-Octamethylene tetrahydrophthalic anhydride I.—Yield of the oily anhydride 7.4%; b.p. in a collar flask 170-175°C. (outside temperature) at 0.6 mm. Calculated for $C_{16}H_{22}O_3$: C, 73.24; H, 8.45%. Found: C, 73.00, 73.03; H, 8.35, 8.25%.

Cyclotridecene-one-3.—Yield 46%; b.p. 119-125°C. at 0.5 mm.

Cyclotridecene-ol-3.—Yield 88%; b.p. 129-134°C. at 1 mm. Calculated for $C_{13}H_{24}O$: C, 79.54; H, 12.32; act. H, 0.51%. Found: C, 79.64; H, 12.30; act. H, 0.52%.

Cyclotridecadiene.—Yield 45%; b.p. 82°C. at 1 mm. Ultraviolet max. 232 mμ. Calculated for $C_{13}H_{22}$: C, 87.54; H, 12.44%. Found: C, 86.79; H, 12.48%.

2-5-Nonamethylene tetrahydrophthalic anhydride II.—Yield of oily anhydride 17.2%. Recrystallized from ether – petroleum ether to a constant melting point, it melted at 148-150°C. Calculated for $C_{17}H_{24}O_3$: C, 73.88; H, 8.75%. Found: C, 73.69; H, 8.88%.

DEHYDROGENATION OF ANHYDRIDE I

Compound I (200 mgm.) was mixed with 200 mgm. of Pd-charcoal and heated for 30 min. to 340°C. After this the product was saponified by stirring 24 hr. with 10 ml. of 10% potassium hydroxide and separated into acidic and neutral material. The neutral product was a colorless oil (35 mgm.) which boiled in a collar flask at 65-67° at 4 mm. and gave an infrared spectrum identical with cyclododecadiene. The acidic material was reconverted into the anhydride by sublimation. It had no ultraviolet absorption.

SELENIUM DEHYDROGENATION OF ANHYDRIDE II

Compound II (2.18 gm.) and 8.7 gm. of selenium were heated in a sealed tube for 19 hr. at 370°C. The content of the tube was then extracted with ether and the residue, after the evaporation of the ether, saponified by stirring 24 hr. with 130 ml. of 10% potassium hydroxide. The products were then separated into neutral (453 mgm.) and acidic (720 mgm.) material. The neutral material was chromatographed on 18.1 gm. of alumina. Petroleum

ether eluted from this column 106 mgm. of an oil which distilled in a collar flask at 85-95°C. at 0.05 mm. The middle fraction was analyzed. Calculated for $C_{15}H_{22}$: C, 89.02; H, 10.97%. Found: C, 88.92; H, 10.97%.

The acidic material was converted by sublimation in high vacuum into the oily anhydride.

The ultraviolet spectrum is given in Fig. 1, Curve 1.

OXIDATION WITH PERMANGANATE

This oxidation was done on 686 mgm. of 2-5-nonamethylene phthalic anhydride in exactly the same way as before (2). The yield after several recrystallizations was 14 mgm. of pure benzene 1,2,3,4-tetracarboxylic methylester, which melted at 129-131°C. alone and in admixture with an authentic specimen. Also the infrared spectra of both compounds were identical.

ACKNOWLEDGMENTS

This work was performed on a grant from the National Research Council, Ottawa. The microanalyses were performed by the microanalytic laboratory of Dr. Robert Dietrich, Zurich, Switzerland.

The infrared spectra were taken by Dr. Bohon in the Anderson Physical Laboratory, Champagne, Ill. To him we are also indebted for their interpretation.

REFERENCES

1. INGRAHAM, R. B., MACDONALD, D. M., and WIESNER, K. Can. J. Research, B, 28: 453. 1950.
2. WIESNER, K., MACDONALD, D. M., INGRAHAM, R. B., and KELLY, R. B. Can. J. Research, B, 28: 561. 1950.

THE MECHANISMS OF GLUCOSE PENTAACETATE ANOMERIZATION AND LEVOGLUCOSAN FORMATION[1]

By R. U. Lemieux and Carol Brice[2]

ABSTRACT

The stannic chloride catalyzed anomerization of the pentaacetyl-D-glucopyranoses in chloroform solution is specific for the C1-acetoxy group. The reactions involve complete dissociation of the C1-carbon atom to acetoxy group bond with an intermediate formation of carbonium ions. The initial step of the *beta* to *alpha* rearrangement is a rapid dissociation, involving the participation of the C2-acetoxy group, to a resonance-stabilized carbonium ion with the lactol carbon atom occupied in the α-configuration. The rate-controlling step in the reaction appears to be the rearrangement of this ion to other ions which are capable of recombining with acetate ion to yield the α-acetate. The α-acetate is highly stable, as compared to the β-anomer, and the dissociation of the C1-carbon atom to acetoxy group bond is the rate-controlling step in its rearrangement. The stability of the α-acetate toward a variety of acidic reagents which readily dissociate the β-form is pointed out. For example, although the α-acetate is highly stable toward titanium tetrachloride, the reaction of the β-anomer with this reagent, to yield tetraacetyl-β-D-glucopyranosyl chloride, is extremely fast. This product is unstable under the reaction conditions used and rearranges to the α-form at a measurable rate. 1, 2, 3, 4-Tetraacetyl-β-D-glucopyranose with stannic chloride in chloroform solution yielded triacetyl-D-glucosan <1, 5>β <1, 6>. The alkaline hydrolysis of triacetyl-D-glucosan <1, 5> α <1, 2> yielded D-glucosan <1, 5> β <1, 6>. The mechanisms of these reactions are discussed.

Since our first communication[1], Bonner (1) has published the results of a mechanistic study of the *alpha–beta* rearrangement of the glucose pentaacetates in acetic acid – acetic anhydride mixtures with sulphuric acid as catalyst. We have studied the rearrangement under the conditions described by Pacsu (15) which involve the use of stannic chloride as catalyst with pure chloroform as solvent.

The rearrangement of methyl tetraacetyl-β-D-glucopyranoside to the α-form in chloroform solution with stannic chloride (15), titanium tetrachloride (16), or boron trifluoride (21) as catalysts suggests that the analogous stannic chloride catalyzed *beta* to *alpha* rearrangement of the glucose pentaacetates is specific for the C1-acetoxy group. Bonner (1) has shown that tetraacetyl-β-D-glucopyranosyl benzene was essentially unaffected by solution in propionic anhydride which contained sulphuric acid. Under the same conditions, pentaacetyl-β-D-glucopyranose was converted rapidly to 1-propionyl-tetraacetyl-α-D-glucopyranose and Bonner concluded that the anomerization involved no structural change other than that at the anomeric center.

[1] *Manuscript received December 17, 1951.*
Contribution from the National Research Council, Prairie Regional Laboratory, Saskatoon, Sask. Issued as Paper No. 136 on the Use of Plant Products and as N.R.C. No. 2689. Presented in part at the 34th Annual Conference, the Chemical Institute of Canada, Winnipeg, Man., June 18-20, 1951.

[2] *This paper is based partly on a thesis submitted by Carol Brice to the School of Graduate Studies of the University of Saskatchewan, Saskatoon, Sask., in partial fulfillment of the requirements for the degree of Master of Arts.*

We have carried out the following transformations in order to establish definitely that the stannic chloride catalyzed *beta* to *alpha* isomerization of pentaacetylglucopyranose in chloroform solution involves only the inversion of the lactol carbon atom. Acetobromoglucose (I) with silver propionate in propionic acid yielded a substance (III), m.p. 104-105°C., specific rotation + 3.5° in chloroform. Although there could be little doubt about the structure of III, it seemed desirable to prepare the substance in an independent manner since it could not be predicted with certainty that the decomposition of an intermediate such as VII would not involve replacement at the C6-carbon atom to yield tetraacetyl-6-propionyl-β-D-glucopyranose (VI). 2,3,4,6-Tetraacetyl-β-D-glucopyranose (II) with propionyl chloride gave a substance identical with III. It has been suggested (4) that 1,2,3,4-tetraacetyl-β-D-glucopyranose (V) possesses or can assume the *ortho*acid structure VIII. Since II depresses the melting point of V, the compounds are not identical (4). However, if V should in fact possess the structure VIII, then it might be expected that under reaction conditions the substance II could also assume the structure VIII. Thus, the propionylation of either II or V would yield the same product. However, the propionylation of V yielded a new compound believed to be tetraacetyl-6-propionyl-β-D-glucopyranose (VI), m.p. 112-113°C., specific rotation + 5.8° in chloroform. Therefore, the substance III is in fact 1-propionyl-tetraacetyl-β-D-glucopyranose. Bonner (1) reported this compound to melt at 97-97.5°C. with zero specific rotation at 25°C. in chloroform. The product (IV) obtained on the anomerization of III in stannic chloride – chloroform solution was converted to acetobromoglucose using hydrogen bromide in propionic acid. The identity of the acetobromoglucose was substantiated by converting the compound to methyl tetraacetyl-β-D-glucopyranoside. Since 1-propionyl-tetraacetyl-β-D-glucopyranose (III) could be converted to methyl tetraacetyl-β-D-glucopyranoside in the same manner, it can be concluded that IV, m.p. 71.3-72.3°C., specific rotation + 102° in chloroform, was 1-propionyl-tetraacetyl-α-D-glucopyranose. Bonner (1) reported this compound to melt at 72-73°C. with specific rotation + 95° at 22°C. in chloroform.

Stereochemical considerations render it highly improbable that the *beta* to *alpha* rearrangement involves a continuous shift of the C1-acetoxy group from one side of the pyranose ring to the other. However, the anomerization could conceivably proceed through an open chain intermediate such as IX.

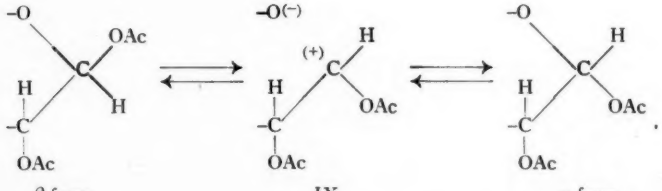

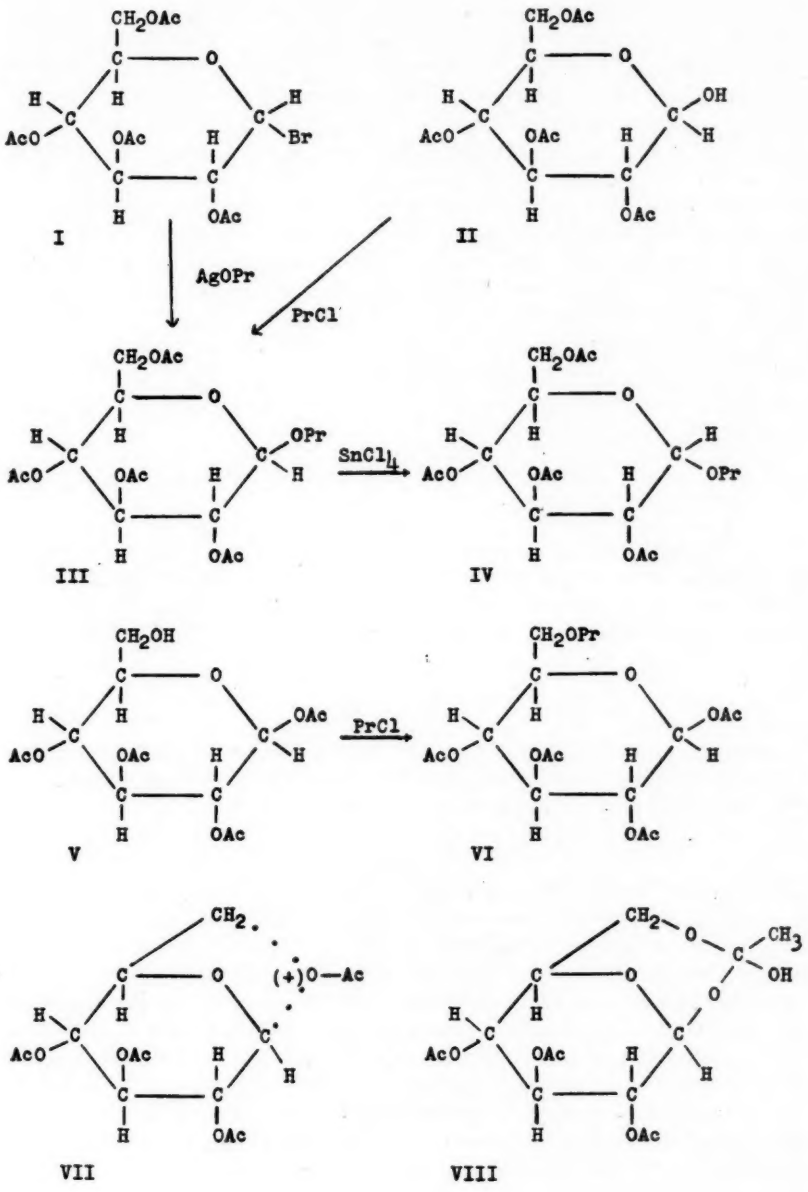
I
II
AgOPr
PrCl
III
IV
SnCl4
V
VI
PrCl
VII
VIII

Evidence which disposed of this possibility and established the reaction to involve a complete dissociation of the C1-carbon atom to acetoxy group bond was obtained by anomerizing pentaacetyl-β-D-glucopyranose with carbon-14 labeled C1-acetoxy group in the presence of an equal amount of nonradioactive pentaacetyl-β-D-galactopyranose. The pentaacetyl-α-D-glucopyranose and pentaacetyl-α-D-galactopyranose thus formed were isolated by the addition of inactive carrier and recrystallization to constant activity. The activity was found to be distributed between the two sugar acetates with a slight preponderance in the galactose derivative. This exchange requires that the reaction involve a complete dissociation of the acetoxy group to lactol carbon atom. The difference in radioactivity found in the products was undoubtedly due to different rates in the formation of acetochloro derivatives, compounds which are known to form under the conditions used (15).

A quantitative yield of silver chloride was obtained on treating silver acetate with an excess of stannic chloride in chloroform and it seems probable that there resulted a chloroform solution of stannic chloride and stannic trichloride acetate (X).

$$SnCl_4 + AgOAc \rightarrow SnCl_3OAc + AgCl$$

X

The Lewis acid, stannic chloride, undoubtedly catalyzes the anomerization of β-glucose pentaacetate by complexing with the C1-acetoxy group to lead to the equilibrium represented by Equation 1. If the anomerization were carried out in the presence of carbon-14 labeled stannic trichloride acetate and

(1) $$SnCl_4 + AcO\text{-}Gl(OAc)_4 \rightleftarrows SnCl_4OAc^{(-)} + Gl(OAc)_4{}^{(+)}$$

XI

if exchange between this substance and the ion XI were rapid (Equation 2), it would be expected that the resulting anomerized glucose pentaacetate mixture would contain radioactive C1-acetoxy groups.

(2) $$SnCl_3OAc^* + SnCl_4OAc^{(-)} \rightleftarrows SnCl_3OAc + SnCl_4OAc^{*(-)}$$

This was the case and the following data establish this exchange reaction to be very rapid. When pentaacetyl-β-D-glucopyranose was anomerized in chloroform solution in the presence of such a source of radioactive acetate ions, the radioactivity in the reaction product, the α-anomer, indicated that exchange was 93% complete. However, when pentaacetyl-α-D-glucopyranose was treated under the same reaction conditions—conditions which were much more vigorous than required for completing the *beta* to *alpha* rearrangement—the radioactivity of the recovered α-anomer indicated only 29% exchange. It was therefore evident that the dissociation of the C1-carbon atom to acetoxy group bond is accomplished much more readily for the β-anomer than for the α-anomer.

Lemieux (9) has shown that pentaacetyl-α-D-glucopyranose is much more stable toward acid catalyzed mercaptolysis than is the β-anomer and the high

reactivity of the β-compound was attributed to a participation of the C2-acetoxy group in the dissociation of the C1-carbon atom to acetoxy group bond. It has been widely assumed that the anomeric forms of a sugar acetate are equally suitable as starting materials for the preparation of their aceto-chloro derivatives by reaction with titanium tetrachloride and, in fact, it has been proposed (16) that pentaacetyl-α-D-glucopyranose is an intermediate in the conversion of the β-acetate to α-acetochloroglucose. However, we have

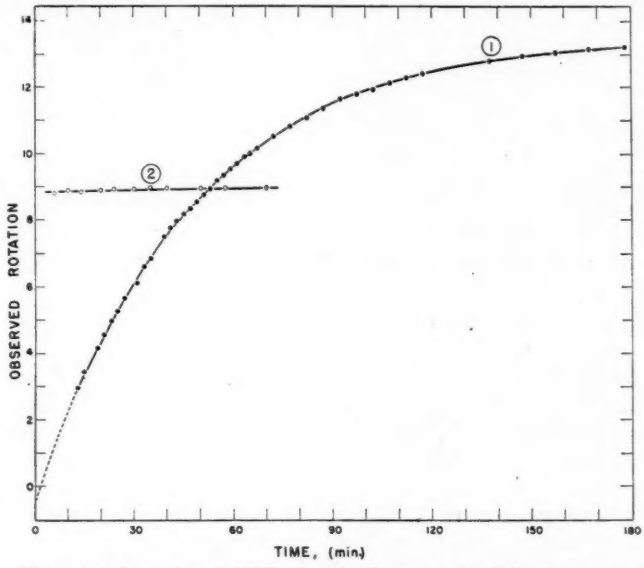

FIG. 1. The rates of reaction at 40°C. of equimolar amounts of the glucose pentaacetates and titanium tetrachloride in chloroform solution. 1. Pentaacetyl-β-D-glucopyranose. 2. Pentaacetyl-α-D-glucopyranose.

found pentaacetyl-α-D-glucopyranose to remain essentially unchanged under conditions which converted the β-anomer to tetraacetyl-α-D-glucopyranosyl chloride in excellent yield (7) and the difference in reactivity is illustrated by Fig. 1. Using the integrated polarimetric rate expression,

$$k = \frac{2.303}{t} \log \frac{a_0 - a_\infty}{a_t - a_\infty},$$

the rate of the reaction using the β-anomer was found to be first order as shown by the rate constants calculated at various times given in Table I. It was therefore apparent that the rate-controlling step for the reaction is a rearrangement or decomposition of a rapidly formed intermediate which, under the conditions used, required about three hours at 40°C. to go to completion. When the reaction was allowed to proceed for only five minutes at 40°C. and the mixture was washed free of titanium tetrachloride, tetraacetyl-β-D-glucopyranosyl chloride (17) was readily isolated from the resulting chloroform solution. Furthermore, the solution displayed the slow mutarotation described by Schlubach, Stadler, and Wolf (18) for β-acetochloro-

TABLE I

REACTION AT 40°C. OF EQUIMOLAR AMOUNTS OF PENTAACETYL-β-D-GLUCOPYRANOSE AND TITANIUM TETRACHLORIDE IN CHLOROFORM SOLUTION

Time, min.	Observed rotation	k, min.$^{-1}$
0	− 0.50° (calc.)	—
15	3.47	0.0223
25	5.29	0.0215
35	6.89	0.0216
45	8.21	0.0218
55	9.24	0.0218
65	10.03	0.0216
87	11.39	0.0220
97	11.83	0.0222
212	13.45	—
227	13.45	—

glucose in chloroform solution. It was therefore evident that pentaacetyl-β-D-glucopyranose reacts extremely rapidly with titanium tetrachloride to yield tetraacetyl-β-D-glucopyranosyl chloride and that the reaction which was followed to yield the data described in Fig. 1 and Table I is actually the rearrangement of the latter compound to the α-anomer.

It has been pointed out (9) that a variety of reactions of pentaacetyl-β-D-glucopyranose appear to involve a ready formation of an intermediary resonance-stabilized carbonium ion and it would be expected that the first step in the *beta* to *alpha* rearrangement of glucose pentaacetate (XII) would lead to the carbonium ion XIII. This idea was confirmed by carrying out the anomerization in the presence of the stannic chloride acetate source of radioactive acetate ions for only five minutes—conditions which bring about the formation of only a small amount of α-anomer. The recovered starting material possessed a radioactivity which indicated that in this short period of time about 75% exchange had occurred. Therefore, under the anomerizing conditions, the β-anomer is readily dissociated to the carbonium ion XIII of α-D-configuration which readily recombines with acetate ion to revert to starting material.

Pacsu (15) has shown that the stannic chloride catalyzed rearrangement is accompanied by the formation of acetochloroglucose and we were unable to follow the course of the reaction under conditions which gave a chlorine-free product. As pointed out by Pacsu, it would be expected that the reaction be first order, however, rate constants calculated from our data using the above first order rate equation yielded values which decreased considerably in magnitude with increasing time. This result probably is related to the decrease in catalyst concentration with time brought about by the side reactions. The plots of Fig. 2 show the high stability of the α-anomer as compared to the β-form.

The above information allows the following interpretation for the mechanism of the *beta* to *alpha* rearrangement of the pentaacetylglucopyranoses. Under the reaction conditions used, the β-anomer (XII) is rapidly dissociated to the carbonium ion XIII. Recombination of the ions proceeds readily with a

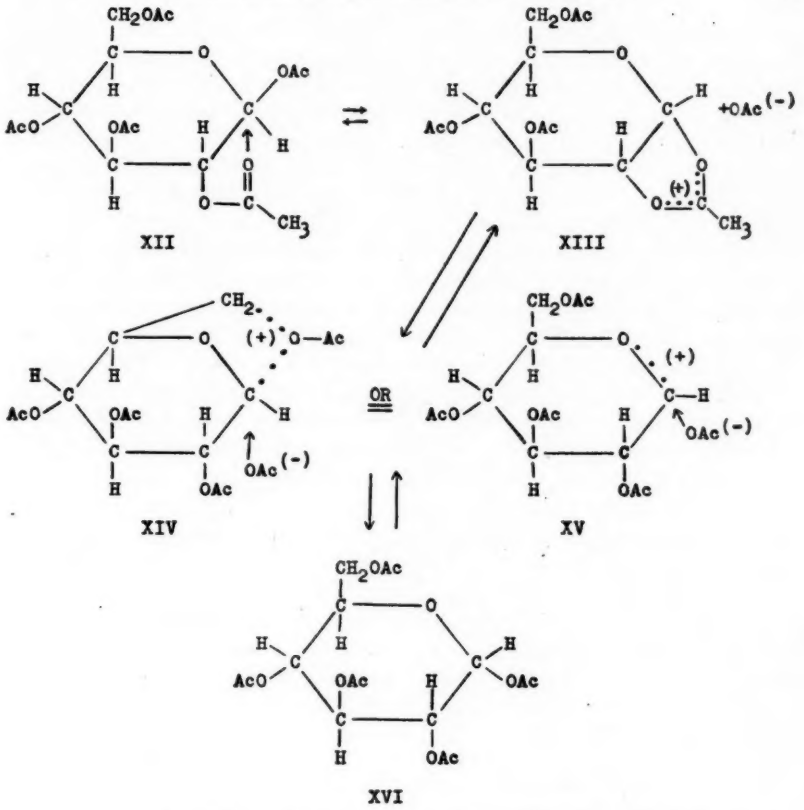

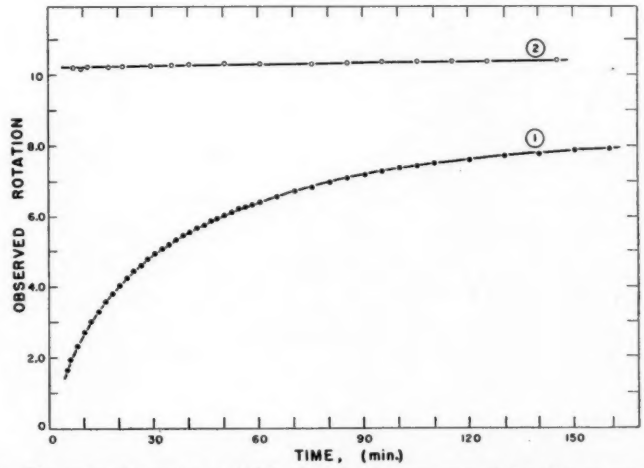

FIG. 2. The rates of reaction at 40°C. of equimolar amounts of the glucose pentaacetates and stannic chloride in chloroform solution. 1. Pentaacetyl-β-D-glucopyranose. 2. Pentaacetyl-α-D-glucopyranose.

second inversion of the lactol carbon to reform the starting material. The formation of the α-anomer from the ionic intermediates requires that the lactol carbon atom be liberated from its attachment in the α-D-configuration of XIII. This ion must therefore be in equilibrium with carbonium ions of different structure such as XIV or XV. It is possible that such a rearrangement of XIII is facilitated by an approach of a negatively-charged ion. Nevertheless, the formation of the α-anomer would require an interaction of acetate ion with ionic intermediates such as XIV or XV. From the rate plots of Fig. 2, it is obvious that the α-anomer, after having formed, has no effect on the observed reaction rate for the β-anomer. That is, the observed reaction rate must be related to the forward reaction—the *beta* to *alpha* anomerization. Since the dissociation of the β-anomer appears to be much faster than the observed reaction rate, this step cannot be rate-controlling for the forward reaction. Therefore, the rate-controlling step of the forward reaction must be concerned with the rate of formation of the α-anomer from the intermediary ions which, in turn, is related to the rearrangement of the carbonium ion XIII to other carbonium ions such as XIV or XV.

Treatment of the radioactive pentaacetyl-α-D-glucopyranose, which was prepared by subjecting nonradioactive α-anomer to anomerizing conditions in the presence of a source of radioactive acetate ions, with hydrogen bromide in acetic acid yielded, after two recrystallizations, an acetobromoglucose preparation with only 5% of the activity of the starting material. Thus, the *alpha* to *beta* rearrangement is also specific for the anomeric center. The high stability of the α-anomer has already been discussed and there can be little doubt that the dissociation of this compound is the rate-controlling step in its conversion to the β-anomer.

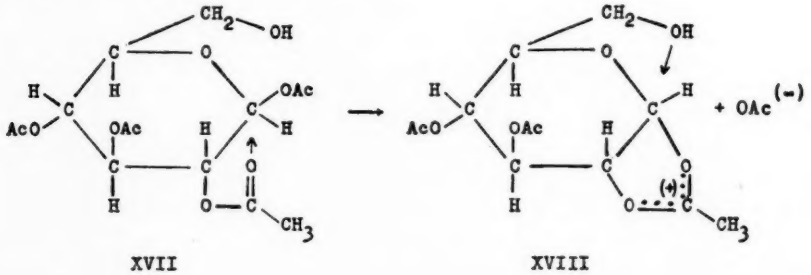

XVII XVIII

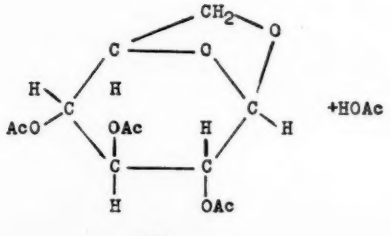

XIX

When 1,2,3,4-tetraacetyl-β-D-glucopyranose (XVII) was treated with a chloroform solution of stannic chloride, triacetyl-D-glucosan <1, 5>β<1, 6> (XIX) was isolated in good yield from the reaction product. This observation is further evidence for the participation of the C2-acetoxy group in the dissociation of the C1-carbon atom to acetoxy group bond and the formation of a transient carbonium ion of structure XVIII. The formation of β-glucosan under these acidic conditions should be contrasted to its formation by the alkaline hydrolysis of phenyl β-D-glucopyranoside (12). The high resistance to alkaline hydrolysis of phenyl α-D-glucopyranoside as compared to the β-anomer (12) could be the result of a participation of the C2-oxygen atom in the hydrolysis of the β-glucoside, a neighboring group participation which is not possible for the α-glucoside. On the basis of these ideas and the observation that such phenyl glucosides as phenyl 2,3-dimethyl-β-D-glucopyranoside were highly resistant to alkaline hydrolysis, McCloskey and Coleman (10)

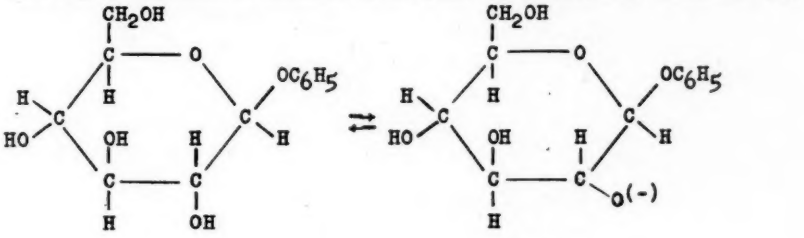

XX ⇌ XXI

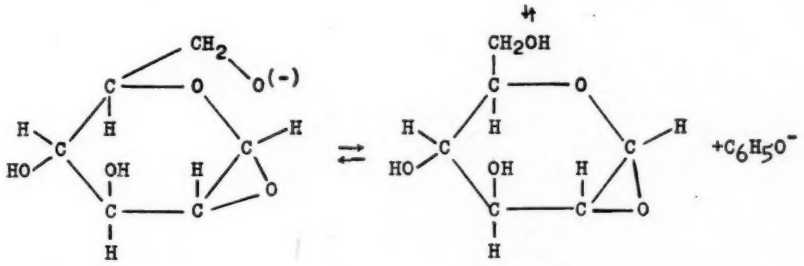

XXIII ⇌ XXII + $C_6H_5O^-$

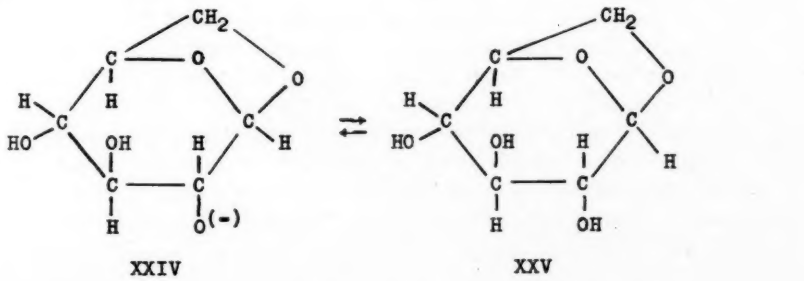

XXIV ⇌ XXV

have postulated the intermediary formation of D-glucosan <1, 5> α <1, 2> in the hydrolysis of phenyl β-D-glucopyranoside. We have found the alkaline hydrolysis of triacetyl-D-glucosan <1, 5> α <1, 2> to lead to the formation of D-glucosan <1, 5> β <1, 6>, an observation which confirms the mechanism proposed by McCloskey and Coleman. The reaction can therefore be considered to proceed as follows. Phenyl β-D-glucopyranoside (XX) in alkaline solution can be assumed to exist to some extent as the anion XXI. The decomposition of this ion to D-glucosan <1, 5> α <1, 2> (XXII) and phenolate ion is undoubtedly the rate-controlling step for the transformation. In the presence of alkali, the glucosan XXII probably passes into the anion XXIII which rearranges to the more stable form XXIV, an anionic form of the product, D-glucosan <1, 5> β <1, 6> (XXV). The instability of aryl β-glucosides (13) toward alkaline conditions as compared to alkyl β-glucosides is undoubtedly related to the high stability of aryloxide ions as compared to alkoxide ions. It is noteworthy that Heddle and Percival (5) have demonstrated the acidic properties of the C2 and C6 hydroxyl groups of glucosides.

The formation of the 1,6-glucosan ring from the ions XVIII and XXIII indicates that it is sterically possible for the C6-oxygen atom of pentaacetyl-α-D-glucopyranose to participate in a dissociation of the C1-carbon atom to acetoxy group bond. However, the high stability of this compound suggests that the ion VII is very unstable and unlikely to form. The same considerations apply to the formation of the ion XXVI.

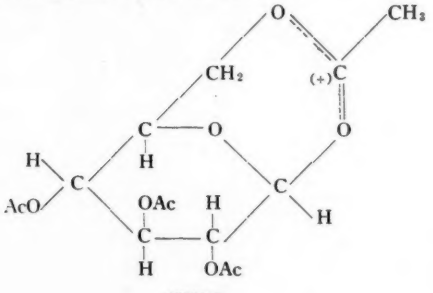

XXVI

EXPERIMENTAL

Instrumentation

The rotations were measured at room temperature, 23 to 28°C. The melting points are corrected. The radioactivities of "infinitely thick" samples were determined with a windowless counter operating with helium–isobutane in the Geiger region. Appropriate resolving-time and background corrections were made. The samples were mounted by filtration using Skellysolve F as dispersing agent on disks of Whatman Number 3 paper using a special funnel which ensured uniform distribution and constant surface area (14). All counts were referred to a carbon-14 labeled cellulose acetate standard of the same surface area. Successive mounts of a material gave results which did not differ by more than 3%.

1-Propionyl-tetraacetyl-β-D-glucopyranose

A mixture of tetraacetyl-α-D-glucopyranosyl bromide, 5 gm., silver propionate, 7 gm., and propionic acid, 50 ml., was shaken at room temperature for 15 min. and filtered. Both the filtrate, after dilution with water, and the filter cake were extracted with chloroform. The chloroform extract was neutralized with aqueous sodium bicarbonate solution, filtered, and evaporated to an oil which soon crystallized. After one recrystallization from ethanol, the yield was 4.0 gm., 82%, m.p. 96-98°C. Several further recrystallizations from ethanol raised the melting point to 104-105°C. with $[\alpha]_D + 3.5°$ (*c*, 1.2 in chloroform). Calc. for $C_{17}H_{24}O_{11}$: C, 50.50; H, 5.98%. Found: C, 50.42; H, 5.99%.

Propionyl chloride, 0.35 gm., was added to a mixture of 20 ml. dry benzene and 5 ml. pyridine at 0°C. To the resulting mixture, 1.00 gm. of 2,3,4,6-tetraacetyl-β-D-glucopyranose, m.p. 137-139°C., $[\alpha]_D + 14.2°$ (*c*, 2.9 in chloroform) (2), was added. After shaking at 0°C. for 15 min, then at room temperature for 90 min., the mixture was poured into ice water. The aqueous mixture was extracted with benzene and the benzene extract, washed several times with water, was evaporated to a syrup which soon crystallized. One recrystallization from ethanol gave 0.71 gm., 61% yield, of material melting at 93-96°C. After several recrystallizations from ethanol the substance melted at 104.5-105°C. A mixture with the substance prepared from acetobromoglucose melted at 104-105°C.

1-Propionyl-tetraacetyl-α-D-glucopyranose

1-Propionyl-tetraacetyl-β-D-glucopyranose, 8.1 gm., and anhydrous stannic chloride, 5.2 gm., were dissolved in 100 ml. of pure chloroform (15) and the solution was refluxed for five hours. The cooled solution was washed twice with ice water, the combined water extracts were extracted once with chloroform, and the combined chloroform extracts after washing with sodium bicarbonate solution were dried over calcium chloride. Evaporation of the solvents gave a syrup which soon crystallized. One recrystallization from ethanol gave 3.8 gm. of material, 47% yield, m.p. 62-66°C., $[\alpha]_D + 97.6°$ (*c*, 1 in chloroform). Four further recrystallizations from ethanol raised the melting point to 71.3-72.3°C. with $[\alpha]_D + 102°$ (*c*, 1 in chloroform). Calc. for $C_{17}H_{24}O_{11}$: C, 50.50; H, 5.98%. Found: C, 50.36; H, 5.97%.

Methyl Tetraacetyl-β-D-glucopyranoside from the 1-Propionyl-tetraacetyl-D-glucopyranoses

1-Propionyl-tetraacetyl-α-D-glucopyranose, 1.5 gm., was dissolved in 15 ml. of a 50% solution of hydrogen bromide in propionic acid. After 2.5 hr. at room temperature, a product, 0.60 gm., was isolated in the usual manner. After four recrystallizations from ether–Skellysolve C, the melting point was 87.5-88.2°C. with $[\alpha]_D + 199°$ (*c*, 0.73 in chloroform). This material, 230 mgm., was treated for three hours at room temperature with 230 mgm. of silver carbonate in 10 ml. of methanol. The product, 90 mgm., isolated in the usual manner melted at 103-104°C. with $[\alpha]_D - 18°$ (*c*, 0.79 in chloroform)

after two recrystallizations from methanol. A mixed melting point with methyl tetraacetyl-β-D-glucopyranoside, m.p. 104-105°C., was 103-104°C.

The above procedure was used to convert 1-propionyl-tetraacetyl-β-D-glucopyranose to acetobromoglucose, m.p. 87-88°C., in 52% yield from which methyl tetraacetyl-β-D-glucopyranoside, m.p. 103-104°C., was prepared in 48% yield.

Tetraacetyl-6-propionyl-β-D-glucopyranose

Propionyl chloride, 5 ml., was added at 0°C. to a solution of 30 ml. of pyridine in 30 ml. of dry benzene. Eight grams of 1,2,3,4-tetraacetyl-β-D-glucopyranose, m.p. 127.5-129°C., $[\alpha]_D$ + 11° (*c*, 2.5 in chloroform) (6), was added and the mixture was shaken first at 0°C. for 20 min. then at room temperature for three hours. The resulting mixture was poured into ice water and extracted with benzene. The benzene extract was washed several times with water and decolorized by filtration through a bed of Magnesol–Celite (5:1) (11). Removal of the benzene *in vacuo* and recrystallization of the product from ethanol gave 6.0 gm. of material, m.p. 110-112°C. Three further recrystallizations from ethanol raised the melting point to 112-113°C. with $[\alpha]_D$ + 5.8° (*c*, 1.1 in chloroform). Calc. for $C_{17}H_{24}O_{11}$: sapon. equiv., 80.5. Found: sapon. equiv., 80.1.

Radioactive Silver Acetate

The radioactive silver acetate used in this work was prepared by mixing aqueous solutions containing equivalent amounts of silver nitrate and sodium acetate labeled in the carboxyl group with carbon-14. The precipitate was washed with cold water, recrystallized from water, washed with ethanol, and dried *in vacuo* at 65°C.

1-Acetoxy-labeled Pentaacetyl-β-D-glucopyranose

A mixture of radioactive silver acetate, 25,600 counts per minute, 0.45 gm., acetobromoglucose, 1.00 gm., and 10 ml. of dry acetonitrile was refluxed for 30 min. The silver salts were removed by filtration and the filtrate after dilution with water was extracted with chloroform. The chloroform extract was washed with water, dried over sodium sulphate, and evaporated *in vacuo* to a syrup. The syrup was dissolved in ether and Skellysolve F was added until crystallization began. The yield was 0.31 gm. of material which gave 9900 counts per minute. The material was recrystallized from ethanol to yield 0.26 gm. of product, m.p. 130-132°C., 10,500 counts per minute. Recrystallization from ethanol gave 0.23 gm. of material, m.p. 131-132°C., 10,600 counts per minute. A third recrystallization from ethanol gave 0.22 gm. of product, m.p. 131.5-132°C., 11,000 counts per minute. Assuming equal self-absorption for the samples of silver acetate and glucose pentaacetate, the calculated radioactivity for the product would be 11,000 counts per minute.

Exchange on the Simultaneous Anomerization of Pentaacetyl-β-D Derivatives of Glucose and Galactose

Radioactive pentaacetyl-β-D-glucopyranose, 4640 counts per minute, 500 mgm., which was labeled in the 1-acetoxy group and nonradioactive

pentaacetyl-β-D-galactopyranose, 500 mgm., were dissolved in 30 ml. of dry chloroform and 1.57 gm. of stannic chloride was added. The solution was refluxed for five hours, cooled, and washed twice with ice water. The combined wash waters were extracted with chloroform and the combined chloroform solutions were washed with water, sodium bicarbonate solution, and again with water. The resulting chloroform solution was filtered and diluted to 100 ml. Nonradioactive pentaacetyl-α-D-galactopyranose, 1.00 gm., was added to a 50 ml. aliquot and nonradioactive pentaacetyl-α-D-glucopyranose, 1.00 gm., was added to the remaining solution. The chloroform was removed *in vacuo* and the crystalline residues were recrystallized from ethanol until pure. After six recrystallizations, the yield of pentaacetyl-α-D-galactopyranose was 623 mgm., m.p. 96-97°C., $[\alpha]_D$ + 109° (*c*, 1 in chloroform), 290 counts per minute. After seven recrystallizations, the yield was 460 mgm., m.p. 96-97°C., $[\alpha]_D$ + 108° (*c*, 1 in chloroform), 300 counts per minute. After five recrystallizations, the yield of pentaacetyl-α-D-glucopyranose was 938 mgm., m.p. 110.2-111.2°C., $[\alpha]_D$ + 103° (*c*, 1 in chloroform), 176 counts per minute. After six recrystallizations, the yield 726 mgm., m.p. 111.5-112°C., $[\alpha]_D$ + 103° (*c*, 1.2 in chloroform), 179 counts per minute.

Exchange on the Anomerization of Glucose Pentaacetates in the Presence of a Source of Radioactive Acetate Ions

Radioactive silver acetate, 60,800 counts per minute, 0.501 gm. (3 m.e.), and 1.57 gm. stannic chloride were added to 30 ml. of dry chloroform. Pure dry pentaacetyl-β-D-glucopyranose, 1.08 gm. (2.77 mM.), was added and the mixture was refluxed for seven hours. The insoluble salts were recovered by filtration and washed with chloroform. The yield of salts was quantitative, based on the formation of silver chloride, and treatment with sulphuric acid liberated no steam-volatile acidity. The chloroform filtrate was washed twice with ice water, then with sodium bicarbonate solution, dried over sodium sulphate, and evaporated *in vacuo* to a syrup which soon crystallized. Purification was by recrystallization from ethanol. After one recrystallization, the yield was 629 mgm., m.p. 99-104°C., 12,900 counts per minute. After two recrystallizations, the yield was 443 mgm., m.p. 110-111°C., $[\alpha]_D$ + 102° (*c*, 0.76 in chloroform), 12,600 counts per minute. After three recrystallizations, the yield was 368 mgm., m.p. 111.2-112°C., 12,600 counts per minute.

The percentage exchange in this reaction and the other exchange reactions described below can be calculated from the formula,

$$\% \text{ Exchange} = \left(\frac{a+b}{b}\right)\left(\frac{MA}{mB}\right) 100,$$

where a = mM. of glucose pentaacetate, b = m.e. of silver acetate, M is the molecular weight, 390, of glucose pentaacetate of A counts per minute, and m is the molecular weight of silver acetate, 167, of B counts per minute. Thus, the percentage exchange in the above experiment was,

$$\left(\frac{2.77+3}{3}\right)\left(\frac{390 \times 12{,}600}{167 \times 60{,}800}\right) 100 = 93\%.$$

Pure dry pentaacetyl-α-D-glucopyranose, 1.08 gm. (2.77 mM.), was treated under the same conditions as described above for the β-anomer using 0.501 gm. (3 m.e.) of silver acetate, 60,800 counts per minute. The product was purified by recrystallization from ethanol. After one recrystallization, the yield was 0.649 gm. of material, m.p. 109-111°C., 3500 counts per minute. A second recrystallization gave a substance, m.p. 111-111.5°C., with $[\alpha]_D + 104°$C. (*c*, 1.0 in chloroform) and a radioactivity of 3940 counts per minute, which was essentially pure pentaacetyl-α-D-glucopyranose. The percentage exchange was 29%. The radioactive α-glucose pentaacetate, 301 mgm., was dissolved in 2.5 ml. of 50% hydrogen bromide in glacial acetic acid and the solution was kept at room temperature for three hours. The product, isolated in the usual manner, weighed 106 mgm. after one recrystallization from ether and Skellysolve F, melted at 89-89.5°C., and possessed a radioactivity of 210 counts per minute. A second recrystallization gave a product, m.p. 89-89.5°C. with 197 counts per minute. Thus, at least 95% of the radioactivity of the starting material resided in the C1-acetoxy group.

Pure dry pentaacetyl-β-D-glucopyranose, 1.08 gm. (2.77 mM.), was treated under the same anomerizing conditions as described above using 0.501 gm. (3 m.e.) of silver acetate, 83,100 counts per minute, except that the reaction mixture was refluxed for only five minutes. The product was purified by recrystallization from ethanol. After one recrystallization, the material, 0.557 gm., melted at 127.8-129.8°C. and gave 12,700 counts per minute. A second recrystallization gave 0.505 gm. of product, m.p. 130.5-131.5°C., $[\alpha]_D + 5.50$ (*c*, 1 in chloroform) with 14,000 counts per minute. After a third recrystallization, the yield was 0.380 gm. of pure pentaacetyl-β-D-glucopyranose, m.p. 131.5-132.5°C., $[\alpha]_D + 3.4°$ (*c*, 1 in chloroform), which gave 13,900 counts per minute. This radioactivity corresponds to 75% exchange.

Rates of the Reactions of the Pentaacetyl-D-glucopyranoses with Stannic Chloride

The data plotted in Fig. 2 were obtained by dissolving at 40°C. and zero time 1.253 gm. (3.21 mM.) of dry glucose pentaacetate in 25 ml. of a solution of 0.879 gm. (3.37 mM.) of stannic chloride in pure dry chloroform (15). The acetate dissolved very rapidly and, as soon as solution was complete, the mixture was transferred to an all-glass 2 dm. polarimeter tube kept at 40 ± 0.1°C.

Rates of the Reactions of the Pentaacetyl-D-glucopyranoses with Titanium Tetrachloride

The data plotted in Fig. 1, part of which are listed in Table I, were obtained by dissolving with vigorous shaking at 40°C. and zero time 0.901 gm. (2.31 mM.) of dry glucose pentaacetate in 20 ml. of a solution of 0.440 gm. (2.29 mM.) titanium tetrachloride in chloroform. As soon as solution was complete, the mixture was transferred to the polarimeter tube as described above. The rotation at zero time was obtained by extrapolation.

A solution of 2.00 gm. pentaacetyl-α-D-glucopyranose in pure dry chloroform, 9.4 ml., was added to 0.98 gm. titanium tetrachloride in 3.3 ml. of the chloroform and the mixture was refluxed for three hours. The product,

isolated in the usual manner (16), weighed 1.19 gm. after one recrystallization from ether and Skellysolve C. After one more recrystallization the substance, $[\alpha]_D$ + 102° (*c*, 1.1 in chloroform), melted at 112-114°C. and this melting point was not depressed by the addition of the starting material.

Titanium tetrachloride, 0.88 gm., was dissolved in 40 ml. of pure dry chloroform and to the solution at 40°C. pentaacetyl-β-D-glucopyranose, 1.80 gm., was added. After shaking for five minutes at 40°C., the mixture, which still contained some yellowish precipitate, was poured into 100 ml. of ice water. After vigorous shaking, the chloroform layer was washed with sodium bicarbonate solution, then water, and dried over sodium sulphate for about 10 min. After 20 min. had elapsed from the time the reaction mixture had been added to the water, part of the dried chloroform solution, 15 ml., was added to a 2 dm. polarimeter tube kept at 25°C. and the remainder was worked up as described below. The initial rotation was + 1.89°. After 7, 24, and 48 hr., the rotations were + 3.26°, + 4.80°, and + 5.48°, respectively. Dry benzene, 25 ml., was added to the remaining chloroform solution and the mixture was evaporated *in vacuo* at 25°C. to a dry syrup. The syrup was dissolved in about 10 ml. of pure ether and the solution was cooled in a dry ice–acetone bath. On adding Skellysolve F to turbidity and scratching the side of the flask with a glass rod, a substance, m.p. 90-94°C., was soon precipitated. After recrystallization from the same solvents, the nicely crystalline material, $[\alpha]_D$ − 6° (*c*, 1.3 in pure chloroform), melted at 95-97°C. One more recrystallization gave a product, $[\alpha]_D$ − 8° → + 16° after 24 hr. (*c*, 1.1 in pure chloroform), which melted at 96-97°C. When ordinary chloroform was used the mutarotation was from − 8° to + 63° in 24 hr. Calc. for $C_{14}H_{19}O_9Cl$: Cl, 9.67%. Found: Cl, 9.68, 9.67%. Schlubach (17) has reported tetraacetyl-β-D-glucopyranosyl chloride to melt at 99-100°C. with $[\alpha]_D^{17}$ − 13.0° → + 81.2° after 24 hr. (*c*, 1 in pure chloroform) after many recrystallizations from ether.

*Acid Catalyzed Formation of Triacetyl-*D*-glucosan <1, 5> β <1, 6>*

1,2,3,4-Tetraacetyl-β-D-glucopyranose, 1.00 gm., was dissolved in 15 ml. of dry chloroform and 0.75 gm. of stannic chloride was added. After refluxing for five hours, the reaction mixture was washed twice in cold water, the wash waters were extracted with chloroform, and the combined chloroform extracts were washed with water, then sodium bicarbonate solution, and again with water. After drying over calcium chloride, the chloroform solution was evaporated to yield 0.30 gm. of a nicely crystalline material. After three recrystallizations from ethyl acetate, the material, $[\alpha]_D$ − 51° (*c*, 1.1 in ethanol), melted at 109-110°C. Tanret (19) has reported triacetyl-D-glucosan <1, 5> β <1, 6> to melt at 107-108°C. and the specific rotation in alcohol to be − 45.5°, Hurd and Cantor (7) have reported the constants m.p. 108°C., $[\alpha]_D^{20}$ − 58.6° (*c*, 0.18 in ethanol), while Vongerichten and Müller (20) have reported the substance to melt at 110°C. Our product possessed an infrared spectrum which was identical to that reported by Kuhn (8) for levoglucosan triacetate and deacetylation gave a material with the physical constants expected for D-glucosan <1, 5> β <1, 6>.

Base Catalyzed Formation of D-*glucosan* <1, 5> β <1, 6>

Crystalline triacetyl-D-glucosan <1, 5> α <1, 2> (3), m.p. 57-58°C., 0.600 gm., was dissolved in 20 ml. of dry acetone and 25 ml. of *N* aqueous potassium hydroxide solution was added. After 15 min. at room temperature the colorless solution was made only faintly alkaline to phenolphthalein indicator by a dropwise addition of 10% sulphuric acid. The salts which precipitated were removed by filtration and the filtrate was concentrated *in vacuo* to a dry semicrystalline syrup. Pyridine, 25 ml., and acetic anhydride, 25 ml., were added and the mixture was shaken at room temperature for four hours then kept at room temperature for 20 hr. The resulting mixture was poured into 200 ml. of ice water and the aqueous solution was extracted with chloroform. The chloroform extract was washed twice with water, filtered, and concentrated *in vacuo* to a yellow-colored oil. The oil was dissolved in 20 ml. of chloroform and this solution was extracted twice with 10 ml. of 10% hydrochloric acid, once with water, and finally with sodium bicarbonate solution. The resulting chloroform solution was dried by filtration and concentrated to a syrup which soon crystallized. Recrystallization from 2 ml. of ethyl acetate with the addition of Skellysolve F to turbidity gave 0.346 gm., 58% yield, of material, m.p. 107-108°C. After two further recrystallizations, the material, $[\alpha]_D$ − 51° (*c*, 1 in ethanol), possessed a melting point, 109-110°C., which was not depressed by admixture of the above described triacetyl-D-glucosan <1, 5> β <1, 6>.

ACKNOWLEDGMENTS

The authors wish to acknowledge their indebtedness to Dr. A. C. Neish for putting the counting equipment used in this work at their disposal, for providing them with the radioactive sodium acetate, and for many useful suggestions regarding the measurement of radioactivities.

REFERENCES

1. Bonner, W. A. J. Am. Chem. Soc. 73: 2659. 1951.
2. Georg, A. Helv. Chim. Acta, 15: 924. 1932.
3. Gladding, E. K. and Purves, C. B. J. Am. Chem. Soc. 66: 154. 1944.
4. Haworth, W. N., Hirst, E. L., and Teece, Ethel G. J. Chem. Soc. 1405. 1930.
5. Heddle, W. J., and Percival, E. G. V. J. Chem. Soc. 1690. 1938; 249. 1939.
6. Helferich, B. and Klein, W. Ann. 450: 219. 1926; 455: 173. 1927.
7. Hurd, C. D. and Cantor, S. M. J. Am. Chem. Soc. 60: 2677. 1938.
8. Kuhn, L. P. Anal. Chem. 22: 276. 1950.
9. Lemieux, R. U. Can. J. Chem. 29: 1079. 1951.
10. McCloskey, C. M. and Coleman, G. H. J. Org. Chem. 10: 184. 1945.
11. McNeely, W. H., Binkley, W. W., and Wolfrom, M. L. J. Am. Chem. Soc. 67: 527. 1945.
12. Montgomery, Edna M., Richtmyer, N. K., and Hudson, C. S. J. Am. Chem. Soc. 65: 3. 1943.
13. Montgomery, Edna M., Richtmyer, N. K., and Hudson, C. S. J. Org. Chem. 10: 194. 1945.
14. Neish, A. C. and Spyker, J. W. In preparation.
15. Pacsu, E. Ber. 61: 137. 1928.
16. Pacsu, E. Ber. 61: 1508. 1928.
17. Schlubach, H. H. Ber. 59: 840. 1926.
18. Schlubach, H. H., Stadler, P., and Wolf, Irene. Ber. 61: 287. 1928.
19. Tanret, G. Ber. 27: 665. 1894.
20. Vongerichten, E. and Müller, Fr. Ber. 39:245. 1906.
21. Whistler, R. L., Kimmell, K. Ann, and Durso, D. F. J. Am. Chem. Soc. 73: 3530. 1951.

MEASUREMENTS OF SELF-DIFFUSION IN AQUEOUS SOLUTIONS OF SODIUM DIHYDROGEN PHOSPHATE[1]

By J. E. Burkell and J. W. T. Spinks

ABSTRACT

Measurements of self-diffusion in aqueous solutions of sodium dihydrogen phosphate have been made using P^{32} as tracer. The method involves the preparation of two similar solutions differing only in the fact that one is "labeled" by means of the P^{32} isotope. A capillary cell is filled with the radioactive solution and immersed in a relatively large volume of inactive solution, maintained at a constant temperature. After diffusion has proceeded for a measured length of time, the cell is removed and the radioactivity of the liquid remaining in it measured by counting. The self-diffusion coefficient may be calculated from the length of the capillary cell, the period of diffusion, and the ratio of the final activity to the original activity. The method was checked by repeating some work on the self-diffusion of Na^+ in sodium iodide solution. Self-diffusion measurements were made with sodium dihydrogen phosphate solutions of several concentrations between 1.0 and 10^{-4} molar.

INTRODUCTION

In the past, many diffusion studies have been made in which a concentration difference exists between two portions of a medium.

The results of such experiments are evaluated in terms of one or another of the different forms of Fick's Law.

$$dm = - Dq \frac{dc}{dx} . dt \tag{1}$$

where dm is the amount of solute diffusing through an area, q, in time, dt, when dc is the concentration difference between two points in the solution, dx apart, and D is the diffusion coefficient. Physically, the diffusion constant, D, represents the amount of solute which would diffuse across unit area in unit time under unit concentration gradient.

An alternative form is

$$\frac{\partial c}{\partial t} = \frac{\partial}{\partial x}\left(D\frac{\partial c}{\partial x}\right) \tag{2}$$

which reduces to

$$\frac{\partial c}{\partial t} = D\frac{\partial^2 c}{\partial x^2} \tag{3}$$

when D is independent of concentration.

In general, the diffusion coefficient is not independent of the concentration and it becomes necessary, therefore, to distinguish between an average or integral value over a finite concentration interval and the differential value corresponding to a definite concentration. The differential diffusion coefficient has a much greater theoretical significance than an integral value. However, with many types of apparatus only an integral value may be obtained, since the diffusion results in a concentration change during the experiment. It

[1] *Manuscript received November 14, 1951.*
Contribution from the Department of Chemistry, University of Saskatchewan, Saskatoon, Sask. Paper presented at the Winnipeg meeting of the Chemical Institute of Canada, June 1951.

has been shown for some cases, notably steady state diffusion (6) and diaphragm diffusion (7) that differential values may be computed from integral coefficients. Gordon, stressing the necessity for caution in the interpretation of the experimentally measured diffusion coefficient, has written:

"One of the most curious phenomena in the whole field of diffusion has been the failure of many experimenters to recognize the distinction between the differential diffusion coefficient, valid for a concentration, and the integral coefficient which results from a measurement over a range of concentrations. The resulting confusion has had some unfortunate consequences since the 'diffusion constant' is usually only a constant in a Pickwickian sense of the term" (7).

In principle, any type of experiment will yield differential values if the concentration difference is made sufficiently small, but it is not possible in most cases to approach this condition at all closely. However, the utilization of tracer methods makes possible the study of diffusion under conditions of zero concentration difference. In this ideal case, a limiting value of the diffusion constant, called the self-diffusion coefficient, is obtained.

There is a second advantage in using tracer methods. The much greater sensitivity possible in the determination of materials by radioactive assay permits extension of the investigations to the range of very dilute solutions, where Fick's diffusion equations are strictly applicable. However, the qualifying assumption must be made in every case that, despite the slight mass difference, the tracer atom behaves precisely as the inactive isotope. This assumption appears to hold quite well for ions in aqueous solution where the ions are hydrated and presumably the mass differences are relatively small (2).

The increasing availability of radiosotopes over the past few years has led to the recent application by several workers of tracer methods to diffusion studies. The first experiments were actually done by Hevesy (9). In his experiments, radioactive lead (Th B) was plated onto the end surface of a lead cylinder and the penetration of the lead into itself was followed by measuring the intensity of the emerging radioactive rays from time to time. Similar studies have been made for other metals and more recently the method has been extended to salt crystals. In a study of the diffusion of sodium ion in a sodium chloride crystal, sodium chloride, labeled with Na^{22}, was coated onto one face of a sodium chloride crystal. After allowing the $Na^{22}Cl$ to penetrate for a suitable time, the crystal was pared down, slice at a time, and the activity of successive slices measured (11). The self-diffusion coefficients of various ions in solution have also been determined, and, in several instances, comparisons made with the values predicted from the theories of Nernst and Onsager. Self-diffusion measurements have been utilized in the study of high molecular weight compounds, and as a method of following changes in molecular complexity.

The diaphragm cell and several types of capillary cell have been successfully employed. The diffusion of the tracer isotope is followed by standard coun-

ting procedures. On the assumption of identical behavior, the diffusion behavior of the ion in question is thus revealed, and the self-diffusion coefficient is calculated by inserting these experimental data into the Fick equation, integrated for the boundary conditions of the experiment.

Brady and Salley (4), using a diaphragm cell, have determined the self-diffusion coefficient of Na^+ in sodium chloride solutions, and Jehle (10) has determined the values for Na^+ and Cl^- in solution by a capillary cell method. Some experiments of Adamson, Cobble, and Nielson (2) on self-diffusion coefficients of sodium ion in sodium chloride solutions are of particular interest. They used the isotopes Na^{22} and Na^{24} but no differences in diffusion behavior were observed. This is possibly due to the fact that the mass difference for the hydrated ions is relatively small. Self-diffusion coefficients for Na^+ and I^- in aqueous solution at 25°C. have been measured independently by Adamson (1) with a diaphragm cell, and by Wang and Kennedy (15) using a capillary cell with a shearing mechanism. The agreement between the results is very good. While the value for I^- ion lies close to that predicted by theory, the self-diffusion coefficient for Na^+ ion is found to be appreciably greater than the theoretical. It has been found by Whiteway *et al.* (16) that for Ag^+ ion diffusing in silver nitrate solution, this deviation in the self-diffusion coefficient does not occur. The value of tracer diffusion experiments as a test of theory is emphasized by the report of Robinson and Drew (13) of measurements with solutions of $10^{-5}M$. It is noteworthy that earlier, Onsager and Fuoss (12) were unable to obtain reliable results below 0.05 M with which to test their equation although since then, accurate data have been published for $10^{-3}M$ (8). Brady and Salley (4) appear to have been the first to study colloidal electrolytes by self-diffusion measurements in aqueous solutions. Anderson and Saddington (3) have applied self-diffusion coefficient measurements to the study of the reversible processes of aggregation in solution. A distinctive type of capillary cell was employed in which diffusion takes place from a capillary into a large body of liquid. This method has the special advantage that the measurement is relatively insensitive to slight vibrations as compared to larger capillaries (14).

A similar type of cell has been used in the present work for the determination of the self-diffusion coefficient of $H_2PO_4^-$ ion in aqueous sodium dihydrogen phosphate solutions. In experiments under conditions such that a concentration gradient is present, the gradient in specific gravity may be used to suppress convection and bulk mixing. This stabilizing effect is absent in self-diffusion experiments. The difficulty is overcome by the use of narrow capillary tubes as diffusion cells. The radioactive solution is contained in the capillary which is immersed in a relatively large volume of inactive solution of the same concentration. The success with which convection effects have been eliminated is evidenced by the independence of the measured self-diffusion coefficient of the duration of diffusion.

The experimental conditions are such that diffusion proceeds from a confined region of finite length across the interface into an infinite medium.

Integration of the general Fick equation

$$\frac{\partial c}{\partial t} = D\frac{\partial^2 c}{\partial x^2} \tag{4}$$

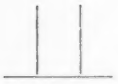

gives the ratio R of the average activity in the capillary after diffusion to that before diffusion,

$$R = \frac{8}{\pi^2}\left(\frac{e^{-\pi^2 Dt/4L^2}}{1} + \frac{e^{-9\pi^2 Dt/4L^2}}{9} + \frac{e^{-25\pi^2 Dt/4L^2}}{25}\right). \tag{5}$$

The series is rapidly convergent and sufficient accuracy is obtained if only the first term is used (the error due to neglecting higher terms is about 0.3% (5)). L is the length of the capillary.

$$\text{i.e. } R = \frac{8}{\pi^2}e^{-\pi^2 Dt/4L^2},$$

$$\ln R = \ln\frac{8}{\pi^2} - \frac{\pi^2 Dt}{4L^2},$$

$$\text{and } D = \frac{4L^2}{\pi^2 t}\left(\ln\frac{8}{\pi^2} - \ln R\right) = \frac{9.21L^2}{\pi^2 t}\left(\log\frac{8}{\pi^2} - \log R\right). \tag{6}$$

The main error in determining D will be due to errors in R. Differentiating Equation 6 with respect to R indicates that the effect of inaccuracies in R will be least when R is about 0.3. The effect does not change much for values of R up to 0.5 and owing to practical considerations in the experiments, the activity ratios were nearer this value (5).

EXPERIMENTAL

Capillary tubes about 1 mm. in diameter and from 2 to 4 cm. in length were used in the experiments. The cells were cut from a length of Pyrex tubing which was found, by measuring the length of a mercury thread in the bore, to have a uniform bore. Suitable lengths were cut and one end ground flat and square. The other end was ground to a taper to reduce the disturbance caused by immersion. The length of each was accurately measured with a micrometer. The capillary cells were held tight against the base of a lucite carrier by fitting them with threaded lucite collars and screwing these into suitably tapped holes in the carrier (Fig. 1). A good seal was ensured by a smear of silicone grease. Three such capillaries were held by the carrier consisting of the lucite base held horizontally by an upright glass rod. This apparatus had the advantage that the cells were conveniently removable for cleaning or replacement.

In carrying out an experiment, 200 ml. of inactive solution was filtered into a 250 ml. beaker, which rested on a cork disk in a 400 ml. beaker. The 400 ml. beaker was placed in a domed lid vacuum desiccator which was heavily weighted. The capillary cells were filled with a radioactive solution of the same concentration as the inactive solution and the glass rod of the carrier

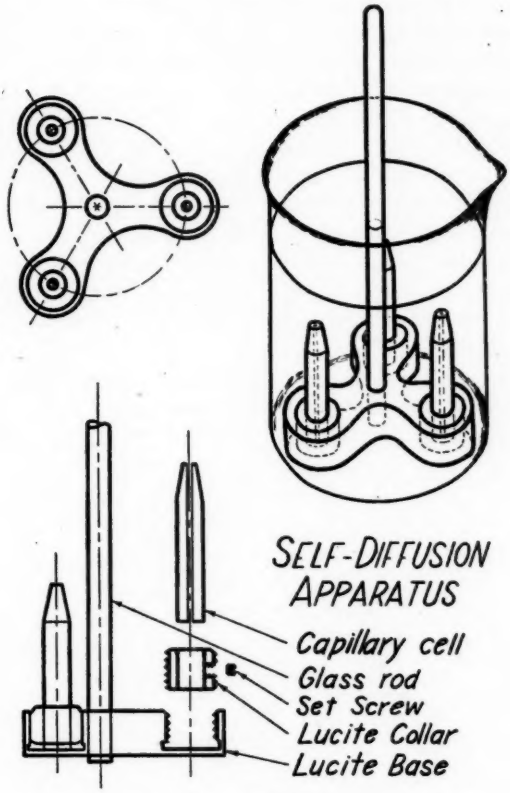

FIG. 1. Self-diffusion apparatus.

passed through a stopper fitted into the hole in the desiccator lid. The lid was placed on, and the desiccator put in the thermostat whose temperature was maintained at 25.0°C. The water level was such that the desiccator was almost completely covered. The carrier was then lowered until the open ends of the capillaries were just above the surface of the outer solution, and left in this position. When temperature equilibrium had been attained, the

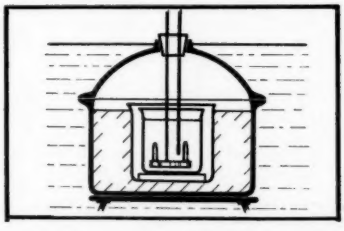

FIG. 2. Arrangement for self-diffusion experiment.

carrier was gently lowered until the cells were completely immersed. At the end of a known diffusion period, the carrier was raised, removed, and the exterior of the cells dried. The contents of each capillary cell was transferred to an aluminum counting tray by means of a fine pipette, the cell was washed three to five times with distilled water, these washings were added to the same tray, and the liquid content evaporated to dryness. A reference sample was then prepared by refilling the cell, previously dried, with the active solution, and transferring the cell contents to a tray as outlined above.

The radioactive content of the tray was then measured, using the G.M. counter, the reference sample being counted immediately before and after the experimental tray, so that no decay correction was required. From the radioactive ratio R, the self-diffusion coefficient is calculated.

Experiments with Na^{22}

In order to check the accuracy of the method, the self-diffusion coefficient of Na^+ in 0.1 M sodium iodide was measured, using Na^{22}, for comparison with the value obtained by Wang and Kennedy (15). The results are given in Table I.

TABLE I

SELF-DIFFUSION COEFFICIENT OF Na^+ IN 0.1 MOLAR NaI; 25.0°C.

Cell dimensions, mm.		Diffusion time, min.	R	$D \times 10^5$ cm.^{2} sec.$^{-1}$
Length	Diam.			
38.75	0.961	5208	0.415	1.30
40.23	0.961	5208	0.440	1.28
40.86	0.961	5208	0.455	1.25
38.75	0.961	7366	0.325	1.26
40.86	0.961	7366	0.349	1.29

The mean value is 1.282×10^{-5} cm.^{2}sec.$^{-1}$ as compared with 1.274×10^{-5} obtained by Wang and Kennedy under the same conditions.

The self-diffusion coefficients were calculated from the experimental results as in the following example:

The length of the cell was 38.75 mm. The diffusion time was 5208 min. The results of counting the diffusion sample and the reference samples prepared before and after the experiment were as follows:

	Observed counting rate, R/M*	Counting rate corrected for resolving time error, R/M	Background counting rate, R/M	Net counting rate, R/M
Reference sample	60.37	62.50	0.37	62.13
Diffusion sample	26.12	26.50	0.54	25.96
Reference sample	61.13	63.40	0.34	63.06

R/M = registers/minute; 1 register = 64 counts.
Mean value of net counting rate of reference samples = 62.60 R/M.

Proportion of activity remaining in cell after diffusion

$$= R = \frac{25.96}{62.60} = 0.415.$$

Hence,

$$D = \frac{9.21\ L^2}{\pi^2 t}\left(\log \frac{8}{\pi^2} - \log R\right)$$

$$= \frac{9.21\ (3.875)^2}{\pi^2 \times 5208 \times 60}\{(.9088 - 1) - (.6180 - 1)\}$$

$$= 1.30 \times 10^{-5}\text{cm.}^2\text{sec.}^{-1}$$

Experiments with P^{32}

Solutions of sodium dihydrogen phosphate were prepared by dissolving reagent grade $NaH_2PO_4.H_2O$ in distilled water.

The tracer P^{32} was obtained from Chalk River as phosphoric acid in solution. In preparing a radioactive solution, an amount of this phosphoric acid solution sufficient to give the desired counting rate was evaporated to dryness with nitric acid, to ensure that the activity was in the $PO_4^{\equiv}$ form. The residue was unweighable. The labeled solution was prepared by taking this activity up in about 20 ml. of the inactive solution.

Viscosities of the sodium dihydrogen phosphate solutions were determined using an Ostwald viscometer.

The results of self-diffusion measurements are given in Table II. Each value of D is a mean value from four to six experiments. (Actual values plotted in Fig. 3.)

TABLE II

SELF-DIFFUSION COEFFICIENTS IN P^{32} LABELED NaH_2PO_4 SOLUTIONS AT 25.0°C.

Concentration, moles/l.	$D \times 10^6$ cm.^{2} sec.$^{-1}$	Viscosity, η, centipoise	$D \times \eta \times 10^6$	pH	$\frac{[H_2PO_4^-]}{[H\ PO_4^-]}$
1.006	5.19	1.323	6.86	3.72	2.55×10^3
0.506	7.03	1.075	7.56	3.86	1.84×10^3
0.0991	7.67	0.924	7.09	4.21	8.22×10^2
0.0493	7.78	0.922	7.17	4.44	4.85×10^2
0.0102	7.91	0.916	7.25	4.76	2.32×10^2
0.00488	8.30	0.913	7.58	4.83	1.97×10^2
0.00103	8.68	0.905	7.85	5.32	$.64 \times 10^2$
0.000503	8.33	0.902	7.51	5.48	$.44 \times 10^2$
0.0000987	8.74	0.897	7.85	5.70	$.27 \times 10^2$

The diffusion coefficient is plotted against the log of the concentration in Fig. 3. It is seen that there is an approximately linear relation between D and log c for concentrations between 10^{-1} to 10^{-4} M. The equation for the linear portion is $D \times 10^6 = 7.30 - 0.363 \log c$ with a standard deviation of 0.28. The rapid rise in the value of D for solutions between 1 and 10^{-1} M may be due to the large change in viscosity. Table II indicates that the

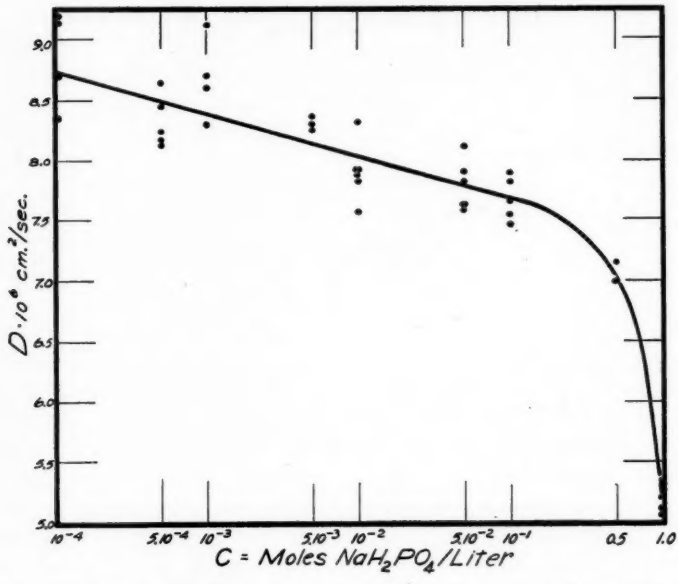

FIG. 3. Plot of diffusion coefficient versus the log of the concentration of sodium dihydrogen phosphate.

product $D\eta$ is approximately constant. The self-diffusion coefficient is plotted against the square root of the concentration in Fig. 4. By extrapolation, the value of the self-diffusion coefficient at infinite dilution is found to be $D_0 = 8.9 \times 10^{-6}$ cm.^{2}sec.$^{-1}$ Table II also records the values of the pH of the solutions and the ratio, $[HPO_4^{=}]/[H_2PO_4^{-}]$ as determined from

$$\frac{[H^+][HPO_4^{=}]}{[H_2PO_4^{-}]} = K_2 = 7.5 \times 10^{-8}.$$

The calculations indicate that for concentrations greater than 0.005 M the

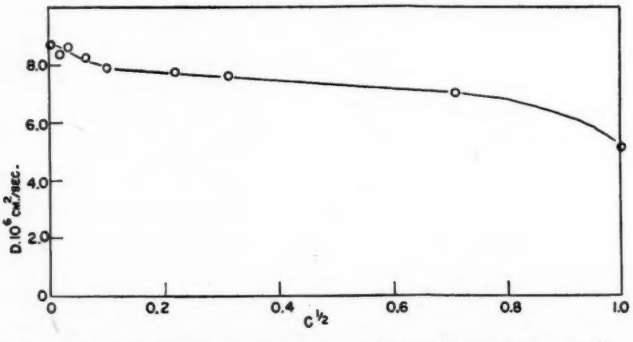

FIG. 4. Plot of diffusion coefficient versus (moles NaH_2PO_4 per liter)$^{\frac{1}{2}}$.

contribution of $HPO_4^=$ ion may be neglected, and that it is still small even at 10^{-4} molar. Similar calculations, using

$$[H_3PO_4] = \frac{[H^+][H_2PO_4^-]}{[K_1]} = \frac{[H^+][H_2PO_4^-]}{1.2 \times 10^{-2}},$$

indicate that the contribution of phosphoric acid is also very small.

ACKNOWLEDGMENT

We wish to acknowledge financial support from the National Research Council of Canada. We are grateful to the Saskatchewan Research Council for a Scholarship (JEB).

REFERENCES

1. ADAMSON, A. W. J. Phys. Chem. 15: 762. 1947.
2. ADAMSON, A. W., COBBLE, J. W., and NIELSON, J. M. J. Chem. Phys. 18: 229. 1949.
3. ANDERSON, J. A. and SADDINGTON, K. J. Chem. Soc. Supp. No. 2, 381. 1949.
4. BRADY, A. P. and SALLEY, J. D. J. Am. Chem. Soc. 70: 914. 1948.
5. BURKELL, J. E. Thesis, University of Saskatchewan, Saskatoon. 1951.
9. CLACK, B. W. Proc. Phys. Soc. London, 36: 313. 1924.
7. GORDON, A. R. Ann. N.Y. Acad. Sci. 46: 285. 1945.
8. HARNED, H. S. and NUTTALL, R. L. J. Am. Chem. Soc. 69: 736. 1947.
9. HEVESY, G. and OBRUTSCHEWAN, A. Nature, 115: 674. 1925.
10. JEHLE, L. P. PhD. Thesis, University of California, Berkeley. 1938.
11. MAPOTHER, D., CROOKS, N. N., and MAWER, J. J. Chem. Phys. 18: 1231. 1950.
12. ONSAGER, L. and FUOSS, R. L. J. Phys. Chem. 36: 2689. 1932.
13. ROBINSON, L. B. and DREW, S. B. J. Chem. Phys. 15: 417. 1947.
14. WANG, J. H. J. Am. Chem. Soc. 73: 510. 1951.
15. WANG, J. H. and KENNEDY, J. W. J. Am. Chem. Soc. 72: 2081. 1950.
16. WHITEWAY, S. G., MACLENNAN, D. F., and COFFIN, C. C. J. Phys. Chem. 18: 229. 1950.

THE BINDING OF ANIONS BY LYSOZYME, CALF THYMUS HISTONE SULPHATE, AND PROTAMINE SULPHATE[1]

By J. Ross Colvin

ABSTRACT

The adsorption of a large series of anions by positively charged lysozyme, calf thymus histone sulphate, and protamine sulphate has been studied by dialysis equilibrium. One group of anions was not adsorbed by lysozyme while the adsorption isotherms for Orange I, Orange II, and 2, 4-dinitro-1-naphthol-7-sulphonic acid were S-shaped. These anomalous isotherms, which were also obtained with histone sulphate and protamine sulphate, have an appreciable temperature coefficient at intermediate dye concentrations. It is emphasized that this type of adsorption is inconsistent with the exclusively electrostatic view of protein binding of anions. It is also shown that $-\Delta F$, $-\Delta H$, and ΔS per mole of anion bound must pass through a maximum for intermediate free anion concentrations in such systems. The lack of binding of some anions and the anomalous isotherms for others is interpreted in terms of a solvation sheath about the charged protein. Their significance for the general process of binding of ions by proteins is discussed.

INTRODUCTION

Although the combination of ions with various proteins has been the subject of many investigations (8), our understanding of the detailed mechanisms involved in the formation of many such complexes is still limited. In recent years, however, the binding of anions by negatively charged proteins has been explained almost exclusively in terms of electrostatic forces between the components (14, 16, 22, 25). Such an interpretation assumes that the Coulomb attraction between the anions and one of a series of identical cationic centers on the protein is chiefly responsible for the formation of the complexes. Using this idea, the binding of many anions may be described quite adequately by a Langmuir adsorption isotherm, modified in certain instances by electrostatic repulsion (16). However, the concept of identical sites cannot be generally valid (12, 13, 24). Furthermore, because of the known importance of ion–dipole and dispersion forces in analogous systems (6) it seems doubtful that electrostatic forces can be the only important factor in binding of anions by proteins. Klotz and Walker have reported (15) that methyl orange, the anion most widely used in studies of this kind, is not bound to lysozyme although this protein has an isoelectric point of 11 (1) and possesses 20 cationic groups in the region of neutrality (7). If the hypothesis referred to above were generally applicable, methyl orange should be bound quite strongly at pH 7.6. Accordingly, the discrepancy between observation and prediction has been investigated.

METHODS AND MATERIALS

All adsorption isotherms were obtained by the dialysis equilibrium technique in which anions are distributed between a protein solution on one side of a semipermeable membrane and a buffer solution on the other. Detailed

[1] *Manuscript received December 19, 1951.*
Contribution from the Division of Applied Biology, National Research Laboratories, Ottawa, Canada. Issued as N.R.C. No. 2701.

descriptions of this method are available elsewhere (12, 13, 16). The screw caps of all vials were lined with aluminum foil and controls on the adsorption of dye by the 18/32 Visking cellulose tubing were included in all experiments. The vials, of approximately 15 ml. total capacity, were equilibrated on a rotating dialyzer for six hours at room temperature. Model experiments showed that this interval was sufficient to attain anion equilibrium, while Klotz (15) has demonstrated that the transfer of lysozyme across the membrane in this interval may be neglected to a first approximation. Any errors due to this source would tend to reduce rather than enhance the effects reported in this study. Lysozyme concentrations, corrected for moisture content determined by heating under vacuum at 100° for 16 hr., were usually of the order of 1×10^{-4} *M* assuming a molecular weight of 14,000 (20). Except where otherwise mentioned, the lysozyme and anions were dissolved in 0.05 *M* phosphate buffer, pH 6.8. The total volume of liquid in each vial was 10 ml., being equally distributed between the protein solution and the external buffer.

After equilibration, concentrations of each anion in the external buffer were estimated by a Beckman quartz spectrophotometer, Model DU, from simultaneously determined calibration curves. Wave lengths used for the various anions were as follows: Methyl orange, Orange II, Orange I, phenol red, methyl red: 5400 Å; *p*-nitrophenol: 4500 Å; *p*-hydroxyerioglucine (fast green F.C.F.): 4300 Å; 2,4-dinitro-1-naphthol-7-sulphonic acid: 4800 Å; picrate: 4800 Å; fluorescein: 5200 Å.

Lysozyme and serum albumin used in this study were crystalline products obtained from Armour and Co., Chicago. Histone sulphate was prepared by the procedure of Kossel (19) and was shown to be positively charged at pH 6.8. It was heterogeneous both electrophoretically and in the ultracentrifuge. Protamine sulphate, obtained from Brickman and Co., Montreal, was positively charged at pH 6.8 and appeared to be quite homogeneous electrophoretically. It was heterogeneous, however, in the ultracentrifuge.

The sodium salts of the dyes were obtained as follows: methyl orange, Orange I, Orange II, and sodium *p*-nitrophenolate were purified by recrystallizing commercial products once from water, washing with alcohol and ether, and subsequently drying the residue over calcium chloride. Sodium picrate and the disodium salt of 2,4-dinitro-1-naphthol-7-sulphonic acid were prepared by neutralizing the free acid with sodium hydroxide and then recrystallizing the salts once from water. After washing with alcohol and ether they were dried over calcium chloride. Phenol red (Merck's reagent grade), methyl red (Mallinckrodt's indicator), the disodium salt of *p*-hydroxyerioglucine (fast green F.C.F.) obtained from Anachemia, and fluorescein (Eastman Kodak) were used without further purification, after drying over calcium chloride.

All buffers were made up according to Clark (4) from reagent grade material and checked against commercial standards.

Those experiments involving a determination of the temperature dependence of binding were carried out in rooms maintained at a given temperature ± 0.5°C.

RESULTS

In preliminary experiments, Klotz's observation that methyl orange was not detectably bound by native lysozyme was confirmed. Likewise, lysozyme in 6 *M* urea does not adsorb methyl orange (Table I) although lysozyme denatured by heating at 100° for one hour takes up appreciable quantities of the dye (Table II).

TABLE I

NONINTERACTION OF METHYL ORANGE AND LYSOZYME IN 6 *M* UREA IN DIALYSIS EQUILIBRIUM EXPERIMENTS*

Optical density of buffer external to lysozyme: 6 *M* urea	Optical density of buffer external to control
0.009	0.007
0.062	0.067
0.147	0.147
0.294	0.297

**Equal quantities of methyl orange added to external solutions of each pair of vials prior to equilibration.*

TABLE II

ADSORPTION OF METHYL ORANGE BY HEAT DENATURED LYSOZYME IN DIALYSIS EQUILIBRIUM EXPERIMENTS

Sample	Opt. density of buffer external to cellulose tubing after equilibration*			
	Series 1	Series 2	Series 3	Series 4
A	0.18	0.28	0.47	0.52
B	0.18	0.29	0.43	0.55
C	0.30	0.58	0.83	0.90
D	0.26	0.57	0.83	1.00

NOTE:

A = *Aliquot of lysozyme denatured directly in the sac of cellulose tubing.*

B = *Aliquot of lysozyme denatured prior to pipetting into the sac of cellulose tubing, with the coagulum ground as finely as was practicable and suspended before pipetting.*

C = *Control sac, without lysozyme, treated in the same manner as Sample A.*

D = *Control, without lysozyme. Aliquot of buffer only, without heat treatment.*

**Equal quantities of methyl orange added to the external solutions of each series before equilibration.*

In addition, since lysozyme alone has a mobility of 3.82×10^{-5} cm.^{2} per v. sec. while in the presence of serum albumin it has a mobility of 3.97×10^{-5} cm.^{2} per v. sec., positively charged lysozyme cannot interact with negative serum albumin at pH 6.8. This result had been predicted previously by Klotz and Walker (15) on the basis of precipitation experiments.

These preliminary experiments confirmed the basis of the investigation for they demonstrated clearly that the simple electrostatic theory must be revised. Further work showed that the anions of methyl red, *p*-nitrophenol,

p-hydroxyerioglucine, picrate, and fluorescein were not adsorbed by lysozyme at pH 6.8. Experiments with phenol red, 2,4-dinitro-1-naphthol-7-sulphonic acid, and Orange I (Fig. 1) and with Orange II (Fig. 2) showed that all these

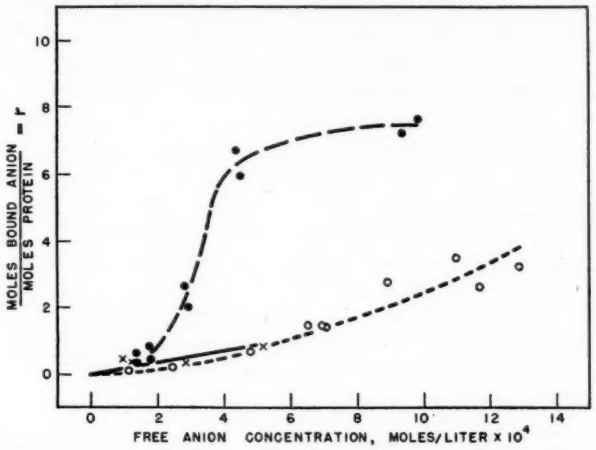

FIG. 1. The binding of phenol red, 2, 4-dinitro-1-naphthol-7-sulphonic acid, and Orange I by lysozyme at pH 6.8. ● Orange I; × phenol red; ○ 2, 4-dinitro-1-naphthol-7-sulphonic acid.

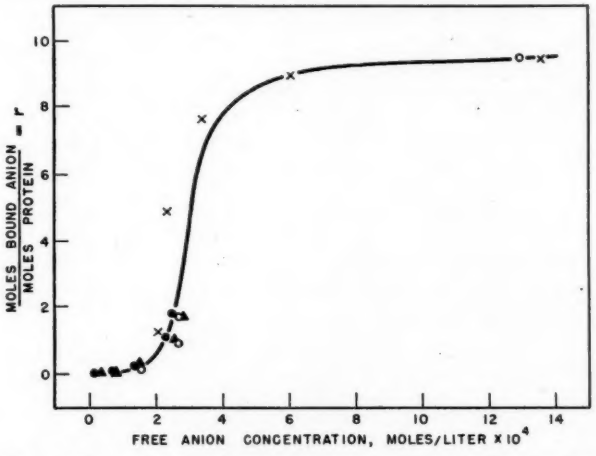

FIG. 2. The binding of Orange II by lysozyme at pH 6.8. Similar symbols identify the points belonging to the same independent experiment.

anions were bound by lysozyme in increasing order of binding strength. In all figures the isotherms were fitted visually to the series of individual points which represent estimates from up to four independent experiments.

Although *p*-nitrophenol has a pK of 6.5 (18) lysozyme did not absorb this anion even at pH 8.0 where ionization is practically complete.

The results for the first group of anions were quite unexpected because of the high positive charge possessed by lysozyme and because the anions are all adsorbed strongly by negative proteins. Lack of binding of the nitrophenols was particularly surprising in view of their high relative affinity for serum albumin and wool (23, 24, 25). Certainly, on the basis of simple electrostatic theory, the doubly charged anion, *p*-hydroxyerioglucine (18), ought to be very strongly held; but no evidence of this was found.

Ordinarily, in systems containing both proteins and ions, if binding occurs at all, the isotherm is concave to the concentration axis over the whole range. However, from Figs. 1 and 2 the binding of Orange I, Orange II, and 2,4-dinitro-1-naphthol-7-sulphonic acid by lysozyme under these conditions is anomalous. The isotherm is clearly convex to the concentration axis at low dye concentrations in what will be referred to as the exponential phase. Quite clearly, throughout this phase the adsorption of one anion promotes the adsorption of another. However, for Orange I and Orange II this part of the isotherm is succeeded by a linear interval and then a logarithmic phase, the sum of the two corresponding to the usual form for negative proteins.

Moreover, a considerable amount of work has established that this shape of the curve is not due to experimental error. Four independent experiments covering a wide range of total anion concentrations confirmed this shape as shown by Fig. 2. Control experiments for the adsorption of Orange II on serum albumin and β-lactoglobulin and for methyl orange on serum albumin under similar conditions gave the normal pattern. It is also significant that the isotherm for Orange II on lysozyme given here is in good agreement with the portion of the curve obtained by Klotz (14) for the same system at high concentrations of the dye. Finally, because Beer's law is obeyed by Orange II up to very high concentrations the inflection point and subsequent leveling of the isotherm for this anion on lysozyme cannot be due to micelle formation.

The binding of Orange II by lysozyme is strongly suppressed by high concentrations of urea (Table III). Denaturation, however, does not appreciably inhibit the binding of Orange II. Unfortunately, insolubility of the denatured lysozyme prevents quantitative estimation of the degree of binding under these conditions.

TABLE III

INHIBITION OF BINDING OF ORANGE II BY LYSOZYME IN THE PRESENCE OF UREA; 0.05 *M* PHOSPHATE BUFFER, pH 6.8

Initial molarity of urea	Average number of Orange II molecules bound per molecule of protein
0	1.68
0.1	1.54
0.25	1.19
0.50	0.67
1.00	0.57
2.00	0.27

NOTE: *All vials contained equal quantities of total dye anion and of lysozyme.*

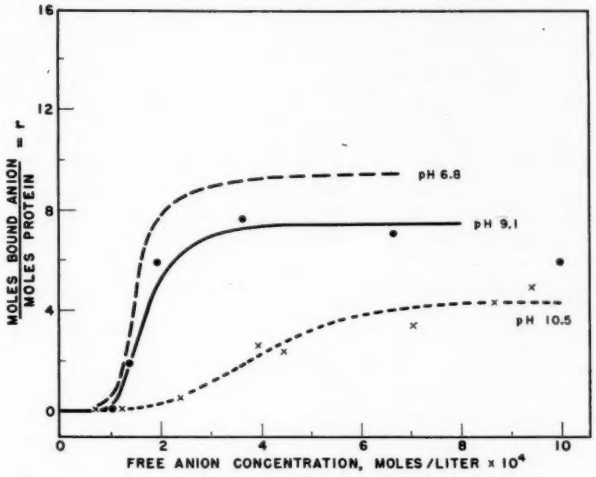

FIG. 3. The effect of pH change on binding of Orange II by lysozyme.

The effect of increasing pH on the binding of Orange II by lysozyme is shown in Fig. 3. Glycinate buffers (0.1 *M* sodium hydroxide and 0.1 *M* glycine with 0.1 *M* sodium chloride) were used for the higher pH's. In this comparison, the small differences in the competitive effects of the glycinate and phosphate ions were neglected (17). As expected the amount of binding decreases as the pH increases but the anomalous form of the isotherm persists even at pH 10.5. Experiments, not indicated on the graph in the interests

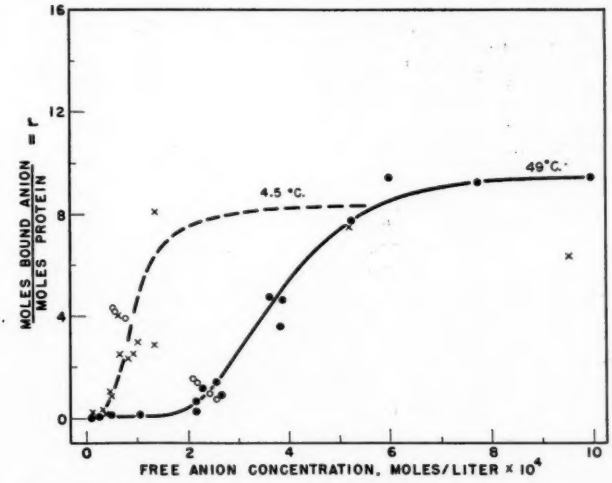

FIG. 4. The effect of temperature change on binding of Orange II by lysozyme at pH 6.8. The open circles identify the points obtained, in duplicate, by equilibration first at one temperature followed by re-equilibration at the second temperature.

of clarity, showed all the isotherms to be horizontal at very low anion concentration. All these results indicate that this cooperative binding of anions by positive proteins is a valid reproducible observation and is not an artifact of the analytical methods employed.

Fig. 4 shows the effect of temperature change on the adsorption of Orange II on lysozyme. Since the isotherms converge at their extremes, the temperature coefficient of binding decreases at both very low and high concentrations of free anion but is appreciable at intermediate concentrations. The effect is completely reversible, and is in sharp contrast to the behavior usually found for most other protein-ion complexes (14).

The unusual shape of the isotherms for Orange I and Orange II on lysozyme suggested an investigation of the adsorption properties of the positively

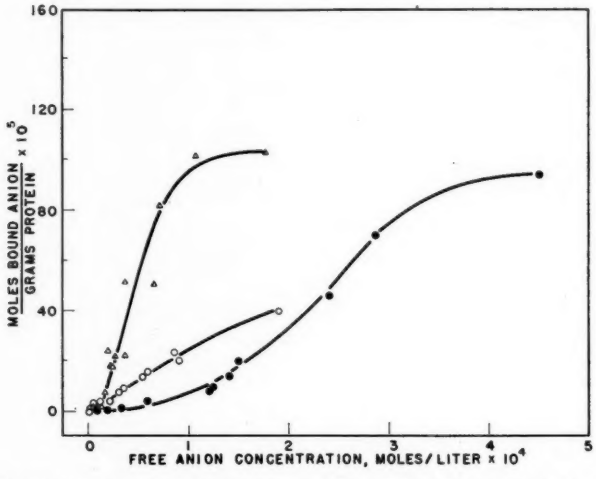

FIG. 5. The binding of methyl orange, Orange II, and 2, 4-dinitro-1-naphthol-7-sulphonic acid by histone sulphate at pH 5.5, ● methyl orange; △ Orange II; ○ 2, 4-dinitro-1-naphthol-7-sulphonic acid.

charged proteins, calf thymus histone sulphate and protamine sulphate. The binding of methyl orange, Orange II, and 2,4-dinitro-1-naphthol-7-sulphonic acid on histone sulphate and protamine sulphate at pH 5.5 is recorded by Figs. 5 and 6 respectively. The lower pH was made necessary by the low solubility of the histone salt in phosphate buffers at pH 6.8. The isotherm found for 2,4-dinitro-1-naphthol-7-sulphonic acid on protamine sulphate at very high free anion concentrations is shown in Fig. 7. Except for the binding of 2,4-dinitro-1-naphthol-7-sulphonic acid by histone, all isotherms show an exponential period during the adsorption of the anion. In those systems where this cooperative adsorption could be studied it was followed by an interval with normal decreasing free energy change per mole of anion bound.

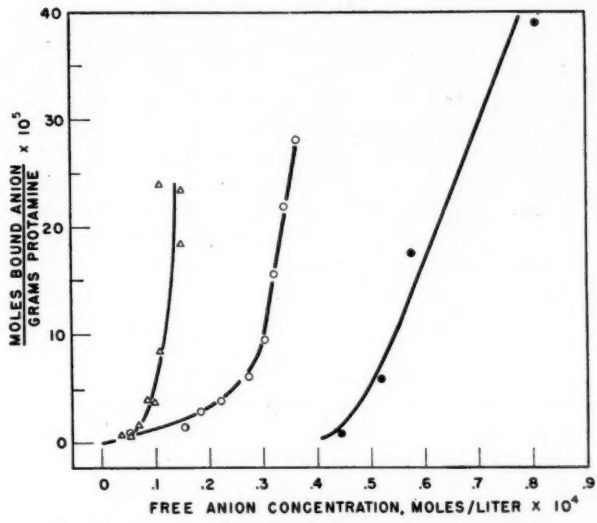

FIG. 6. The binding of methyl orange, Orange II, and 2, 4-dinitro-1-naphthol-7-sulphonic acid by protamine sulphate at pH 5.5, ● methyl orange; △ Orange II; ○ 2, 4-dinitro-1-naphthol-7-sulphonic acid.

Finally, it will be observed that the isotherms plotted for 2,4-dinitro-1-naphthol-7-sulphonic acid (Figs. 6 and 7) do not join smoothly in their common range of free dye concentration. This discrepancy between consecutive experiments is presumed due to the high temperature coefficient noted earlier.

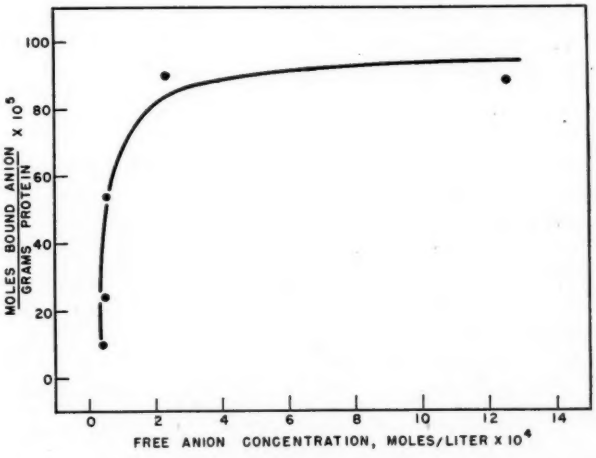

FIG. 7. The binding of 2, 4-dinitro-1-naphthol-7-sulphonic acid by protamine sulphate at pH 5.5.

DISCUSSION

Because of the presence of the exponential phase, the form of these isotherms precludes any application of the simple theory of Klotz *et al.* (16) except possibly at very high free anion concentrations. The shape of the curves, together with the relative binding affinities of the various anions, shows that factors other than electrostatic forces must be important in the binding of anions to protein. Otherwise, the anions of methyl orange, methyl red, *p*-nitrophenol, and sodium picrate should be bound as strongly as Orange II to lysozyme. This conclusion is reinforced by the differences in binding capacity of lysozyme for the isomers Orange I and Orange II, as well as the existence of specific buffer effects (17). Furthermore, if the electrostatic attraction were the predominant contribution to binding, the doubly charged anion, *p*-hydroxyerioglucine, would be held much more strongly than Orange II. Finally, the displacement of Orange II from lysozyme by urea, and the failure of native lysozyme to combine with serum albumin, cannot be resolved solely in terms of simple Coulomb forces. Their effects must often be strongly modified by steric factors and ion–dipole or dispersion forces.

The idea that nonelectrostatic forces are operating in the combination of anions and proteins is not new or surprising because of the known importance of modifying factors in analogous systems (6). It must be re-emphasized only because of recent criticism (14). Klotz, indeed, has recognized the evidence for participation of van der Waals' forces but has rejected the idea of their general importance on the ground that the ΔH of binding of most anions to proteins is known to be small. This argument is not valid, since it arbitrarily assumes that, for negligible changes in volume, by far the greater part of the increase in energy required to detach the water of solvation from the protein is balanced by the decrease in electrostatic energy between the components. Such an assumption cannot be generally true and, as a consequence, the van der Waals' component may be appreciable, especially for larger anions or proteins.

The isotherms obtained in this study suggest that cooperative binding of anions at low free dye concentrations may be a general property of small, positively charged proteins. However, even if this group proves to be an isolated case, possible explanations of the anomaly in terms of statistical mechanical models are of the greatest interest. One such model, often used in gas–solid systems to explain curves of a similar shape, postulates direct attractive interaction between uncharged, adsorbed molecules on the surface of the adsorbent due to mutual van der Waals' forces (3). Unfortunately, for small proteins in the liquid systems under consideration here, any direct interaction between adsorbed anions must be repulsive, since the electrostatic forces decrease as r^{-2} while the van der Waals' forces decrease as some higher inverse power of r. In addition, this simple model cannot explain why there should be an initial resistance to binding of nearly all anions by these positive proteins. Because of the opposite sign of the charge on protein and anion Verwey and Overbeek's concept of electrical double layer repulsion

(26) likewise provides no solution of this problem. Finally, the phase change which usually accompanies binding of anions to these proteins cannot be considered the cause of the exponential form of the isotherm at low concentrations. Such an interpretation requires the postulate that the total number of sites or the intrinsic binding constants of the groups on the protein are greater for precipitated material than for monodisperse, soluble preparations. The validity of such a premise seems extremely unlikely.

An extension of the old notion of electrostriction of solvent about charged centers on a protein does provide a model which rationalizes these observations. The solvation mantle which exists about ions in solution, protein or otherwise (5, 9, 10, 11, 14), is particularly evident for cations (2, 21). Accordingly, around the strongly positively charged centers of lysozyme, histone, and protamine there is a sheath of solvent molecules partially immobilized and orientated by the strong inhomogeneous local field. Although the strength of attachment of solvent will certainly vary from point to point, this mantle must hinder the approach of any other particle to the protein because of the work which must be done to remove the "sheath". In general, of course, regions of the protein–solvent interface affected by such electrostriction will be isolated. Such is the case for most large negative proteins, e.g., like serum albumin, where the cationic centers are separated by anionic groups. Consequently, the local field about any one group is decreased, the solvent-sheath is restricted in extent, and the work required to remove one solvent molecule is diminished. If the protein molecules are small, however, and carry a sufficient number of positive charges, the mantle will extend over the whole "surface" of the protein and will prevent combination with other ions. This mantle would be particularly evident for a protein like lysozyme with only one free carboxyl (7), thus explaining the nonbinding of many anions such as methyl orange. If, however, the anion is large or its structure is such that close approach to the protein is favored, the electrostatic factor plus the dispersion forces are sufficient to overcome the barrier, especially at higher concentrations of free anion. The resultant binding of the ion reduces the total strength of the composite field about the positive protein, and therefore the work necessary to remove additional "frozen" water molecules. Later anions are thus bound more easily, accounting for the exponential phase of adsorption. Eventually, however, electrostatic repulsion between the bound anions as well as spatial limitations on small proteins must prevent further binding. As a result the isotherm passes through an inflection point and reaches a plateau.

This interpretation is supported by the following. At constant temperature, the point at which the isotherm attains a detectable curvature upwards is shifted towards higher free anion concentrations with increasing pH (Fig. 3). This change would be expected on the basis of the above speculations since the hydrogen bonds and the London dispersion forces would be affected only to a small extent by a change in charge on the protein. The sum of these forces may thus contribute a substantial component, which is relatively insensitive to the net charge, to the local field about any given group on the

protein. Therefore, a higher concentration of free anion would be required to initiate the exponential phase. In this process, the effect of the reduction of the total number of positive groups with increasing pH is greater than the effect of decreasing the electrostatic component of the composite field about the protein (Fig. 3). This too is in accord with the above scheme, especially since the effect of a change from pH 6.8 to 9.1 is much less than the effect of a change from 9.1 to 10.5. It is also significant that denaturation of lysozyme increases its capacity to bind methyl orange since the unfolding and disorientation would reduce the total height of the barrier about any given cationic group without greatly reducing the total number of positive centers. Finally, comparison of the isotherms for the three proteins will show that the affinity for binding of the anions is in the order Orange II > 2,4-dinitro-1-naphthol-7-sulphonic acid > methyl orange. The constant order for each of the proteins implies that similar processes may be involved. Admittedly, this assumption cannot be pushed too far since 2,4-dinitro-1-naphthol-7-sulphonic acid shows no hint of cooperative adsorption on histone. In this instance, electrostatic attraction plus the other forces mentioned appears to be sufficient to overcome the barrier at all concentrations of free dye.

If the hypothesis outlined in the preceding paragraph is correct, the binding of Orange II by lysozyme has a larger temperature coefficient (Fig. 4) than the binding of an equivalent amount of water. Unfortunately, no direct means of testing this conclusion exists.

Although it is impossible at the present time to give a quantitative analysis of these isotherms either by statistical mechanics or from a thermodynamic point of view, some interesting conclusions can be drawn from their general properties. Obviously $-\Delta F$ per mole of anion bound increases (numerically) from a small value at the outset to a maximum and then decreases as total free dye concentration increases. In addition, study of Fig. 4 demonstrates that the $-\Delta H$ (and $-\Delta E$ also if the volume change is assumed to be negligible) per mole of anion bound also rises to a maximum and then decreases. Hence the character of the successive reactions $PA_n + A \rightarrow PA_{n+1}$ changes radically, as adsorption on a protein molecule proceeds from a low average number of anions bound per protein molecule to a high one. Since ΔF in the initial stages of binding is very nearly zero while ΔH is zero or slightly negative, ΔS must be very close to zero for the initial stages of binding. As the average number of anions held by a protein molecule increases, however, ΔS must also rise to a maximum and then decrease. This follows from Fig. 4 which shows that when $-\Delta H$ is decreasing as a function of free anion concentration, $-\Delta F$ is still increasing. This conclusion is quite different from those reached by a study of binding of anions by negative proteins (14). The most obvious interpretation of the course of ΔS is that the first anions are bound without displacement of solvent while binding of later anions involves the simultaneous release of solvent. Such a view also explains the maximum in the numerical values of $-\Delta H$ and $-\Delta E$.

If this hypothesis is substantially correct there should be a positive correlation between the degree of hydration of cationic proteins and the charge of

each. Furthermore, assuming that the strength of binding of solvent molecules is proportional to the differential heat of hydration of the protein, there should be an inverse correlation between the binding affinities of proteins per unit weight, for a given ion, and their heats of hydration. Unfortunately, data of this kind are meager at present and are complicated by the wide differences in composition of the proteins. Work is continuing on these systems, however.

Finally, the presence of a charge effect, as postulated here, complicates the interpretation of any comparison of the competitive binding effects of buffer anions, such as that of Klotz and Urquhart (17).

In brief, the general process of protein–anion binding is more complex than has been admitted lately. With particular systems under favorable conditions, electrostatic attraction may be chiefly responsible for the negative ΔF of binding. However, the effects of the electrostatic contribution may be equaled or even exceeded by the van der Waals' component. In addition, the effect of both of these attractive forces may also be modified markedly by the work required to remove part of the solvation mantle of the protein. Consequently, any wide generalizations are dangerous. Each system must be studied separately or, at best, as a member of a narrow class.

ACKNOWLEDGMENTS

The author is indebted to Drs. D. B. Smith, D. R. Whitaker, E. Hughes, and particularly to Dr. W. H. Cook for stimulating discussion and criticism of the manuscript.

REFERENCES

1. ANDERSON, E. A. and ALBERTY, R. A. J. Phys. & Colloid Chem. 52: 1345. 1948.
2. BERNAL, J. D. and FOWLER, R. H. J. Chem. Phys. 1: 515. 1933.
3. BRUNAUER, S. The adsorption of gases and vapors. Vol. I. Physical adsorption. Princeton University Press. 1945.
4. CLARK, W. M. The determination of hydrogen ions. 3rd ed. The Williams and Wilkins Company, Baltimore. 1928.
5. COHN, E. J. and EDSALL, J. T. Proteins, amino acids and peptides. Reinhold Publishing Corp., New York. 1943.
6. DE BOER, J. H. Advances in Colloid Sci. 3: 1. 1950.
7. FROMAGEOT, C. and DE GARILHE, M. P. Biochim. et Biophys. Acta, 4: 509. 1950.
8. HAUROWITZ, F. Chemistry and biology of proteins. Academic Press, Inc., New York. 1950.
9. HÖBER, R. Physical chemistry of cells and tissues. The Blakiston Company, Philadelphia. 1945.
10. HUNT, J. R. and TAUBE, H. J. Chem. Phys. 19: 602. 1951.
11. JIRGENSONS, B. J. Polymer Sci. 1: 475. 1946.
12. KARUSH, F. J. Am. Chem. Soc. 72: 2705. 1950.
13. KARUSH, F. and SONENBERG, M. J. Am. Chem. Soc. 71: 1369. 1949.
14. KLOTZ, I. M. Cold Spring Harbor Symposia Quant. Biol. 14: 97. 1949.
15. KLOTZ, I. M. and WALKER, F. M. Arch. Biochem. 18: 319. 1948.
16. KLOTZ, I. M., WALKER, F. M., and PIVAN, R. B. J. Am. Chem. Soc. 68: 1486. 1946.
17. KLOTZ, I. M. and URQUHART, J. M. J. Phys. & Colloid Chem. 53: 100. 1949.
18. KOLTHOFF, I. M. Acid-base indicators. The MacMillan Company, New York. 1937.
19. KOSSEL, A. The protamines and histones. Longmans, Green and Co., London, 1928. p. 73.
20. PALMER, K. J., BALLANTYNE, M., and GALVIN, J. A. J. Am. Chem. Soc. 70: 906. 1948.
21. ROBINSON, R. A. and STOKES, R. H. Ann. N. Y. Acad. Sci. 51: 593. 1949.
22. SCATCHARD, G. and BLACK, E. S. J. Phys. & Colloid Chem. 53: 88. 1949.
23. STEINHARDT, J., FUGITT, C. H., and HARRIS, M. J. Research Natl. Bur. Standards, 28: 201. 1942.
24. TERESI, J. D. J. Am. Chem. Soc. 72: 3972. 1950.
25. TERESI, J. D. and LUCK, N. M. J. Biol. Chem. 174: 653. 1948.
26. VERWEY, E. J. W. and OVERBEEK, J. Th. G. Theory of the stability of lyophobic co oids. Elsevier Publishing Co, Inc., Amsterdam. 1948.

PREPARATION OF KETENE FROM GLACIAL ACETIC ACID, METHYL ACETATE, AND ETHYL ACETATE[1]

By K. K. Georgieff

ABSTRACT

Laboratory studies were carried out to determine whether methyl and ethyl acetates could be pyrolyzed to give yields and conversions to ketene comparable to those obtainable from acetic acid. Acetic acid was pyrolyzed to ketene and water in the presence of 0.33% triethyl phosphate or phosphoric acid catalyst at 680°-760°C. and 140-160 mm. Hg absolute. Maximum yield obtained was 80.6% and maximum conversion 34.5%. Methyl acetate was cracked to ketene and methanol at 610°-685°C. and 95-400 mm. absolute, using triethyl phosphate, phosphoric acid, sulphuric acid, dimethyl sulphate, butyl borate, and silica gel–boric acid as catalysts. High yields could be obtained only with phosphates in 2-3% concentration. Maximum yield to ketene, including ketene recovered as acetic acid, was 76% (conversion 31-34%). Maximum yield to methanol was 81.3% (conversion 33-34%). Methyl acetate containing 18% methanol was also cracked but results were poorer. Ethyl acetate, in the presence of 0.33% triethyl phosphate, was pyrolyzed to ketene, ethylene, and water at 630°-685°C. and 140-190 mm. absolute. Maximum yield of ketene, including ketene recovered as acetic acid, was 85.8%. Maximum conversion to ketene was 35.4% and to ketene plus acetic acid 85.7%. Yields to ethylene were nearly quantitative.

INTRODUCTION

The production of ketene from acetic acid and its conversion to acetic anhydride for the manufacture of cellulose acetate have been carried on industrially for many years. However, to determine whether high yields and conversions to ketene could also be obtained from esters of acetic acid, investigations were carried out on methyl acetate and ethyl acetate, as well as on acetic acid.

The preparation of ketene from acetic acid has already been described somewhat extensively in the literature but was repeated here so that yields, conversions, catalyst consumption, etc. could be compared with those obtained with methyl acetate and ethyl acetate. Industrially, ketene is produced with a yield of 90% and a conversion of 75% by passing acetic acid, together with 0.2% by weight of triethyl phosphate, through a stainless steel tube at 700°-730°C. and 100-450 mm. absolute (5). Our experiments were carried out under essentially these conditions, and the ketene was passed into glacial acetic acid to convert it into acetic anhydride. When satisfactory yields were obtained with acetic acid, the investigation was continued with methyl acetate and ethyl acetate.

The pyrolysis of acetate esters to ketene has already been described. Wilsmore (9) discovered that ethyl acetate could be pyrolyzed to ketene by a heated wire, but his apparatus gave only low yields. Hurd (2) pyrolyzed ethyl acetate in a vertical glass tube and obtained chiefly acetic acid and ethylene but he also obtained traces of ketene. Loder (6) described the pyrolysis of esters of saturated aliphatic carboxylic acids in a heated copper tube to ketenes and the corresponding alcohols. He claimed a ketene yield of

[1] *Manuscript received September 19, 1951.*
Contribution from the Research Laboratories, Shawinigan Chemicals Limited, Shawinigan Falls, Que.

87.8% from methyl acetate using silica gel impregnated with boric acid as catalyst, but he gave no indication either of his methanol yield or his conversions. However, since this was the only prior disclosure of high yields of ketene from acetate esters, it was decided to first try out Loder's silica gel–boric acid catalyst. We were able to obtain only very low yields and conversions. In any case, it was obvious from these preliminary experiments that the catalyst would probably require frequent regeneration and the regeneration was not likely to be easily accomplished. To avoid this difficulty, it was decided to try to find a volatile catalyst which could be added to the feed. Triethyl phosphate and 85% orthophosphoric acid proved to be satisfactory.

Loder (6) also indicated that ethyl acetate pyrolyzed to ketene and ethanol, but in this investigation ketene, ethylene, and water were obtained. Since completion of this work,* a patent (7) has been issued describing the use of a mixture of triethyl phosphate and pyridine as catalyst and giving the products as ketene, ethylene, and water. Optimum conditions disclosed were essentially the same as those found in this investigation, but the yields and conversions claimed were higher.

EXPERIMENTAL

Pyrolysis of Acetic Acid and Ethyl Acetate

The same apparatus, procedure, catalyst, feed rate, and absolute pressure were used for acetic acid and ethyl acetate. Both materials used were manufactured by Shawinigan Chemicals Ltd. and analyzed at least 99.5%. The apparatus is shown in Fig. 1. Acetic acid containing 0.33% by weight of triethyl phosphate was fed at a constant rate from a feed bottle into a stainless steel pyrolysis tube heated by an electric furnace. The products of reaction (i.e. ketene, water, and permanent gases) and the unconverted acetic acid were passed through one water-cooled and two brine-cooled condensers to condense out the water, acetic acid, and some acetic anhydride formed by the interaction of ketene with acetic acid. The remaining ketene then passed into two fritted glass scrubbers containing acetic acid where it was quantitatively converted to acetic anhydride. The residual permanent gas was scrubbed with 20% potassium hydroxide solution, dried with calcium chloride, and exhausted by two Presso-Vac pumps operating in parallel. Its volume was then measured by a wet-test meter. Since the reaction of ketene and acetic acid is highly exothermic, the rate of production of ketene was followed by observing the temperature of the cooling bath required to maintain any given temperature within the acetic acid scrubber. The length of most runs was five and one-half to six hours.

A constant feed of acetic acid, which is absolutely essential for good operation, was obtained by maintaining a near constant head of liquid above a glass capillary of the proper size. Some difficulty was encountered owing to plugging of the capillary, but this was largely overcome by introducing the

**Experimental work on ethyl acetate was completed in October 1945.*

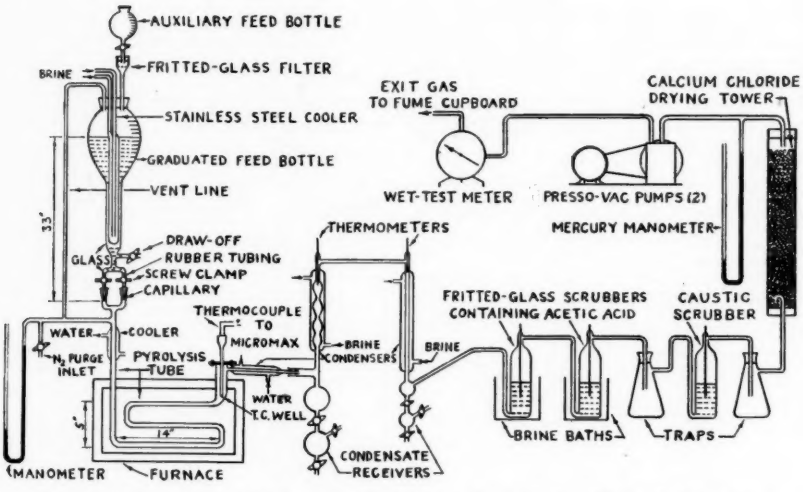

FIG. 1. Apparatus for the preparation of ketene from acetic acid or ethyl acetate.

acid into the feed bottle through a fritted glass filter and by keeping in readiness a stand-by capillary.

The pyrolysis tube, which was heated by electrical resistance elements, consisted of an S-shaped stainless steel tube, 13/32 in. I.D. and 50 in. long, to which was welded an 8 in. length of 1 in. pipe containing a ½ in. O.D. thermocouple well. The temperature was measured by means of a thermocouple connected to a Micromax recorder, and was varied by adjusting the voltage to the resistance elements with a Variac transformer. A slow gradual deposition of carbon occurred in the tube, and after a few weeks of operation it was necessary to burn it out with a stream of air.

Three runs with acetic acid were also made in the methyl acetate cracking apparatus. In two runs, 0.33% triethyl phosphate was used as catalyst and in the other 0.4% orthophosphoric acid (chemically pure, 85% grade). Optimum yield conditions were not attained. The results are given in Table VI.

Pyrolysis of Methyl Acetate

Methyl acetate of 98–99% purity was obtained by acetylation of chemically pure methanol with acetic anhydride. Operation was the same as in the pyrolysis of acetic acid but the apparatus was slightly modified. A larger diameter reaction tube (½ in. I.D.) was used so that a lower pressure drop through the tube would result which would make possible lower absolute pressures. The desired reaction pressure was obtained by properly throttling a bronze globe valve inserted between the reaction tube and the first condenser. The condenser system was modified to permit dry ice cooling. The first condenser was lengthened from 6 in. to 30 in., the first 18 in. being cooled with brine at −5°C. and the remaining 12 in. with a dry ice–methanol mixture at −30°C. The second condenser consisted of a glass U-tube with a bulb

appropriately attached to store the condensate, and was cooled by a dry ice–methanol bath at –35°C. The third condenser was a spiral copper tube with an attached condensate storage bulb and was cooled by a bath at –50 to –55°C.

Pyrolyses were carried out without catalyst, with one solid catalyst, i.e., silica gel supporting boric acid (6), and with the following compounds dissolved in the methyl acetate feed: triethyl phosphate (redistilled Tennessee Eastman Corporation material), orthophosphoric acid (chemically pure, 85%), sulphuric acid (chemically pure, 96%), fuming sulphuric acid, dimethyl sulphate (Eastman Kodak, practical grade), butyl borate (Eastman Kodak), hydrochloric acid (chemically pure, 20% acid in water), boron fluoride–ethyl ether complex (redistilled, Eastman Kodak, practical grade), and pyridine (redistilled Barrett's Grade 2A).

Pyrolysis of Methyl Acetate–Methanol Azeotropic Mixture

The same apparatus and general procedure were used as for pure methyl acetate. Only triethyl phosphate and 85% orthophosphoric acid were used as catalysts.

ANALYTICAL

Pyrolysis of Acetic Acid

The condensate from the first and second condensers consisted of a mixture of acetic acid and water. The acetic acid was determined by titration with standard ½*N* sodium hydroxide solution using phenolphthalein as indicator. The condensate from the third condenser, as well as the scrubber product, consisted chiefly of acetic anhydride and acetic acid with only traces of high-boiling tars. The acetic anhydride was determined by the "aniline method" (1) and the acetic acid by difference.

Pyrolysis of Methyl Acetate

The constituents of the condensate from the first and second condensers were determined by standard methods as follows:—

Methanol: by acetylation with acetic anhydride–pyridine mixture.

Acetic acid: by titration with standard aqueous ½*N* sodium hydroxide solution.

Methyl acetate: by saponification with an excess of standard aqueous ½*N* sodium hydroxide solution followed by back-titration with standard ½*N* hydrochloric acid.

Water: by titration with Karl Fischer reagent.

The condensate from the third condenser, as well as the scrubber product, consisted of acetic anhydride, acetic acid, and methyl acetate. The anhydride was determined by the "aniline method" (1) and the acetic acid by calculation from the difference between the "total acidity" titer and twice the "aniline" titer. (A negligible percentage of the methyl acetate was found to hydrolyze when the anhydride was hydrolyzed with water alone at room temperature.) The sample, which had already been used to obtain the "total acidity" titer,

was afterwards used to obtain the percentage of methyl acetate by saponification with an excess of standard alkali.

Pyrolysis of Ethyl Acetate

The scrubber product and condensate were analyzed as in the previous investigations on acetic acid and methyl acetate. The permanent gases were analyzed using a standard Burrell type apparatus and standard reagents. Carbon dioxide was determined by absorption in 30% potassium hydroxide solution; total unsaturates by absorption in fuming sulphuric acid; oxygen by absorption in alkaline pyrogallol; nitrogen by multiplying the percentage of oxygen by four; carbon monoxide by absorption in acidic cuprous chloride; and hydrogen by oxidation with copper oxide. Acetylene in the unsaturates was determined in a separate sample by absorption in alkaline silver nitrate followed by estimation of the nitric acid formed (8).

RESULTS

Pyrolysis of Acetic Acid

The results, using 0.33% by weight of triethyl phosphate in the feed and an absolute pressure of 140–160 mm. Hg at the inlet end of the pyrolysis tube are plotted in Fig. 2. It will be noted that on increasing the feed rate from 190 ± 10 gm. per hour to 240 ± 10, the maximum yield increased somewhat, but that on further increasing it to 315 ± 10, the yield remained approximately constant while the conversion decreased considerably, thus

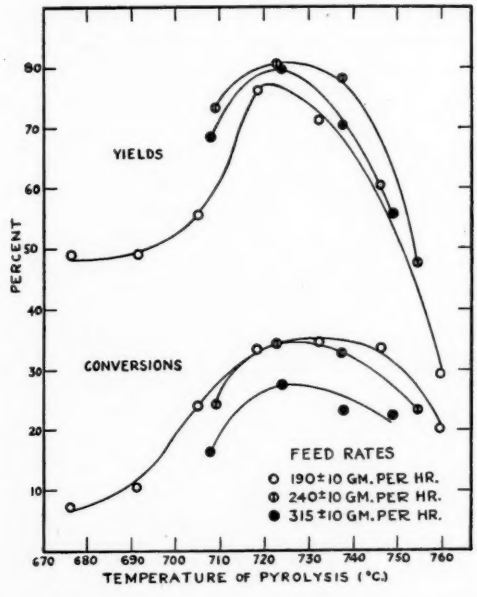

FIG. 2. Pyrolysis of acetic acid: effect of temperature on yield and conversion to ketene at various feed rates.

indicating that the optimum capacity of the tube had been exceeded. The maximum yield and conversion were thus obtained at a feed rate of 240 ± 10 gm. per hour and a temperature of 724°C., and were 80.6% and 34.5% respectively. Of the 19.4% loss in yield, 14.4% was due to the formation of permanent gases and 5.0% to the sweeping out of acetic acid and anhydride from the scrubbers by the permanent gases. The percentage of the acid which decomposed to permanent gases increased with increase in temperature.

Pyrolysis of Methyl Acetate

The pyrolysis of methyl acetate without a catalyst produced extremely low yields of ketene and methanol. Of the potential catalysts tried, only triethyl phosphate and orthophosphoric acid were found entirely satisfactory.

Triethyl Phosphate Catalyst

The maximum yields were obtained at 670 ± 10°C. and 150–250 mm. Hg absolute, and were as follows:— to ketene, including ketene recovered as acetic acid, 76.2% at a conversion of 31.3%; to methanol, 81.3% at a conversion of 33.4%. A feed rate of 6.2 gm. per minute was used. About 2.5 to 3.0% of phosphate catalyst, based on the weight of methyl acetate, was required to give the maximum conversion. It was also necessary to add 5-6% water to the methyl acetate feed stock.

No attempt was made to determine systematically the optimum feed rate for this larger tube, as had been done with acetic acid for a somewhat smaller tube, since optimum yields were obtained over a fairly wide range of feed rate. It was merely assumed that the new optimum feed rate, in moles per minute, would be directly proportional to the ratio of the area of the heated (inside) surface of the larger tube to the smaller, i.e.,

$$507 \text{ sq. cm.}/412 \text{ sq. cm.} \times 4/60 = 0.0820 \text{ moles per minute}$$
$$= 6.08 \text{ gm. methyl acetate per minute.}$$

The validity of this assumption was substantially confirmed by the experimental results. However, it was necessary to determine the effect of the following variables on the yield and conversion:—

(i) *Effect of Addition of Water to the Feed*

It had already been reported (6) that if up to 8% water is added to the feed, some of the ketene which would otherwise go to valueless by-products would be recovered as acetic acid. This has been confirmed. The addition of 5 to 6% water did not increase the yield or conversion to ketene, as such, but did increase the yield and conversion to ketene plus acetic acid for any given concentration of catalyst in the feed. Some improvement in the methanol yield was also noted. The presence of the water tended to depress the formation of both permanent gas and paraformaldehyde. The experimental results are summarized in Table I.

(ii) *Effect of Per cent Catalyst in Feed on Per cent Conversion*

Under conditions of constant contact time and constant temperature in the pyrolysis tube, it was found that the conversions to ketene, ketene plus acetic acid, and methanol increased rapidly with increase in the concentra-

TABLE I

PYROLYSIS OF METHYL ACETATE
EFFECT OF ADDITION OF WATER TO THE FEED

Run No.	% Et_3PO_4 in feed	Feed rate, gm./min.	% H_2O in feed	Temp. of pyrolysis, °C.	Abs. press., mm. Hg	% Yield			% Conversion		
						To ketene alone	To ketene and HOAc	To CH_3OH	To ketene alone	To ketene and HOAc	To CH_3OH
M 2	0.33	6.1	0.7*	632 ± 10	94	38.3	40.5	41.2	9.4	10.3	10.4
M 3	0.33	5.1	0.7*	610 ± 10	96	37.4	38.0	44.1	9.7	10.0	11.6
*M*13	0.33	6.0	5.2	660 ± 15	92	38.6	45.3	47.4	8.8	11.6	12.1
M 6	0.67	6.5	0.6*	626 ± 5	106	51.2	52.2	60.0	12.5	13.0	14.9
*M*14	0.7	5.4	5.5	654 ± 10	93	52.8	57.2	65.6	14.8	17.5	20.2

**No water added.*

tion of triethyl phosphate up to 2%, but then leveled off between 2 to 3%. Results are shown in Fig. 3.

(iii) *Effect of Pressure on Conversion*

The per cent conversion was found to be almost independent of the pressure between 95 mm. Hg absolute and 325 mm. and at optimum temperature, as can be seen from Fig. 4. The highest yields and conversions, using 2% triethyl phosphate as catalyst, were obtained at about 150 to 250 mm. Hg absolute. Above 325 mm., yields decreased rather rapidly and conversions decreased somewhat less rapidly, owing to the formation of larger percentages of per-

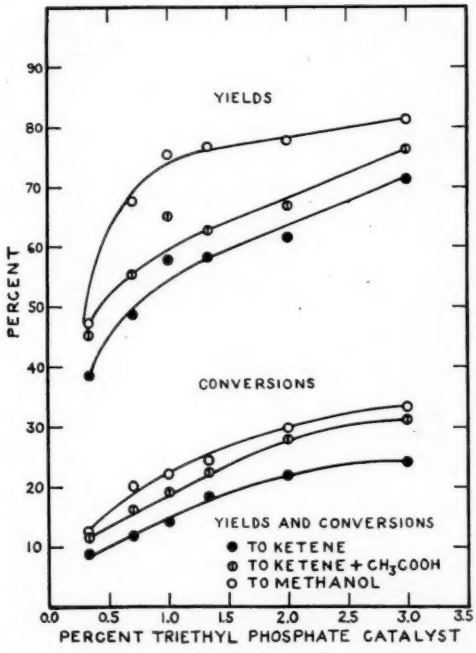

FIG. 3. Pyrolysis of methyl acetate: effect of percentage of triethyl phosphate catalyst in feed on yield and conversion. Temperature = 663 ± 10°C.; absolute pressure = 230-270 mm. Hg; feed rate = 6 gm. per minute; per cent water in feed = 5.3.

manent gases. The optimum temperature apparently decreased from 662 ± 5°C. at 95 mm. absolute to 626 ± 10°C. at 402 mm.

Orthophosphoric Acid as Catalyst

Yields and conversions with orthophosphoric acid (85%) were approximately the same as those obtained with triethyl phosphate for the same percentage, by weight, of catalyst in the feed. Some difficulty was experienced in starting up the runs, but once started, operation was smooth. The general composition of the condensate, as well as the by-products, e.g., paraformalde-

hyde, were also similar. Table II gives a comparison between triethyl phosphate and orthophosphoric acid as catalysts.

Other Catalysts

Sulphuric acid (96%) and fuming sulphuric acid also catalyzed the reaction to ketene and methanol but the highest yields obtained were only 45-50% and the highest conversions 8-10%. Increasing the percentage of catalyst above 0.67% did not appear to improve the conversion. Sulphuric acid appeared to be easily reduced, as evidenced by the strong odor of hydrogen sulphide and organic sulphur compounds in the condensate.

Dimethyl sulphate had only a slight catalytic effect.

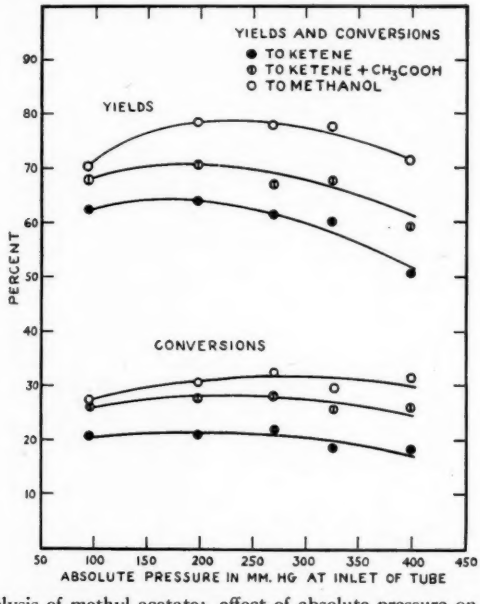

FIG. 4. Pyrolysis of methyl acetate: effect of absolute pressure on yields and conversions. Per cent triethyl phosphate in feed = 2.0.

Butyl borate was also a poor catalyst. It was better than dimethyl sulphate but poorer than sulphuric acid. Much larger quantities of paraformaldehyde were formed with the above three catalysts than with the phosphates. The largest quantity was formed with dimethyl sulphate.

The only solid catalyst tried was silica gel impregnated with boric acid (6). Even with a fresh catalyst, very low yields and conversions were obtained.

Hydrochloric acid (20% solution in water), boron trifluoride–ethyl ether complex, and pyridine were found to have no catalytic effect at all.

Pyrolysis of Methyl Acetate–Methanol Azeotropic Mixture

Methyl acetate containing 18% methanol was also pyrolyzed, but conversions were only 38% to 56% of those obtained with pure methyl acetate for the

TABLE II

PYROLYSIS OF METHYL ACETATE
COMPARISON BETWEEN TRIETHYL PHOSPHATE AND PHOSPHORIC ACID AS CATALYSTS

Run No.	% Et_3PO_4	% H_3PO_4 (85%)	Feed rate, gm./ min.	% H_2O in feed	Temp. of pyrolysis, °C.	Abs. press., mm. Hg	% Yield			% Conversion		
							To ketene alone	To ketene and HOAc	To CH_3OH	To ketene alone	To ketene and HOAc	To CH_3OH
M 40	0.0	0.67	6.0	5.2	660 ± 10	228	48.1	55.7	72.0	11.8	15.9	20.5
M 29	0.70	0.0	6.1	5.2	658 ± 5	275	48.7	55.4	70.2	11.9	16.2	20.4
M 41	0.0	1.33	5.7	5.2	666 ± 5	242	52.9	61.8	73.6	15.0	21.6	25.7
M 16	1.33	0.0	5.6	5.6	660 ± 10	94	58.2	62.8	76.8	18.5	22.5	24.5
M 42	0.0	2.0	5.3	5.0	644 ± 10	232	68.3	75.6	75.5	19.4	28.1	28.0
M 22	2.0	0.0	6.1	5.1	638 ± 10	198	64.0	70.2	78.2	21.0	27.7	30.8

same percentage of triethyl phosphate or orthophosphoric acid in the feed, all other conditions being essentially the same. (For details see Table III.) Increasing the percentage of catalyst increased the conversion, but conversions as high as the maximum obtained with pure methyl acetate could not be obtained with up to 5% catalyst. When the dry azeotrope was cracked, very large amounts of paraformaldehyde and permanent gases were formed.

The very much lower conversions obtained with the azeotrope as compared with pure methyl acetate for any given percentage of catalyst, would appear to be due to at least three factors. Firstly, the feed stock already contains 33.7 mole % of methanol and this exerts an unfavorable influence on the final equilibrium. Secondly, methanol appears to react with phosphate catalysts reducing them to catalytically ineffective compounds. Hence, the higher concentration of methanol present when the azeotrope is cracked is responsible for the higher concentration of catalyst required to produce any given conversion. (Further details are given in the section on "Side-Reactions".) And thirdly, there is probably a greater loss of ketene by recombination with methanol in the condenser system.

Side Reactions

The major loss in yield in the pyrolysis of methyl acetate and methyl acetate–methanol azeotropic mixture was due to the formation of permanent gases, e.g., carbon monoxide, hydrogen, ethylene, etc. The average molecular weight of the gas was determined for many runs by dividing the weight of methyl acetate not recovered as liquid or solid by the total number of molecular volumes of gas formed. Molecular weights varied from run to run, but most values fell between 25 and 28 with an over-all average of 26.6.

Other important side reactions were the reduction of the phosphate catalysts to catalytically ineffective compounds and the oxidation of methanol to formaldehyde with its subsequent polymerization to paraformaldehyde. Several factors indicate that the methanol was the chief reducing agent of phosphate. Firstly, acetic acid pyrolyzes to ketene and water, and ethyl acetate to ketene, ethylene, and water and both require only 0.2-0.33% phosphate to give the maximum conversion. On the other hand methyl acetate which pyrolyzes to ketene and methanol requires 2.5-3.0%. Hence, since ketene and ester are not responsible for the higher consumption of catalyst, methanol probably is. Secondly, since a much higher concentration of phosphate is required to bring about the maximum or near maximum conversion with methyl acetate–methanol azeotrope than with pure methyl acetate, it would appear that the higher concentration of methanol present in the former is responsible for the higher consumption of catalyst. Thirdly, the formation of significantly large quantities of paraformaldehyde and water, along with the disappearance of phosphate (as described below), add further weight to the hypothesis of simultaneous oxidation of methanol and reduction of phosphate.

Some paraformaldehyde and water (over and above that added to the feed) were obtained in the condensate in all runs, including those in which catalysts other than phosphates were used. The paraformaldehyde was identified by

TABLE III

COMPARISON OF PYROLYSIS OF PURE METHYL ACETATE AND METHYL ACETATE – METHANOL AZEOTROPIC MIXTURE

Run No.	Substance cracked	% Et_3PO_4	% H_3PO_4 (85%)	Feed rate, gm./ min.	% H_2O in feed	Temp. of pyrolysis, °C.	Abs. press., mm. Hg	% Yield			% Conversion		
								To ketene alone	To ketene and HOAc	To CH_3OH	To ketene alone	To ketene and HOAc	To CH_3OH
M 31	Azeotrope	2.0	—	5.1	5.4	676 ± 10	230	38.0	50.4	48.0	7.9	13.0	12.4
M 22	Pure MeOAc	2.0	—	6.1	5.1	638 ± 10	198	64.0	70.2	78.2	21.0	27.7	30.8
M 51	Azeotrope	—	2.0	5.2	5.2	666 ± 5	100	48.4	57.6	46.4	10.9	15.8	12.8
M 42	Pure MeOAc	—	2.0	5.3	5.0	644 ± 10	232	68.3	75.6	75.5	19.4	28.1	28.0
M 32	Azeotrope	4.0	—	5.4	5.3	710 ± 5	227	58.0	67.4	69.4	16.5	24.8	25.5
M 33	Azeotrope	4.9	—	6.3	0.3	676 ± 10	224	59.8	63.4	44.9	14.6	17.0	12.0

treating it with dilute sulphuric acid to convert it to formaldehyde and then applying the standard qualitative tests, i.e., fuchsin, chromotropic acid, resorcinol condensation, and odor. It was noted that the addition of water to the feed reduced the amount of paraformaldehyde formed, and increased the yield of methanol somewhat. It was also noted that the amount of water recovered in the condensate, over and above that added to the feed, increased somewhat with increase in conversion.

Analyses of condensates of two runs for phosphate by precipitation as magnesium ammonium phosphate and ignition to magnesium pyrophosphate (4) showed only 0.20% to 0.24% phosphate, calculated as phosphoric acid even though 2.5 to 4% phosphate was used in the feed. This indicates that the phosphate phosphorus may have been reduced to highly volatile compounds, perhaps to its hydrides or perhaps even to elemental phosphorus. In the pyrolysis of acetic acid, when the first condenser was taken down for cleaning, small amounts of what may have been elemental phosphorus were observed to ignite with a bright flash when given a sharp blow with a metallic object.

Pyrolysis of Ethyl Acetate

Ethyl acetate was pyrolyzed to ketene, ethylene, and water in the presence of 0.33% by weight of triethyl phosphate. The maximum yield to ketene, including ketene recovered as acetic acid, was obtained at 644± 5°C. and 154 mm. Hg absolute, and was 85.8%. The maximum conversion to ketene was 35.4% and to ketene plus acetic acid 85.7%. A feed rate of 4.2 gm. per minute was used and all the ethyl acetate was cracked in a single pass through the tube at temperatures above 628°C. The yield of ethylene was determined for only Run No. E7 and was found to be 104% of theory, assuming that all the ethylene was derived from the ethyl radical. However, it is known that ketene also decomposes to ethylene, carbon monoxide, and other gases, and if it is assumed that all the acetate radical which is not recovered as ketene or acetic acid is converted quantitatively to ethylene, carbon monoxide, and water according to the equations,

$$2CH_3 - \overset{\overset{O}{\parallel}}{C} - OC_2H_5 \rightarrow 2CH_2 = C = O + 2H_2O + 2C_2H_4,$$
$$\downarrow$$
$$C_2H_4 + 2CO$$

TABLE IV

PYROLYSIS OF ETHYL ACETATE

Run No.	% Et_3PO_4 in feed	Feed rate, gm./min.	% H_2O in feed	Temp. of pyrolysis, °C.	Abs. press., mm. Hg	% Yield to ketene and acetic acid	% Conversion	
							To ketene alone	To ketene and HOAc
E 4	0.33	3.7	< 0.1	600 – 628	155	76.5	6.7	64.5
E 5	0.33	4.2	< 0.1	644 ± 5	154	85.8	21.8	85.7
E 6	0.33	4.2	< 0.1	666 ± 5	188	76.0	32.4	76.0
E 7	0.33	3.6	< 0.1	685 ± 10	148	72.2	35.4	72.2

then the yield to ethylene from the ethyl radical becomes 90%. Of the 10% loss, about 5.3% was recovered as acetylene. A summary of the results is given in Tables IV and V.

TABLE V

PERMANENT GASES FORMED IN THE PYROLYSIS OF ETHYL ACETATE

Run No.	Spot gas analysis*						
	% CO_2	% C_nH_{2n} + C_2H_2	% C_2H_2	% CO	% H_2	% O_2	% N_2
E 4	1.3	84.4		2.9			
E 5	4.0	70.8		5.4			
E 6	2.5	68.4		3.4			
E 7	1.4	77.2	3.9	8.3	0.7	2.0	8.0

**The gas analysis given for Run No. E7 is the average for the whole run. All others are only typical analyses and are not necessarily the average.*

DISCUSSION

The highest yield of ketene obtained from acetic acid in this investigation was comparable to that obtained industrially, but the highest conversion was a little less than half as great. The low conversion would appear to be due to recombination of ketene and water to acetic acid and acetic anhydride. In several experiments, the presence of a substantial quantity of acetic anhydride in the aqueous condensate from the first and second condensers was established by cooling the condensate to −10°C. to retard the hydrolysis of the anhydride until it could be determined quantitatively by the "aniline" method (1). Results are shown in Table VI. Since the anhydride in the aqueous condensate could not be easily isolated by distillation it was considered, for yield purposes, as recovered acetic acid, and in most runs was allowed to hydrolyze to acetic acid. Further evidence of recombination of ketene and water was obtained in another investigation on a much larger scale, details of which are not given here. Yields of 90-92% and conversions of 70-72% were obtained by using linear velocities 10 to 12 times those used in this investigation, and by adding a catalyst neutralizer (gaseous ammonia) at the inlet or outlet of the pyrolysis tube. The higher linear velocity permitted a much more rapid separation of ketene and water in the condenser system, and the ammonia probably neutralized the phosphate catalyst which otherwise would have catalyzed the hydrolysis of ketene. In the present small-scale investigation no attempt was made to add any neutralizer owing to the difficulty of metering in such a small flow.

The highest conversion obtained in the pyrolysis of methyl acetate was also much lower than that obtained in the industrial pyrolysis of acetic acid but was of the same order as that obtained in our laboratory pyrolysis of acetic acid. It would appear probable that the conversion could be greatly increased by employing the same expedients as with acetic acid.

In the pyrolysis of methyl acetate–methanol azeotropic mixture, conversions were lower and catalyst consumption was much higher than for pure methyl

TABLE VI

PYROLYSIS OF ACETIC ACID

Run No.	Catalyst used	% Catalyst in feed	Feed rate, gm. per min.	Temp. of pyrolysis, °C.	Abs. press., mm. Hg	% yield to ketene	% Conv. to ketene	% Conversion to ketene if Ac_2O in first and second condensates is included
M 37	Et_3PO_4	0.33	6.1	732 ± 10	270	72.0	22.7	27.5
M 38	Et_3PO_4	0.33	4.4	720 ± 5	245	59.8	26.3	30.6
M 55	H_3PO_4 (85%)	0.4	4.1	724 ± 5	200	66.2	34.3	42.9

NOTE:—*The three above experiments (only) were carried out in the methyl acetate apparatus.*

acetate. It would thus appear advisable to obtain first substantially pure methyl acetate from the azeotropic mixture.

In the pyrolysis of ethyl acetate, much higher conversions to ketene than those obtained in this investigation are also undoubtedly possible. In fact, conversions of 85% and quantitative yields have already been claimed in the patent literature (7). The optimum temperature of pyrolysis was found to be about 60° to 80°C. lower than for pure acetic acid, which would indicate that the primary products of the pyrolysis are not acetic acid and ethylene, followed by dehydration of the acetic acid. Instead it would seem probable that the pyrolysis is exactly analogous to that of methyl acetate but that, in this case, the alcohol (ethanol) is unstable under the conditions of pyrolysis and dehydrates to ethylene and water, according to the equations,

$$CH_3 - \overset{\overset{O}{\parallel}}{C} - OC_2H_5 \rightarrow CH_2 = C = O + C_2H_5OH$$
$$\rightarrow CH_2 = C = O + C_2H_4 + H_2O.$$

Some of the ketene then recombines with water giving a mixture of ketene and acetic acid. No ethanol was isolated, which is not surprising, since it is well known that ethanol dehydrates in the presence of catalysts such as alkali and alkaline-earth metal phosphates containing free phosphoric acid at temperatures of 480°C. (3).

ACKNOWLEDGMENT

The author wishes to thank Dr. W. E. Barker for his collaboration on the work on acetic acid, and also Shawinigan Chemicals Limited for permission to publish this paper.

REFERENCES

1. COLLINS, W. D. *et al.* Ind. Eng. Chem. 18: 636. 1926.
2. HURD, C. D. and BLUNK, F. H. J. Am. Chem. Soc. 60: 2419. 1938.
3. I. G. FARBENINDUSTRIE A.-G. Brit. Patent 326,185. 1930.
4. KOLTHOFF, I. M. and SANDELL, E. B. Textbook of quantitative inorganic analysis. The Macmillan Co., New York. 1936. p. 367.
5. LOASBY, G. and BROWN, F. S. Brit. Ministry of Supply and U.S. Tech. Ind. Intelligence Comm. FIAT Final Rept. No. 145. 1945.
6. LODER, D. J. U.S. Patent 2,175,811. 1939. Brit. Patent 504,626. 1939.
7. LONZA ELEKTRIZITÄTSWERKE and CHEMISCHE FABRIKEN A.-G. Swiss Patent 233,176. 1944. Chem. Abstracts, 43: 6643. 1949.
8. ROSS, W. H. and TRUMBULL, H. L. J. Am. Chem. Soc. 41: 1180. 1919.
9. WILSMORE, N. T. M. J. Chem. Soc. 91: 1938. 1907.

THE FLOW OF FLUIDS THROUGH ACTIVATED CARBON RODS. I[1]

By E. A. Flood, R. H. Tomlinson, and A. E. Leger

ABSTRACT

The flow rates of the vapors of benzene, ethyl chloride, diethyl ether, methanol, and water through activated carbon rods have been found to exceed, considerably, flow rates calculated by classical equations. The excess flow rates show maxima in widely different relative pressure regions and are ascribed to flow of adsorbed material. An empirical equation is presented which correlates the observed flow rates with relevant adsorption isotherms. Classical equations of flow through elliptical and rectangular pipes are discussed with reference to flow through fine-grained porous materials. It is shown that equations of the Adzumi type are roughly valid as applied to fine-grained porous bodies, but that without a knowledge of the frequency distributions of pore sizes and shapes, flow data cannot be related to pore dimensions in any literal sense. End effects are discussed.

INTRODUCTION

While the rates of flow of gases through capillaries and porous bodies may be described approximately by various classical equations, we have shown in previous papers (17, 27) that when appreciable adsorption occurs, these flow equations may be considerably in error. Since flow rate data are extensively used to gain information concerning the fine structure of porous material, it is important to determine the magnitude of the errors which adsorption phenomena may introduce into such experiments. Further, if the flow of adsorbate contributes appreciably to the over-all flow rate and this contribution can be distinguished from gaseous flow and described mathematically, a new and valuable tool for the study of the very fine structure of active adsorbents might be developed. Finally, there is a broad, largely unexplored field where transport of fluids occurs under the influence of compressive surface forces, and where information is needed concerning such processes.

Accordingly, we have carried out some additional measurements of flow rates of adsorbable vapors through activated carbon rods and have attempted to correlate the observed flow rates with the structure of the carbon rods and their adsorptive properties.

The results of this investigation are presented in three parts. In Part I we present this general introduction and most of the experimental results together with a theoretical discussion of gaseous flow through porous bodies. In Part II it is shown that the flow rates of nonadsorbable gases are consistent with well-established facts concerning the macropore structure of zinc dichloride activated carbon rods. In Part III it is shown that the flow rates of adsorbable gases may be correlated with relevant adsorption–desorption isotherms. Equations are deduced which correlate micropore structure, adsorptive properties, and flow rates. It is further shown that surface forces which compress gases to high densities within micropores may increase flow rates by very large factors. The increased flow rates are due in the main to

[1] *Manuscript received August 16, 1951.*
Contribution from the Division of Chemistry, National Research Council, Ottawa. Issued as N.R.C. No. 2704.

an increase in the effective pressure gradient and to the direct effect of the increase in fluid density. Evidence is presented which suggests that where considerable adsorption occurs the rate controlling mechanism of flow of the adsorbates studied is a laminar viscous flow of liquid films.

EXPERIMENTAL

Materials

The activated carbon rods used in these experiments were supplied through the courtesy of the National Carbon Company. They consist of very uniform, zinc-chloride-activated, extruded and calcined, rods. The rods as supplied were all close to 0.38 cm. in diameter, 3 or 4 in. long and fairly straight. From these rods, plugs 1 cm. long were cut and the ends carefully ground. By a little care in selection to avoid pieces with obvious cracks, etc., plugs of remarkable uniformity regarding permeability and adsorption characteristics can be obtained. A number of plugs were cut; those of lengths 1.00 ± 0.02 cm. were numbered and kept for further investigation. Plugs Nos. 11 and 18 were used for most of the experiments reported in this paper. Plugs Nos. 9, 10, 11, 12, 13, and 14 were reported on previously (27). All of these plugs except No. 13 were very similar as regards permeability. The charcoal has the following general characteristics:

Helium density, 2.22 ± 0.05 gm. per cc.

Mercury density, 0.707 ± 0.001 gm. per cc.

Void fraction, 0.68 (from mercury and helium densities).

Void fraction at saturation, assuming adsorbate has density of the liquid at the same temperature,

(*a*) diethyl ether, 0.24; (*b*) water, 0.30.

Adsorption B.E.T. surface areas,

(*a*) nitrogen, 1100 sq.m. per gm.; (*b*) diethyl ether, 1200 sq. m. per gm.; (*c*) ethyl chloride, 900 sq. m. per gm.

The benzene, diethyl ether, ethyl chloride, and methane were all of reagent quality, were carefully dried, redistilled in vacuum, and checked as to vapor pressure. The nitrogen was a commercial grade of nitrogen, dried by passage through a liquid nitrogen trap.

Methods, Procedures, Apparatus

The transpiration experiments which we have carried out are all of the same type as those described in our earlier papers (17, 27). These experiments consist essentially in forcing a gas through an activated carbon rod by means of a pressure gradient. The system is maintained at a constant temperature and the pressure difference across the charcoal rod, as well as the mean pressure, maintained at constant values, while observations of either the volume or weight of gas passing through the charcoal per minute are made. When the flow rate has been constant over a period of some hours it is recorded. In order to ensure a reasonably steady state of flow, it is neccessary that the total weight of gas entering or leaving the charcoal, during the period while

the flow rate appears to be constant, be large in comparison with the weight of gas adsorbed.

The apparatus and procedures we have used to obtain the flow data reported in this paper are similar to those described by Tomlinson and Flood (27) with minor modifications and improvements such as enclosing the whole of the input system, as well as a considerable part of the output system, within a thermostatic fluid envelope. In case of some of the experiments in the lower pressure regions it was necessary to carry out the flow rate measurements during a period of a week or more and to use gravimetric methods to determine the quantity of vapor actually passing through the sample per minute. By maintaining a liquid at a suitable constant low temperature a source of constant low pressure gas was provided and by observing the loss in weight of the liquid the quantity of gas passing through the charcoal obtained. The flow in volume units is then calculated using the ideal gas laws. At the lowest pressures used, mercury vapor distills into the cold liquid during the 6 to 10 day period of the experiments and it is necessary to correct for this back distillation. The liquid remaining was distilled into a second weighted tube to separate it from the mercury collected during the run.

The procedure followed for the water vapor flow was essentially similar to that used for the other adsorbable vapors, but was varied slightly to take into account the hysteresis of the isotherm. Thus, in adsorption flow the plug was brought to equilibrium at the effluent pressure and the influent pressure then raised to obtain the required pressure gradient, care being taken that this pressure was not exceeded at any time. In the case of desorption flow, the plug was equilibrated at the influent pressure and the effluent pressure reduced to obtain the pressure gradient. The equilibrium at the influent pressure in desorption state flow measurements was approached from higher pressures and conversely in adsorption flow experiments.

It may be remarked that it was found that after repeated exposures to various adsorbable gases, especially benzene, the permeability of the charcoal rods to nitrogen showed a downward trend, falling some 5-10%, depending on the treatment. After evacuation during three or four hours at a temperature between 350-400°C. the original nitrogen-permeability can be restored to within the probable experimental error.

The adsorption–desorption isotherms were determined by the standard McBain technique, the system including the manometer being immersed in the water of the thermostatic bath. However, the lowest pressure readings were made on a McLeod gauge which was outside of the thermostatic bath.

Results

It was hoped to obtain adsorption isotherms for each gas on the charcoal plug actually used for the flow measurements. However, this has not been done owing to the accidental destruction of plug No. 18 after some of the most careful and time-consuming flow measurements had been made and before adsorption measurements could be obtained. Consequently, most of the isotherm data were obtained on a small plug cut from the same rod as plug

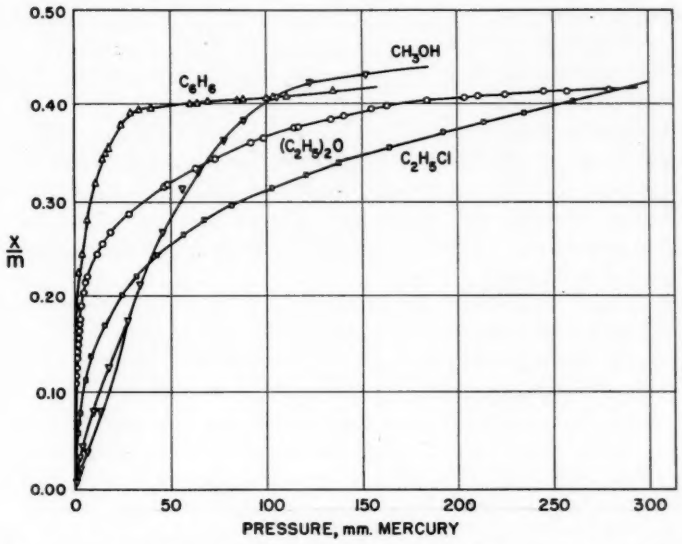

FIG. 1. Adsorption isotherms for benzene, methanol, diethyl ether, and ethyl chloride. X/m is weight adsorbed in gm. per gm. of carbon.

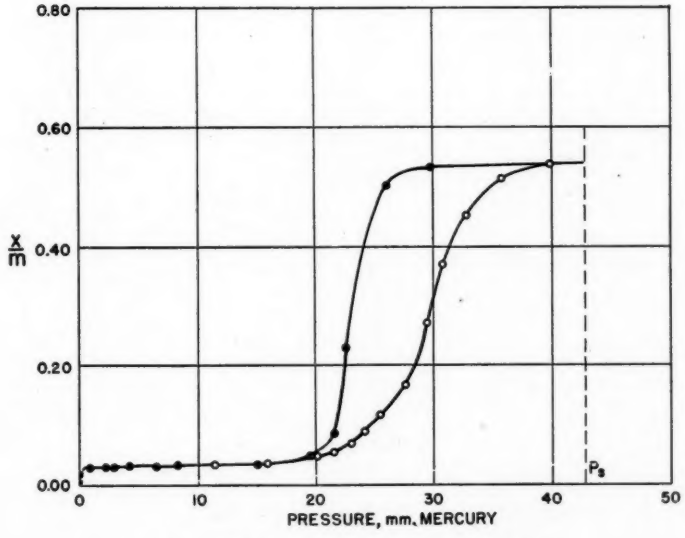

FIG. 2. Water adsorption–desorption isotherms.

No. 18 while the flow data applies to different plugs, as shown by the tables. As a check, the adsorption–desorption isotherms were determined with plug No. 11 for methanol and the isotherm was essentially the same as obtained on the specially cut plug.

The adsorption results given here were calculated from the weight of the charcoal after it had been heated to 350-400°C. for some hours and evacuated under high vacuum. In some cases, especially benzene and water, the original weight of the charcoal could not be obtained by pumping at the end of isotherm measurements. This accounts for the slight rise shown on the water isotherm at low pressures.

The isotherms for benzene, methanol, ethyl chloride, and diethyl ether are given in Fig. 1, while that of water, in Fig. 2. The ethyl chloride isotherm is the same as that reported previously (27) with added experimental measurements below 360 mm. pressure.

Flow rate data are presented graphically in Figs. 3 to 8 inclusive. The ordinates shown in the graphs represent flow rates expressed in K' units, i.e., in cubic centimeters per minute measured at the input pressure and multiplied by the ratio of the input pressure to the pressure difference across the plug. The flow rates are plotted against $\bar{p}$, the mean of the input and output pressures expressed in mm. Hg.

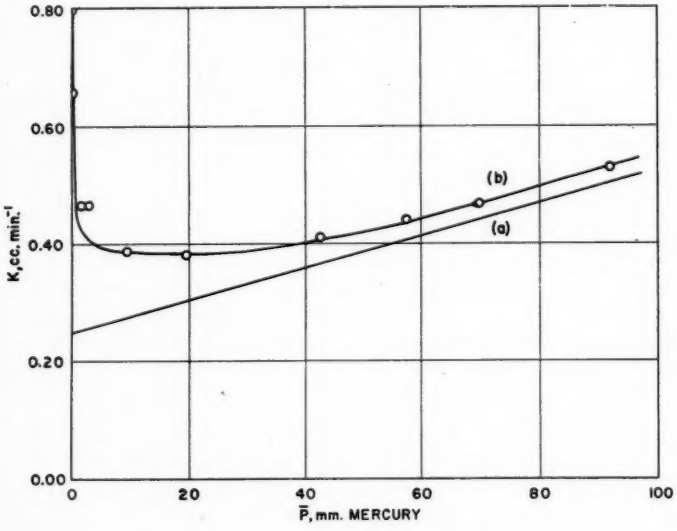

FIG. 3. Flow rate of benzene through plug No. 18.
O = Observed points.
(*a*) Adzumi line, $K' = 2.79 \times 10^{-3}\,\bar{p} + 0.249$.
(*b*) $K = K' + 0.05\,\bar{X} + 0.32 \times 10^{2}\left(\frac{X_1^{2.2} - X_2^{2.2}}{\Delta p}\right)$.

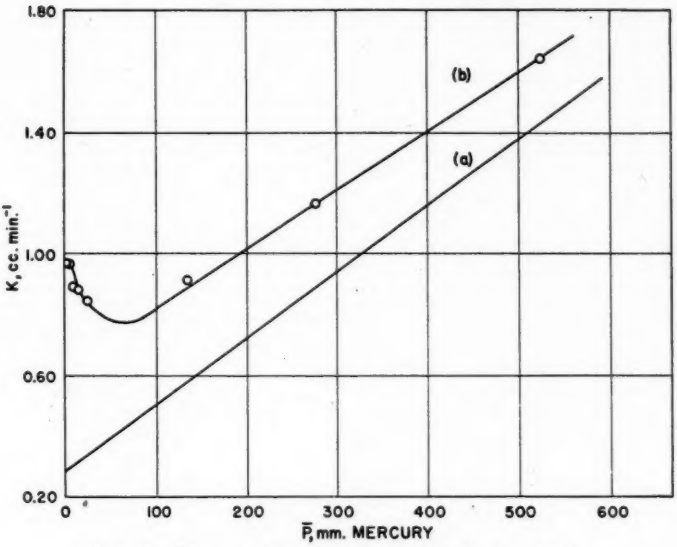

FIG. 4. Flow rate of ethyl chloride through plug No. 11.
O = Observed points.
(*a*) Adzumi line, $K' = 2.18 \times 10^{-3}\,\bar{p} + 0.285$.
(*b*) $K = K' + 0.37\,\overline{X} + 0.38 \times 10^{3}\left(\frac{X_1^{2.1} - X_2^{2.1}}{\Delta p}\right)$.

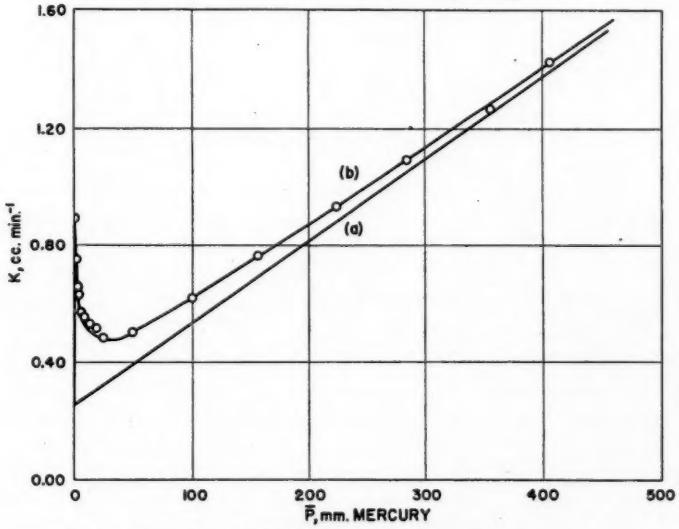

FIG. 5. Flow rate of diethyl ether through plug No. 18.
O = Observed points.
(*a*) Adzumi Line, $K' = 2.80 \times 10^{-3}\,\bar{p} + 0.255$.
(*b*) $K = K' + 0.09\,\overline{X} + 0.218 \times 10^{3}\left(\frac{X_1^{3} - X_2^{3}}{\Delta p}\right)$.

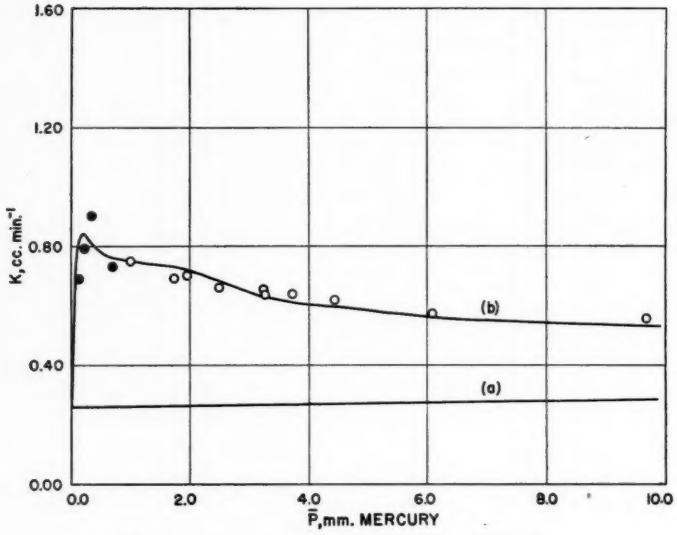

FIG. 6. Low pressure region corresponding to Fig. 5.
○ = Volumetric observed points.
● = Gravimetric observed points.
(*a*) and (*b*) as given for Fig. 5.

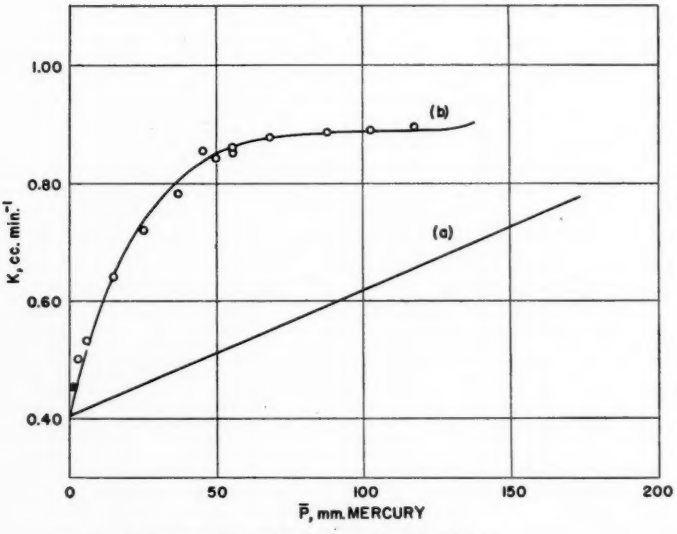

FIG. 7. Flow rate of methanol through plug No. 11.
○ = Observed points.
(*a*) Adzumi Line, $K' = 2.31 \times 10^{-3}\,\bar{p} + 0.405$.
(*b*) $K = K' + 0.357\,\bar{X} + 0.89 \times 10^{2}\left(\dfrac{X_1^{1.7} - X_2^{1.7}}{\Delta p}\right)$.

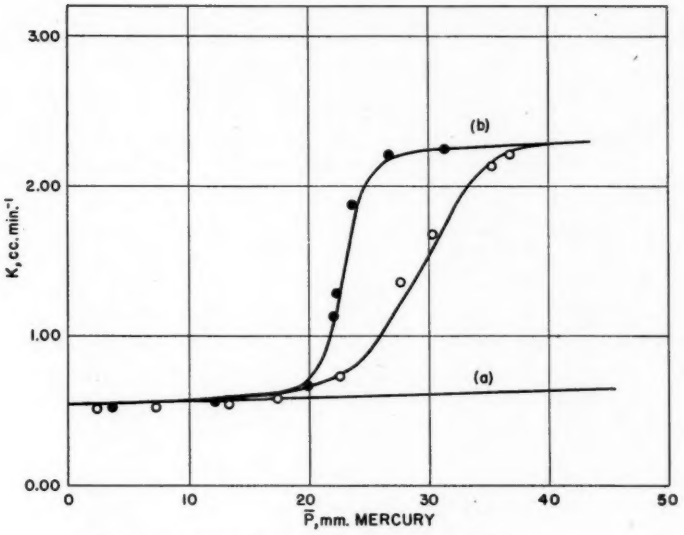

FIG. 8. Flow rate of water through plug No. 11.
○ = Observed points, adsorption state.
● = Observed points, desorption state.
(*a*) Adzumi line, $K' = 2.23 \times 10^{-3}\ \bar{p} + 0.540$.
(*b*) $K = K' + 3.26\ \bar{X}$.

The straight lines (*a*) shown in the figures are calculated from nitrogen flow rates by means of the Adzumi equation,

$$K' = \frac{A}{\eta}\bar{p} + \frac{B}{\sqrt{M}}$$

where η is the viscosity and M the molecular weight of the gas and A and B are constant characteristics of the porous plug but independent of the gas. Usually in theoretical discussions where c.g.s. units are used, K is expressed in cubic centimeters per second and pressures in dynes cm.$^{-2}$

An example of the calculations involved and the degree of precision obtained is presented in Table I for a methanol flow measurement. This point is shown on Fig. 7 for a mean pressure, $\bar{p}$, of 45.4 mm. and is average in precision. The nitrogen flow rates at 35°C. are linear functions of $\bar{p}$, above a $\bar{p}$ of 50 mm. and are described by the following equations,

$$\text{Plug No. 11, } K = 1.26 \times 10^{-3}.\ \bar{p} + 0.433$$

$$\text{Plug No. 18, } K = 1.19 \times 10^{-3}.\ \bar{p} + 0.415.$$

It may be pointed out that the constants for Plug No. 11 as determined some years previously and as reported by Tomlinson and Flood (27) differ somewhat from those given above, the previously reported slope and intercept being 1.23×10^{-3} and 0.460, respectively.

TABLE I

AN EXAMPLE OF FLOW MEASUREMENT: METHANOL AT 35°C. THROUGH PLUG NO. 11

INFLUENT PRESSURE, $p_1 = 7.055$ cm.
EFFLUENT PRESSURE, $p_2 = 2.025$ cm.
PRESSURE GRADIENT, $\Delta p = 5.030$ cm.
MEAN PRESSURE, $\bar{p} = 4.540$

Measurements were begun four hours after pressure conditions were set

Burette reading, cc.	Volume flowing, cc.	Time, hr. : min. : sec.	Time of flow, sec.	Flow, cc. sec.$^{-1}$
97.0		2 : 18 : 50		
92.4	4.6	2 : 26 : 10	440	0.01045
85.0	7.4	2 : 38 : 15	725	0.01021
79.0	6.0	2 : 48 : 05	590	0.01017
75.8	3.2	2 : 53 : 25	320	0.01000
71.6	4.2	3 : 00 : 35	430	0.00977
48.8	22.8	3 : 38 : 40	2285	0.00998
31.0	17.8	4 : 07 : 05	1705	0.01044
14.6	16.4	4 : 33 : 45	1600	0.01025
99.0		4 : 59 : 30		
85.8	13.2	5 : 20 : 55	1285	0.01027
79.6	6.2	5 : 31 : 10	615	0.01008
63.6	16.0	5 : 57 : 10	1560	0.01026
46.4	17.2	6 : 26 : 00	1730	0.00994

NOTE: *Total volume = 135.0.*
Total time of flow = 13285.
Mean flow rate = 0.01016.

Calculations:

$$K = \frac{Vp_1}{\Delta p \,.\, time}$$

$$K = \frac{135.0 \times 7.055}{5.030 \times 13285} = 0.01425 \text{ cc. sec.}^{-1}$$

$$= 0.855 \text{ cc. min.}^{-1}.$$

"Burette readings" and "volume flowing" represent cubic centimeters measured at the influent pressure p_1.

The solid curves, (*b*), shown in the figures represent calculated flow rates based on an empirical equation in which the terms $\alpha \bar{X}$ and $\beta (X_1^n - X_2^n)/\Delta p$ are added to the Adzumi flow equation (cf. Part III of this paper). Thus the curves are drawn from,

$$K = \frac{A}{\eta}\bar{p} + \frac{B}{\sqrt{M}} + \alpha\bar{X} + \beta\frac{X_1^n - X_2^n}{\Delta p},$$

where α, β, and n are adjustable constants; $\bar{X}$ is the mean value of the ordinate of the relevant isotherm averaged over the pressure interval Δp; X_1 and X_2 are the values of the ordinates corresponding to the pressures p_1 and p_2, respectively, i.e., to the influent and effluent pressures; Δp is $p_1 - p_2$ in mm. of Hg. The other symbols are as above. The various values of the constants are given in the legends describing the figures. In the case of water the value of β is so small that the term in $(X_1^n - X_2^n)/\Delta p$ is omitted altogether. The values of the viscosities and molecular weights used are given in Table II.

TABLE II

PHYSICAL CONSTANTS OF VARIOUS LIQUIDS AND VAPORS AT 35°C.

Substance	Molecular weight	Gas viscosity, poises × 10^{-4}	Liquid viscosity, poises × 10^{-4}
Benzene	78.11	78.2	53.0
Ethyl ether	74.12	77.4	20.7
Ethyl chloride	64.52	105.0	24.0
Methanol	32.04	98.9	48.2
Water	18.02	102.4	72.25
Nitrogen	28.02	181.5	

Most points given are considered to be reliable to within about 5%. However, the lowest ether and benzene flow measurements are probably not much better than ± 20%. The ether maximum is believed to be real and fairly close to the indicated $\bar{p}$ value; the maximum ether experimental value was obtained from two independent measurements which gave practically identical flow rates. Values obtained for very low pressure ethyl chloride flow by a pressure decay method are not reported as these were found to be very inaccurate owing to adsorption–desorption complications. However, the results indicate that a maximum exists somewhat below the rise shown on Fig. 4. No maximum was found in the case of benzene but it is thought that at a low enough pressure it would appear. No evidence of a maximum in nitrogen flow was found although the flow rate measurements were extended to mean pressures as low as 0.037 mm. of Hg.

DISCUSSION

In order to form any sort of notion as to what interpretation is to be given to the experimental results reported in this paper, it seems necessary to be able to describe with some accuracy the flow of gases through our charcoal rods when not complicated by adsorption. In what follows, we prepare a foundation for correlating flow rates of nonadsorbable gases with pore diameters in statistical assemblies of pores of various shapes and sizes.

The Adzumi Equation

Many empirical equations have been put forward to describe the flow of fluids through porous materials. Notable among them are the equations of Darcy (14), Kozeny (21), Adzumi (1-4), Carman (10), and Arnell (6-7). Practically all of these equations have certain features in common which are perhaps most conveniently discussed by references to Adzumi's equations.

The Adzumi (4) equation relates the rate of flow of gases to the pore radii of capillaries in a porous body. The equation is based on Knudsen's "long-tube" formula, namely,

$$K = \frac{Q_{pv}}{\Delta p} = \frac{\pi r^4}{8\eta l}\bar{p} + \gamma\frac{4}{3}\frac{r^3}{l}\sqrt{\frac{2\pi RT}{M}}, \tag{1}$$

K = flow rate in cubic centimeters per second measured at an arbitrary pressure and multiplied by this pressure, and divided by the

difference between the input and outflow pressures, $p_1 - p_2$. (if p_2 is zero, K is numerically equal to the flow rate in cubic centimeters per second measured at a constant input pressure.)

Q_{pv} = flow rate in pv units.
$\Delta p = p_1 - p_2$ in dynes cm.$^{-2}$
r = radius of capillary in cm.
l = length of capillary in cm.
η = viscosity of fluid in poise.
$\bar{p} = \frac{1}{2}(p_1 + p_2)$ in dynes cm.$^{-2}$
R = gas constant in ergs per mole per degree of temperature.
T = the absolute temperature.
M = the molecular weight.
γ = an empirical function of pressure often assumed to be a constant.

In case of n capillaries of constant length connecting two large reservoirs containing gas at pressures p_1 and p_2 respectively, in the absence of inertial and other end effects, the total simultaneous flow will be, of course, the sum of the flows through each capillary. Thus we can follow Adzumi (4) and write for the total flow rate,

$$K = n\frac{\pi\overline{r^4}}{8\eta l}\bar{p} + n\gamma\frac{4}{3}\frac{\overline{r^3}}{l}\sqrt{\frac{2\pi RT}{M}}, \tag{2}$$

provided that γ is the same for each capillary and is independent of pressure.

Adzumi considers also the case of capillaries in series and arrives at the conclusion that in the case of m capillaries in series,

$$K = A\frac{1}{\sum_m \frac{l_i}{r_i^4}}\bar{p} + \gamma B\frac{1}{\sum_m \frac{l_i}{r_i^3}},$$

neglecting other nonlinear pressure dependent terms which he considers to be small. He gives some data in support of the contention that the other pressure dependent terms are small and may be neglected. However, it is easily shown that the contribution of nonlinear pressure dependent terms is not by any means always small. Actually K will only be a linear function of $\bar{p}$ when either the capillaries in series have nearly the same radii, i.e., behave as part of a single capillary or when r^4/l and r^3/l for one capillary are much smaller than the values of these quantities for any of the other capillaries in the series, i.e., when the one capillary controls the flow rate.

Adzumi goes on to treat a collection of m capillaries in series and n in parallel, and writes,

$$K = A\bar{p}\sum^n \frac{1}{\sum_m \frac{l_i}{r_i^4}} + \gamma B\sum^n \frac{1}{\sum_m \frac{l_i}{r_i^3}}, \tag{3}$$

or,

(3a) $$K = A\bar{p}E + \gamma BF,$$

where A and B represent the constants other than those in r and l appearing in the Knudsen long tube formula. If the capillaries all have radius R and length L, the equation becomes simply,

(4) $$K = nA\bar{p}\frac{R^4}{L} + n\gamma B\frac{R^3}{L},$$

and

$$R = E/F.$$

Adzumi tests Equation 3a by measuring the flow rates of gases through porous plates where r is not a constant and finds that the equations are in fact linear, in that K can be expressed by an equation of the form of Equation 3a. It is reasonably well established that in the case of flow through many porous or granular beds, K actually is a linear function of $\bar{p}$ over a wide range of pressure; in fact, over a wider range of pressure than it is for a single capillary, the rise at low pressures characteristic of the long single capillary being conspicuously absent. Experimentally, it is found that the slope of K as a function of $\bar{p}$ varies inversely as the viscosity, as it should, and that the intercept varies inversely as the square root of the molecular weight.

Equations of the type of Equation 4 form the basis of the various methods of determining surface areas of granular beds from gas permeability measurements. Arnell has shown that with minor empirical adjustments such equations give excellent correlations between granule surface areas, mean pore sizes, etc., and flow data.

There is, however, need for caution in the application of permeability methods to the determination of "pore sizes". Unless there is evidence independent of flow data that "pore sizes" are constant, even if the pores are all cylinders of the same length and are all of circular cross section, the quotient $\overline{r^4}/\overline{r^3}$ is by no means in general equal to $\bar{r}$. The correct relation is, $\overline{r^4}/\overline{r^3} \geqslant \bar{r}$ and $\overline{r^4}/\overline{r^3}$ may be greater than $\bar{r}$ by a factor of any magnitude, i.e., a thousandfold or more. Adzumi's application of Equation 4 to calculate R for porous plates assumes that R is practically constant.

It must be emphasized that in a complex assembly of even straight round capillaries, entirely different capillaries may control the values of $\bar{r}$, $\overline{r^2}$, $\overline{r^3}$, and $\overline{r^4}$. Thus without a knowledge of pore-size frequency distribution, no correlation can be made as between the surface area, the void volume, the intercept, and the slope. In such cases the "surface area", mean "pore size", etc., as measured by permeability methods will be entirely fictitious.

In the case of granular beds the pores are interstitial spaces and the void space does not resemble a system of parallel cylindrical capillaries but rather a system of "bottle necks". The permeability is controlled by the "bottle necks", the sum of whose lengths will in general be considerably less than the length of the bed. The cross sections of the "bottle necks" will, in general, have a number of irregular shapes and the "average shape" might be represented by almost any ideal geometrical figure other than the circle. Of

course, the areas of these cross sections will not usually be constant. Finally, when it is realized that γ itself in the original Knudsen equation is a pressure dependent factor, it is surprising that such equations can be used at all to correlate pore structure and permeability.

It may be emphasized again that for capillaries in series, K cannot be an exactly linear function of $\bar{p}$ unless the capillaries in series which control the flow rate are all the same. Since undoubtedly this cannot be the case in granular beds of material of widely varying granule size, the fact that K usually is a linear function of $\bar{p}$ implies that the pressure is uniform across the granular bed at right angles to the direction of flow. Consequently, the flow is the same as though the different capillaries were in parallel, or in other words, each section perpendicular to the direction of flow is identical and the granular bed behaves as though it consisted of a parallel system of capillaries, each capillary consisting of a series of shorter identical capillaries. Such a situation might be expected in a system of a great many capillaries which were all cross connected so as to form a space lattice, where the rate of flow—and hence the pressure drop—due to any one capillary is negligible compared to that of the whole system.*

The second term of the right-hand member of Equation 1, i.e., the intercept when K is plotted against $\bar{p}$, is usually referred to as the "slip" term. While the association of "slip" with the viscous flow of fluids was perhaps first introduced by Helmholtz (16) and its possible existence demonstrated by Kundt and Warburg (22), it is chiefly to Maxwell (23) that we owe our knowledge of this term. Maxwell's evaluation of the "slip" was based upon an elaborate analysis of stresses arising in gases obeying the classical Boltzman equations. In the case of gases which are Maxwellian with respect to velocity components perpendicular to the direction of flow and where velocity components may be treated as independent, the "slip" term, as shown by Millikan (24) and Kennard (18) must be very nearly as given by Maxwell in all cases where laminar viscous flow prevails in the body of the fluid remote from the walls and where velocity gradients are all small.

Maxwell pointed out that where the pressures are so low that nothing like laminar flow can exist in the body of the gas, the transport of matter must, in the limit, become a phenomenon of molecular effusion, an entirely different phenomenon from viscous flow with slip. When a gas is so dilute that even over long distances (e.g., down the length of a long tube) collisions may be neglected, the flow problem can be solved without much difficulty granting a simple law of reflection of molecules striking the walls of the tube. Assuming diffuse reflections from the walls (i.e., that molecules leave the walls with equal probabilities in all directions, independently of incident angles) and that the gas is Maxwellian we get what is known as "Knudsen flow". The case of Knudsen flow or molecular effusion has been studied very thoroughly

**If two quite different pore systems are cross connected at such intervals that Δp per interval is relatively large, then the equation of continuity cannot be applied to each system independently. This situation has been commented on by Babbitt (8).*

by Clausing (12) following Smoluchowski (26) and Knudsen (19, 20). The region between Maxwellian flow or laminar flow with slip and Knudsen flow has been practically ignored until quite recently when it has been studied by Pollard and Present (25).

Maxwell's original equation when integrated and expressed in K units is,

$$K = \frac{\pi r^4}{8\eta l}\bar{p} + \frac{2-f}{f}\frac{\pi r^3}{4l}\sqrt{\frac{2\pi RT}{M}},$$

where f is the fraction of the surface from which molecules are diffusely reflected and $(1-f)$ is the fraction of the surface from which molecules are specularly reflected; the other symbols are as above. If f may have almost any value and especially if f is any function of $\bar{p}$ the equation is practically meaningless. The implicit assumption is that f is independent of $\bar{p}$ and nearly unity.

That f is independent of $\bar{p}$ and nearly one in most cases where the contribution of the Poiseuille term is appreciable has been shown by Knudsen and many others. The fact that $(2-f)/f$ is a measure of a real physical quantity dependent on the surface has been shown by Millikan and co-workers who show that the nature of the surface whether covered with oil, shellac, etc., does in fact produce a measurable difference in the rate of transfer of momentum to the surface. This point is important since it demonstrates the existence of "slip". If the intercept were fundamentally due to some sort of gaseous diffusion superimposed on the laminar flow or to any property of the gas alone, the nature of surface could not change the rate of transfer of tangential momentum to the wall if the thin fluid layer adjacent to the wall were not moving, apparent variations in apparatus dimensions, due to possible variations in layer thickness, being quite negligible in Millikan's experiments.

The Knudsen long tube formula was obtained by considering that in the low pressure limit the phenomenon must become one of molecular effusion, which with $f = 1$ requires,

$$K = \frac{4}{3}\frac{r^3}{l}\sqrt{\frac{2\pi RT}{M}}.$$

Adding this term to the Poiseuille or viscous, high pressure limit term, Knudsen obtained Equation 1 without the factor γ. This procedure, although physically plausible, is of course not strictly permissible since the two mechanisms of flow are mutually exclusive. Knudsen introduced the empirical term, γ, where

$$\gamma = \frac{1 + C_1 p}{1 + C_2 p},$$

in order to make the expression give the Maxwellian "slip" intercept in the higher pressure regions. At higher pressures, γ approaches c_1/c_2 and Knudsen put $c_1/c_2 = 0.81$. The Knudsen intercept is greater than the Maxwellian intercept by $16/3\pi$ when $f = 1$. Hence the value of 0.81 for γ

corresponds to a value of f of about 0.85 in Maxwell's expression. Thus at higher pressures the Knudsen expression becomes practically identical with the Maxwell equation with $f \simeq 0.9$, which is in accordance with a good deal of experimental evidence. Smoluchowski derived the Knudsen long tube formula for the case where f may differ from unity and obtained the Knudsen expression with the added factor $(2 - f)/f$. If f can be appreciably less than unity at low pressures, the limiting intercept may be considerably greater than the Knudsen intercept. While Pollard and Present have presented an analysis of gaseous self-diffusion, including the intermediate pressure region, they do not discuss the question as to the value of f but assume the "cosine law" of reflection or in other words f is taken as unity. While the evidence is by no means conclusive it seems to be the general opinion that f should be taken as unity in molecular effusion problems.*

In pressure regions intermediate between Knudsen or effusive flow and Maxwellian or laminar viscous flow with slip, the situation concerning f, as well as the exact nature of the flow, is obscure. Pollard and Present point out that the development of the drift velocity necessary for laminar flow results from collisions terminating long free paths and necessarily reduces the net transport from these long free paths parallel to the walls of a long tube and hence leads to a minimum in the usual plots of K against p. These authors consider that the difference between the numerical values of Maxwell's "slip" term and Knudsen's effusion term are largely "fortuitous" which certainly appears to be the case from a strictly theoretical viewpoint. However, the bulk of the evidence indicates that the Maxwellian slip term is essentially correct in the laminar flow region. The evidence is also fairly clear that the effusion intercepts are larger, in cases of long tubes, and close to Knudsen's intercept. It may seem that it makes very little practical difference which intercept is considered to be correct since these two intercepts are not very different numerically and especially since a more or less indeterminate empirical term of the type $(2 - f)/f$ is probably involved in both cases. However, it is necessary to make this distinction because it is only in the case of capillaries having certain length–diameter ratios that the numerical values are nearly the same. In the case of a tube whose length is much less than its diameter, the effusion intercept, as shown by Clausing, is much less than that of the Maxwellian intercept. Further, the distinction is not only a matter of the numerical values of the constants, but makes a considerable difference in the effects to be expected from a series of short capillaries joining large volumes, i.e., a series of "bottle necks" such as might be encountered in granular or porous beds. While the "slip" term associated with a series of identical capillaries separated by relatively large volumes is the same as the slip term for a single capillary, equal in length to the sum of the lengths

**It will be noted that f is not by any means identical with the accommodation coefficient of Smoluchowski and Knudsen, nor is it identical with a somewhat similar coefficient used by Alty (5). It would be quite possible for the f used above to be equal to unity where the accommodation coefficient was much less than unity. However, if the accommodation coefficient were unity, it would seem to imply that f must also be unity.*

of the short capillaries, this is not the case when the phenomenon is one of molecular effusion. Clausing has worked out in detail the values of the intercept for cylindrical tubes of arbitrary cross section and length, where the transport process is one of molecular effusion. We may express the Knudsen, Maxwellian, and Clausing intercepts respectively as follows:

$$K_1 = \frac{r}{L}\frac{8}{3}A,$$

$$K_2 = \frac{r}{L}\frac{2-f}{f}\frac{\pi}{2}A,$$

$$K_3 = WA,$$

Where $A = r^2\sqrt{\frac{\pi RT}{2M}}$, and r = radius, L = length, $f \approx 0.9$, and W is a complex function of r and L. In the following table a few values of these intercepts are given for circular tubes of constant radius and varying lengths, A being taken as unity (i.e., $A = 1$ cubic centimeter per second)

L/r =	0.1	0.5	1	2	4	10	100
K_1 =	26.7	5.33	2.67	1.33	0.67	0.27	0.027
K_2 =	19.2	3.84	1.92	0.96	0.48	0.19	0.019
K_3 =	0.91	0.80	0.67	0.51	0.36	0.19	0.027

A single long capillary where $L/r = 100$ would thus give an intercept of 0.027 in the case of Knudsen or effusive flow and an intercept of about 0.019 for Maxwellian or laminar flow. While if this capillary were divided into 100 equal parts and relatively large volumes were placed between the short capillaries, the intercept for the series would still be 0.019 for laminar flow but only 0.007 for effusive flow (i.e., 1/100 the Clausing intercept for $L/r = 1$). In a granular bed we might expect the "bottle necks" to have lengths comparable with their diameters and should expect the deviation from linearity at low pressures to appear not as a rise, but rather as a fall. The analysis of Pollard and Present suggests that the limiting low pressure intercept would be obtained only in regions where the radius was much less than the mean free path. Consequently the region of transition from Maxwellian to Knudsen flow will cover a considerable pressure range. In the transition region the relative contributions of "slip" and effusive flows will vary for gases having different collision cross sections. If pore lengths are either much less or much greater than their diameters, the flow rates in K units will not be inversely proportional to $\sqrt{M}$. Where pore diameters are considerably greater than their lengths we should find that the flow rates expressed in $K \times \sqrt{M}$ units increase in the order of the collision cross section, e.g., increasing in the order He, H_2, N_2, and CO_2. Where pore diameters are much less than their lengths the flow rates in $K \times \sqrt{M}$ units will decrease in the order given, while where diameters and lengths are nearly the same, the flow rates in these units will be the same. If the flow rates of several gases through a porous bed, as expressed in K units, are accurately linear functions of $\bar{p}$ from regions where viscous flow is considerable to regions where effusive flow must prevail, it implies that pores which control the flow rate are cylindrical pores which

have lengths comparable with their diameters, and also that either the pores are all of the same diameter or that pressures are uniform across sections everywhere perpendicular to the direction of flow. Where the K, $\bar{p}$ plot is almost parallel to the $\bar{p}$ axis, few inferences can be drawn with any certainty. Pollard and Present point out that the failure to observe minima in the flow through porous bodies is due to the absence of long free paths in such bodies. If we apply the Clausing intercept to a series of short capillaries connecting large volumes we are in effect removing the contribution from the long free paths. Pollard and Present state that, in the case of porous media, observations show that flow rates are accurately linear down to pressures where the mean free path is of the order of several hundred times the mean pore radius. While a good deal of published data, as well as our own, suggest a fall at low pressures, the fall is too small to allow any very definite conclusions to be drawn, especially in view of the fact that the gases used are treated as ideal and end effects are ignored.

Evidently we know the general behavior of the "slip" and "effusion" intercept terms fairly well as applied to cylinders of circular cross section. In some respects we know more about the intercepts than we know about the Poiseuille term, since we know the values of the limiting intercepts for tubes of almost any cross section, while the problem of Poiseuille flow with slip has been worked out for only a comparatively few special cases. As far as we are aware, only the circular tube has been treated formally in the case of laminar flow with slip. If we wish to apply these flow equations to granular or porous beds where the "pores" are essentially interstitial spaces, we must be able to form at least some idea of what is to be expected when we have a laminar flow with slip through pipes of various forms. Accordingly we will discuss this question briefly.

Laminar Viscous Flow with Slip

The general differential equations of motion when applied to fluids with suitable assumptions lead to what are known as the Navier-Stokes equations. For a steady state of laminar viscous flow through a cylindrical pipe these equations may be reduced to,

$$\frac{\delta p}{\delta z} = \eta\left(\frac{\partial^2 V}{\partial x^2} + \frac{\partial^2 V}{\partial y^2}\right), \tag{5}$$

where $\delta p/\delta z$ is the pressure gradient along the axis of the pipe, η the viscosity, and $V(x, y)$ the velocity of the fluid, the coordinates being taken with the axis of the cylinder as z axis.

$V(x, y)$ is obtained from Equation 5 and the boundary condition, $V = 0$, at the wall. The rate of discharge, Q_V, is then obtained by integrating $V(x, y)$ over the area of the cross section, A. Thus,

$$Q_V = \iint_A V(x, y)dxdy. \tag{6}$$

Equation 5 may be derived very simply as follows.

Let the following figure represent a section of the flowing liquid bounded by a velocity contour surface whose perimeter is S and area is $S.\delta z$.

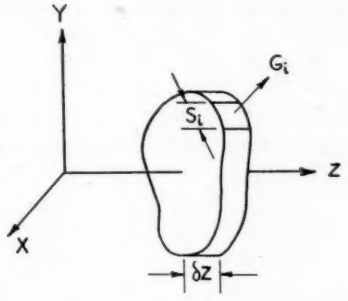

If G_i is the velocity gradient at the element of surface $S_i\delta z$ and A is the area enclosed by the contour and δp the pressure difference across the section, then we have by definitions,

$$\text{Pressure force} \quad = \iint_A \delta p dx dy = A\overline{\delta p},$$

$$\text{Viscous force} \quad = \eta\delta z \sum_S S_i G_i = \eta\delta z S\bar{G},$$

where $\bar{G}$ is the mean value of the gradient over the length S and δp is the mean value of the pressure difference over the area A. Hence balancing forces, we have,

$$A\,\overline{\delta p} = \eta\delta z S\,\overline{G},$$

or,

$$\iint_A \delta p dx dy = \eta\delta z \int_S \frac{dv}{dn}\, ds,$$

where dV/dn is the velocity gradient. Hence we can write by Green's theorem,

$$\iint_A \delta p dx dy = \eta\delta z \iint_A \left(\frac{\partial^2 V}{\partial x^2} + \frac{\partial^2 V}{\partial y^2}\right) dx dy,$$

which, with suitable assumptions concerning the nature of the functions involved, leads to Equation 5. Equations 5 and 6 involve the tacit assumption that the viscosity remains constant for all values of x and y. In general we would not expect this assumption to hold exactly since the traction between wall and fluid would almost certainly be different from that between fluid and fluid. Accordingly the rate of discharge Q_V as given by Equation 6 will be somewhat too low or too high. If this lack of constancy of η is limited to a small region near the limiting values of x and y we can still describe the flow quite accurately by assuming the viscosity constant but altering the

boundary condition and assuming a finite positive or negative "slip" velocity at the perimeter. Since the velocity gradient is a measure of the shearing force, it is natural to assume that the slip velocity, V_s, is proportional to the mean value of the velocity gradient at the perimeter $\bar{G}$. Thus we write,

$$V_s = -\xi\bar{G} = -\xi\frac{A}{\eta S}\frac{\delta p}{\delta z}$$

where ξ is the coefficient of slip and A and S are, respectively, the cross-sectional area and perimeter of the pipe. Hence we can write for the general case of Poiseuille flow with slip,

$$Q_V = \iint_A V(x, y)dx\,dy - \xi\frac{A^2}{\eta S}\frac{\delta p}{\delta z}. \tag{7}$$

The first term of the right-hand member of Equation 7 is identical with that in Equation 6 and is the classical Poiseuille flow expression assuming no slip. In the case of a Maxwellian gas ξ is positive and is given by,

$$\xi = \frac{\eta}{p}\sqrt{\frac{\pi RT}{2M}}\cdot\frac{2-f}{f}.$$

Thus ξ has the dimensions of length and is roughly equal to the mean free path. Hence at low pressure ξ may become quite large. In the case of liquids ξ is usually assumed to be zero. While it seems improbable that the influence of the wall can extend much beyond a molecular diameter in such dense fluids as ordinary liquids, and hence that ξ could be appreciable, nevertheless, it might be positive or negative and quite appreciable for liquids strongly repelled or attracted by the walls of very small capillaries.

For a pipe whose cross section is the ellipse having major semiaxis ab and minor semiaxis b, the formal solution of Equation 7 gives,

$$Q_V = -\frac{\pi a^3b^4}{4(a^2+1)\eta}\frac{\delta p}{\delta z} - \xi\frac{\pi^2a^2b^4}{\eta S}\frac{\delta p}{\delta z}, \tag{8}$$

or approximately,

$$Q_V = -\frac{\pi a^3b^3}{4(a^2+1)\eta}\cdot\frac{\delta p}{dz}\left(b + 4\xi\right). \tag{9}$$

This approximation weights the slip term somewhat too heavily. However, in the case of pores having somewhat irregular cross-sectional shapes the apparent sizes of the equivalent elliptical pipes will be larger when representing areas than when representing flow terms. This type of influence will be relatively greater on Poiseuille terms than on slip terms. Accordingly the simple approximate Equation 9 is probably as good as, or better than, the more exact Equation 8 for correlating pore dimensions and flow rates through parallel assemblies of nearly elliptical pipes of various dimensions.

In the case of pipes whose cross sections are simple figures bound by straight lines, the formal solution of the Poiseuille flow problem may become very

complex and solutions in closed form not attainable. While Boussinesq (9) has evaluated numerically the rates of discharge from rectangular pipes of various dimensions, it is not possible to express these results in any simple parametric form. In the case of the elliptical pipe, the velocity contour lines are geometrically similar to the pipe and this fact greatly simplifies the solution of the problem. If we assume that velocity contours in rectangular, triangular, etc., pipes are also geometrically similar to the containing pipes, approximate solutions in closed form can be obtained very readily. In general, these "solutions" give somewhat smaller Poiseuille terms than do the corresponding formal classical solutions and hence weight the slip terms somewhat too heavily. These approximate solutions thus resemble Equation 9 and like Equation 9 are perhaps better for correlating pore dimensions of porous bodies and flow data than are the more exact expressions.

In the case of pipes whose cross sections can be described in terms of geometrically similar figures converging on their centers of area, the assumption that velocity contours are geometrically similar to the cross section of the pipes enables us to obtain solutions in terms of a single variable.

For example, in the case of a rectangular pipe whose cross section has side lengths $2b$ and $2ab$ respectively, taking the origin at the center and the x axis parallel to side $2b$,

$$A(x) = 4ax^2, \quad S(x) = 4(a+1)x, \quad \text{and} \quad \overline{G} = \frac{a^2+1}{a(a+1)}\frac{dv}{dx}.$$

Hence,

$$\frac{dv}{dx} = \frac{a^2x}{(a^2+1)\eta}\frac{\delta p}{\delta z}, \qquad 0 \leqslant x \leqslant b,$$

and,

$$V(x) = \frac{a^2}{2(a^2+1)\eta}(x^2 - b^2 - 2\xi' b)\frac{\delta p}{\delta z},$$

where,

$$V(x=b) = V_s = -\xi\overline{G} = -\xi'\frac{dv}{dx} = \text{slip velocity.}$$

If the fluid density is ρ, the flow rate in mass units, Q_m, becomes

$$Q_m = \rho Q_V = -\rho\frac{a^3b^3}{(a^2+1)\eta}(b + 4\xi')\frac{\delta p}{\delta z}. \tag{10}$$

Values of Q_V when $\xi' = 0$, as given by Equation 10, may be compared with the relevant classical values. For $a = 1$ and $a \to \infty$ the rates of discharge

as given by Equation 10 are about 11 and 27% respectively, less than those given by Boussinesq.*

In the case of steady flow, Q_m is constant throughout the length of the pipe, i.e., independent of z. Accordingly the variables z and p are easily separated and integrated over their respective intervals, $o \leqslant z \leqslant L$, $p_1 \geqslant p \geqslant p_2$. For an ideal gas,

$$\xi' = \frac{a^2+1}{a^2+a}\frac{\eta}{p}\sqrt{\frac{\pi RT}{2M}}\cdot\frac{2-f}{f} \quad \text{and} \quad \rho = \frac{pM}{RT}.$$

Hence putting these expressions in Equation 10, integrating and expressing the result in K units, we get,

$$K = \frac{a^3b^4}{(a^2+1)\eta L}\bar{p} + \frac{4a^2b^3}{(a+1)L}\sqrt{\frac{\pi RT}{2M}}\cdot\frac{2-f}{f}, \tag{11}$$

or in terms of the long or short order lengths of the rectangle, W and D respectively,

$$K = \frac{W^3D^3}{16(W^2+D^2)\eta L}\bar{p} + \frac{W^2D^2}{2(W+D)L}\sqrt{\frac{\pi RT}{2M}}\cdot\frac{2-f}{f}.$$

Equation 11 can be written in a somewhat different form, namely,

$$K = \frac{a^3D^4}{16(a^2+1)\eta L}\bar{p} + \frac{a^3D^3}{2(a^2+1)L}\sqrt{\frac{\pi RT}{2M}}\cdot\frac{2-f}{f},$$

where the slip term has been changed. This approximation involves a

Gaede (15) measured the rate of flow of hydrogen through two long, shallow, very narrow (4×10^{-4} cm.) slits by a rather indirect pressure decay method. The very striking minimum in the K, $\bar{p}$ plot that he obtained is very well known. At higher pressures the K, $\bar{p}$ plot is a straight line whose slope is about one-third of that calculated by classical methods and about one-half of that calculated by Equation 10. The observed ratio of the limiting low pressure intercept to the intercept of the straight line is 3.0 while the ratio of the Clausing intercept to that calculated by Equation 10 is also 3.0. Clausing (13) and Carman (11) interpret Gaede's data on the assumption that the classical flow equations are applicable and hence find that the critical dimension is 2.81×10^{-4} (Clausing), 2.88×10^{-4} (Carman) instead of 4.0×10^{-4} as reported by Gaede. Since this dimension was measured by interferometric methods such an error involving the missing of two or three interference fringes seems rather improbable. An alternative possibility is that the units used by Gaede are double the usual units (not by any means an impossibility in pressure decay methods using two volumes and two slits). If this were the case the data are almost exactly as calculated by Equation 10 as well as being consistent with the Clausing intercept. However, as the data stand, Equation 10 gives both a slope and intercept which, although somewhat better than the classical values, are much too large.

As a check on the validity of Boussinesq's numerical values for the rates of laminar viscous flow through rectangular pipes, we have measured the rates of discharge of a viscous oil of known viscosity through round and rectangular pipes. The rectangular pipe was about 40 cm. long and the cross section roughly 3×0.3 cm. It was constructed from optically flat parts ground to the limits of precision of the ordinary lens grinding equipment of the optics section of the N.R.C. Its dimensions were measured independently by the metrology section and by ourselves and it is thought that all of its dimensions were known to within ±0.1%. The round glass tube was commercial precision bore and was about of the same length and of about 0.6 mm. diameter. The apparent viscosity of the oil in Stokes was determined in the round tube before and after determining its apparent viscosity in the rectangular tube. The following results were obtained: 10.79 and 10.85 in the round tube, before and after respectively. According to Boussinesq's formula for the rectangular tube, 10.70. Bureau of Standards value 10.72. Estimated error in absolute units ±1%.

Evidently Boussinesq's numerical values may be used for calculating rates of discharge of viscous oils (and probably Newtonian fluids without slip, generally) from rectangular pipes.

maximum change in the shape factor of the slip term of about 17% when $a = 2.4$ and is exact for $a = 1$ and $a = \infty$. In this form the equation is more convenient since we can now write

$$K = f(a)\left[\frac{D^4}{8\eta L}\bar{p} + \frac{D^3}{L}\sqrt{\frac{\pi RT}{2M}}\cdot\frac{2-f}{f}\right], \tag{12}$$

where $f(a) = \frac{1}{8}\pi a^3/(a^2+1)$ for elliptical pipes, and $f(a) = \frac{1}{2}a^3/(a^2+1)$ for rectangular pipes.

Similar expressions can be obtained for cylinders whose cross sections are triangular, cruciform, star-shaped, etc.

For a collection of N capillaries of varying lengths, L, in a parallel arrangement, where shapes, lengths, and parameters, D, are statistically independent, we can write,

$$K = N\overline{f(a)}\;\left|\frac{\overline{1}}{L}\right|\left[\frac{\overline{D^4}}{8\eta}\bar{p} + \overline{D^3}\sqrt{\frac{\pi RT}{2M}}\cdot\frac{2-f}{f}\right]. \tag{13}$$

According to Equation 13, the ratios of Poiseuille to slip terms are independent of shape factors and in this respect the equation may be regarded as a form of Adzumi equation. Under the conditions stated, Equations 12 and 13 might be expected to hold within perhaps 5 to 10% for nearly round or square capillaries, while holding within perhaps 30 to 40% in the case of very long, narrow, slitlike channels. It is, of course, to be borne in mind that all of these flow equations involve highly arbitrary assumptions and are only to be considered as approximately valid under certain idealized conditions where laminar viscous flow with slip is known to be the dominant flow mechanism. In all of these expressions involving the term $(2-f)/f$, f should be taken as about 0.9, and may be reduced or increased a little for different gases and surfaces, if such adjustments are supported by experimental evidence. We must know the frequency distribution of shape factors, $f(a)$, of side lengths D, etc., in order to evaluate the various means in Equation 11. In a system of rectangular pores grown more or less at random, there would probably be a greater statistical correlation between relative lengths of sides than there would be between relative side lengths and their magnitudes. Thus for a considerable range in values of D, we might expect $f(a)$ to be comparatively constant.

The above discussion has been limited to cylindrical capillaries. In granular or porous beds there must be many capillary passages which diverge and converge along the direction of flow. In the general case of viscous flow with slip through relatively coarse-grained converging–diverging channels, K will not be a linear function of $\bar{p}$. When K is a linear function of $\bar{p}$ it implies that such convergent–divergent flow paths are either fine-grained or absent. However, we must recognize that the existence of divergent–convergent flow paths may invalidate the relations put forward above, even when K appears to be an accurately linear function of $\bar{p}$. While the possible effects of marked convergence and divergence of capillaries is very difficult to estimate with any

accuracy in the case of Poiseuille flow with slip, these effects are easily estimated in the case of effusive flow, following the method of Clausing. It may be remarked that in the case of pores whose diameters are about equal to their lengths a very great increase in diameter of the central portion of the pore makes practically no difference to the Clausing intercept. The Clausing intercept for a round tube whose length is equal to the diameter, is practically identical with that corresponding to two holes in series, the holes being of the same diameter as the tube.

Up to this point we have ignored corrections associated with turbulence, kinetic energy of the flowing fluid, distance of travel to develop the velocity distribution characteristic of laminar flow, bent tubes, etc. There is a good deal of experimental evidence which indicates that turbulence does not occur under any of the experimental conditions likely to be encountered in permeability measurements of fine-grained porous beds. Kinetic energy corrections estimated by any reasonable method will be found quite negligible. (It may be remarked that in the case of gases, it is sometimes stated that because of the increase in the velocity of volume elements flowing down a pressure gradient, an additional kinetic energy correction is to be added to that usually applied to incompressible fluids. This correction, sometimes referred to as the Hagenback correction, depends on the distribution law of molecular velocities assumed applicable to the moving gas and may be positive, negative, or zero. Kinetic theory considerations suggest that it should be zero.) The apparent viscosity of extremely viscous liquids is known to increase if measured in capillaries below certain critical sizes. Such effects might be appreciable in the case of common liquids in capillaries whose radii were comparable with molecular dimensions but should not be appreciable in porous beds where the capillary radii controlling flow rates are considerably larger.* As far as we are aware, practically all of these so-called "end effects" are negligible in the case of the slow permeation of fluids through fine-grained porous materials.

From the foregoing discussion the following conclusions are drawn:

1. Without a knowledge of the frequency distributions of pore sizes and shapes we cannot relate flow data to pore dimensions in any literal sense.

2. Where there is evidence, independent of flow data, from which frequency distributions of pore sizes and shapes may be inferred, the relations between steady state flow rates of nonadsorbable gases and pore dimensions of fine-grained porous bodies may be based on the following roughly valid statements:

(*a*) Pressures may be regarded as uniform across thin sections perpendicular to the direction of flow.

(*b*) Flow rates are controlled by pores whose cross sections are uniform throughout their lengths.

(*c*) Rates of Knudsen or effusive flow through these rate-controlling pores are to be related to pore dimensions by the method of Clausing.

**It has been shown that the viscosities of common liquids are perfectly normal in films of the order of 10^{-4} cm. cf. Bastow, S. H. and Bowden, F. P. Proc. Roy. Soc. (London), A, 151: 220. 1935.*

(*d*) If these pores are of nearly constant elliptical or rectangular shape, rates of Maxwellian or laminar viscous flow with slip through these pores may be described by Equation 11.

(*e*) End effects may be ignored.

In Part II of this paper, inferences concerning the structure of our carbon rods are drawn from published data. Using the above roughly valid conclusions as basic assumptions, we show that the flow rates of nonadsorbable gases are consistent with the pore structure of the carbon rods.

REFERENCES

1. ADZUMI, H. Bull. Chem. Soc. Japan, 12: 199. 1937.
2. ADZUMI, H. Bull. Chem. Soc. Japan, 12: 285. 1937.
3. ADZUMI, H. Bull. Chem. Soc. Japan, 12: 292. 1937.
4. ADZUMI, H. Bull. Chem. Soc. Japan, 12: 304. 1937.
5. ALTY, T. Proc. Roy. Soc. (London), A, 190: 59. 1947.
6. ARNELL, J. C. Can. J. Research, A, 24: 103. 1946.
7. ARNELL, J. C. Can. J. Research, A, 25: 191. 1947.
8. BABBITT, J. D. Can. J. Research, A, 28: 449. 1950.
9. BOUSSINESQ, J. J. Math. pures appl., 13: 377. 1868.
10. CARMAN, P. C. J. Soc. Chem. Ind. (London), 57: 225T. 1938.
11. CARMAN, P. C. Proc. Roy. Soc. (London), A, 203: 55. 1950.
12. CLAUSING, P. Verslag Nederland. Akad. Wetenschap. 35: 1023. 1926.
13. CLAUSING, P. Ann. Physik, 14: 134. 1932.
14. DARCY, H. P. G. Les fontaines publiques de la ville de Dijon, exposition et application des principes à suivre et des formules à employer dans les questions de distribution d'eau. Victor Dalmont, Paris. 1856. (*cf.* Dalla Valle, J. M. Micromeritics—the technology of fine particles. Pitman Pub. Corp., New York. 1943.)
15. GAEDE, W. Ann. Physik, 41: 289. 1913.
16. HELMHOLTZ, H. von. Sitzber. Akad. Wiss. Wien., Math. natur-w. Klasse. 40 : 607. 1860.
17. HODGINS, J. W., FLOOD, E. A., and DACEY, J. R. Can. J. Research, B, 24: 167. 1946.
18. KENNARD, E. H. Kinetic theory of gases. McGraw-Hill Book Co. Inc., New York. 1938.
19. KNUDSEN, M. Ann. Physik, 28: 75. 1909.
20. KNUDSEN, M. Ann. Physik, 35: 389. 1911.
21. KOZENY, J. Sitzber. Akad. Wiss. Wien, Math. natur-w. Klasse, Abt. II a, 136: 271. 1927.
22. KUNDT, A. and WARBURG, E. Ann. Physik, 155: 337. 1875.
23. MAXWELL, J. C. Scientific papers, vol. 2, *edited by* W. D. Niven. The University Press, Cambridge. 1890.
24. MILLIKAN, R. A. Phys. Rev. 21: 217. 1923.
25. POLLARD, W. G. and PRESENT, R. D. Phys. Rev. 73: 762. 1948.
26. SMOLUCHOWSKI, N. Ann. Physik, 33: 1559. 1910.
27. TOMLINSON, R. H. and FLOOD, E. A. Can. J. Research, B, 26: 38. 1948.

THE FLOW OF FLUIDS THROUGH ACTIVATED CARBON RODS

II. THE PORE STRUCTURE OF ACTIVATED CARBON[1]

BY E. A. FLOOD, R. H. TOMLINSON, AND A. E. LEGER

ABSTRACT

The flow rates of adsorbable gases through zinc chloride activated carbon rods are considerably greater than might be expected from classical considerations. From data independent of flow measurements, the pore-size frequency distributions of the activated carbon are deduced and a model macropore system presented. It is shown that flow rates of nonadsorbable gases are consistent with a mean macropore diameter of about 3×10^{-5} cm., as well as being consistent with what can be inferred concerning such structures. The macropore system is regarded as an interstitial structure and is described as a random assembly of "bottle necks" joining relatively large void spaces. The assembly is described by means of two constant parameters and one stochastic variable. The mean micropore diameter of zinc chloride activated carbons is generally regarded as being of the order of 2×10^{-7} cm. or less. It is shown that no ordinary type of effusive or diffusive flow through pores of the order of 2×10^{-7} cm. can be appreciable compared with the flow through the macropore system, unless surface forces increase flow rates by large factors. In the case of strongly adsorbed gases the anomalous flow rates are ascribed to a flow through the micropore system and hence it is inferred that surface forces introduce large factors tending to increase flow rates in these very small pores.

Elaborate studies of the structure of highly activated carbons were carried out in the United States and Canada during the war. The results of these studies have been partially published in a number of NDRC and other reports and a summary of this work has been presented recently by Emmett (4). In the immediately following paragraph, we quote a few reasonably well-established general facts concerning the structure of charcoal which have a direct bearing on flow problems.

The majority of high density, highly activated carbons are porous bodies in which the void volume usually consists of more than half the total volume. The void volume consists of two main parts known respectively as the micropore and macropore volumes. These volumes are usually of about the same size, the micropore volume being perhaps generally somewhat larger than the macropore volume in the case of carbons of very high activity and high density. The micropore volume is responsible for most of the adsorptive properties of the material, the macropore volume providing access to the micropore structure, but otherwise not contributing appreciably to the adsorption phenomena. One rather striking fact brought out by Juhola's work as reported by Emmett (4) is that P.C.I.* pulverized briquetted coal before activation has a macropore structure very similar to that of the highly activated material, and also very similar to the macropore structures of other highly activated carbons made from entirely different sources. Apparently inactive pulverized briquetted coal can be activated in stages, developing a micropore structure without changing the macropore structure appreciably.

[1] *Manuscript received August 16, 1951.*
Contribution from the Division of Chemistry, National Research Council, issued as N.R.C. No. 2698.

**Pittsburgh Coke and Chemical Company, formerly Pittsburgh Coke and Iron.*

In this case, the macropore structure must have been originally an interstitial type of structure. Hence the inference is strong that in the case of carbons having macropore structures similar to those of the P.C.I. carbons, these structures are also to be regarded as essentially interstitial structures. It is further noted that most of the high density, highly activated carbons have rather similar pore structures; this is especially notable in the case of the extruded zinc chloride activated carbons made by the National Carbon Co. The methods of manufacture and general properties of the carbons designated CWSN-19, CWSN-44, and CWSN-45 (the last is designated N-145 by Juhola (5)) correspond very closely to those pertaining to our carbon rods. The pore structures of these three carbons are very similar to one another and accordingly we assume that the pore structures of these three carbons are also very similar to those of our carbon rods.

We proceed to determine whether our flow data are consistent with the pore-size distributions as given by Emmett for carbons CWSN-19, CWSN-44, and CWSN-45.

In the case of the macropores, the "pore-size distributions" were obtained by Juhola (5) by forcing mercury into the porous body and observing the increments of pressure corresponding to increments in volume of mercury forced into the carbon. The holes were assumed square and the classical relations between pressure, surface tension, diameter (side length of square), etc., applied. Micropore distributions were based on capillary condensation as applied to water desorption isotherms. In order to apply the volume pore-size distributions to flow problems, it is necessary to convert the data into a pore-size frequency distribution. As a first statement of the problem we write,

$$V = N\overline{f(a)LD^2}$$

where V is the total pore volume per cubic centimeter of porous material, N is the number of pores per cubic centimeter, $f(a)$ is a shape factor, L a pore length, and D a side length of some plane figure enclosing an area.

If we can suppose that the lengths, shapes, and side lengths are statistically independent (i.e., that we can describe the pore system in terms of pores of average shapes, lengths, and diameters), we can write,

$$V = N\,.\,\overline{f(a)}\,.\,\overline{L}\,.\,\overline{D^2} = N'\overline{D^2} = \sum D^2 N'(D)$$

where,

$$\sum N'(D) = N'.$$

$N'(D)$ as defined above is a sort of pore-size frequency distribution for volume expressed in units of length. N' thus might be regarded as the total length of a large number of pores multiplied by some numerical shape factor.

Where the total void volume is made up of two possibly quite different pore systems, we should distinguish between them and write,

$$N'\overline{D^2} = N_1'\overline{D_1^2} + N_2'\overline{D_2^2}$$

where $N_1'\overline{D_1^2}$ and $N_2'\overline{D_2^2}$ refer to the two different systems.

If we suppose that the pore volume of activated charcoal can be described in any such manner, we can equate $N_1'\overline{D_1^2}$ and $N_2'\overline{D_2^2}$ to the observed micropore and macropore volumes, respectively, and attempt to find, by trial, functions $N_1'(D_1)$ and $N_2'(D_2)$ which will fit the observed pore-size volume distribution. It is found that by putting,

$$N_1'(D_1) = \frac{N_1 h_1^7}{6!} D_1^6 e^{-h_1 D_1}, \qquad 0 \leqslant D_1 \leqslant \infty,$$

$$N_2'(D_2) = N_2' h_2 e^{-h_2 D_2}, \qquad 0 \leqslant D_2 \leqslant \infty,$$

where,

$$h_1 = 6 \times 10^7 \text{ and } h_2 = 3 \times 10^4,$$

and where,

$$\frac{N_1' h_1^7}{6!} \int_0^\infty D_1^8 e^{-h_1 D_1} dD_1$$

is the micropore volume per cc. and,

$$N_2 h_2 \int_0^\infty D_2 e^{-h_2 D_2} dD_2$$

is the macropore volume per cc., the plot of pore volume as a function of D agrees very well with Juhola's plots as reported by Emmett for the three National Carbon Co. carbons referred to above. The values of h determine the mean pore size as well as the values of D for which the rate of increase of volume with diameter is a maximum. The values of N determine the total void volume. The mean values of the pore diameters (or side lengths of squares, if assumed square) are,

$$\overline{D}_1 = 1.2 \times 10^{-7} \text{cm.},$$

$$\overline{D}_2 = 3.3 \times 10^{-5} \text{cm.},$$

for the micropore and macropore systems respectively.

It may be noted that the macropore volume distributions of nearly all of the carbons studied by Juhola (5) indicate a distribution, $N_2'(D_2)$ of the form Ae^{-hD}, and further, the spread of values of $\overline{D}_2$ is not great, ranging from the smallest for the high-density National Carbon Co. carbons, namely, about 3×10^{-5} cm., to about 15×10^{-5} cm. for various carbons from other sources having large macropore volumes.

It will be noted that nearly all of the micropore structures reported by Juhola are also very similar and yield similar values of $\overline{D}_1$. The distribution we have adopted for the micropore system yields a mean pore radius that is perhaps somewhat too small for the National Carbon Co. carbons. A larger value of the exponent of D (i.e., D^8 in place of D^6) would give a better fit

with the experimental data, but in view of the considerably increased labor in calculation entailed thereby, as well as the doubtful validity of basing the distributions on the desorption isotherms, we have not thought it worthwhile to improve the empirical distribution function. As far as the two pore-size distributions are concerned, for a given assumed shape of pore, the mercury pressure method of measurement is more direct than is the capillary condensation method and it would seem that perhaps more confidence may be placed on mean pore diameters of macropores than on those of micropores.

If we accept the values of $\overline{D_1}$ and $\overline{D_2}$ as given above, and can suppose that the pore "lengths" and "shapes" are at all comparable in the two systems, it is evident that if fluids flow through these pore systems by the same mechanism, uninfluenced by surface forces, the micropore structure cannot contribute appreciably to the over-all flow rate. In the case of the permanent gases where adsorption at room temperatures is negligible, it seems safe to assume that only the macropore structure need be considered in describing the flow of permanent gases through our carbon rods.

Since, as we have seen, the macropore structure is essentially an interstitial type of structure and is fine grained, we shall assume that the pressure may be regarded as uniform throughout any thin section perpendicular to the applied pressure gradient, i.e., we assume that the flow is equivalent to a flow through capillaries in parallel.

As we have shown in Part I of this paper, the flow through a single cylinder of quite a variety of shapes may be represented by,

$$K = f(a)\frac{1}{L}\left[\frac{D^4}{8\eta}\bar{p} + D^3\sqrt{\frac{\pi RT}{2M}}\cdot\frac{2-f}{f}\right], \tag{1}$$

where the symbols are as previously indicated; ($f(a)$ here is not the same as the shape factor for volume. For square cylinders $f(a)$ may be taken as $\frac{1}{4}$.) For N capillaries in parallel assuming statistical independence of shapes, lengths, and diameters, we may write,

$$K = N\overline{f(a)}\,\left|\overline{\frac{1}{L}}\right|\left[\frac{\overline{D^4}}{8\eta}\bar{p} + \overline{D^3}\sqrt{\frac{\pi RT}{2M}}\cdot\frac{2-f}{f}\right].$$

The slope, S, of K as a function of the mean pressure, $\bar{p}_m$, measured in mm. Hg is thus,

$$S = N\overline{f(a)}\,\left|\overline{\frac{1}{L}}\right|\,\overline{D^4}\,\frac{c}{8\eta},$$

where $\bar{p}$ dynes cm.$^{-2}$ $= c\bar{p}_m$.

The intercept, I, is,

$$I = N\overline{f(a)}\,\left|\overline{\frac{1}{L}}\right|\,\overline{D^3}\sqrt{\frac{\pi RT}{2M}}\cdot\frac{2-f}{f}.$$

Therefore,

$$\frac{\overline{D^4}}{\overline{D^3}} = \frac{S}{I}\,\frac{8\eta}{c}\sqrt{\frac{\pi RT}{2M}}\cdot\frac{2-f}{f}.$$

If the form of the frequency distribution of pore sizes is at all consistent with Juhola's data for macropores, then as we have seen,

$$N(D) = Ae^{-hD},$$

and hence,

$$\overline{D^4}/\overline{D^3} = 4\overline{D},$$

regardless of the values of A and h, and hence we have,

$$\overline{D} = \frac{S}{I}\frac{2\eta}{c}\sqrt{\frac{\pi RT}{2M}}\cdot\frac{2-f}{f}.$$

The flow data for nitrogen reported in Part I of this paper and in our previous paper (6) yield a mean value of $S/I = 2.7 \times 10^{-3}$. Taking $\eta = 181.5 \times 10^{-6}$ poise as the viscosity of nitrogen at 35°C. and $f = 0.9$, we get,

$$\overline{D} = 3.4 \times 10^{-5}.$$

The maximum reasonable spread of values of $\overline{D}$ based on the flow data would be obtained by taking the smallest experimental value of S/I with the smallest reasonable value of $\frac{2-f}{f}$, i.e., with $f = 1$, and the largest value of S/I with $f = 0.8$. Values of $\overline{D}$ thus obtained range from 2.6 to 4.5×10^{-5}. This range of values covers the range of values of $\overline{D}$ for National Carbon Co. carbons of this type very nicely.

The agreement between the apparent values of the mean pore diameter (or side length, if square) as measured by the flow method and as determined by the mercury pressure method is really excellent and would seem to justify some of the underlying assumptions. Perhaps the most important assumption is that our carbon rods have macropore structures very similar to those reported by Emmett. Some of the other important assumptions are as follows. (*a*) Shape factors and lengths are statistically independent of the parameter used to describe the variation in cross-sectional area of the "pore". These assumptions are common to both methods and are inherent in the idea that the "average pore" may have a length, shape, and diameter. Thus $N(D)$ should have the same form for the two methods. It is to be emphasized that physically the pore system is really one interconnected whole and the attempt to describe this volume in terms of "pores" is necessarily somewhat arbitrary. (*b*) The mechanism of flow through the macropore system at higher pressures is the normal Maxwellian flow as observed for small capillaries. The system behaves as a system of parallel rectangular or elliptical capillaries of nearly constant shape. The micropore system does not contribute appreciably to the flow rate of nitrogen. These assumptions are, of course, peculiar to the flow method of determination of $\overline{D}$. (*c*) The usual relations between surface tension and capillary depression of mercury as observed for small holes prevail in such a pore system. The holes are effectively square or round.

It may be emphasized that in the flow method of determination of $\overline{D}$ the "shapes" and "lengths" of pores are not explicitly concerned, while in Juhola's mercury-pressure method the value of $\overline{D}$ depends on the assumed shape. Thus, as pointed out by Emmett, if the pores were assumed to be long rectangular slits, the value of $\overline{D}$, as determined by this method, would be only half as large as given above. Our results seem to justify Juhola's assumption of nearly square holes.

Even assuming square holes we cannot calculate the flow through such a system unless we also know the lengths of the pores. By comparing the observed values of the slope or intercept with the macropore void volume, it becomes immediately apparent that the effective length of the pores is considerably less than the length of the sample. This can only occur if the pore system is a system of "bottlenecks", a conclusion consistent with an interstitial structure.

In order to illustrate the nature of the various factors and assumptions involved in such considerations, we shall present a model pore system based on a literal interpretation of the above assumptions.

It may be remarked that the most commonly used model pore system is a parallel bundle of round straight capillaries. Such a pore system is incompatible with an interstitial structure. It leads to serious inconsistencies between observed void volumes and flow data. Moreover, the "average shape" of a cylindrical* pore is almost certainly not circular. A model pore system should be some simple idealization of the space between packed particles. It should, if possible, lead to simple calculations, have some flexibility but not be too arbitrary; it should provide for dispersion of pore sizes and should, of course, be consistent with known data and be physically reasonable. It is to be emphasized that such a model pore system is not to be regarded in any sense as a picture of a real pore system. The model is rather to be regarded as an explicit statement of the assumptions made concerning such structures, and thus provide a method of testing these assumptions for self-consistency and for consistency with observed data. As will be seen, some very arbitrary assumptions are involved.

MODEL PORE SYSTEMS

We first construct a frame of reference as follows. A cube of side length L is cut into a very large number of very thin sections parallel to a face of the cube. The thickness of a section will be a stochastic variable represented by l_i. Each section of thickness l_i is cut into L/l_i right square cylinders of length L and cross section l_i^2. Each square cylinder is cut again into L/l_i cubes l_i^3. If there are $M(l_i)$ sections of thickness l_i, there will be $L/l_i\ M(l_i)$ square cylinders of length L, and cross sections l_i^2. If we put, $L/l_i\ M(l_i) = N(l_i)$ then the total area of one face of the cube L^3 will be given by $\Sigma l_i^2 N(l_i) = L^2$. If L is taken as unity, $N(l_i)$ becomes the number of cylinders of cross section, l_i^2, per unit area or the number of squares of side length, l_i,

Cylindrical in its general sense.

contained in a plane cutting L^3 at right angles to the cylinders. The cubes are now rearranged so as to form an assembly which has the same distribution of squares of side length, l_i, i.e., $N(l_i)$, in any plane cutting the cube parallel to any face. (This will involve a change in $M(l_i)$, of course.) The number of cubic cells of side length l_i will be $L/l_i\ N(l_i)$, say, $P(l_i)$. Thus the total volume may be represented by any of the following,

$$L^2 \sum l_i M'(l_i) \equiv L^2 M' \bar{l}_m, \quad L \sum l_i^2 N(l_i) \equiv LN\,\overline{l_n^2},$$

$$\sum l_i^3 P(l_i) \equiv P\,\overline{l_p^3},$$

according as we consider the volume as made up of M' sections, N square cylinders, or P cubic cells. (The subscripts m, n, and p are used to indicate that the three distribution functions are different; while $M'\bar{l}_m = L$, $N^{\frac{1}{2}}\bar{l}_n$ and $P^{\frac{1}{3}}\bar{l}_p$ do not equal L unless l_i is a constant.) This type of construction imposes limits on possible forms of $N(l_i)$. However, if $\bar{l}$ is very small compared with L, distributions of the form $N(l_i) = Nl^n e^{-kl}$, $0 \leqslant \bar{l} \leqslant \infty$, can be used for most purposes with reasonable approximation.

If we wish to construct a model porous system we may regard the system of cubic cells as merely a frame of reference within a solid continuum. We now place within each cubic cell some pore of "average shape" so that the volume of each pore has some definite constant relation to the volume of the cell into which it is placed. Such a pore should penetrate the faces of the cubic cells so that each cell may have the same permeability perpendicular to any face of the cell. We suppose the average pore to be an idealization of the void space between cubic packed spheres. The void space between cubic packed spheres has certain "bottleneck" features reminiscent of porous adsorbents and the "bottlenecks" are approximately square as suggested by Juhola's data. However, it is difficult to treat the flow through such cells because of the converging-diverging channels. While a number of idealizations of such a void space or "pore" can be made, we adopt what seems to be the simplest possible model having two parameters, namely the following,

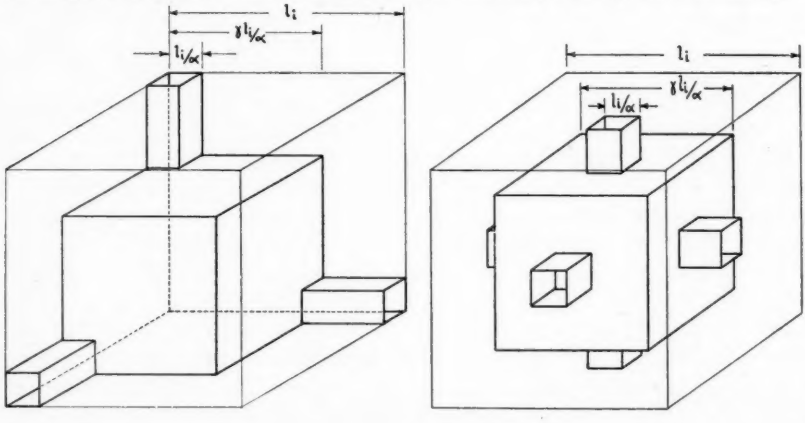

The two figures are different arrangements of the same voids and solids and would have identical properties with respect to mercury pressure pore-size volume distributions as well as identical permeabilities, except perhaps at low gas pressures where molecular effusion prevails. l_i/α is the side length of the square cylindrical capillary of length $l_i(1 - \gamma/\alpha)$. $\gamma l_i/\alpha$ is the side length of the larger cube contained within the cell. α and γ are assumed constant, while l_i is a stochastic variable such that $\bar{l}$ is very small compared with the side length, L, of the whole assembly.

The void volume is obviously the volume of the large cube plus the volume of the "bottlenecks". If the volume of the cell is taken as unity, the void volume per cell is the void fraction of the whole assembly since α and γ are assumed constant.

In an assembly of a great many such cells, the permeability of any small section (of cross section Ll_i and length L) is large compared with that of the corresponding cylinder (of cross section l_i^2 and length L). Accordingly, when fluids flow through such a medium the pressure will be constant throughout a section and independent of the relative positions of cells in following sections.

Hence the permeability is independent of whether the system is regarded as made up of cylinders or an assembly of cubic cells such that $N(l_i)$ is the same for any section parallel to any face. In addition, the flow through a regular assembly of cells of constant size of this type is independent of the direction of the pressure gradient. For example, if the applied pressure gradient is along a diagonal of the cube, three arms or "bottlenecks" contribute to the flow, whereas when the gradient is parallel to one arm, only the one arm contributes, and it might appear that the permeability was markedly dependent on orientation. However, in the former case, the number of flow paths per unit area is greater, not by 3, but by $\sqrt{3}$, while the effective length of pore is increased by $\sqrt{3}$, as compared to the latter case. Hence the two orientations give the same permeability. Similar results will be obtained with other orientations. Accordingly, we shall assume that the permeability of the whole system of cells is independent of the orientation of the faces of the unit cells with respect to the whole cube L^3, and in the case of flow problems calculate the permeability as though the pressure gradient were parallel to one arm of the unit cells.

We proceed to determine whether or not a distribution function $N(l_i)$ and values of the parameters α and γ can be found, which are self-consistent and physically reasonable, and which are consistent with known data concerning the macropore structure of similar National Carbon Co. carbons.*

The following relations hold:

The void volume V_i per cell will be given by,

$$V_i = \frac{l_i^3}{\alpha^3}(\gamma^3 + 3\alpha - 3\gamma), \qquad \alpha \geqslant \gamma \geqslant 1.$$

**We consider it more reasonable to assume that the "average pore" is square rather than circular. If circular cylindrical bottlenecks are assumed, it will lead to slightly different values of α and γ but $\bar{D}$, and all of the more important features of the model, will be unchanged.*

Letting $n_i = L/l_i$, then for $N(l_i)$ cylinders of length, L, and cross section, l_i^2, we have,

$$V_i' = n_i N(l_i) \frac{l_i^3}{a^3} (\gamma^3 + 3a - 3\gamma)$$
$$= LN(l_i) \frac{l_i^2}{a^3} (\gamma^3 + 3a - 3\gamma).$$

The total void volume will be given by,

$$V = LN \frac{\overline{l^2}}{a^3} (\gamma^3 + 3a - 3\gamma),$$

where $N\overline{l^2} = L^2$. Hence, for $L = 1$, and $D_i = l_i/a$,

$$V = N \left[\frac{\gamma^3 + 3a - 3\gamma}{a} \right] \overline{D^2} = \frac{\gamma^3 + 3a - 3\gamma}{a^3},$$

where V is the void volume per cubic centimeter of porous material. This is equivalent to our assumption that we can write,

$$V = N . \overline{f(a)} . \overline{L} . \overline{D^2}.$$

If $N(l_i)$ or $N'(D_i)$ can be represented by means of a continuous function and we suppose D to vary, then the total volume of macropores per cc. of carbon whose bottleneck diameters lie between D_1 and D_2 will be given by,

$$V_{D_1,_2} = \left[\frac{\gamma^3 + 3a - 3\gamma}{a} \right] \int_{D_1}^{D_2} D^2 N'(D) dD.$$

Assuming that $N'(D)$ can be represented by Nhe^{-hD}* as suggested by Juhola's data for a great many quite different kinds of carbon, then we have,

$$V_{D_1,_2} = \left[\frac{\gamma^3 + 3a - 3\gamma}{a} \right] Nh \int_{D_1}^{D_2} D^2 e^{-hD} dD.$$

The volume contained within the central cubes** between cube side lengths l_1 and l_2 will be,

$$V^+ = \frac{\gamma^3}{a} Nh \int_{D_1 = l_1/\gamma}^{D_2 = l_2/\gamma} D^2 e^{-hD} dD.$$

The permeability of the system can be determined very readily. From (1) we can write for the Poiseuille flow through a square cylinder,

*For this distribution function N becomes the number of cylinders or the number of squares per unit area in a plane section of the cube. If construed strictly, the number of cubic cells per cubic centimeter becomes infinite where $0 \ll l \ll \infty$. The basic relations are

$$\overline{D^n} = \frac{n!}{h^n}, N\overline{l^2} = Na^2\overline{D^2} = 1.$$

**It will be noted that the shape of this central volume is more or less arbitrary.

$$K = \frac{D^4}{32\eta L} \cdot c\bar{p}_m,$$

where $c = 1.332 \times 10^3$ and $\bar{p}_m$ is the mean pressure in mm. of Hg. Neglecting the resistance to flow offered by the common large cube compared with the resistance of the arms, and since we have $D_i = l_i/\alpha$ and $L' = l_i/\alpha\ (\alpha - \gamma)$ we can write for the slope S_i, for a single cell,

$$S_i = \frac{l_i^4}{\alpha^3 l_i(\alpha - \gamma)} \frac{c}{32\eta},$$

For n_i identical cells in series, where $n_i l_i = L$, we have,

$$S_i' = \frac{l_i^4}{\alpha^3(\alpha - \gamma)} \frac{1}{L} \frac{c}{32\eta},$$

and for $N(l_i)$ cylinders in parallel,

$$S_i'' = \frac{N(l_i) l_i^4}{\alpha^3(\alpha - \gamma)} \frac{1}{L} \frac{c}{32\eta}.$$

Hence, for all cells,

$$S = \frac{N\overline{l^4}}{\alpha^3(\alpha - \gamma)} \frac{1}{L} \frac{c}{32\eta} = N\frac{\alpha}{\alpha - \gamma} \frac{1}{L} \overline{D^4} \frac{c}{32\eta}.$$

Similarly for the intercept, we get,

$$I = N\frac{\alpha}{\alpha - \gamma} \frac{1}{L} \overline{D}^3 \frac{1}{4} \sqrt{\frac{\pi RT}{2M}} \cdot \frac{2 - f}{f}.$$

For a cylinder of length, L, and cross-sectional area, O, assuming the same distribution as above, we have,

$$S = 12\overline{D}^2 \frac{1}{\alpha(\alpha - \gamma)} \frac{c}{32\eta} \frac{O}{L},$$

$$I = 3\overline{D} \frac{1}{\alpha(\alpha - \gamma)} \frac{1}{4} \sqrt{\frac{\pi RT}{2M}} \cdot \frac{2 - f}{f} \cdot \frac{O}{L}.$$

We use the values of S, I, and V to solve for $\overline{D}$, α, and γ. Taking the values of S and I for plugs Nos. 11 and 18 as reported in Part I of this paper and assuming macropore void volumes to be 30% of plug volumes, we find $\overline{D} = 3.65 \times 10^{-5}$, $\alpha = 7.6$, and $\gamma = 4.9$, while for the five plugs (excluding 13) reported previously (6), $\overline{D} = 3.41 \times 10^{-5}$, $\alpha = 7.2$, $\gamma = 4.7$. These values of the constants yield calculated slopes and intercepts within 3% of the relevant observed values. The difference between the two sets of values is probably not significant. Hence, taking $\overline{D} = 3.5 \times 10^{-5}$, $\alpha = 7.4$, and $\gamma = 4.8$, which seem physically reasonable values, we get very consistent results. Thus the calculated macropore volume is 0.29 cc. per cc. of carbon, while that based on the water desorption isotherm is 0.30 cc. and that based on the ether adsorption isotherm is 0.24 cc. The pore-size volume distribution curve falls very nicely within the curves given by Emmett for the three similar carbons. The calculated and observed

slopes* and intercepts of the flow rates of nitrogen, hydrogen, helium, and carbon dioxide through all of the plugs (excluding 13) agree probably within the experimental error. (The calculated value for hydrogen is a little high. Since f usually varies a little for the different gases, we may expect some variation due to this factor.)

The calculated surface area of the macropore volume is 0.6 sq. m. per cc., while the calculated surface area of the system thought of as constructed from granules is about 1.2 sq. m. per cc. The surface area of the granules calculated from the flow data and void volume of macropores by the Arnell (1) method is 6 to 7 sq. m. per cc. It may be remarked that the Arnell and similar methods correlate empirically the actual total granule surface with flow data and necessarily give larger surface areas than those corresponding to the void spaces, since these areas include areas of surfaces actually in contact as well as areas of surfaces effectively in contact as far as flow is concerned.

There is a marked hysteresis in the mercury-pressure method of measuring pore-size distribution, i.e., generally most of the mercury forced into the carbon stays there when the pressure is released. Assuming that the mercury

**As an additional check as to the validity of regarding the slope terms as describing a Poiseuille flow, the permeability of plug No. 11 to liquid water at 35°C. was measured. The apparatus used permitted measurement of flow rates both entering and leaving the sample. Flow rates were considered valid when these rates were practically indistinguishable. The results are recorded in the following graph.*

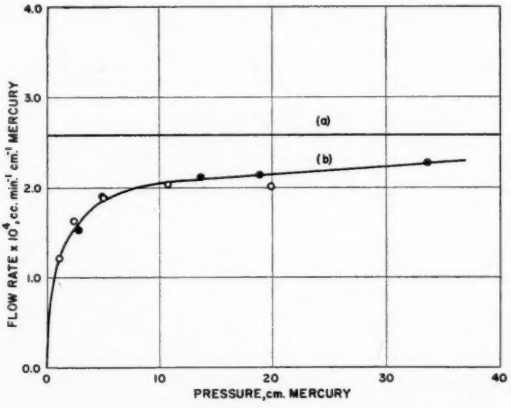

The experimental points are shown at (b). The open circles are the flow rates with decreasing pressure heads, the solid circles with increasing heads. The straight line (a) is the calculated liquid water flow rate based on the nitrogen permeability as determined after the liquid water permeability measurements. It was found that the nitrogen and adsorbable gas permeability, as well as the adsorptive capacity of the sample (plug No. 11) were considerably reduced by the passage of the liquid water through the sample, no doubt owing to the filtering action of the plug. The flow rate in K units per minute corresponding to (a) is roughly 28 at $\bar{p}$ = 760 mm.

It will be noticed that the observed flow rates of liquid water approach the calculated value asymptotically with increasing pressure head. Apparently the macropore structure contains hydrophobic surfaces or capillaries having negative wetting angles. Appreciable quantities of organic material were almost certainly adsorbed by the carbon during the establishment of the experimental conditions necessary for the liquid permeability measurements, accordingly hydrophobic regions are not necessarily inherent in the carbon structure.

threads in the "bottlenecks" will always break on release of the pressure, our model indicates that 93% of the mercury should be retained by the sample. If the walls of the bottlenecks were comparatively smooth and free from adsorbed gas, the mercury threads would be less likely to break and the sample retain considerably less mercury after release of the pressure. Thus we might expect unactivated material to retain $< 93\%$. According to Emmett (4) usually 90 to 95% is retained in the case of activated carbons while as little as 35% is retained in some cases of unactivated material of similar macropore structure. The calculated pore volume of bottlenecks and central volumes, whose diameters lie between 1800-18000 Å (i.e., the volume that would fill by capillary condensation of nitrogen in the adsorption relative pressure range 0.99 to 0.999) is about 0.047 cc. per cc. (roughly 0.018 from the bottlenecks and 0.029 from the central volumes). The corresponding volumes as observed for CWSN charcoals range from 0.039 to 0.050. The calculated value of what Emmett calls the free volume although somewhat too high is consistent with values given by Emmett. One further point may be mentioned. The Clausing or low pressure limiting intercept for our model where the "pore" lengths are two or three times their diameters would be about $\frac{4}{5}$ of the Maxwellian intercept,* i.e., according to the model, the plot of K against $\bar{p}$ should show a slight downward curve in pressure regions where the mean free path is greater than about 10^{-4} cm., i.e., at values of $\bar{p}_m$ less than 50 mm. This is qualitatively in agreement with the observed data.

The rather surprisingly good agreement between calculated and observed properties obtained above seems to justify some of the numerous underlying assumptions. In any case, there can be little doubt that the flow of gases which are not strongly adsorbed is entirely consistent with what can be inferred concerning the structure of our activated carbon rods. It seems safe to conclude that the flow rates of nitrogen, hydrogen, etc., are controlled almost wholly by the macropore system of the carbon.**

ANOMALOUS FLOW RATES

The flow rates of condensable vapors through relatively large capillaries obey the normal Maxwellian flow relations, even at mean pressures fairly close to saturation; in spite of the considerable surface adsorption which must occur under such circumstances and in spite of any surface mobility of adsorbed material. Consequently, we must conclude that the flow rates of condensable vapors through the greater part of the macropore system follows the normal Maxwellian flow, and hence conclude that the anomalous flow rates observed are, in the main, due to an additional flow through the micropore system. Such a conclusion is consistent with Babbitt's (2) very interesting study of the permeability of wood to water vapor and nitrogen. This conclusion is also consistent with the well-known discrepancies between "surface

*cf. Part I.

**Somewhat different model pore systems have been discussed recently by L. G. Joyner in some interesting papers. Conclusions concerning micropore permeability would be essentially as given above.

areas" as measured by flow and by adsorption methods in cases where highly active adsorbants are involved. Accordingly, we shall assume that our anomalous flow rates are due, at least in part, to an additional flow through the micropore system and examine the consequences of this assumption.*

We can regard the micropore system as made up from an assembly of cells contained within the macropore system and construct a model to describe the system along the lines used above in describing the macropore system. Making allowance for the different average path lengths and using Juhola's data together with various estimates of void space surface areas, we can obtain rough limiting estimates within which the values of the slope S_1 and of the intercept I_1 for the micropore system should fall. We find,

$$S_1 = S_2 \times (10^{-4} \text{ to } 10^{-6}),$$

$$I_1 = I_2 \times 5(10^{-2} \text{ to } 10^{-4}),$$

where S_2 and I_2 are the slope and intercept, respectively, applicable to the macropore system. The intercepts given above are the Maxwellian intercepts. The Clausing intercepts have roughly similar values for such models. Accordingly, neither molecular effusion nor Maxwellian flow, in its usual form, nor any ordinary type of diffusion** through the micropore system can make an appreciable contribution to the over-all flow rate, unless surface forces introduce very large factors tending to increase the flow rate through such very fine-grained systems. Evidently in the case of gases which are not strongly adsorbed, these factors are not large. In the case of gases which are strongly adsorbed, one of the most obvious and direct effects of surface forces is to increase the density of fluid in the immediate neighborhood of the surface as compared with the equilibrium gas density remote from the surface. If the micropore system has a mean pore diameter anything like 1.2×10^{-7} cm., the pore diameters are small compared to the mean free

According to our model, the mean flow path length of the capillaries of the micropore system is somewhat less than one-half of the length of sample. However, if the macropore system be filled with mercury, the mean path length will be somewhat greater than the sample length. Thus the micropore flow rate should be reduced by a factor of about 0.3, if the macropore structure were completely filled with mercury. To check this point and as a check on the independence of the two pore systems, flow rate measurements were made on rods into which mercury had been forced. When the mercury was forced into the sample at 360 p.s.i., approximately 54% of the macropore void volume remained mercury filled after handling at atmospheric pressure. The methanol adsorption isotherm was not changed by this treatment, the nitrogen permeability was reduced to 0.09 of its former value. Assuming the micropore flow rate to be the difference between the observed flow rate and that calculated on the basis of the nitrogen permeability, the methanol flow rate was reduced to 0.34 of its former value. It may be remarked that the methanol flow rate showed a pronounced maximum when plotted as a function of $\bar{p}$ (cf. Part III, Fig. 4). These results are consistent with our model and with the assumption that the two pore systems may be treated as independent of one another. However, in another experiment mercury was forced into the sample under a pressure of 2400 p.s.i. and after handling at atmospheric pressure 86% of the macropore volume remained mercury filled. In this case the mercury filled sample showed very little adsorptive capacity for methanol even after long exposure. Also the methanol permeability was greatly reduced and no nitrogen permeability could be detected at all. While evidently the micropore and macropore structures cannot be treated as entirely independent of one another, the total flow rate may be regarded as essentially the sum of the micropore and macropore flow rates.

**In order to yield a flow rate of the observed order of magnitude, the diffusion constant can hardly be less than 10^{-4}. Barrer's (3) very thorough study of diffusion through fine-grained porous materials indicates diffusion constants of a much lower order of magnitude, e.g., 10^{-8} to 10^{-17}.

paths (λ) of gases at densities corresponding to pressures up to one atmosphere. Hence any transport phenomena will be controlled by wall collision phenomena (from kinetic theory, the number of molecular collisions between successive wall collisions when a gas diffuses down a tube of diameter D is D/λ) and will be a molecular effusion process. However, if surface forces compress the gas to densities at all comparable with the liquid density (the value of D/λ in this case is of the order of unity and drift velocities should develop) the flow should become essentially laminar flow with slip, unless, of course, the condensed material is strongly held on isolated "sites", i.e., unless the adsorbed material is in some sort of solid state. It is immediately evident that, other things being equal, a large increase in density is quite capable of increasing the flow rate as measured in K units.

While the dimensions of a piece of active carbon are slightly changed by adsorption, these changes are usually very small and can hardly account for any very large increase in permeability.

Again a very low value of f in the term $(2 - f)/f$, due possibly to an adsorbed layer, could, of course, lead to a very rapid transport of matter. However, as we have pointed out, the flow of condensable vapors through large capillaries is perfectly normal under pressure conditions such that considerable adsorption on the walls must occur. If the adsorbed layer were capable of sliding over the surface at speeds considerably in excess of the gas slip velocity, it would increase the velocities of all the lamina and the flow rate would be much higher than observed. However, it may be pointed out that a slowly moving layer of high density may transport a great deal more material (as measured in K units) than a rapidly moving layer of low density. Accordingly, if the cross-sectional area of the adsorbed layer is appreciable compared to the cross section of the capillary, the contribution of a slowly moving adsorbed layer to the total flow rate may be considerable. About the only other immediately obvious variable involved is the viscosity and we would not, in general, expect the viscosity to decrease markedly as a result of the action of compressive surface forces.

It would seem that by far the simplest assumption to make is that the micropore flow mechanism is essentially Maxwellian, the abnormally high rate being due to the increased densities and stresses that result from the action of surface forces. Accordingly, we shall make this assumption and in Part III we shall enquire as to whether or not compressive surface forces can give rise to pressure dependent factors of any such form and magnitude as are required to be consistent with our data.

REFERENCES

1. ARNELL, J. C. Can. J. Research, A, 25: 191. 1947.
2. BABBITT, J. D. Can. J. Research, A, 28: 449. 1950.
3. BARRER, R. M. Quart. Rev. Chem. Soc. (London), 3: 293. 1949.
cf. Also numerous other articles and books by this author.
4. EMMETT, P. H. Chem. Rev. 43: 69. 1948.
5. JUHOLA, A. J. Division 10, NDRC Formal Report, June, 1945.
6. TOMLINSON, R. H. and FLOOD, E. A. Can. J. Research, B, 26: 38. 1948.

NOTE

The Papilionaceous Alkaloids. XVI. Trilupine and Dilupine*

Recently Galinovsky and Kainz (5) obtained from the bases of *Lupinus albus*, together with *d*-lupanine, a quantity of a sublimate evincing properties and yielding analytical figures similar to those described by Couch (3, 4) for the alkaloid that he designated trilupine. They tried to ascertain whether their sublimate had the improbable *d*-lupanine di-N-oxide structure assigned by Couch (3). However, they established that their substance was not an N-oxide, but *d*-lupanine monohydrochloride dihydrate which was also the product they obtained in attempting to prepare *d*-lupanine di-N-oxide by Couch's method (3).

Not long before his death Dr. J. F. Couch had generously given the present author his entire supply of lupine alkaloids including both his trilupine and his synthetic sample. It is deemed worthwhile to record that the findings of Galinovsky and Kainz (who had not in their possession a sample of Couch's trilupine) have been confirmed by a comparison of the infrared absorption spectra and the X-ray diffraction patterns of trilupine, synthetic trilupine, and *d*-lupanine monohydrochloride dihydrate. All three were identical.

The ready formation of base hydrochlorides by a base-catalyzed hydrolysis of chloroform has already been reported concerning spathulatine and nonalupine which are both identical with pusilline monohydrochloride monohydrate (6); consequently it does not depend on the presence of a lactamic nitrogen as Galinovsky and Kainz seem to assume (5) since pusilline contains no oxygen.

Of the alkaloids described by Couch, dilupine (3) is also of dubious identity. It was assigned the empirical formula $C_{16}H_{26}O_2N_2$ and, tentatively, the structure of a C-methyl-lupanine N-oxide. However, it forms salts containing one oxygen less than the original base. The base liberated from dilupine hydrobromide yielded analytical figures corresponding to the formula $C_{16}H_{26}ON_2$ (3). A base N-oxide does not usually lose its oxygen on salt formation since oxymatrine forms normal salts (7). Couch (3) stated that dilupine after extraction with chloroform deposited some trilupine (*d*-lupanine monohydrochloride dihydrate). Hence, it is plausible that dilupine might consist of impure *d*-lupanine probably contaminated with some of the hydrochloride. Unfortunately Dr. Couch's collection of alkaloids did not contain any dilupine so that it was not possible to make a direct comparison. However, this assumption finds support in the fact that *Lupinus barbiger* which is reported to yield trilupine, sparteine, and dilupine (3) must, because of the nature of trilupine, have contained some *d*-lupanine. Furthermore, the melting points of the hydrobromide (233-4°) and methiodide (253°) are not very different from the uncorrected melting point of *d*-lupanine hydrobromide

*Issued as N.R.C. No. 2702.

(238°) and the reported uncorrected melting point of the methiodide (263°) (2). The specific rotation of *d*-lupanine methiodide (+ 51.48°) (1) and that of dilupine methiodide (+ 51.1°) are identical.

EXPERIMENTAL

Trilupine

The sample of trilupine obtained from Dr. Couch sintered at 120° and melted at 250-253°.* It was sublimed at 200-210° at 0.1 mm. and the sublimate dissolved in boiling acetone containing a few drops of water. On cooling, the solution deposited colorless prismatic needles sintering at 125-130°, resolidifying, and melting at 260-263°. Calcd. for $C_{15}H_{24}ON_2 \cdot HCl \cdot 2H_2O$: C, 56.15; H, 9.11. Found: C, 56.20; H, 9.35%. $[\alpha]_D^{21} + 56.9°$ (*c*, 3.71 in water).

The synthetic *d*-lupanine di-N-oxide received from Dr. Couch was purified exactly as described above for trilupine. It had the same melting point either before or after admixture with trilupine. A freshly sublimed sample of each substance was used for the infrared absorption spectra which were determined in nujol mulls with a model 12B Perkin-Elmer single beam spectrometer. The two spectra were exactly superposable.

A sample of *d*-lupanine monohydrochloride dihydrate was prepared as described by Galinovsky and Kainz. It fused at 125-130°, resolidified, and melted at 266°. In admixture with trilupine, it fused at 125-130°, and melted at 262-263°. The X-ray diffraction powder patterns of this salt and of trilupine were identical.

d-Lupanine Monohydrobromide

A small quantity of *d*-lupanine in methanol was neutralized to Congo red with a solution of hydrobromic acid in methanol added dropwise. The solution was evaporated to dryness, the residue dissolved in methanol, and the solution again evaporated to dryness. The residue was now dissolved in acetone containing a little methanol and the solution was cooled in the refrigerator. After some time it deposited the hydrobromide as colorless prisms, m.p. 244° (238° uncorr.).

ACKNOWLEDGMENT

The author expresses his gratitude to Dr. W. H. Barnes and Mrs. H. Sheppard who prepared the X-ray powder diagrams; also to Dr. R. N. Jones and Mr. R. Lauzon for the infrared absorption spectra.

1. Beckel, A. Arch. Pharm. 249: 339. 1911.
2. Clemo, G. R. and Leitch, G. C. J. Chem. Soc. 1813. 1928.
3. Couch, J. F. J. Am. Chem. Soc. 58: 1296. 1936.
4. Couch, J. F. J. Am. Chem. Soc. 59: 1469. 1937.
5. Galinovsky, F. and Kainz, G. Monatsh. 82: 926. 1951.
6. Marion, L. Can. J. Chem. 29: 959. 1951.
7. Ochiai, E. and Ito, Y. Ber. 71: 938. 1938.

Received January 3, 1952.
Léo Marion
Division of Chemistry,
National Research Council of Canada,
Ottawa, Canada.

**All melting points are corrected unless otherwise mentioned.*

CANADIAN JOURNAL OF CHEMISTRY

Notice to Contributors

GENERAL: Manuscripts should be typewritten, double spaced, and the **original and one extra copy** submitted. Style, arrangement, spelling, and abbreviations should conform to the usage of this Journal. Names of all simple compounds, rather than their formulas, should be used in the text. Greek letters or unusual signs should be written plainly or explained by marginal notes. Superscripts and subscripts must be legible and carefully placed. Manuscripts should be carefully checked before being submitted, to reduce the need for changes after the type has been set. If authors require changes to be made after the type is set, they will be charged for changes that are considered to be excessive. **All pages, whether text, figures, or tables, should be numbered.**

ABSTRACT: **An abstract of not more than about 200 words, indicating the scope of the work and the principal findings, is required.**

ILLUSTRATIONS:

(i) *Line Drawings:* All lines should be of sufficient thickness to reproduce well. Drawings should be carefully made with India ink on white drawing paper, blue tracing linen, or co-ordinate paper **ruled in blue only**; any co-ordinate lines that are to appear in the reproduction should be ruled in black ink. Paper ruled in **green, yellow, or red should not be used** unless it is desired to have all the co-ordinate lines show. Lettering and numerals should be neatly done in India ink preferably with a stencil (**do not use typewriting**) and be of such size that they will be legible and not less than one millimeter in height when reproduced in a cut three inches wide. All experimental points should be carefully drawn with instruments. Illustrations need not be more than two or three times the size of the desired reproduction, but the ratio of height to width should conform with that of the type page. **The original drawings and one set of small but clear photographic copies are to be submitted.**

(ii) *Photographs:* Prints should be made on glossy paper, with strong contrasts; they should be trimmed to remove all extraneous material so that essential features only are shown. Photographs should be submitted **in duplicate**; if they are to be reproduced in groups, one set should be so arranged and mounted on cardboard with rubber cement; the duplicate set should be unmounted.

(iii) *General:* **The author's name, title of paper, and figure number should be written in the lower left hand corner (outside the illustration proper) of the sheets on which the illustrations appear.** Captions should not be written on the illustrations, but typed together at the end of the manuscript. All figures (including each figure of the plates) should be numbered consecutively from 1 up (arabic numerals). **Each figure should be referred to in the text.** If authors desire to alter a cut, they will be charged for the new cut.

TABLES: Each table should be typed on a separate sheet. Titles should be given for all tables, which should be numbered in Roman numerals. Column heads should be brief and textual matter in tables confined to a minimum. **Each table should be referred to in the text.**

REFERENCES: **These should be listed alphabetically by authors' names, numbered in that order, and placed at the end of the paper.** The form of literature citation should be that used in this Journal. **Titles of papers should not be given.** The first page only of the references cited should be given. **All citations should be checked with the original articles.** Each citation should be referred to in the text by means of the key number.

REPRINTS: A total of 50 reprints of each paper without covers are supplied free to the authors. Additional reprints will be supplied according to a prescribed schedule of charges. On request, covers can be supplied at cost.

Approximate charges for reprints may be calculated from the number of printed pages, obtained by multiplying by 0.6 the number of manuscript pages (double-spaced typewritten sheets, 8½ in. by 11 in.) and making allowance for space occupied by line drawings and halftones (not inserts). The cost per page is tabulated at the back of the reprint request form sent with the galley.

Contents

Page

The Action of Liquid Ammonia on Wheat Straw Holocellulose—*C. T. Bishop* - 229

The Reaction between Silver and Triphenylmethyl Chloride—*E. J. Perry and C. A. Winkler* - - - - - - - - - - - - 235

Dicumarol-2-C^{14}: Synthesis and Metabolism Studies—*H. R. Eisenhauer, J. M. Pepper, L. B. Jaques, and J. W. T. Spinks* - - 245

Some Methyl Ethers and Acetates of Purpurogallin—*G. Denis Thorn and L. R. C. Barclay* - - - - - - - - - - - - - 251

The Quantitative Determination of the Free Monoxides of Calcium, Strontium, and Barium, and of Calcium Ethylate by the Alcohol–Glycerol Method—*E. G. Swenson and T. Thorvaldson* - 257

Reaction of Oxymercurials with Hydrazine—*George F Wright* - 268

Thermal Decarboxylation of Uronic Acids—*A. S. Perlin* - - - - 278

Synthesis of Para-bridged Benzene Compounds. III.—*M. F. Bartlett, S. K. Figdor, and K. Wiesner* - - - - - - - - - 291

The Mechanisms of Glucose Pentaacetate Anomerization and Levoglucosan Formation—*R. U. Lemieux and Carol Brice* - 295

Measurements of Self-diffusion in Aqueous Solutions of Sodium Dihydrogen Phosphate—*J. E. Burkell and J. W. T. Spinks* - 311

The Binding of Anions by Lysozyme, Calf Thymus Histone Sulphate, and Protamine Sulphate—*J. Ross Colvin* - - - 320

Preparation of Ketene from Glacial Acetic Acid, Methyl Acetate, and Ethyl Acetate—*K. K. Georgieff* - - - - - - - - - - 332

The Flow of Fluids Through Activated Carbon Rods. I.—*E. A. Flood, R. H. Tomlinson, and A. E. Leger* - - - - - - - - 348

The Flow of Fluids Through Activated Carbon Rods. II. The Pore Structure of Activated Carbon—*E. A. Flood, R. H. Tomlinson, and A. E. Leger* - - - - - - - - - - - - - - - - 372

The Papilionaceous Alkaloids. XVI. Trilupine and Dilupine—*Léo Marion* - 386

Printed in Canada *by* University of Toronto Press